ANTIWEAR BEHAVIOUR OF ORGANO-PHOSPHORUS (III) ESTERS

by

Ian Nigel Lacey

A thesis submitted for the degree of Doctor of Philosophy of the University of London and for the Diploma of Membership of the Imperial College of Science and Technology (D.I.C.)

April 1985

Mineral Technology Section
Department of Mineral Resources Engineering
Royal School of Mines
Imperial College of Science and Technology
London SW7

"..... Something lingering with boiling oil in it, I fancy.
Yes, I think boiling oil comes into it somewhere."

(The Mikado, W.S. Gilbert 1836-1911)

ABSTRACT

This thesis investigates the antiwear properties of a number of dialkyl and diaryl phosphonates under elastohydrodynamic (EHD) conditions. The surface films produced by the phosphonates under rolling conditions have been studied and compared with the products obtained when the phosphonates were heated with iron powder.

The laboratory preparation and purification of the esters used in these studies have been described. Infrared Spectroscopy, ^{31}P n.m.r. Spectroscopy, Mass Spectroscopy and Elemental Analysis have been used to characterise the synthesised esters.

The reaction of dialkyl and diaryl phosphonates with iron under a variety of conditions has been investigated. The effects of temperature, oxygen and water on the rate of the reaction have been studied, and the reaction has been shown to involve the oxidation of iron and was to be promoted by the presence of oxygen and/or water and by elevated temperatures. Trialkyl phosphites have been shown not to undergo a similar reaction to disubstituted phosphonates. Dialkyl phosphonates have been shown not to react on being heated with chromium metal.

The phosphonate-iron reaction products have been analysed by a number of methods. As well as the methods used to characterise the pure esters, other analytical methods have been used; i.e. Electron Spin Resonance Spectroscopy and Mossbauer Spectroscopy. The results of these analytical methods are discussed. The results have shown that the phosphonate-iron reaction products are polymeric compounds largely composed of Iron (III) mono alkyl (or aryl) phosphate groups.

The EHD film forming properties of the dialkyl and diaryl phosphonates dissolved in synthetic hydrocarbon lubricants have been studied using a heated optical interferometry EHD test rig. The phosphonates have been shown to form chemical films of 200 nm thickness in the rolling contact under EHD conditions at elevated temperatures.

These surface films have been analysed using Scanning Electron Spectroscopy, Reflective Infrared Spectroscopy and Mass Spectroscopy. The results of these analyses show that the chemical films are similar to the products formed by heating the phosphonates with iron.

ACKNOWLEDGEMENTS

My thanks are extended to my supervisors Dr. G.H. Kelsall and Dr. H.A. Spikes, and in the early part of the project, Dr. H.L. Shergold, for their encouragement and guidance.

Much gratitude is owed to both students and staff of the Departments of Mineral Resources Engineering, Mechanical Engineering and Chemistry at Imperial College and to the staff of the n.m.r. service at Kings College London for all the assistance and advice given to me in this project.

My thanks to Barbara and Sally at Shared Office Services for the typing of this thesis.

I am grateful to Mobil Oils Ltd., for the supply of Lubricating Oils.

I am indebted to the Ministry of Defence for the funding of this project.

TABLE OF CONTENTS

		Page
ABSTRACT		3
ACKNOWLEDGEMENTS		5
TABLE OF CONTENTS		6
LIST OF FIGURES		12
LIST OF TABLES		15
LIST OF PLATES		16
NOMENCLATURE		17
Chapter 1.	**An Introduction to Lubricant Antiwear Additives**	18
1.1	General Introduction	19
1.2	Background to Phosphorus Additive Behaviour	21
1.2.1	Comparative to Phosphorus Additive Behaviour	22
1.2.2	Nature of the Film formed	25
1.2.3	Evidence from "Solution Chemistry"	28
1.3	External Factors Influencing Additive Performance	33
1.3.1	Influence of Base Oil Types	33
1.3.2	Influence of Steel Types	35
1.3.3	Influence of Water	36
1.3.4	Influence of Oxygen	38
1.3.5	The Effect of Temperature	40
1.4	The "Thick Film" Effect	42
1.5	Discussion and Conclusions	44
Chapter 2	**Phosphites - Structure and preparative methods**	48
2.1	Structure and Nomenclature	48
2.2	General Preparative Methods	51
2.3	Synthesis of Tri-Alkyl and Aryl Phosphites	54

		Page
2.3.1	Hydrolysis of PCl_3	54
2.3.2	Transesterification	55
2.3.3	Disproportionation	56
2.4	Preparation of Di-Alkyl and Aryl Phosphonates	57
2.4.1	Hydrolysis of PCl_3	57
2.4.2	Transesterification	58
2.4.3	Disproportionation of $(RO)_3P$	58
2.4.4	Esterification of H_3PO_3	59
2.4.5	Miscellaneous Methods	60
2.5	Preparation of Mono-Alkyl and Aryl Phosphonates	61
2.5.1	Hydrolysis of PCl_3	61
2.5.2	Disproportionation of $(RO)_3P$	62
2.5.3	Alkaline Hydrolysis of $(RO)_2PHO$	62
Chapter 3.	**The Preparation and Purification of the Esters**	63
3.1	Preparation	63
3.1.1	Introduction	63
3.1.2	Apparatus	63
3.1.3	Preparation of Tri Hexyl Phosphite	66
3.1.4.	Preparation of Di Hexyl Phosphonate	67
3.1.5	Preparation of Mono Phenyl Phosphonate	69
3.2	Practical Observations	72
3.2.1	Heats of Reaction	72
3.2.2	Effect of Temperature	72
3.2.3	Solvent	73
3.2.4	Distillation	73
3.3	Conclusions	74
Chapter 4	**Characterisation of the Phosphorus Esters**	75
4.1	Infrared Asbsorption Spectra	75
4.1.1	Introduction	76
4.1.2	Equipment	78

			Page
	4.1.3	Technique	81
	4.1.4	Infrared Spectra	83
	4.2	^{31}P Nuclear Magnetic Resonance (n.m.r.) Spectra	99
	4.2.1	Introduction to ^{31}P n.m.r.	99
	4.2.2	Equipment and Technique	101
	4.2.3	Spectra	101
	4.3	Mass Spectra	103
	4.3.1	Introduction	103
	4.3.2	Results	104
	4.4	Elemental Microanalysis	107
	4.4.1	Introduction	107
	4.4.2	Method	107
	4.4.3	Results	108
	4.5	Summary	108
Chapter 5		**Reaction of Phosphonates and Iron**	109
	5.1	Experimental	109
	5.1.1	General Experimental Method	110
	5.1.2	Heating in a 'Semi-closed' System	111
	5.1.3	Effect of Temperature	113
	5.1.4	Effect of Oxygen	113
	5.1.5	Effect of Water	114
	5.1.6	Reaction with Oxidised and Reduced Iron Samples	115
	5.1.7	Reaction with Iron (III) Oxide	115
	5.1.8	Effect of Surface Area of the Iron on Reaction	116
	5.1.9	Tests in Liquid Paraffin Solution	120
	5.1.10	Reaction with Chromium Powder	122
	5.1.11	Reaction of Trihexyl Phosphite and Iron Powder	122

		Page
5.2	Monitoring of the Reaction Progress	123
5.2.1	Measurement of dissolved Iron Content	124
5.2.2	Infrared Spectrophotometry	127
5.2.3	^{31}P Nuclear Magnetic Resonance Spectrometry	132
5.2.4	Summary of the Methods of Monitoring the Reaction	133
5.3	Results and Discussion	134
5.3.1	General Experimental Method	134
5.3.2	Heating in a 'Semi-closed' System	136
5.3.3	Effect of Temperature	139
5.3.4	Effect of Oxygen	141
5.3.5	Effect of Water	143
5.3.6	Reaction with Oxidised and Reduced Iron Samples	147
5.3.7	Reaction with Iron (III) Oxide	149
5.3.8	Effect of Surface Area of the Iron on Reaction	151
5.3.9	Tests in Liquid Paraffin Solution	153
5.3.10	Reaction with Chromium Powder	160
5.3.11	Reaction of Trihexyl Phosphite and Iron Powder	160
5.4	Summary	164
Chapter 6	**The Analysis of the Phosphonate-Iron Reaction Product**	167
6.1	Infrared Spectroscopy	167
6.1.1	Method	168
6.1.2	Infrared Spectra	168
6.1.3	Discussion	169
6.2	^{31}P n.m.r. Spectroscopy	179
6.2.1	Method	179
6.2.2	^{31}p n.m.r. Spectra	179
6.2.3	Results and Discussion	181

		Page
6.3	Mass Spectrometry	184
6.3.1	Method	184
6.3.2	Spectra	185
6.3.3.	Results and Discussion	187
6.4	Elemental Analysis	199
6.4.1	Method	199
6.4.2	Results and Discussion	200
6.5	Electron Spin Resonance Spectroscopy	204
6.5.1	Introduction	204
6.5.2	Spectra	208
6.5.3	Results and Discussion	208
6.6.	Mossbauer Spectroscopy	210
6.6.1	Introduction	210
6.6.2	Spectra	212
6.6.3	Results and Discussion	212
6.7	Discussion of the Analytical Results	216
6.7.1	Similarity	217
6.7.2	Polymeric Nature	217
6.7.3	Oxidation State of the Iron	217
6.7.4	Bonding State of the Phosphorus Atom	218
6.7.5	Co-ordination around the Iron Atoms	220
6.7.6	Molecular Formula	222
6.7.7	Possible Structures	223
Chapter 7	**Optical Interferometric Study of EHD Film Thickness**	227
7.1	Elastohydrodynamic Lubrication	228
7.2	EHD Film Thickness Measurement by Optical Interferometry	231
7.2.1	Introduction	231
7.2.2	Chromatic Interferometry	233
7.2.3	Refractive Index	237

		Page
7.3	The Optical EHD Test Apparatus	238
7.3.1	General Description	238
7.3.2	Speed Control and Measurement	244
7.3.3	Temperature Control and Measurement	247
7.3.4	Oil Circulating System	248
7.4	Experimental Work	249
7.4.1	Materials	249
7.4.2	Preparation of Fluids	249
7.4.3	Test Procedure	250
7.4.4	Measurement of the Refractive Index	251
7.4.5	Calibration of Rolling Track Diameter	252
7.5	Results and Discussion	255
7.5.1	"Pure" Rolling Tests	255
7.5.2	"Sliding" Tests	268
7.5.3	Effect of Corrosion Inhibitors	270
7.6	Analysis of the Surface Film	272
7.6.1	Appearance of the Film	272
7.6.2	Scanning Electron Microscopic Analysis	275
7.6.3	Infrared Spectra	283
7.6.4	Mass Spectral Analysis	292
7.6.5	Summary of the Analysis of the Surface Film	294
7.7	Discussion	296
Chapter 8	**Summary and General Conclusions**	300
8.1	The Reaction of Phosphonates with Iron	300
8.2	The EHD Film Forming Properties	303
8.3	A Possible Mechanism of Interaction	304
8.4	Implications	305
8.5	General Conclusions	307
Chapter 9	**Suggestions for Future Work**	309
References		312

LIST OF FIGURES

Figure		Page
3.1	Preparation Apparatus	64
3.2	Distillation Apparatus	64
4.1	Variable Temperature Infrared Cell	79
4.2 - 4.6	Infrared Spectra - dialkyl phosphonates	84 - 88
4.7 - 4.8	Infrared Spectra - diaryl phosphonates	89 - 90
4.9 - 4.10	Infrared Spectra - trialkyl phosphites	91 - 92
4.11 - 4.12	Infrared Spectra - triaryl phosphites	93 - 94
4.13 - 4.14	Variable Temperature Infrared Spectra	95 - 96
4.15	^{31}P n.m.r. spectrum dihexyl phosphonate	102
4.16	Mass Spectrum Line Diagram dihexyl phosphonate	105
5.1	Apparatus for "Semi-closed" heating tests	112
5.2	Calibration graph-iron by A.A.S.	126
5.3	Infrared spectrum - dihexyl phosphonate-iron reaction product	129
5.4	Method of measuring absorbances	131
5.5	Method of construction of spectral baselines	131
5.6	Iron concentration with time for four di-phosphonates on heating with iron	135
5.7	Infrared spectrum - condensate from the dioctyl phosphonate-iron heating test, octan-1-ol and dioctyl phosphonate	137
5.8	Effect of temperature on the dihexyl phosphonate-iron reaction	140
5.9 - 5.10	Effect of oxygen on the phosphonate-iron reaction	142
5.11 - 5.12	Effect of water of the phosphonate-iron reaction	144

		Page
5.13 - 5.14	Effect of oxygen and water on the phosphonate-iron reaction	146
5.15	Effect of oxidation and reduction of iron on the rate of the dihexyl phosphonate-iron reaction	148
5.16	A comparison of the rates of reaction of dihexyl phosphonate with oxidised iron and with 'as received' iron in the presence of oxygen and/or water	148
5.17	A comparison of the rates of reaction of dihexyl phosphonate with Fe_2O_3 and with iron	150
5.18	A comparison of the rates of reaction of dihexyl phosphonate with Fe_2O_3 and with "oxidised iron"	150
5.19	Effect of particle size on the dihexyl phosphonate-iron reaction	152
5.20	Effect of surface area of the iron foil on the rate of the dihexyl phosphonate-iron reaction	152
5.21	A comparison of the rate of reaction of dihexyl phosphonate with iron in liquid paraffin solutions and in 'neat' solution	154
5.22	Effect of oxygen on the rate of reaction of dihexyl phosphonate and iron in liquid paraffin solution	156
5.23 - 5.24	Effect of water on the rate of reaction of dihexyl phosphonate and iron in liquid paraffin solution	156 - 157
5.25 - 5.26	Infrared spectra of trihexyl phosphite before and after heating with iron	161 - 162
6.1 - 6.5	Infrared spectra of the phosphonate-iron reaction products	170 - 174
6.6	Infrared spectra of the dihexyl phosphonate-iron reaction product at 25° - $175^{o}C$	175
6.7	^{31}P n.m.r. Spectrum for the dihexyl phosphonate - iron reaction product	180
6.8a	Representation of a portion of the mass spectrum of the dihexyl phosphonate-iron reaction product	186

6.8 - 6.11	Mass spectrum line diagrams for the dialkyl phosphonate-iron reaction product	188 - 191
6.12	e.s.r. spectrum for the dihexyl phosphonate-iron reaction product	209
6.13	Mossbauer spectrum for the dihexyl phosphonate-iron reaction product	213
6.14	Temperature dependence of the Mossbauer Isomer shift	214
7.1 - 7.2	Film profiles of a rolling point contact	229
7.3	Two beam interferometry	232
7.4	Sectional view of EHD test rig	240
7.5	Schematic diagram of power train layout	245
7.6	Calibration of rolling track radius	253
7.7 - 7.10	Film build up as a function of a decrease in rolling speed at constant EHD film thickness.	256 - 259
7.11	Film build up as a function of an increase in EHD film thickness at constant rolling speed.	260
7.12	Effect of inadequate cleaning on the rate of film formation	266
7.13 - 7.14	Film build up at constant rolling speed under rolling/sliding conditions	269
7.15 - 7.20	Elemental analysis by SEM/EDAX of the surfaces of the balls from the lubrication tests	277 - 282
7.21 - 7.24	Infrared spectra of the surfaces of the balls from the lubrication tests	285 - 288
7.25	Mass spectrum line diagram for the surface film of a ball used in a dihexyl phosphonate lubrication test	291
7.26	Comparison of experimental Film build up at constant rolling speed with values calculated from a constant film thickness test	299

Page

LIST OF TABLES

4.1	Literature Values for the Infrared absorptions of Organophosphorus Esters	80
4.2 - 4.3	Determined values for the phosphorus group frequencies	97
4.4	Recorded chemical shifts for several phosphites and phosphonates	103
4.5	Assignment of major m/e ratios in the mass spectrum of dihexyl phosphonate	106
5.1	Iron powder size ranges and estimated surface areas	118
5.2	Masses of iron foils and calculated surface areas	120
5.3	Infrared absorbances for octanol, dioctyl phosphonate and "reaction condensate"	138
6.1	Absorption frequencies for the "new" absorption found in the infrared spectra of the phosphonate-iron reaction products	176
6.2 - 6.3	^{31}P n.m.r. chemical shifts for the phosphonate-iron reaction products	181 - 183
6.4	m/e ratios for the primary mass spectra peaks for the dialkyl phosphonate-iron reaction products	192
6.5	Elemental compositions for a series of dihexyl phosphonate-iron reaction samples	201
6.6	Elemental ratios for a series of dihexyl phosphonate-iron reaction samples	202
7.1	Absorbance peaks in the Infrared spectra of the surface films	289

Page

LIST OF PLATES

7.1	Typicical EHD point contact interferogram	230
7.2	Front view EHD test rig	239
7.3	Front elevation ball and loading arm	242
7.4	Stationary contact after 'growth' of a film	264
7.5	Stationary contact at start of test	264
7.6 - 7.9	Photomicrographs of the surface films	273 - 274

NOMENCLATURE

Symbols not found here may be found in the text

nmr	nuclear magnetic resonance
esr	electron spin resonance
t	time
δ	chemical shift (in ppm)
ρ	density
w/w	weight for weight (percentage)
ppm	part per million
DHP	di hexyl phosphonate
DOP	di octyl phosphonate
DDDP	didodecyl phosphonate
DPP	diphenyl phosphonate
BOPP	bis 4 tert-Octylphenyl phosphonate
λ	wavelength
cm^{-1}	reciprocal centimetre, wave number
nm	nano (10^{-9}) metre
μ	micron (10^{-6}m)
h	film thickness
ho	central film thickness
EHD	Elastohydrodynamic
EHL	Elastohydrodynamic Lubrication

Chemical elements are represented by the appropriate chemical symbol

Chapter 1.

An Introduction to Lubricant Antiwear Additives

Modern lubricating oils are a complex mixture of base oils and various additives. As the demands placed on the oil by faster running and hotter temperatures have increased, so oils have become more specially formulated to cope with these demands.

Of great interest currently is the lubrication regime known as "Boundary Lubrication". In this regime only thin films are formed, with resultant frequent contact between the higher asperities of the metal parts in the rolling or sliding contact. Under these conditions wear becomes very significant, and, as boundary lubrication frequently occurs in gas turbine engines and transmissions of both fixed and rotary winged aircraft, it is clear that "catastrophic failure", due to excessive wear, could have serious if not disastrous consequences.

To reduce wear under these conditions, a number of compounds have been added to oils to act as 'antiwear' agents. One of the best known of these is Molybdenum Disulphide or "Molyslip" as sold for addition to car engine oils. A common feature of antiwear additives is the presence of a Sulphur, Chlorine or Phosphorus atom, or combinations of them. Other examples of antiwear agents in use include chlorinated waxes, benzyl disulphide, metal (especially zinc) dialkyl dithio-phosphates, chlorinated organo phosphates, and organophosphorus esters.

The mechanism by which these additives perform as antiwear agents is unclear. The purpose of this project has been to study how one particular class of organophosphorus compound, the alkyl and aryl esters of phosphorous acid (H_3PO_3), act as antiwear additives.

1.1 General Introduction

Phosphorus containing compounds have been employed for many years as "antiwear" and "extreme pressure" additives in lubricating oils. Several types of phosphorus compounds have been used as additives, of which the most commonly used are tricresyl phosphate and Zinc dialkyl dithiophosphates (ZddP's). Other phosphorus additives used are organophosphites and organophosphonates [$(RO)_3P$ and $(RO)_2PHO$ respectively, where 'R' is an alkyl or aryl group]. It is upon these latter compounds that this research project has been based.

The mechanisms by which these compounds function as antiwear additives is only poorly understood, and, as will be shown later, a number of different and often contradictory theories have been proposed. It is known that a surface film is formed, which in some way reduces wear at the metal surface. However, neither the nature, nor the mechanism of formation of these films has been clearly resolved.

Generally the mechanism accepted until recently was as follows. The additive, or a product of its breakdown, reacts with the metal surface to form a thin metal-organo phosphorus film, normally a few molecular layers in depth, much less than the surface roughness. It is thought that either this film may preferentially shear, so reducing friction, or it may serve to limit metal to metal contacts to only the highest asperity regions.

Because these films are so thin, analysis of their nature is difficult. In addition, many of the methods conventionally used to analyse the surface films (eg Electron Probe Microanalysis (EPMA) or Electron Spectroscopy for Chemical Analysis (ESCA) cannot readily be used to analyse for Carbon, Hydrogen or Oxygen. The presence of Phosphorus can, and has been shown by these techniques. Consequently much of the research carried out provides only indirect clues to the nature of the surface film and its formation.

The role played by the surface film in reducing wear, has become the subject of further interest as a result of recent work done by NASA and the Mobil Oil Corporation (1,2). This work would appear to indicate that at least one phosphonate antiwear additive acts in a very different way to that outlined above.

Under rolling conditions, the additive (in solution) gave rise to 'thick' chemical films built up in the rolling track. A point contact optical elastohydrodynamic (EHD) test rig was used, which permitted the measurement of oil film thickness as a function of speed. At elevated temperatures (80-100°C), a thick film (>100nm) built up in the rolling track. The 'build-up' of this film was observed by the need to reduce the speed in order to maintain the same optical film thickness.

Clearly the role played by this particular additive was substantially different to that previously envisaged. Instead of providing a smoother running surface, this film served to decrease the metal to metal contact by greatly increasing the oil film thickness.

Exceptional antiwear properties have been reported for this additive (1), evidently due to its ability to form thick films, thereby decreasing the metal to metal contact and hence wear. It was not known whether this thick film formation was a unique property of this particular phosphonate reportedly a Bis-(Nonyl-phenyl) phosphonate (3), or whether it is a property of all phosphonates, all organophosphorus compounds or all currently used antiwear additives.

1.2 Background to phosphorus additives behaviour

There are three main methods of approach which have been used to study the antiwear and extreme pressure performance of phosphorus additives. From the results obtained, attempts have been made to understand the role that these additives perform in boundary lubrication. The three methods, which are complimentary, are:-

(i) Comparing the performance of different types and structures of phosphorus additives. For example comparing the performances of a series of trialkyl phosphites, or contrasting phosphites against the corresponding phosphates.

(ii) Studying the film formed on the rubbed or non rubbed metal surfaces by electron diffraction or other surface analysis techniques.

(iii) Studying the "solution chemistry" of phosphorus additives under antiwear/extreme pressure conditions to try to determine the mechanism of film formation.

1.2.1 Comparative performance

Comparisons of different phosphorus additives have been made using both dynamic and static testing methods. In such tests the aim has been to gain information on the mechanism by considering the different results obtained with respect to the differences in the structure or composition of the esters. The comparative tests have, for example, compared phosphates with the corresponding phosphite or phosphonate, or have measured changes in antiwear performance or reactivity of a series of phosphates of different alkyl groups.

Barcroft and Daniel (4) compared the antiwear performance of triaryl phosphates with their hydrolytic and pyrolytic stabilities. Increasing antiwear performance was found to be in the same order as increasing ease of hydrolysis. That is, antiwear performance increased in the order phenyl, tolyl. The ease of pyrolysis was found to increase with decreasing antiwear performance, that is xylyl, tolyl, phenyl Consequently the authors deduced that the mechanism of interaction involved hydrolysis of the ester.

The relative performance of trialkyl phosphates as extreme pressure agents was studied by Davey (5). In these tests the longer alkyl groups gave improved antiwear and antiscuff properties. This trend was less noticeable with the trialkyl phosphites although some improvement in antiwear properties with increasing alkyl chain length was noticeable. Davey also showed that trialkyl phosphates and phosphites were better antiwear and extreme pressure agents than triaryl phosphates.

Davey found that phosphites gave better antiwear and antiscuff behaviour than did the corresponding phosphates. As the presence of phosphide films had been recorded, Davey concluded that phosphites gave better antiwear behaviour since they were more readily reduced to phosphides than would the corresponding phosphates. However, as is discussed in the next section, it is now generally considered tht the iron phosphide eutectic proposed by both Beeck et al (6) and by Davey is not involved in the antiwear mechanism of organophosphorus esters.

The results obtained by Davey have been reported by other authors, but only as a result of less ranging comparative studies.

Hall (7) compared the relative wear scars and scar appearances for tri-and di-phosphates, triphosphites and diphosphonates. In comparing the relative performances of the tri-p-tolyl phosphate and phosphite, Hall was able to show the superior performance of the phosphite to the phosphate ester.

The superiority of tri-alkyl esters over tri-aryl esters as found by Davey was also reported, but for one example only, by Yamamoto and Hirano (8,9). In their tests the authors compared the antiwear and antiscuff properties of tricresyl phosphate and trioctyl phosphate. Under moderate conditions trioctyl phosphate showed better antiwear properties, due, the authors concluded, to its greater reactivity with the steel surface. Under conditions of high load (the 'antiscuff' region) tricresyl phosphate was found to be superior in preventing scuffing. The films formed by tricresyl phosphate were considered to be of higher mechanical strength and thermal stability than the surface films formed by trioctyl phosphate.

Comparisons between dialkyl phosphates and phosphonates have been made by a number of authors, notably Forbes and Battersby (10) and Hall (7). Here the difference in compounds is much greater than for the tri-esters. Whereas both tri-phosphates and phosphites are neutral compounds, the di-phosphate possesses one acidic hydrogen while the phosphonate is a neutral compound. Forbes and Battersby (8) compared the wear scar diameters and initial seizure load using a four ball machine. The results showed that dialkyl phosphates were better at low loads ('antiwear' region) but worse than the corresponding phosphonate under high loads ('antiscuff' region). In the same work, the authors observed (not suprisingly in view of their acidic nature) that phosphates showed a greater reactivity with iron than did phosphonates. The iron phosphates produced were also readily desorbed into tetradecane solution. The conclusion drawn was similar to that drawn by Yamamoto and Hirano above (8,9), that antiwear behaviour depended on reactive additives whilst good antiscuff properties required the formation of films stable under high loads.

Hall (7) reported similar behaviour between dioctyl phosphate and phosphonates, both giving similar wear scar diameters under loads of up to 50kg. Seizure loads (which Forbes and Battersby had determined (10) to be in the range of 80-225 kg) were not measured and no further comparisons of antiscuff behaviour were made.

Finally comparative tests have been used to investigate the role that the alkyl group plays in the antiwear and antiscuff properties of dialkyl phosphates. Forbes et al (11,12) studied a number of dialkyl phosphates and their amine salts as antiwear and extreme pressure additives.

The results showed that the antiwear activities were porportional to the acid strength (pKa) of the parent ester. Esters of high acid strength (low pKa) gave lower wear scar diameters. Since esters of higher acid strength have greater reactivity with iron this is in keeping the conclusions drawn by Forbes and Battersby (10) and Yamamoto and Hirano (8,9) and mentioned above.

Longer alkyl chain lengths were shown by Forbes and Battersby to be beneficial in reducing wear at moderate loadings. Under heavier loaded conditions the authors reported that the more reactive short alkyl chain esters gave better extreme pressure behaviour. The contradiction between this result and the conclusion drawn (see above) to explain the improved antiwear but lower antiscuff properties of phosphates over phosphonates was not dealt with by the authors. The authors did however conclude that phosphates and phosphonates produced surface films of substantially different nature.

1.2.2 Nature of the film formed

The earliest investigations of the film formed by phosphorus additives at rubbed metal surfaces concluded that an iron: iron phosphide eutectic was formed (6). This low melting eutectic reduced wear by a "chemical polishing" mechanism. Davey in later work (5) supported this mechanism from results obtained using a number of phosphites and phosphates.

Beeck and coworkers (6) concluded from a theoretical viewpoint that a phosphide film was formed. In addition they reported the presence of films adsorbed on iron powder which liberated phosphine on treatment with dilute hydrochloric acid. This latter technique was used by Davey, who also reported phosphine evolution.

Later work has tended to discount this 'iron phosphide eutectic' theory. In lubrication tests wth tricresyl phosphate several authors have reported the presence of phosphates at the surface (4,10,13-17). Furthermore, Barcroft and Daniel (4) showed that phosphide films were not formed on rubbed metal surfaces.

Barcroft and Daniel (4) analysed the surface films formed using an oil containing ^{32}P radiolabelled triphenyl phosphate. Dissolution of the surface film was followed by chemical and radiochemical analysis. The authors showed the presence of phosphate on the surface. Using radiochemical analysis they recorded radioactivity in both the acid solution and in a benzene extract of the acid. Thus the authors were able to show that the surface coating that had dissolved had both inorganic and organic phosphate present.

Godfrey (13) reported only the presence of inorganic phosphate films when using tricresyl phosphate. The wear scars produced in dynamic lubrication tests using tricresyl phosphate to lubricate steel surfaces, were analysed using electron diffraction. A mixture was found of the inorganic iron phosphates $FePO_4$ and $FePO_4.2H_2O$.

The same technique was used by Yamamoto and Hirano (8) to study the films formed from tricresyl phosphate and trioctyl phosphate under dynamic conditions. Again the presence of $FePO_4$ was reported together with FeO and Fe_3O_4. Inorganic iron phosphate films were also reported by Gauthier et al (18). From ESCA analysis of the wear spots obtained using tricresyl phosphate, the authors concluded that $Fe_3(PO_4)_2$ was formed at the surface.

Rounds (19) examined the surface films formed in friction tests with tricresyl phosphate and didodecyl phosphonate. Using X-ray fluorescence, Rounds detected the presence of the hydrocarbon portion of the molecule in the surface film. Contrary to Godfrey, Rounds therefore concluded that the film must be organic in nature. Forbes and Battersby (10) and Hall (7) found that alkyl phosphonates with longer alkyl chain lengths produced more stable surface films and accordingly gave better antiwear properties.

Inorganic iron phosphate films have been reported as being produced in "hot-wire corrosion tests". Sakurai and Sato (14) and Wiegard and Broszeit (20) heated iron wires electrically in the presence of various phosphonates and phosphites. Both groups reported the presence of inorganic iron phosphates on the wires. However the conditions used (400°C, 15 min) were such that an organic film might well be expected to have undergone thermal breakdown.

The antiwear activities of phosphonates and phosphites has been attributed to a similar interaction with the metal surface as that accorded to phosphate esters. As with phosphate esters, tests have shown that the esters give rise to phosphorus containing surface films (10,19,21 - 23). However the nature of the films formed, is, like those obtained from phosphates, not completely resolved.

In addition to the question of whether inorganic or organic surface films are formed, the oxidation state of the phosphorus has been the subject of debate.

Rounds (21,24,25) considered that the phosphonate oxidised to form a phosphate surface coating. X-ray fluoresence was used to analyse the surface coatings formed from didodecyl phosphonate. This technique showed the presence of the hydrocarbon portion of the ester and the presence of phosphorus in the surface coating (19). From a study of the beneficial effect of oxygen Rounds concluded that oxidation of the phosphonate was necessary for good antiwear performance.

Forbes and Battersby (10) found higher surface levels of phosphorus in those surface films formed by dialkyl phosphonates compared to the corresponding phosphate. From their investigations of the effect of oxygen on these esters, they had concluded, contrary to Rounds (19), that oxidation was unlikely to be important to the antiwear activity. The authors concluded that an organic iron phosphate film was formed, which under extreme conditions hydrolysed further to an inorganic iron phosphonate film.

An organic iron phosphonate film was suggested by Barber (16), who had tested a series of dialkyl phosphonates using both static and dynamic testing methods.

1.2.3 Evidence from the "Solution Chemistry"

In attempts to elucidate the mechanism by which phosphorus esters act as antiwear additives, several workers have studied their "solution chemistry". For example lubrication and adsorption tests have been carried out using esters of known acid values or of different stages of

From the observed differences in antiwear behaviour and the known differences between samples, attempts have been made to deduce the mechanism of interaction.

Godfrey (13) compared the friction test results obtained for tricresyl phosphate, with those for orthophosphoric acid (H_3PO_4) and tri-p-tolyl phosphate. Tri-p-tolyl phosphate was used as a 'purer' sample of tricresyl phosphate. The friction values obtained reduced in the order tri p-tolyl phosphate, tri-cresyl phosphate, phosphoric acid. Thus Godfrey concluded that the antiwear performance was due to the presence of free phosphoric acid in the esters. This free acid reacted with the metal surface to form the surface film. Further surface film formation would arise as a result of hydrolysis of the ester to form more phosphoric acid.

The importance of the hydrolysis of the ester to its antiwear performance has been suggested by several other authors. Barcroft and Daniel (4) compared the antiscuff behaviour of a number of aryl phosphates with their hydrolytic stabilities. The tests showed that extreme pressure activity increased in line with the increasing ease of hydrolysis. Furthermore the tests indicated that diphenyl acid phosphate gave better antiscuff performance than triphenyl phosphate or benzyl diphenyl phosphate, of both of which it is the primary hydrolysis product.

In contrast to Godfrey, Barcroft and Daniel considered that the hydrolysis of the ester, was preceded by adsorption of the neutral ester on the metal surface, a mechanism supported by Forbes et al (10,15,16).

Forbes, Upsdell and Battersby (16) compared the relative phosphorus uptake rates on steel surfaces from samples of tricresyl phosphate. Increased levels of phosphorus on the steel surfaces were recorded in tests using samples of tricresyl phosphate, to which products of the hydrolysis of the neutral ester had been added. Preferential adsorption of acidic impurities onto the metal surface was also reported by Klaus and Bieber (27), who used a neutron activation technique to examine for surface phosphorus.

Adsorption tests have been carried out by several authors to further examine the role that adsorptions of the ester has on the antiwear behaviour. Whilst little difference in the adsorption isotherms for tri-phenyl, -tolyl and -xylyl phosphates were found, Barcroft and Daniel (4) found much greater adsorption of diphenyl phosphate from solution. The adsorption of the diaryl phosphates, not surprisingly in view of their acidic nature, was found to be irreversible. Tri-aryl phosphates gave rise to a reversible adsorption.

Results obtained by Goldblatt and Appeldoorn (17) indicated no adsorption of tricresyl phosphate onto iron powder samples. A similar result was obtained by Bieber et al (28), which would appear to be in direct contrast to the results obtained by Barcroft and Daniel and by Forbes et al (16). No temperature is indicated by Goldblatt and Appeldoorn or by Bieber but from the context in which the results were obtained (percolation of the ester through an iron powder column to remove impurities) it seems likely that room temperatures were used. Forbes et al reported no adsorption at temperatures below 50°C. Barcroft and Daniel obtained their adsorption isotherms at 21°C., obtaining maximum phosphorus levels of 100 ug P/25g metal.

Evidence of adsorption of the neutral ester on the metal surface does not in itself prove that hydrolysis of the ester is preceeded by its adsorption onto the metal. Godfrey (13) had concluded that the antiwear performance was due to the presence of acidic "impurities" in the tricresyl phosphate. Indeed the work cited above (4,16,17,27,28) clearly indicated that the acidic products of hydrolysis are more strongly adsorbed. However tests carried out by Goldblatt and Appeldoorn (17) and Hall (7) disputed the importance of these acid phosphates to the antiwear activity.

In both cases, esters were percolated before use in order to remove any acidic impurities that might have been present. The antiwear performance of these treated samples was compared with that of the untreated samples. Goldblatt and Appeldoorn used a sample of tricresyl phosphate percolated through silica gel, a treatment which reduced the acid value from 56 to 3.4 ug KOH/g. The treated sample was found to be as effective in its antiwear behaviour as the original untreated tricresyl phosphate. Hall obtained a similar result with a number of phosphites and phosphonates, which had been passed through an alumina column before use, which reduced the acid value by at least a half (50mg to 27 mg KOH/g in the worst case).

Hydrolysis of esters, when heated in the presence of steel or of iron powders, has been reported by several authors. Godfrey (13) and Forbes et al (16) found high levels of cresols in solution after heating tricresyl phosphate in the presence of steel (13) or iron (16). Forbes et al reported that insufficient cresols was found in solution for complete hydrolysis to have occurred, and concluded, unlike Godfrey, that it was the acid phosphates that were responsible for the stable film.

Forbes and Battersby (10) carried out similar tests with dialkyl phosphonates. Large levels of alcohols were found in the solutions. After heating diethyl phosphonate with iron, the authors analysed the residue. This residue was found to have a composition consistent with iron (III) monoethylphosphonate. Barber reported a similar reaction with di-isopropyl benzyl phosphonate (26).

Unlike the results obtained for tricresyl phosphate (4) these hydrolysis tests for dialkyl phosphonates indicated that the antiwear behaviour improved with increasing hydrolytic stability. Forbes and Battersby observed that the reactivity with iron decreased with increasing alkyl chain length. Phosphonates of longer alkyl chain length gave better antiwear performance. Barcroft and Daniel (4) had found that the triarylphosphates gave better antiwear performance with increasing ease of hydrolysis.

Clearly this would seem to indicate that these two different ester types undergo a different mechanism of interaction, and probably form different surface films. This conclusion has not been assumed in all the work in which comparisons between the two types of ester were made.

It has been reported that phosphite esters give rise to a surface phosphate coating (17). Oxidation of the ester therefore concurrently with its adsorption was necessary for good antiwear activity. Tests with low levels of oxygen showed decreased phosphorus levels on the steel surface (25). In addition higher surface phosphorus levels with correspondingly lower friction values were recorded at higher temperatures (21).

The same work had shown an increase in the oxidation of didodecyl phosphonate at temperatures of greater than 65°C. Using the same infrared analysing technique, Rounds had found no changes in the bulk oil properties and so deduced that oxidation of the phosphonate occurred at the metal surface.

In contrast, Forbes and Battersby (10) found very little oxidation of dibutylphosphonate at 130°C. The authors monitored the oxygen uptake of tetradecane in the presence of iron powder. The addition of dibutyl phosphonate to the tetradecane resulted in only a relatively small increase in the rate of oxygen uptake. The authors concluded that this small increase was due to increased oxidation of the tetradecane as a result of a catalytic effect of the phosphonate. Certainly it would appear that oxidation of the dibutyl phosphonate is a slow reaction, and is possibly not important in the antiwear role.

1.3 External factors influencing additive performance

Additive performance is affected by several factors including temperature, the presence or absence of oxygen or water and the type of base oil used. It is clear that the additive-lubricant-steel interaction is a complex one.

1.3.1 Influence of base oil type

Base oil character has been shown by several researchers to influence the antiwear activity of the additive. Goldblatt and Appeldoorn (17) and Forbes, Upsdell and Battersby (16) investigated the antiwear properties of tricresyl phosphate in various base oils.

Oils of an aliphatic or aromatic character and a mixed aliphatic/aromatic base oil were used. Both groups of workers reported a decrease in antiwear performance as the aromatic character of the base oil was increased. Goldblatt and Appeldoorn suggested that aromatic components competed with the additive for adsorbance on the surface.

This theory of competition for the surface sites was also taken up by Rounds (22,23,24). Rounds investigated the antiwear properties of didodecyl phosphonate in lubricants of varying polar and aromatic character. By taking samples of a naphthenic mineral oil at various stages during its refining, Rounds (22) showed that the removal of polar components during refining improved the antiwear properties of additives tested. In later work (23,24) the author reported the same effect with paraffinic base oils. The antiwear properties of didodecyl phosphonate could be decreased by the addition of either naphthenic hydrocarbon or polar organic compounds containing O,N or S eg quinoline. Highly refined oils had none or very low amounts of this type of compound.

Fowles, Jackson and Murphy (2) used bis (nonyl phenyl) phosphonate in two lubricants. Using a SAE 20 mineral oil, slow film formation was found but eventually thicker surface films were formed. When the same additive was used in a formulated ester oil, film formation occurred very rapidly. However the final film thicknesses obtained were lower (by a factor of three) than those obtained in the mineral oil tests.

1.3.2 Influence of steel type

The surface of a steel is dependent on the composition of the steel and its metallurgical treatment (e.g. whether case - or through - hardened). As the antiwear additives react with the surface of the steel, it follows that the steel type should affect the performance of the additive.

Rounds (25) used six different steels and one "stellite" in both static and dynamic tests. Using didodecyl phosphonate as additive, the author studied the adsorption of phosphorus on the steel surface. As the chromium content of the steel increased, the adsorption of the phosphonate on the steel surface was found to decrease. Rounds attributed this decreased adsorption to the increasing presence of Cr_2O_3 at the surface. The influence of surface oxide ws further demonstrated by artificially increasing the oxide layer on the steel surface. When the oxide layer of the low chromium steels was increased, greater adsorption of phosphonate occurred.

A comparison of antiwear effects involving different steels was made by Hall (7). Two different steels were used, one with a low chromium content (52100, 1.4% Cr) the other steel having a high chromium content (440C, 17% Cr). Using tricresyl phosphate in a neopentyl ester oil, Hall measured the wear scar diameters under different loads. The high chromium steel gave consistently higher wear scar diameters at the same additive loading than those obtained from the low chromium steel. Hall attributed this decreased antiwear activity as due to the relative passivity of the 440C stainless steel.

1.3.3 Influence of water

Several authors have proposed that some form of hydrolysis of the additive is important if it is to show good antiwear properties. It follows therefore that water may have very considerable influence on the additive performance.

Godfrey (13) obtained comparison wear rates for the lubrication of steel with tricresyl phosphate under different atmospheres. Greater wear took place under nitrogen atmospheres than under room air. Godfrey concluded that either the oxygen or water present in air was important to the antiwear behaviour of tricresyl phosphate.

The effect of water and tricresyl phosphate on the lead corrosivity of an ester oil was investigated by Cottington and Ravner (29). Tricresyl phosphate, as received and after percolation through alumina, was added to a pentaerythritol ester base oil and the rate of weight loss from a lead sample compared. Water was added to the tricresyl phosphate - ester solutions and again the corrosion rates were compared. The authors showed that the 'percolated' tricresyl phosphate gave lower initial corrosion rates than an "as received" sample when water was present.

After 168 hours, however, the authors reported that both samples gave similar corrosion rates. They concluded that the corrosion was due either to the direct effect of acidic impurities preserved in tricresyl phosphate, or as a result of the effect of these impurities on the ester. The products of this latter reaction giving rise to the lead corrosion. The effect of water was to enhance the hydrolysis of the tricresyl phosphate to those acidic impurities present in commercial tricresyl phosphate.

Goldblatt and Appeldoorn (17) used tricresyl phosphate in various lubricants and under different atmospheres. The presence of water was found to be detrimental to the formation of a stable surface film. The effect was most noticeable with aromatic oils. The authors concluded that the presence of water enhanced the hydrolysis of the tricresyl phosphate. However, the surface film formed was less stable in the presence of water or aromatic components. The authors considered that this was probably due to competition for adsorption on the metal surface.

Forbes, Upsdell and Battersby (16) reported a similar detrimental effect of water on the performance of tricresyl phosphate. The authors showed that water when added to the tricresyl phosphate led to greater wear scarring. Water when added to solutions of tricresyl phosphate in the presence of iron powder caused increased hydrolysis to acid phosphates. Both the phosphorus uptake and level of cresols in solution increased with increasing amounts of water. From this, and a comparison of the effect of water on a non-hydrolysable additive (stearic acid) with that obtained for tricresyl phosphate, the authors concluded that the antagonistic effect of water was due to increased hydrolysis of the tricresyl phosphate. This increased hydrolysis gave rise to a large amount of acid phosphates which corroded the metal surface.

Forbes and Battersby (10) conducted similar adsorption/reaction tests with dialkylphosphonates. When water was added to the solutions, the adsorption of phosphorus from solution increased. However the authors reported that phosphonates gave rise to surface films which were less soluble than those formed by dialkylphosphates. They concluded, consequently that a small amount of water was beneficial to the antiwear properties of dialkylphosphonates.

1.3.4 Influence of oxygen

The role of oxygen in the formation of phosphorus antiwear films is unclear. While some research has shown good antiwear effects under conditions of low oxygen, other work has indicated that oxygen is important to the formation of antiwear films.

Rounds (21,25) in studying the antiwear properties of didodecyl phosphonate and tricresyl phosphate, reported that diminished phosphorus levels were found in the surface film when lower oxygen levels were used. It was considered that this was due to a decrease in oxidation of the phosphonate to phosphate. However in an investigation of the effect of various steels, Rounds (25) had reported better surface film formation when the oxide layer was artificially increased.

Godfrey (13) found that in the lubrication of steel by tricresyl phosphate, greater wear rates occurred under a nitrogen atmosphere compared to those obtained under air. Godfrey was unable to determine whether this was due to the presence of oxygen, moisture or both.

Goldblatt and Appledoorn (17) also investigated the lubrication of steel by tricresyl phosphate, this time using solutions of the additive in a base oil. Contrary to the results of Godfrey, the authors recorded lower wear scars when tests were run under dry argon atmospheres than under dry air. The results obtained do not appear to have been conclusive, however. Oxygen was reported to have no effect on the wear rate when dry conditions were used.

Under wet conditions, the authors found that wear decreased with increasing oxygen levels. However the authors had also shown that wear rates were increased in the order dry argon, wet argon, dry air, wet air. Thus the results showed a deleterious affect, if any, of oxygen on the performance of tricresyl phosphate. The authors also tested a number of triphosphates and phosphites, with similar results. In 'wet air' conditions greater wear was observed than under 'dry argon'.

Lindinger (30) agreed with the results obtained by Godfrey (13). Using tricresyl phosphate in an ester base oil, Lindinger found that a wear reducing layer was only formed under oxygen, and not under nitrogen. The surface film also formed under a mixed nitrogen-oxygen atmosphere.

Static oxidation tests were carried out by Forbes and Battersby (10). Tetradecane solutions of dibutyl phosphonate were heated in the presence of iron powder. The oxygen uptake was measured and compared to those for tetradecane with and without iron powder present. The authors concluded that little, if any, phosphonate was oxidised to phosphate. They disagreed with Rounds' claim (21,25) that phosphonate oxidation to phosphate was an important step in the formation of antiwear films.

NASA has sponsored a large amount of work on a synthetic hydrocarbon with a phosphonate antiwear additive. In much of the work (1,31-38) low oxygen levels were used (typically 0.1%), primarily to prevent oxidation of the lubricant at the high temperatures used (200-370°C). Exceptional antiwear properties have been reported for this lubricant package, under deoxygenated conditions and under oxygenated conditions (2,39). The presence of oxygen would appear to be unimportant to the performance of this additive.

1.3.5 The effect of temperature

Temperature, as a parameter of additive performance has had little systematic study. By the very nature of rolling and sliding contact testing, heat is generated as a result of friction. The temperature in the contact zone can therefore be raised considerably above that of the bulk oil temperature.

'Static' immersion tests have often been used to study the reaction between the additive and iron or steel. Most of this work has involved heating the additive or a solution of it in a base oil, in the presence of iron powder.

Rounds (21,25) monitored the surface phosphorus levels on iron powder heated in the presence of tricresyl phosphate and didodecyl phosphate. As the temperature was increased, surface levels of phosphorus were found to rise exponentially.

Increased surface levels of phosphorus at higher temperatures was also reported by Forbes et al (16). Tricresyl phosphate was heated in the presence of iron powder at 50°, 130° and $170^{o}C$. In addition to the increased uptake of phosphorus, the amount of cresols found in the solution at the end of the test was also increased. Forbes and Battersby (10) had shown that heating samples of dibutyl phosphonate with iron gave rise to high surface phosphorus levels. Butanol was also found in the tetradecane solutions after the heating tests.

Godfrey (13) heated tricresyl phosphate in the presence of iron powder and steel rings at $230^{o}C$. The resultant solutions showed increased acidity, and the filtered solids gave positive tests for phosphate. The author reported a "strong odour of phenol".

"Hot wire corrosion tests" have been used by some authors to investigate the effect of heating the additives in the presence of iron. In the tests, an electric current is passed through a wire immersed in the additive under test. Sakurai and Sato (14) and Wiegand and Broszeit (20) used the technique to study the antiwear behaviour of a number of phosphonates, phosphites and phosphates (14) and tricresyl phosphate (20). Both reported the formation of inorganic iron phosphates on the surface of the iron wire. The relevance of these results must be questioned however. At the high temperatures (500°C) used, any film formed is very unlikely to retain an organic nature. Additionally the metallurgy of iron, and in particular the surface chemistry, changes with temperature.

Using bis (nonyl-phenyl) phosphonate in a synthetic hydrocarbon lubricant, Parker and Kannel (1) used an X-ray measuring technique to follow the formation of thick chemical films in a rolling contact at temperatures up to 315°C. Film thicknesses of up to 1000nm have been reported at these temperatures.

Using the same additive, Fowles, Jackson and Murphy (2) also reported the 'growth' of thick films. A film thickness of 125nm was reported when a temperature of 99°C was used. At lower temperatures much lower film thicknesses were reported.

Gentle and Day (40) used the same lubricant package as (1) in an optical EHD lubrication rig. At room temperatures, very little film formation was observed. Higher temperatures were used in a 'mercury squeeze film' technique and thicker films were reported to be formed, increasing in thickness with temperature.

1.4 The 'Thick film' Effect

Until recently, phosphorus antiwear additives were considered to function by the formation of a thin layer on the metal surface. This layer was considered to be only a few nanometres thick. Rounds (19) reported the formation of phosphorus containing surface films some 10 to several hundred molecules in depth. Recent work however, has suggested that under certain cirumstances 'thick' chemical films are formed. The advantages of such a thick film in terms of antiwear performance are obvious.

A high-temperature lubricant has been under development by NASA. The lubricant, termed XRM 177F, is a synthetic paraffinic hydrocarbon containing a single additive, an antiwear additive referred to as "an organophosphonate". This additive is believed to be bis (nonyl phenyl) phosphonate (3). From patents recently published, granted to Mobil Oil Corp. (41,42,43), this would appear to be bis (p-(4-methyl-octyl) phenyl) phosphonate.

This lubricant has been shown to possess very good antiwear properties. (1,2,32,33,35,39,44,45,53). The lubricant has been the subject of a large amount of work, primarily to investigate its suitability as a lubricant for high temperature environments (1,31-36,40, 41,46-49).

Parker and Kannel (1) used an X-ray absorbance method to measure the film thicknesses generated in a rolling contact. Using XRM177F as test lubricant, the authors measured the film thickness at temperatures from 65° to 315°C. Film thicknesses of 500 to 1000 nm thicker than those for the base oil alone, were obtained. The 'growth' of the surface film was found to be dependent on the rate of heating used, indicating that a time dependency existed (49).

A time dependency in the growth of the film was also reported by Fowles, Jackson and Murphy (2). Here the same additive was used, in both a mineral oil and an ester base oil. Film thicknesses of up to 150nm were measured using an optical EHD rig. In this work lower temperatures were used, up to 99°C. At a temperature of 66°C, little film formation was found. The authors concluded that the lower temperatures used were the reason for the lower film thicknesses obtained. Using X-ray microprobe analysis, the authors found high levels of phosphorus in the film built up along the rolling track,

Chiu, Hahn and Rosenberg (50) obtained films 12 to 45 nm thicker for the lubricant alone. These results were obtained using toroidal bearings in an optical EHD rig, at room temperatures.

Gentle and Day similarly used XRM177F in an optical EHD rig (40). At room temperatures, the authors found very little evidence of the additive contributing to the oil film thickness. Using a "mercury squeeze" technique, the authors measured the residual films formed at 27°, 93°, and 149°C. A steel bearing was placed in the test fluid for 30 minutes then lowered into mercury to 'squeeze' the fluid from the bearing until a stable residual film was left. The residual film was determined by measuring the capacitance between the bearing and the mercury. Film thicknesses of 43nm at 93°C and 300nm at 149°C were reported. A residual film was found to form only when the additive was present in the lubricant.

Jones et al (51,52) carried out pressure-viscosity measurements on XRM 177F and on the pure lubricant, and showed that the bulk properties of these two lubricants were very similar.

The observed differences (1,2) in the film thicknesses produced by the two lubricants must therefore arise as a result of a reaction of the additive, and is not a result of, for example, differences in pressure-viscosity coefficients.

Trachman and Cheng (47) measured traction coefficients in EHD line contact studies. Lower traction coefficients were recorded for XRM 177F compared to the base oil, when tested at temperatures of 80° and 105°C. The authors deduced that the additive was giving rise to higher film thicknesses when present in the lubricant. No indication of the increase in film thickness, or as to why these higher film thicknesses occurred, was given.

1.5 Discussion and Conclusions

From the work surveyed, it is clear that there still remains a great deal to be discovered about the role played by antiwear additives in reducing friction and wear in rolling and sliding contacts. Despite a large volume of work having been carried out on organophosphorus antiwear additives over the last 40 years, no clear picture of their function has emerged. Much of this work has been done by researchers within commercial organisations. It would appear that many of these studies, understandably perhaps, have been orientated towards showing that a particular additive will function satisfactorily in the required environment. Determining the exact mechanism has seemed of a lower priority.

The earliest proposal concerning the nature of this surface film, that is the "iron-phosphide eutectic-chemical polishing" theory (6) has now been shown to be a 'non-starter'. Less easily disproved, however, have been the inorganic phosphate films suggested by Godfrey (13) and by others.

Although the presence of organic phosphate films has been frequently reported (4,10 for example) there still remains the evidence of the antiwear properties of phosphoric acid. A number of authors reported that phosphoric acid, when dissolved in oil, gave comparable results to commercial tricresyl phosphate (e.g. 13). Thus it would appear that some measure of inorganic phosphate is present on the surface, and it has been suggested (16) that this is formed as a result of further hydrolysis of the already adsorbed products of the hydrolysis of the neutral additive.

However it is clear that there must be a considerable organic component to the film, not only from the X-ray fluoresence studies of Rounds (19). If complete hydrolysis to phosphoric acid were to occur, then antiwear behaviour would be dependant solely on the rate of hydrolysis. Although this would appear to be so for the aryl phosphates (4), it has not been so demonstrated for the alkyl phosphates (10).

These differences between aryl and alkyl phosphates (8,9,13) and the different trends they show between their rates of hydrolysis and antiwear properties (4,10) serve to illustrate further that adsorption is also important to the antiwear function.

Aryl phosphates are more easily hydrolysed than alkyl phosphates with the same number of carbon atoms, because of the increased stability of the aryloxide ion over the alkoxide ion. However aryl groups are sterically "bulky" compared to straight chain alkyl groups. Thus despite their higher rates of hyrolysis, aryl esters form less stable surface films and do not give as good antiwear properties as an equal carbon alkyl ester.

The surface film must therefore retain a considerable organic nature. If no such organic components were present, short term tests would show increased antiwear properties for aryl esters, whilst in the long term all additives would give similar results.

This lack of a long term 'drift' to similar antiwear properties is also a useful indication that phosphates and phosphites produce different coatings. Although this was proposed by some authors (7,10), others have concluded that they both formed phosphate films (21,24,25). If phosphonates formed a phosphate film, then we might expect to find that phosphonates were similar to, or worse than the corresponding phosphate. In fact, the exact opposite has been shown to be the case (5,7,10).

Thus it seems certain that phosphonates and phosphates react differently with the metal surface, and form different surface films. This may well explain the "exceptional antiwear properties" attributed to the additive used by Fowles et al (2) and by other workers. No such antiwear performance has been reported in work with organophosphates.

The nature of the film formed by this additive would appear to be very different from anything previously reported. The thickness and mechanical strength of the film would appear to indicate a polymeric compound, which would be a radical departure from previous thinking. Barber (26) had shown that iron powder and phosphonates reacted to form a "rubbery solid" of a composition approximately that of Iron (III) mono alkyl phosphonate. However, despite the description of a 'rubbery solid' it was not concluded that the additive led to formation of polymeric compounds.

In conclusion therefore, it seems that organophosphates, phosphites and phosphonates adsorb onto the metal surface and react there, probably by partial hydrolysis, to form an organophosphorus film, which may under extreme conditions hydrolyse further. The oxidation of phosphites and phosphonates is, if it occurs at all, slow and probably of little importance.

The formation of an iron phosphide eutectic at the surface has been effectively disproved by a large number of workers and is no longer of any importance in ascribing the mechanism of formation of the antiwear film.

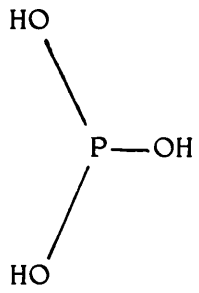
The 'thick' versus 'thin' film argument is not yet sufficiently developed for any true picture to have emerged as to how or why the particular organophosphonate used by Fowles et al (1) gave rise to such 'thick' films. Optical EHD being still a relatively new technique (dating from 1965 (53)), and little film measurement has been carried out at elevated temperatures. It may well be that earlier researchers have been unable to observe that 'thick' chemical film may occur in the rolling contact.

Chapter 2.

Phosphites - Structure and preparative methods

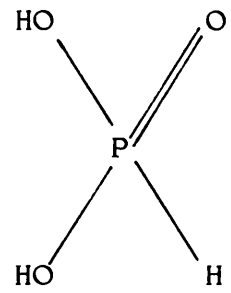
2.1 Structure and Nomenclature

Organo-phosphonates and phosphites are esters of the acid H_3PO_3, usually called phosphorous acid. The name is misleading, however, as the acid exists as the dibasic tautomer phosphonic acid $(HO)_2$ PHO(54,55). The structural formulae of phosphorous acid and phosphonic acid are:-



phosphorous acid

(I)

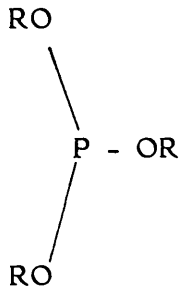


phosphonic acid

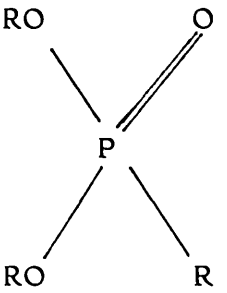
(II)

Mono- and di-substituted esters exist in the form of phosphonic acid (II). They are, therefore correctly called organophosphonates (54-57), however early chemical literature and many lubrication papers (eg 10,19,21) incorrectly refer to them as dialkyl phosphites.

Tri substituted esters and a few metal salts of di-esters exist in the phosphorous form (I). These then are the true 'phosphites' (54). The isomerisation shown can, theoretically at least, occur for all phosphites (55,57), although the rate and temperature required vary greatly. For example, for R=Methyl complete conversion takes place at 200°C in 18 hours, but for R=Butyl the compound is stable to 223°C (57).



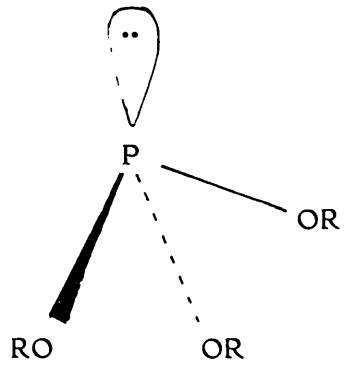
(III)



(IV)

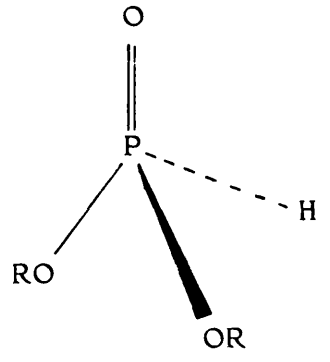
Further confusion arises considering a compound of structure IV. Whilst the parent compound (III) is a phosphite, the product (IV) is a phosphonate and is correctly termed a dialkyl alkyl phosphonate. The rules governing the naming of these and other phosphorus compounds were published jointly by the American Chemical Society and the Chemical Society of London (now the Royal Society of Chemistry) in 1959 (58). Outline forms of these rules are given in several chapters of Corbridge (57). This system of nomenclature is used throughout this thesis.

In terms of structure, a considerable difference exists between phosphites and phosphonates. Phosphites adopt a pyramidal symmetry. In this, phosphorus shows similar behaviour to nitrogen, (the group V element above phosphorus in the periodic table). This structure arises from the sp^3 hybridisation, a lone pair of electrons occupying the fourth "arm" of what may otherwise be considered as a tetrahedron, V.



V

Phosphonates, on the other hand show phosphorus behaving in a manner not found in nitrogen compounds. In phosphonates the 3d orbitals are involved in the orbital hybridisation, although the degree of assistance is not clear (55). Phosphonates possess a true tetrahedral structure, as shown in VI.



VI

These structural differences between phosphites and phosphonates result in considerable differences in their chemical behaviour. Most noticeably is oxidation, trialkyl phosphites being readily oxidised to phosphates (54,55) whereas a very much slower reactivity to oxidising agents is found with phosphonates (54).

2.2 General Preparative Methods

This chapter discusses the methods generally used to prepare phosphonates and phosphites. Details of the specific preparation methods used in this study are given in Chapter 3.

Organophosphonates and phosphites are generally prepared by hydrolysis of phosphorus trichloride with the required alcohol or phenol. The reaction is stepwise, and proceeds with the evolution of hydrogen chloride and formation of the successive alkyl or aryl phosphorochlorides. The series of reactions is shown below (i,ii and iii) (59,60).

i) $PCl_3 + ROH \longrightarrow (RO)\ PCl_2 + HCl$

ii) $(RO)\ PCl_2 + ROH \longrightarrow (RO)_2PCL + HCl$

iii) $(RO)_2\ PCl + ROH \longrightarrow (RO)_3P + HCl$

With most alcohols the major product of this reaction is the disubstituted ester, due to reaction (iv) below (59,60,61)

iv) $(RO)_3P + HCl \longrightarrow (RO)_2\ PHO + RCl$

Further dealkylation is possible in the presence of high concentrations of hydrogen chloride (reactions (v) and (vi)).

v) $(RO)_2\ PHO + HCl \longrightarrow (RO)(OH)PHO + RCl$

vi) $(RO)(OH)PHO + HCl \longrightarrow (HO)_2PHO + RCl$

Limitation of these competitive reactions involves the use of a hydrogen chloride receptor thereby preventing reaction iv from proceeding. With the preparation of aryl phosphites, this dearylation step does not proceed readily, due to the electron displacement of the aryl-oxygen bond (59). Attempts to prepare the trialkyl phosphite in the absence of a hydrogen chloride receptor usually gives rise to the dialkyl phosphonate (59,60).

The reaction is highly exothermic, and many of the preparation methods have used a means of cooling the reaction flask, frequently ice/water baths. Other methods have included controlled evaporation of liquid benzene solvent from under pressure (63). Most workers have used temperatures between 0° and $10^{o}C$. The reaction has been carried out successfully at higher temperatures.

Nearly all the preparative methods reviewed have entailed the use of a solvent. Typically Et_2O, CCl_4, C_6H_6, liquid CH_4 and CH_2Cl_2. The solvent serves to dilute the reactants so moderating the heat rise, and when an amine is used to act as hydrogen chloride receptor, to dilute the contents of the reaction flask to enable stirring to be carried out.

2.3 Synthesis of tri alkyl and aryl phosphites

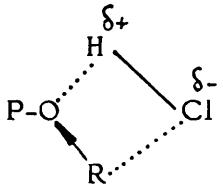
2.3.1 Hydrolysis of PCl_3

This is the general method used for the preparation of tri alkyl or aryl phosphites, as indicated in reaction vii:-

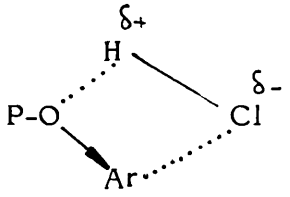
$$PCl_3 + 3ROH + 3 \text{ Base} \longrightarrow (RO)_3P + 3 \text{ Base: HCl} \qquad (vii)$$

The purpose of the base is to act as hydrogen chloride receptor. In the absence of such a base, tri-alkyl phosphites decompose, due to the presence of hydrogen chloride (65). Dealkylation takes place forming the dialkyl phosphonate (reaction iv, section 2.2). Tri aryl phosphites are not so readily dearylated. The aryl group induces a reduced electron density at the oxygen.

The reaction is considered to proceed through a "four centre mechanism" (59,60).



trialkyl



triaryl

In trialkyl phosphites, the nucleophilic attack of Cl on R is stabilized by the small dipole moment R O. In triaryl phosphites this dipole moment is stronger and reversed, thus destabilising the Cl attack on Ar.

Triaryl phosphites have been successfully prepared with no hydrogen chloride receptor (66,67).

Hydrogen receptors used are generally secondary or tertiary amines. Examples of bases used are trialkylamines eg $(C_2H_5)_3N$ (64,68), Pyridine (65), anilines eg $C_6H_5N(CH_3)_2$ (69) and ammonia gas (70,71).

Aqueous extraction of the amine hydrochloride has been used in some preparations as an alternative to filtration (70-73). Thus after completion of the PCl_3 addition, water was added, and the two layers separated.

The organic layer was then dried and distilled. Dilute sodium hydroxide solutions in which the amine hydrochloride is more soluble, have been used instead of water (68).

Most preparative methods have involved addition of the phosphorus trichloride to the solution of alcohol and amine. Trimethyl and triethyl phosphite have been prepared by the addition of the alcohol to $[(CH_3)_2N]_3P$, previously prepared by the reaction of phosphorus trichloride with dimethylamine, $(CH_3)_2NH$ (74,75).

2.3.2 Transesterification

Trialkylphosphites have been prepared by trans-esterification of triarylphosphites with alcohol (76,77). The preparation depends on the equilibria shown in reaction (viii).

$$(ArO)_3P \overset{ROH}{\rightleftharpoons} (ArO)_2POR \overset{ROH}{\rightleftharpoons} (ArO)\ P\ (OR)_2 \overset{ROH}{\rightleftharpoons} P(OR)_3 \qquad \text{(viii)}$$

The equilibrium is moved to the right (ie $P(OR)_3$) by heating and by the use of a catalyst. Catalysts used have included sodium, nickel and $AlCl_3$ (76). Temperatures of 50°C have been used.

The reaction has the advantage in that it enables the preparation of trialkylphosphites in high yield without the risk of dealkylation taking place (reaction iv, section 2.2). Triarylphosphites are more readily prepared than trialkyl phosphites, as triarylphosphites are resistant to dearylation by hydrogen chloride. High yields have been claimed (70%).

2.3.3. Disproportionation

Triphenyl phosphite has been prepared from diphenylphosphonate by disproportionation in the presence of a tertiary amine. The reaction (78) is carried out at room temperature. The reaction is slow, in an example quoted 20 hours at room temperature was required. Diphenyl phosphonate was stirred with pyridine, to give a mixture of 40% $(PhO)_3P$, 19% $(PhO)_2PHO$ and 31% (PhO) P(OH) HO.

Although the reaction avoids the removal of amine hydrochloride, a considerable amount of purification is required.

2.4 Preparation of di alkyl and aryl phosphonates

2.4.1. Hydrolysis of PCl_3

Hydrolysis of phosphorus trichloride by alcohols or phenols is the general preparative method used for di alkyl (or aryl) phosphonates. In its simplest form the reaction is similar to that for the preparation of the tri alkyl phosphites, with the stoichiometry adjusted accordingly.

$$ROH + PCl_3 + 2R'_3N \longrightarrow (RO)_2PCl + 2R'_3N{:}HCl$$

The monochloridite $(RO)_2PCl$ is hydrolysed by the addition of 1 mole equivalent of water to the stirred reaction mixture (60).

$$(RO)_2PCl + H_2O + R'_3N \longrightarrow (RO)_2PHO + R'_3N{:}HCl$$

The reaction has often been carried out in the absence of a hydrogen chloride receptor. Dialkyl phosphonates are less susceptible to dealkylation by hydrogen chloride. Hydrogen chloride being removed by heating or vacuum stripping (79-81).

The susceptibility of trialkyl phosphites to dealkylation by hydrogen chloride has been exploited as a preparative method for dialkylphosphonates. One mole of methyl alcohol is used together with two moles of the required alchohol (80,81,82)

$$2\ ROH + CH_3OH + PCl_3 \rightarrow (RO)_2\ P(OCH_3) + 3\ HCl$$

$$(RO)_2POCH_3 + HCl \rightarrow (RO)_2\ PHO + CH_3Cl$$

Hydrogen chloride and methyl chloride are removed by heating and vacuum stripping.

2.4.2 Transesterification

Dialkyl and diaryl phosphonates of higher alcohols have been prepared by heating 2 moles of the alcohol (or phenol) with diethyl phosphonate (83,84).

$$(C_2H_5O)_2\ PHO \rightarrow (RO)(C_2H_5O)PHO \rightarrow (RO)_2PHO$$

Catalysts have been used to promote the reaction. Catalysts used included phosphoric acid (H_3PO_4) (83) and quaternary ammonium compounds (84).

2.4.3 Disproportionation of $(RO)_3P$

Trialkyl and triaryl phosphites have been used as starting materials for the production of dialkyl phosphonates. The trialkyl (or-aryl) phosphite is refluxed with phosphorous acid, in the molar ratio 2 : 1 to produce the dialkyl phosphonate by a disproportionation reaction (85-88)

$$2(RO)_3P + (HO)_2PHO \rightarrow 3(RO)_2PHO$$

The reaction has been reported as giving yields of 100% of diaryl phosphonates (88)

Again as with the esterification of phosphorous acid (section 2.4.4) this preparative method although "clean" requires the tri substituted ester as feedstock.

2.4.4 Esterification of H_3PO_3

Both dialkyl and diaryl phosphonates have been prepared by esterification of phosphorous acid by the relevant alcohol or phenol (89-92). The reaction produces an equilibrium mixture of the phosphorous acid, alcohol and mono, di and tri substituted esters and water.

$$(HO)_2 + 2ROH \rightleftharpoons (HO)(RO)PHO + ROH + H_2O \rightleftharpoons (RO)_2PHO + 2\ H_2O$$

The equilibrium is forced to the right by the presence of an excess of alcohol or phenol (89-92). Catalysis has been used (89), as has azeotropic removal of water (90-92).

The reaction mixture is refluxed for several hours at 180 - 210°C, although it has been reported that 36 hours is required (89). Excess alcohol is removed by the addition of NaOH to form the olefin (91). The yield has been claimed as 90% (91,92).

Although the reaction has the advantage of being fairly 'clear', a supply of trialkyl phosphite is required.

2.4.5 Miscellaneous methods

Dialkyl phosphonates have been prepared by several other methods.

Heating alkyl halides with phosphorous acid and a tertiary amine gives a dialkyl phosphonate (93).

$$2RX + (HO)_2PHO + 2\ R^1{}_3N \rightarrow (RO)_2PHO + 2R^1{}_3N : HX$$

The reaction is carried out at 80-85°C, in solvent eg toluene. The amine hydrochloride being filtered from the solution. High yields were claimed (90% for $(C_4H_9O)_2PHO$).

On heating disodium phosphite (Na_2HPO_3) with dimethyl sulphate to 85°, an exothermic reaction takes place (94). The temperature rises to 160°C and dimethyl phosphonate is formed in 60% yield.

$$Na_2HPO_3 + (CH_3)_2SO_4 \rightarrow (CH_3O)_2PHO$$

The method is only claimed for dimethyl sulphate. Sulphates of higher alcohols are less ionic, and it would appear unlikely for the reaction to proceed effectively for other alcohols.

Phosphorus trioxide (P_4O_6) reacts readily with water to form phosphorous acid (95). This reaction has been used to produce dialkyl phosphonates (96).

$$P_4O_6 + 8ROH \rightarrow 4(RO)_2PHO + 2H_2O$$

The reaction was carried out at 120-220°C in an organic solvent that forms an azeotrope with water. The analagous reaction with water is a complex one. In hot water the reaction produces phosphoric acid, phosphine and red phosphorus (95). Additionally phosphorus trioxide is highly reactive and toxic which would cause handling and purity problems.

2.5 Preparation of monoalkyl and aryl phosphonates

2.5.1 Hydrolysis of PCl_3

Phosphorus trichloride, if hydrolysed with one mole of the alcohol of phenol, produces (mainly) the mono-alkyl dichlorophosphite $ROPCl_2$ (66). Further hydrolysis of the dichlorophosphite by water or methyl alcohol yields the monoalkyl phosphonate (97).

$$PCl_3 + ROH \longrightarrow RO\ P\ Cl_2 + HCl$$

$$ROPCl_2 + 2CH_3OH \longrightarrow ROP(OCH_3)_2 + 2HCl \longrightarrow ROP(OH)HO + 2CH_3Cl$$

None of the published methods report the use of a hydrogen chloride receptor such as a tertiary amine. The absence of the tertiary amine aids the dealkylation of the phosphite initially formed in the hydrolysis of the dichlorophosphite with methyl alcohol.

The dealkylation is further aided by heating the reaction mixture in a sealed tube (97). Mono alkyl phosphonates have also been prepared by hydrolysis of dichlorophosphonic acid $HP(O)Cl_2$. The chloro-phosphonic acid was refluxed with one mole of the required alcohol and one mole of a lower alcohol, such as methyl alcohol (98).

$$HP(O)Cl_2 + ROH + CH_3OH \longrightarrow HP(O)(OR)(OCH_3) \longrightarrow HP(O)(OR)(OH) + CH_3Cl$$

2.5.2 Disproportionation of $(RO)_3P$

Mono alkyl phosphonates have been prepared by disproportionation of the triphosphite and phosphorous acid.

$$(RO)_3P + 2H_3PO_3 \longrightarrow 3(RO)(OH)PHO$$

The acid and phosphite are heated together in the molar ratio 2:1 for several hours to yield the mono substituted ester (85,86,99). The reaction has been carried out in CCl_4 as solvent and with a tertiary amine present to move the position of equilibrium towards the mono phosphonate (99).

Mono alkyl or aryl phosphonates have also been prepared by disproportionation of the di substituted ester and phosphorous acid in equimolar quantities (85,86).

2.5.3 Alkaline hydrolysis of $(RO)_2PHO$

Dialkyl or aryl phosphonates are hydrolysed under alkaline conditions to form the sodium mono alkyl phosphonate (RO)P(ONa)HO (100,101).

$$(RO)_2\ PHO + NaOH \longrightarrow (RO)P(ONa)HO + ROH$$

The reaction was carried out in a 1 : 1 mixture of water and ethanol as solvent. The mixture refluxed for several hours, and the solvent then removed by vacuum distillation.

The sodium salt is converted to the monoalkyl phosphonate by passing hydrogen chloride through a suspension of the salt in toluene.

Chapter 3.

The Preparation and Purification of the Esters

3.1. Preparation

The phosphonates and phosphites used in this work were prepared and purified in the laboratory using standard preparatory methods.

3.1.1 Introduction

Phosphorus trichloride, in diethyl ether solution was hydrolysed by dropwise addition to 3 equivalents of the relevant alcohol or phenol, together with 3 equivalents of triethylamine dissolved in diethyl ether. Diesters were prepared by the replacement of one mole of the alcohol by one mole of water. This water was added to the reaction mixture after the phosphorus trichloride had been added to the two moles of the alcohol. Attempts to produce monophosphonates by a similar reaction were unsuccessful and alternative methods of preparation were used.

3.1.2 Apparatus

The apparatus used for the production of the phosphates and phosphites was made entirely of glass, and is illustrated in figure 3.1. It consisted of a 2000 cm^3 round bottom flat flange reaction vessel with a five port lid. Into the sockets of this lid were fitted a condenser, a pressure equalising dropping funnel (250cm3), a thermometer and a stirrer guide.

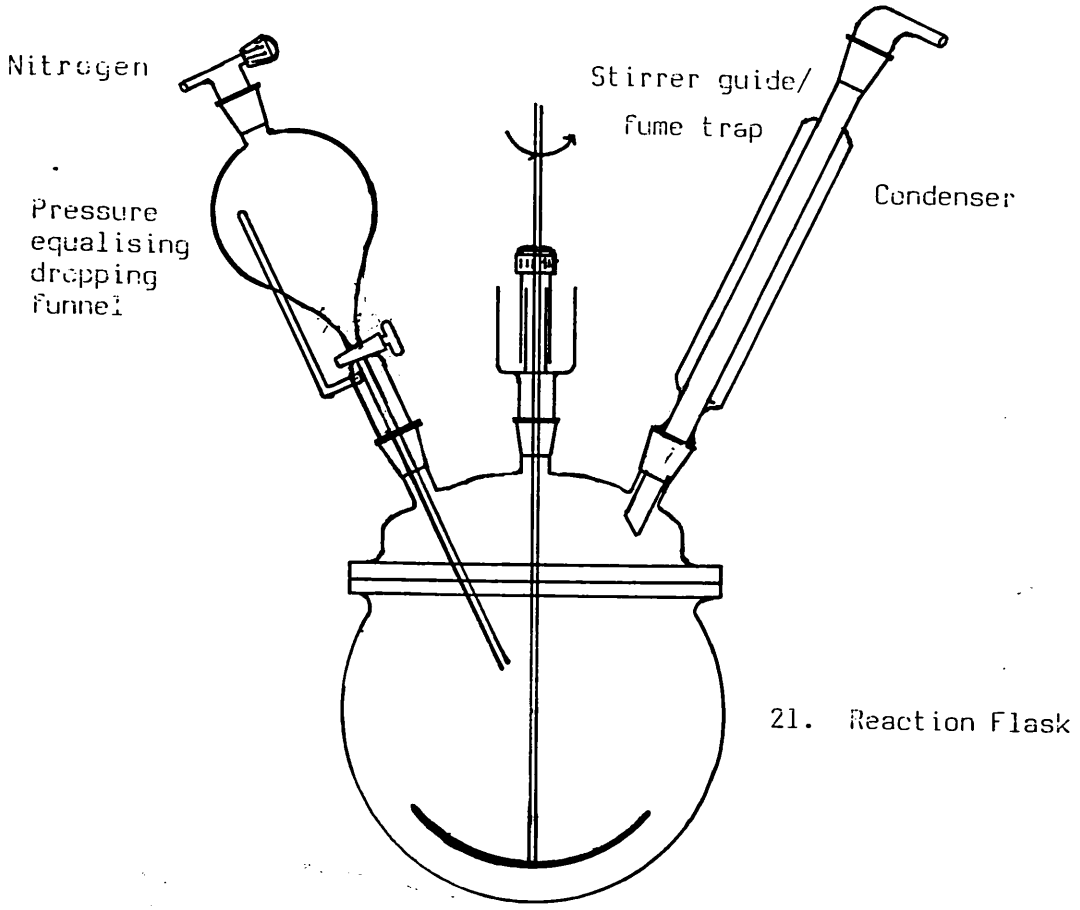


Figure 3.1 Preparation Apparatus

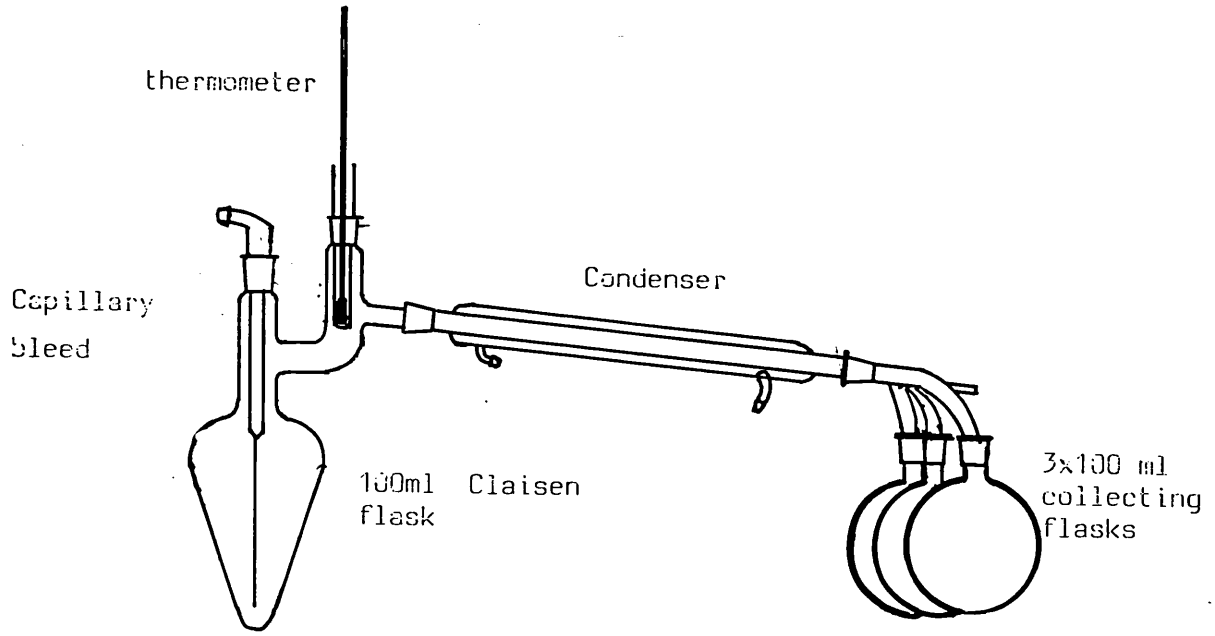


Figure 3.2 Distillation Apparatus

The fifth port was not used and was sealed with a ground glass stopper. To effect a better seal the ground glass joints (with the exception of the stirrer guide) were lightly coated with a silicone grease (LX-51, ICI Ltd). The stirrer guide maintained an effective seal by nature of its design. It consisted of two glass tubes concentrically arranged, the inner tube terminating at its lower end in a ground glass cone joint, whilst the outer tube terminated (at its upper end) in a PTFE "screw" joint for attachment to the stirrer rod. As the stirrer rod rotated, the outer tube rotated around the inner tube which acted as a guide tube. Sealing was effected by the two tubes having been ground to a 'close fit'. Liquid paraffin was placed betwwen the two tubes to act as a seal and lubricant.

Stirring of the reaction mixture was achieved using a glass "anchor" stirrer, passed through the stirrer guide/fume trap and driven by a variable speed electric motor.

A "pressure equalising" dropping funnel was used to deliver the phosphorus trichloride solution to the reaction flask. The delivery pipe was specially lengthened by about 10 cm to enable the phosphorus trichloride solution to drop directly into the centre of the reaction mixture. It was found that when the phosphorus trichloride solution was allowed to run down the side wall, a "crystalline mass" accumulated which trapped unreacted phosphorus trichloride, thereby reducing the yield.

Nitrogen was passed through the apparatus from the top of the dropping funnel, through the side arm of the dropping funnel into the reaction flask. Venting of the reactor was achieved through the condenser attached to the reaction flask.

After filtration and solvent evaporation, distillation of the reaction mixture was carried out. The distillation apparatus used was as shown in figure 3.2.

For distillations of a larger volume than the capacity of the 100ml Claisen flask would allow, a 500ml round bottom flask fitted with a 'Claisen' head was used. Reduced pressure was obtained by using a rotary vacuum pump. Measurements of the vacuum were obtained with a 'Macleod' type vacuum guage.

3.1.3 Preparation of trihexyl phosphite

Trihexyl phosphonate was prepared, in the laboratory, by hydrolysis of phosphorus trichloride by 3 mole equivalents of hexan-1-ol (n - hexanol), in the presence of 3 equivalents of triethylamine.

$$PCl_3 + 3C_6H_{13}OH + 3(C_2H_5)_3N \rightarrow (C_6H_{13}O)_3P + 3(C_2H_5)_3N : HCl$$

Phosphorus trichloride (45.8g, 1/3 mole) in 50 cm^3 anhydrous diethyl ether, was added to a solution of hexan-1-ol (102.0g 1 mole) and triethylamine (101.0g, 1 mole) in diethyl ether (200 cm^3), cooled to 5^oC using an ice-water bath. The mixture was vigourously stirred under a nitrogen blanket.

The addition of the phosphorus trichloride was completed in about 4 hours. The cooling bath was then removed and the mixture left stirring overnight at room temperature to allow further precipitation of triethylamine hydrochloride. Rapid vacuum filtration was then carried out using a sintered glass funnel, the residue being washed with 50 to 100 cm^3 of diethyl ether.

The solvent was removed from the collected filtrate by gently warming the flask and contents with an electric heating mantle.

The produce was distilled twice, under a high vacuum (typically 3mm Hg or less). Trihexyl phosphite $(C_6H_{13}O)_3P$ was distilled at 154.5°C/1.8mm yield = 32.7g (32.1%).

Triethyl phosphite $(C_2H_5O)_3P$, triphenyl phosphite $(C_6H_5O)_3P$ and tris (4-tert. Octyl Phenyl) phosphite were similarly prepared.

$(C_2H_5O)_3P$ b.pt. 38°C/1.0mm
$(C_6H_5O)_3P$ b.pt. 180°C/1.0mm
$(C_8H_{17}C_6H_4O)_3P$ m.pt. 70°C, b.pt 125/1.0mm

3.1.4 Preparation of dihexyl phosphonate

Preparation of dihexyl phosphonate, $(C_6H_{13}O)_2$ PHO was carried out in the laboratory by hydrolysing phosphorus trichloride with 2 equivalent of hexan-1-ol (n-hexanol) in the presence of triethylamine. The resultant dialkyl chlorophosphite was further hydrolysed to yield dihexyl phosphonate.

$$PCl_3 + 2C_6H_{13}OH + 2(C_2H_5)_3N \longrightarrow (C_6H_{13}O)_2\ PHO + 2(C_2H_5N)_3\ N : HCl$$

$$(C_6H_{13}O)_2\ PCl + H_2O + (C_2H_5)_3N \longrightarrow (C_6H_{13}O)_2\ PHO + (C_2H_5)_3\ N : HCl$$

Phosphorus trichloride solution (45.8g, 1/3 mole in 50cm^3 diethyl ether), was added slowly to 68g (2/3 mole), hexan-1-ol and 101g (1 mole) triethylamine dissolved in 200 cm^3 diethyl ether, cooled, using an ice-water bath, to 5°C.

The mixture was vigorously stirred and a nitrogen blanket was kept above the mixture during the addition of phosphorus trichloride.

The addition of phosphorus trichloride was completed in approximately 3.5 hours. The ice-water bath was removed on completion of the phosphorus trichloride addition, and the mixture stirred at room temperature for at least 3 hours to allow equilibration of the reaction mixture. After this time the ice-water bath was replaced and the mixture cooled to $5^{o}C$, and 6g (1/3 mole) of water added very slowly from the dropping funnel. When this addition was completed (1 hour), the mixture was again allowed to warm to room temperature, and left stirring overnight.

The reaction mixture was rapidly vacuum filtered, and the solvent evaporated by gentle heating. The reaction product was distilled twice, under a high vacuum.

Dihexyl phosphonate $(C_6H_{13}O)_2$ PHO was distilled at $118^{o}C$/1.0mm Hg, yield 44%.

Preparation of dihexyl phosphonate in larger quantities was accomplished using a 2l. reaction vessel and reactant weights increased by a factor of 5 throughout.

Similarly prepared were diethyl phosphonate $(C_2H_5O)_2PHO$, dioctyl phosphonate $(C_8H_{17}O)_2PHO$, didodecyl phosphonate $(C_{12}H_{25}O)_2$ PHO, diphenyl phosphonate $(C_6H_5O)_2PHO$ and bis (4 tert Octyl phenyl) phosphonate $(4\text{-}C_8H_{17}C_6H_4O)_2PHO$.

$(C_2H_5O)_2PHO$ b.pt. 37°C / 0.8mm Hg

$(C_8H_{17}O)_2PHO$ b.pt. 170° / 0.5mm Hg

$(C_{12}H_{25}O)_2PHO$ b.pt. 165° / 0.3mm Hg

$(C_6H_5O)_2PHO$ b.pt. 102° / 0.3mm Hg

$(C_8H_{17}.C_6H_4O)_2$ PHO m.pt. - 10°C

3.1.5 Preparation of monophenyl phosphonate

The preparation of monophenyl phosphonate $(C_6H_5O)(OH)PHO$ was attempted in the laboratory using 3 different preparative methods. These preparations were largely unsuccessful, mainly due to the difficulties of purification of the reaction mixture. This can be a complex mixture of the mono-, di- and tri- esters with phenol and phosphorous acid depending on the preparative method used. Very low yields were obtained with all the methods used.

The first method to be used, was the hydrolysis of phosphorus trichloride by one mole equivalent of phenol, and two mole equivalents of water in the presence of triethylamine.

$$C_6H_5OH + PCl_3 + (C_2H_5)_3N \longrightarrow (C_6H_5O)PCl_2 + (C_2H_5)_3N : HCl$$

$$(C_6H_5O)PCl_2 + 2H_2O + 2(C_2H_5)_3N \longrightarrow (C_6H_5O)(OH)PHO + 2(C_2H_5)_3N : HCl$$

Phosphorus trichloride (45.8g) in $50cm^3$ diethyl ether was added slowly (over the course of 3 hours) to a mixture of phenol (31.3g, 1/3 mole) and triethylamine (101g, 1 mole) dissolved in $200cm^3$ diethyl ether and cooled, with the aid of an ice-water bath, to 5°-10°C. After the addition of phosphorus trichloride was completed, the cooling bath was removed and the mixture allowed to warm, with stirring, to room temperature.

The cooling bath was replaced and 12g of water (2/3 mole) was slowly added to the mixture (over 1 hour). The mixture was allowed to stand at room temperature (with stirring) overnight.

The reaction mixture was filtered using a sintered glass filter funnel to yield a colourless liquid, from which the diethyl ether solvent was evaporated by gently warming.

After solvent evaporation, only a small liquid volume ($10cm^3$) remained, which on being allowed to stand for 4 weeks separated into two layers, the top layer of which, some 80% of the total volume, had crystallised out, and was separated by filtration.

In view of the low yield an alternative method was then used.

The second preparative method used was that used by Michalski (101). This method involved the alkaline hydrolysis of the diester.

$$(C_6H_5O)_2PHO + NaOH \rightarrow (C_6H_5O)(ONa)PHO + C_6H_5OH$$

$$(C_6H_5O)(ONa)PHO + HCl \rightarrow (C_6H_5O)(OH)PHO + NaCl$$

Diphenyl phosphonate (234g, 1 mole) was placed in a 500 cm^3 flask, water was slowly added (1 hour). The temperature of the flask contents rose rapidly and a water bath was used to aid cooling.

After the addition of the sodium hydroxide, the cooling bath was exchanged for a heating mantle and the mixture refluxed at 102^oC for 1 hour.

Hydrochloric acid (36.5g HCl in 60 cm^3 water) was added slowly with stirring. The reaction mixture separated to two layers, (lower layer aqueous) the pH of each layer was recorded as pH1

Separation of the organic layer and solvent layer and solvent extraction with iso Butanol followed by distillation yielded only a distillate of phenol.

It is considered that monophenylphosphonate hydrolysed under the conditions used to phosphorous and phenol.

A third method of preparation was then used. This method involved a disproportionation of diphenyl phosphonate acid after Chadwick and Reetz (68).

$(C_6H_5O)_2PHO + H_3PO_3 \longrightarrow 2(RO)(OH)PHO$

Diphenyl phosphonate (234g, 1 mole) and phosphorous acid (82g, 1 mole) were placed in a 500 cm^3 flask, fitted with a stirrer and thermometer. Heating was applied to the flask to melt the phosphorous acid. At a temperature of 60°C the two layers merge. The reaction mixture was held at a temperature of 60 - 70°C for 65 hours during which time the colour changes to yellow/amber.

A sample ($2cm^3$) of the product was extracted with water ($20cm^3$) and the resultant cloudy liquid centrifuged. This gave a clear aqueous layer and lower brown oil layer (diphenylphosphonate). Extraction of the aqueous layer with chloroform gave off-white crystals which by infrared analysis was phenol. Evaporation of the aqueous layer gave a crystalline product insoluble in $CHCl_3$, which was considered to be phosphorous acid.

Distillation under high vacuum proved unsuccessful due to thermal decomposition of the product at 145°C. No distillate was obtained at up to 145° / 0.8mm.

3.2 Practical Observations

3.2.1 Heats of reaction

The hydrolysis of phosphorus trichloride by an alcohol is an exothermic reaction. The degree of exothermicity decreases with the length of the carbon chain of the alcohol used. Thus the most vigorous hydrolysis reactions were those involving ethanol as parent alcohol. The hydrolysis of phosphorus trichloride by an alcohol or phenol was found to be in the following order of decreasing violence

ethyl $\gg$ hexyl $>$ phenyl $>$ octyl $>$ dodecyl $\simeq$ octyphenyl

The hydrolysis of the monochlorophosphite [$(RO)_2PCl$] by water was likewise found to be in the above order of decreasing exothermicity.

3.2.2 Effect of temperature

When a hydrogen chloride receptor such as triethylamine is used, the reaction mixture became very viscous due to the precipitation of the hydrochloride as the reaction proceeds. To maintain mobility of the mixture a solvent such as diethyl ether was used. Thus to limit evaporation of the solvent, cooling to 5°C by means of ice-water bath was used. This allowed a faster rate of addition of the phosphorus trichloride solution.

However it was found that when the reaction was kept stirring overnight at 5°C, the precipitation of the triethylamine hydrochloride was slightly inhibited. On warming the mixture after filtration, further precipitation occurred.

3.2.3 Solvent

As stated in section 3.2.1 solvent is necessary to maintain mobility of the reaction mixture. In addition to this, it was found that dilution of the phosphorus trichloride by solvent before addition to the reaction mixture serves to moderate the reaction. Less phosphorus trichloride is added to the flask with each dropwise addition, and a constant rate of delivery of phosphorus trichloride can be obtained.

3.2.4 Distillation

Distillation was used to purify the prepared esters, and difficulties occasionally arose with this purification method. The distillations of the phosphites and phosphates were hampered by a thermal breakdown of the product if the distillation flask became too hot. This thermal breakdown is most apparent with the aryl phosphites and phosphonates.

At high temperatures, under high vacuum, a deep orange colour appeared in the distillation flask and distillation of the product ceased. For diphenyl phosphonate this temperature was 135°C. Subsequently the flask contents could be heated in excess of 215°C with no further distillation taking place, the flask contents then became a deeper orange in colour. A similar breakdown was found to occur with triphenyl phosphite (at temperatures greater than 170°C) and with dihexyl phosphonate (at temperatures greater than 140°C).

On cooling, the flask contents were found to contain a solid, orange in colour, dispersed in the liquid. Analysis of the solid by elemental microanalysis showed it to be of high (50-60%) phosphorus content. The colouration observed is obviously therefore due to a breakdown of the crude product, probably by loss of the organic portions of the molecule. This breakdown was not investigated further.

3.3. Conclusions

From the work detailed in this chapter the following organophosphorus esters were prepared for further study.

diethyl phosphonate,	$(C_2H_5O)_2PHO$
dihexyl phosphonate,	$(C_6H_{13}O)_2PHO$
dioctyl phosphonate,	$(C_8H_{17}O)_2PHO$
didodecyl phosphonate,	$(C_{12}H_{25}O)_2$
diphenyl phosphonate,	$(C_6H_5O)_2PHO$
bis Octyl phenyl phosphonate,	$(C_8H_{17}.C_6H_4O)_2PHO$
triethyl phosphite	$(C_2H_5O)_3P$
trihexyl phosphite	$(C_6H_{13}O)_3P$
triphenyl phosphite	$(C_6H_5O)_3P$
tris octylphenyl phosphite	$(C_8H_{17}.C_6H_4O)_3P$

Chapter 4.

Characterisation of the Phosphorus Esters

Characterisation of the phosphorus esters, both "bought in" and those prepared in the laboratory, involved mainly two methods of analysis, although other methods were used to a lesser extent.

Characterisation was chiefly obtained by recording the infrared adsorption spectra and ^{31}P n.m.r. (nuclear magnetic resonance) spectra for the esters. In addition mass spectroscopic and elemental microanalysis techniques were used for the dihexyl phosphonate.

4.1 Infrared absorption spectra

Organophosphorus esters are particularly amenable to infrared spectrophotometric analysis due to the strong absorptions in the infrared region shown by the bonds between phosphorus and other atoms.

Absorptions in the infrared region of the electromagnetic spectrum, arise from vibrations of the molecular bonds. Thus the infrared spectrum provides information on the strength and nature of bonding in the molecule. Briefly stated the frequency of vibration of a bond is a function of the masses of the elements bonded together and the strength, and therefore type, of bonding between them. The vibrational frequencies of these groups are largely independent of the other atoms or groups present in the molecule. Thus an assignment of the absorptions present in the infrared spectrum to groups known or considered to be present can be made.

4.1.1 Introduction

In the infrared spectra of organophosphorus esters, several characteristic absorption bands are commonly present. The characteristic absorbances, often termed group frequencies, arise from the bonds of phosphorus to several atoms or groups commonly present in these esters. These group frequencies include the phosphoryl bond (P = O), phosphorus-oxygen-carbon bonds (P-O-C), phosphorus-hydrogen (P-H) and phosphorus-hydroxyl bonds (P-OH). In addition the spectra show absorbances due to the hydrocarbon portion of the molecule, and due to hydrogen bonding. Table 4.1 tabulates the frequencies reported in the literature for absorptions present in the infrared spectra of organophosphorus esters.

Two vibrational frequencies are listed for the P-O-C vibrations. These are variously described as the symmetrical and asymetrical stretching frequencies, or as the (P)-O-C and P-O-(C) stretching frequencies (104). Some confusion exists as to which absorption is due to which of these vibrations, and to what the correct descriptions of these vibrations are. Bellamy (102) and Thomas (105) assign the higher vibration frequency to the P-O-(C) vibration, and the lower frequency to the (P)-O-C vibration. The description P-O-(C) represents the stretching of the phosphorus-oxygen bond, and similarly (P)-O-C the stretching of the carbon-oxygen bond in the P-O-C group.

Hydrogen bonding, present in esters of the phosphonate structure (107, 108) is shown by a strong broad absorption at $\sim$ 3500 cm^{-1} (107).

Table 4.1

Literature Values for the Infrared Absorptions of Organophosphorus Esters

Vibration	(cm^{-1}) ref. 102	ref. 103	ref. 104	ref. 105	ref. 106	ref. 107
P = O	1350 - 1250	1250	1280 - 1250	-	-	-
P-O-C (aromatic)	1240 - 1190	1250 - 1165	-	1242 - 1110	1240 - 1190	-
	995 - 850	1055 - 870	-	996 - 905	-	-
P-O-C (aliphatic)	1150	1110 - 1000	-	1170 - 1105	-	-
	1050 - 990	1000 - 870	-	1041 - 987	1050 - 980	-
P-O-H	2700 - 2560	2630,2220,1665	-	-	-	2725 - 2525 2350 - 2150 1700 - 1600
P-H	2457 - 2270	2500 - 2300	-	-	2440 - 2280	-

4.1.2 Equipment

Two spectrometers were used to record the infrared spectra obtained. The majority of the spectra were recorded using a Perkin Elmer 599B spectrometer. For a few of the variable temperature infrared spectra, a Perkin Elmer 580B spectrometer was used.

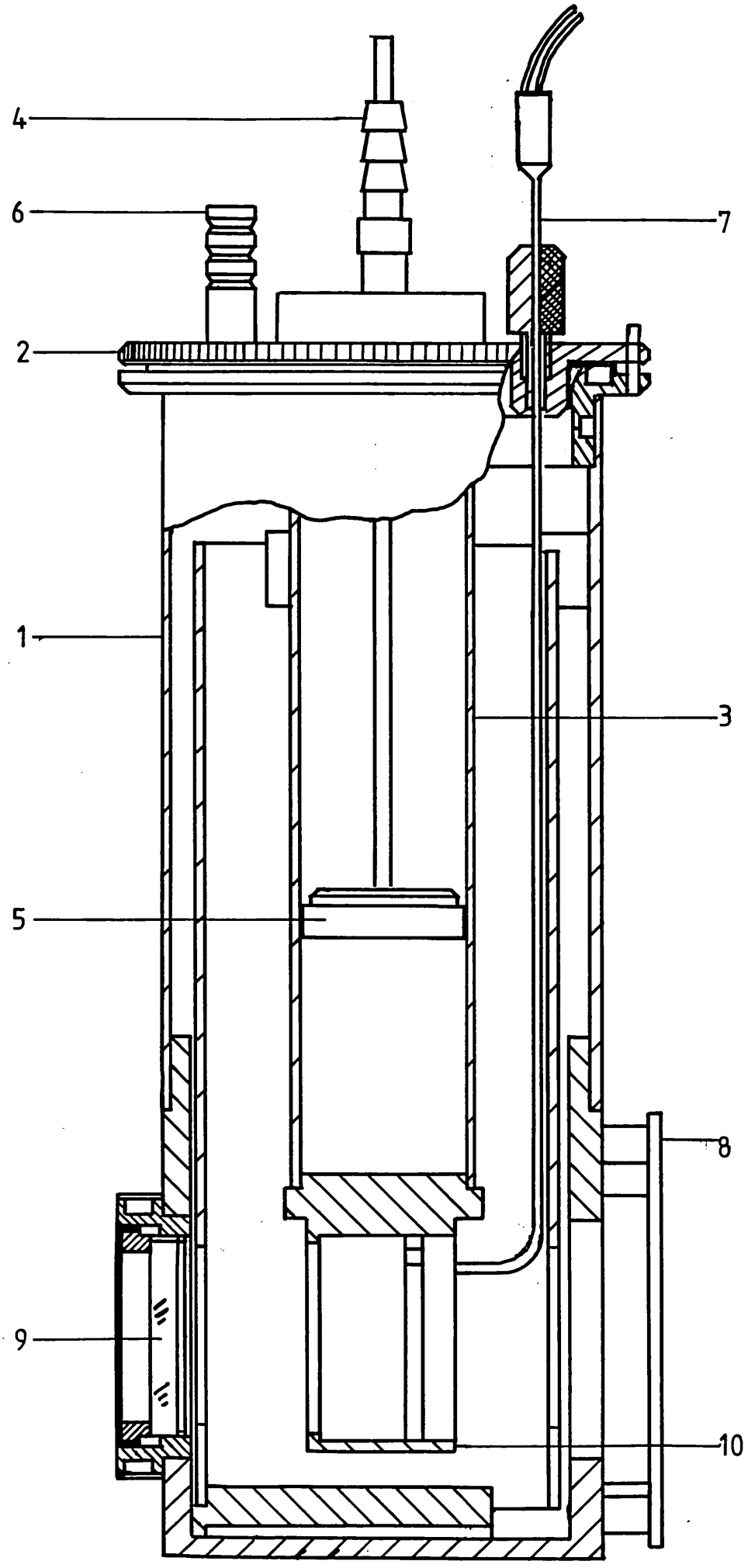
The spectrometers are optically similar both being capable of scanning the infrared spectrum for 4000 to 200 cm^{-1}. The data obtained is handled differently by the two specrometers. The 599B prints out the spectrum as the spectral range is scanned, and although this 'conventional' recording method is available on the PE580B, it was not used. Instead an attached data station was employed to process the spectral data before printing the spectra. The data station can be used to "clean-up" a spectrum by recording the digital signal from the spectrometer. This recorded signal could be amplified, smoothed and processed so as to improve the signal to noise ratio. This technique is especially useful for examining 'weak' spectra or for weak absorptions in an otherwise 'good' spectra.

Variable temperature infrared studies were made using a 'Specac' 21000 variable temperature infrared unit. The unit consists of a heated cell and a thermostatically operated heating control unit. The cell, shown in figure 4.1 is enclosed within an outer chamber which can be sealed and evacuated to limit heat losses from the sample. Sodium chloride windows are fitted to this outer chamber. The sample is placed between the two potassium bromide (KBr) or silver chloride (AgCl) plates of the sample cell before assembly, or by injection through the port of the sample cell.

Fig. 4.1 Variable temperature infrared cell (over)

Key to parts

1. Outer jacket
2. Top plate
3. Refrigerant chamber
4. Regrigerant chamber vent
5. Refrigerant 'mushroom'
6. Evacuation port
7. Thermocouple
8. Mounting plate
9. Outer (NaCl) windows
10. Sample holder


4
6
7
2
1
3
5
8
9
10

Heating of the cell is by means of two electrically heated plates on the sides of the sample holder. These heaters are thermostatically controlled by the heating controller. The controller permits heating of the sample cell from ambient temperatures to 225°C. The power output can be adjusted so as to minimise "overshooting" of the temperature.

4.1.3 Technique

Infrared spectra of the liquid organophosphorus esters and other liquid compounds were recorded as thin liquid films between two sodium chloride (NaCl), potassium bromide (KBr) or silver chloride (AgCl) plates.

The thickness of the liquid film was controlled by placing gaskets of PTFE between the two plates. Film thicknesses of 0.025 and 0.05mm were generally used. Frequently films thinner than 0.025mm (the thinnest gasket available) were required, in order to attenuate the absorption to within the absorbance range of the spectrometer. These were obtained by using the "capillary film" technique, as follows.

A small drop of the sample liquid was placed on one of the pair of plates. The second plate was placed directly upon the lower plate and the two gently squeezed together, by gripping the edges, to spread the sample uniformly between the two plates. The two plates were then clamped in the sample holder before fitting in the spectrometer.

Using the commonly used "interference fringe" method for determination of infrared cell path lengths (109), this capillary film was estimated to be approximately 0.01 mm in thickness.

Sample cells in which a gasket had been fitted were filled through a hole drilled through the front plate which was aligned with a "Luer" type syringe fitting in the cell holder. Liquid samples were injected into the cell, using a hypodermic syringe, care being taken to ensure that no air bubbles were 'trapped' in the cell.

Solid samples were analysed either as solutions in a suitable solvent (eg chloroform or benzene) in which case they were placed in the sample cell in the same way as the liquid samples above. Alternatively a 'nujol' mull of the sample was prepared.

'Nujol' is a high molecular weight liquid paraffin which in its infrared spectrum shows only the absorption bands associated with C-H and C-C bonds. The sample to be analysed was first prepared by dry grinding a small quantity ($\sim$ 50mg) in an agate mortar. When sufficiently fine, a small drop of "Nujol" was added and the sample ground further to disperse the sample through the 'Nujol'. The mull, once prepared was transferred to one of the infrared plates. This was most easily done by using one half of a double edged razor blade. The mull was transferred by flexing the razor blade to a concave shape and using this to remove the sample from the pestle and mortar. Flexing the blade into a convex shape allowed transfer of the mull onto the plate. The sample cell was then assembled in the same way as when preparing capillary liquid films, as outlined above.

The variable temperature infrared spectra were recorded by injecting the samples into the cell, and then running a spectrum at 25°C. The temperature was then increased in steps of 25°C to a temperature of 200° or 225°C.

Once the temperature controller indicated that the required temperature had been reached, the cell was allowed to reach equilibrium for five minutes before the spectrum was recorded. Variable temperature infrared spectra were recorded for samples of dihexyl phosphonate and diphenylphosphonate.

4.1.4 Infrared Spectra

The infrared spectra of several organophosphites and organophosphonates were recorded. Qualitative and quantitative assessments were made of the spectra obtained. Examples of the spectra are shown in figures 4.2 to 4.12.

Figures 4.2 to 4.8 show spectra recorded for dialkyl and diaryl phosphonates. Examples of the infrared spectra recorded for trialkyl and triaryl phosphites are shown in figure 4.9 to 4.12.

The values of the phosphorus group frequencies as determined from these spectra are tabulated in tables 4.2 (diesters) and 4.3 (triesters). It can be seen both from the spectra and from the tabulated group frequencies, that little change in the infrared spectrum occurs with a change of the organic group. It will also be seen that good agreement was obtained between the values obtained for the group frequencies and the literature values tabulated in table 4.1.

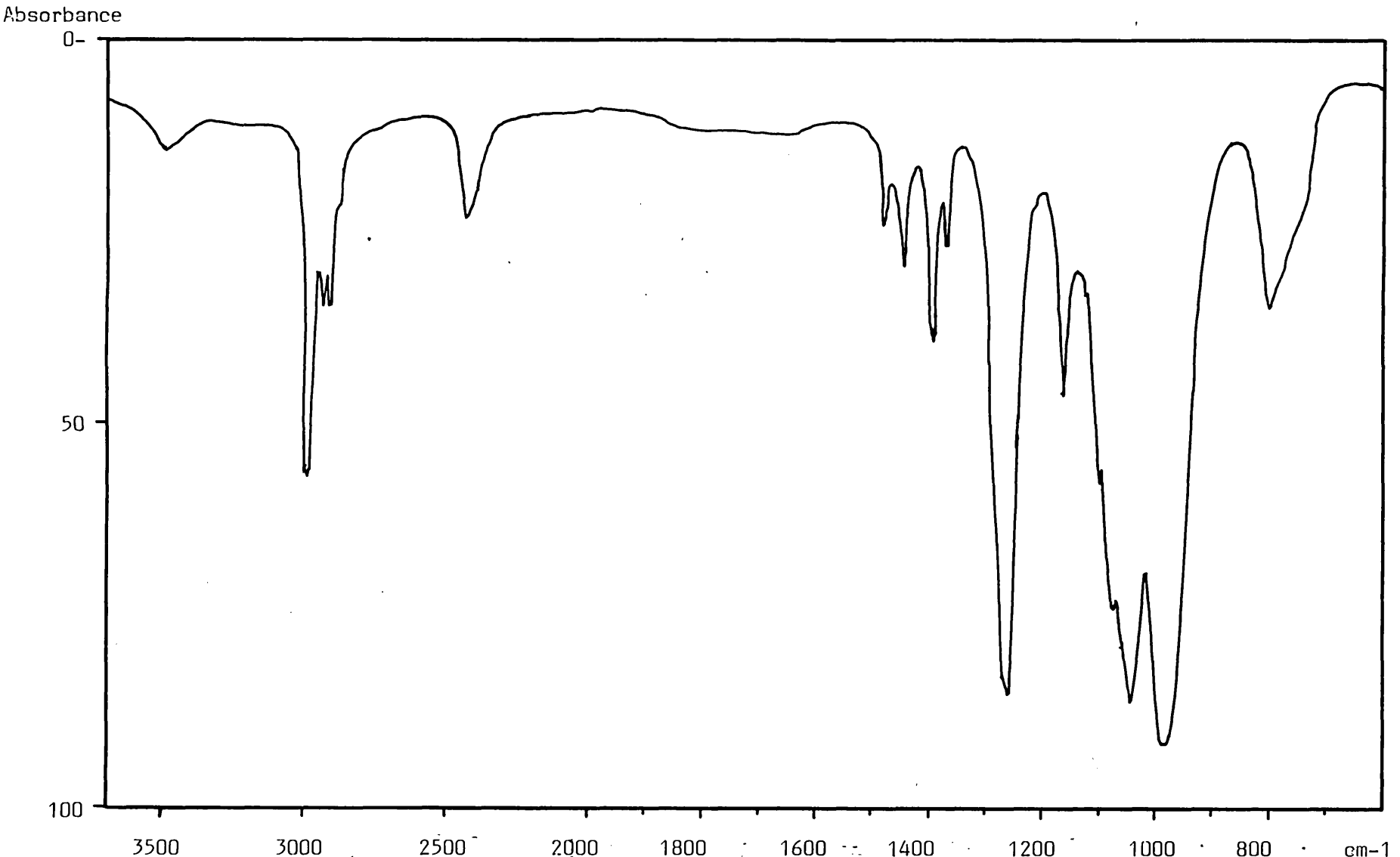


Figure 4.2 Infrared diethyl phosphonate

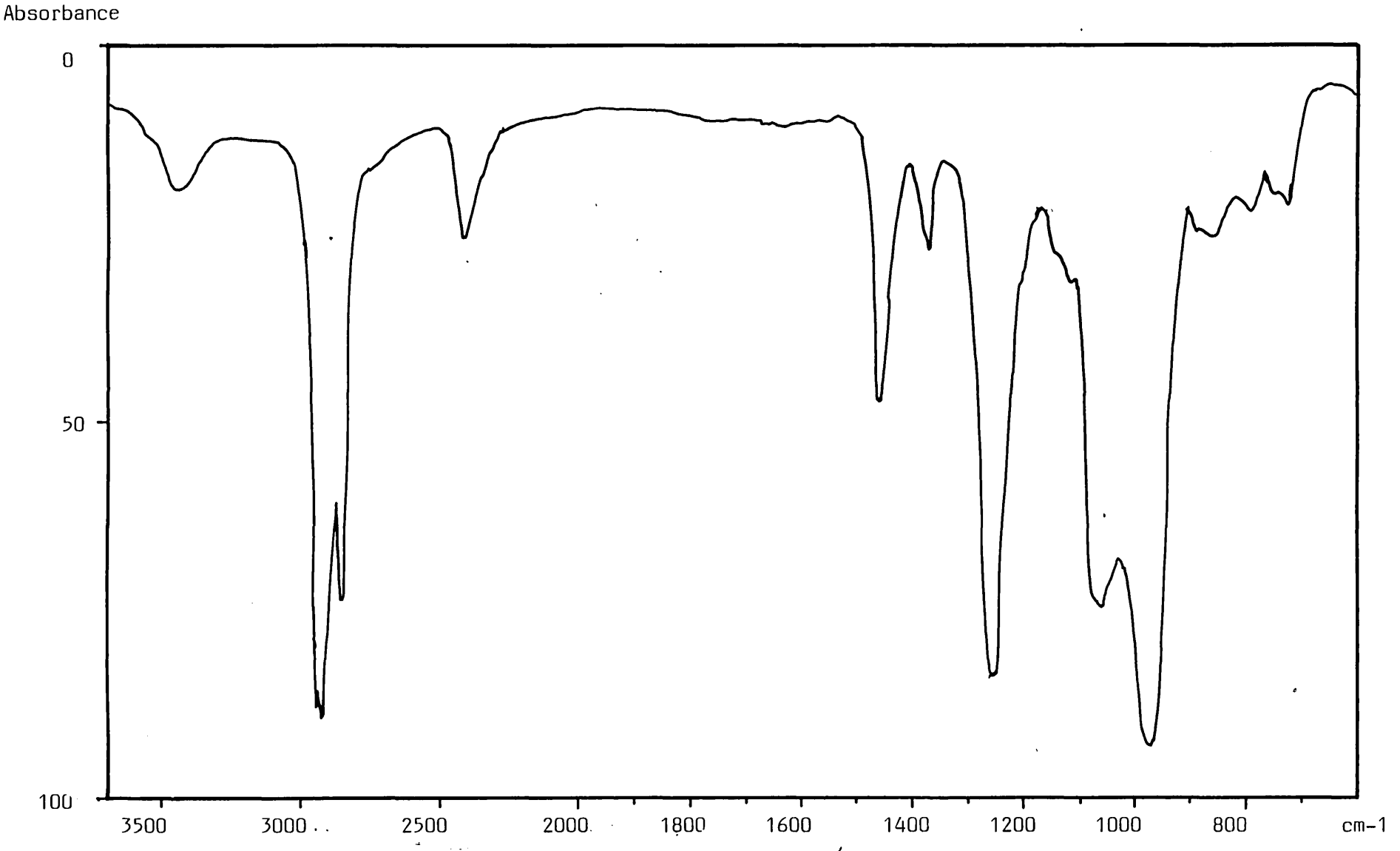


Figure 4.3 Infrared Spectrum - dihexyl phosphonate



Figure 4.4 Infrated spectrum di octyl phosphonate

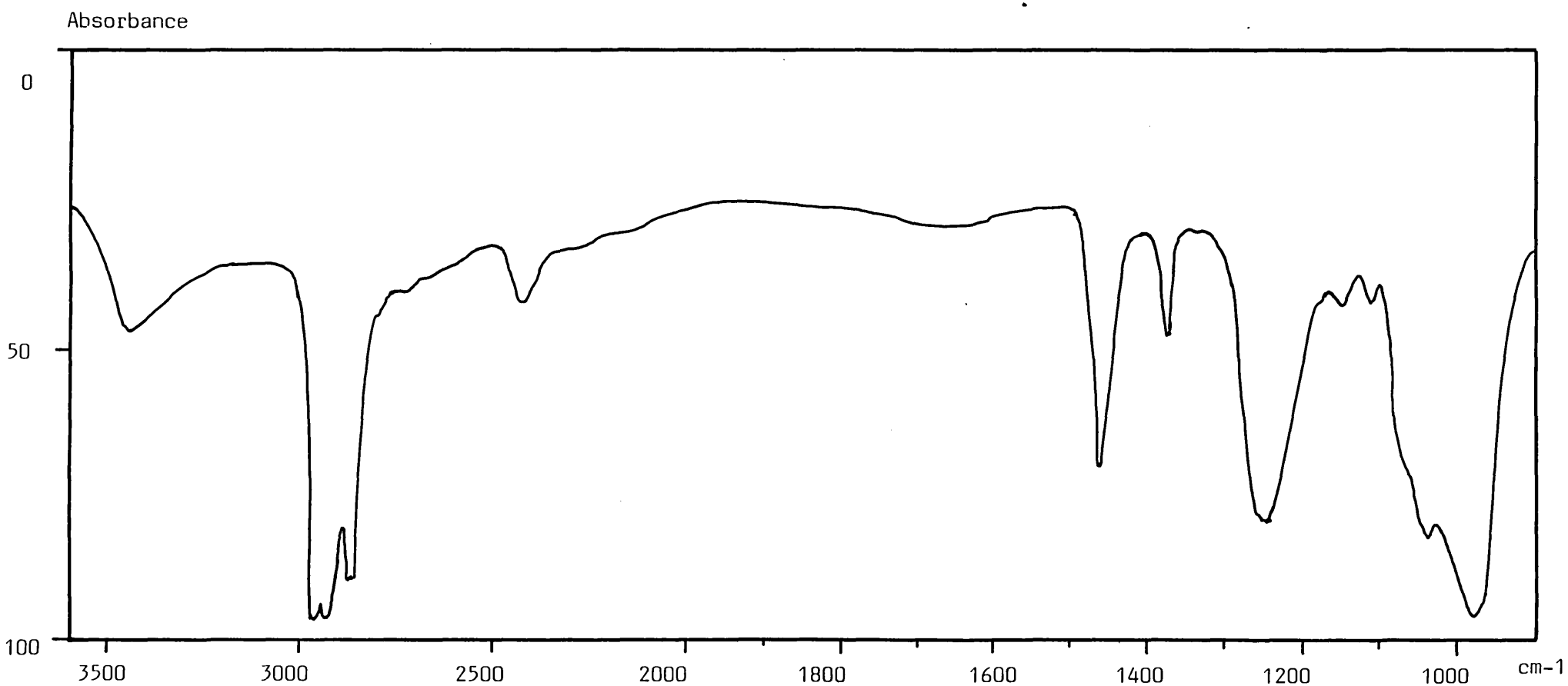


Figure 4.5 Infrared spectrum di (ethyl-hexyl) phosphonate

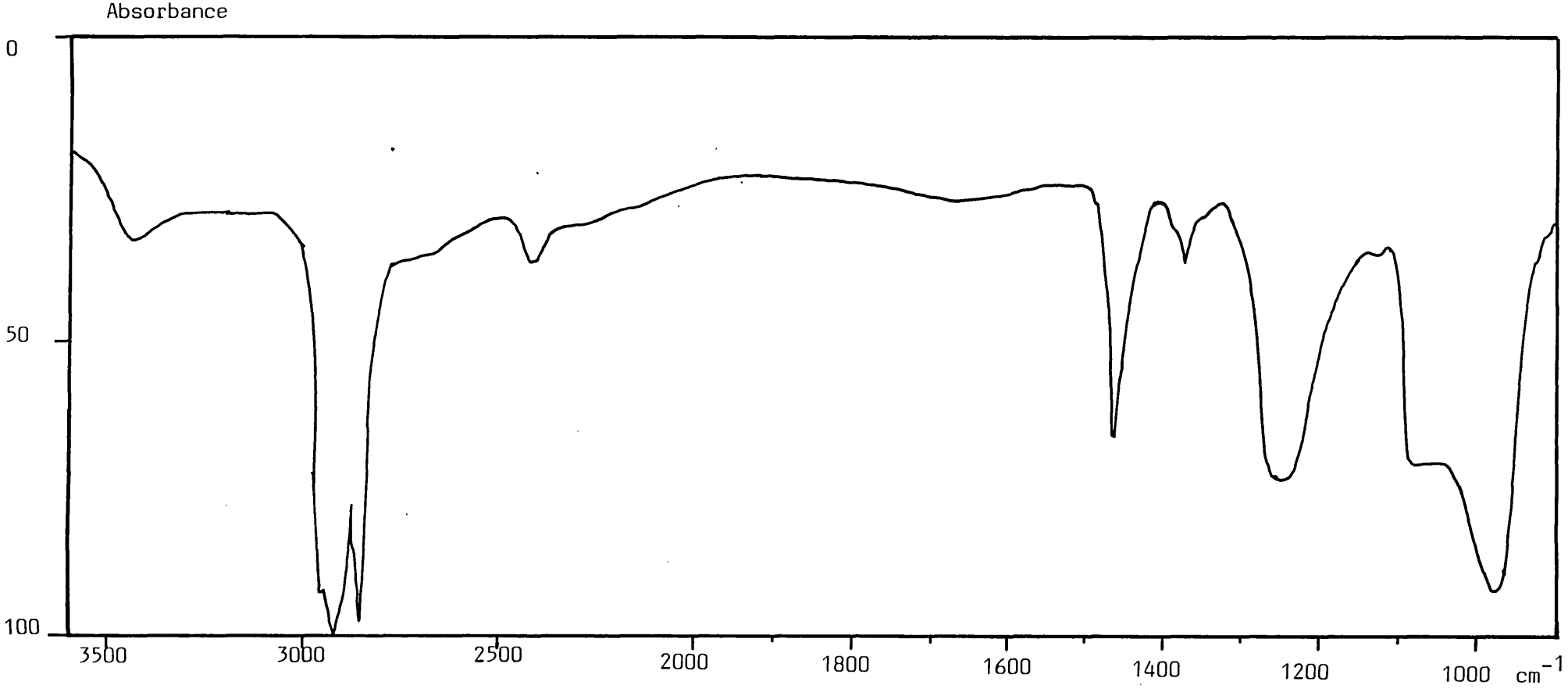


Figure 4.6 Infrared spectrum - didodecyl phosphonate

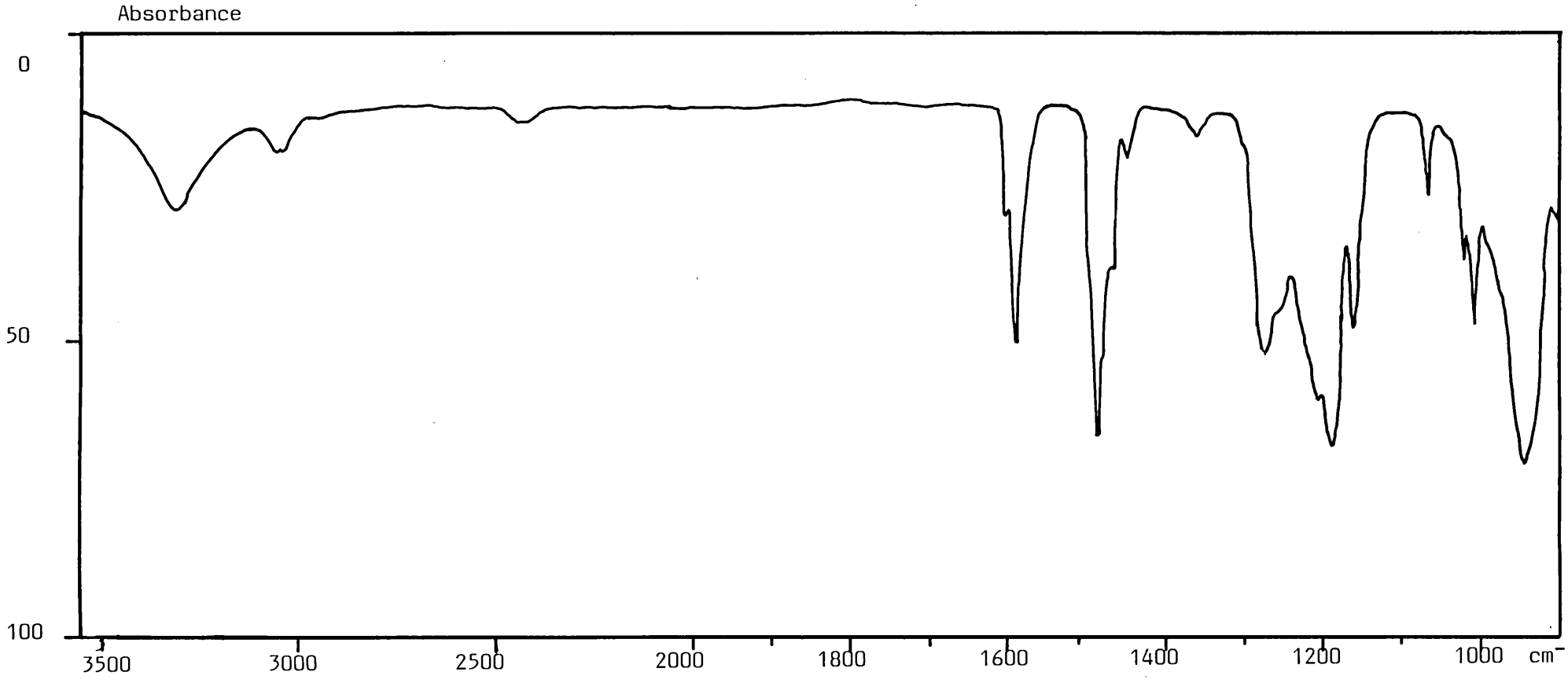


Figure 4.7 infrared spectrum- diphenyl phosphonate

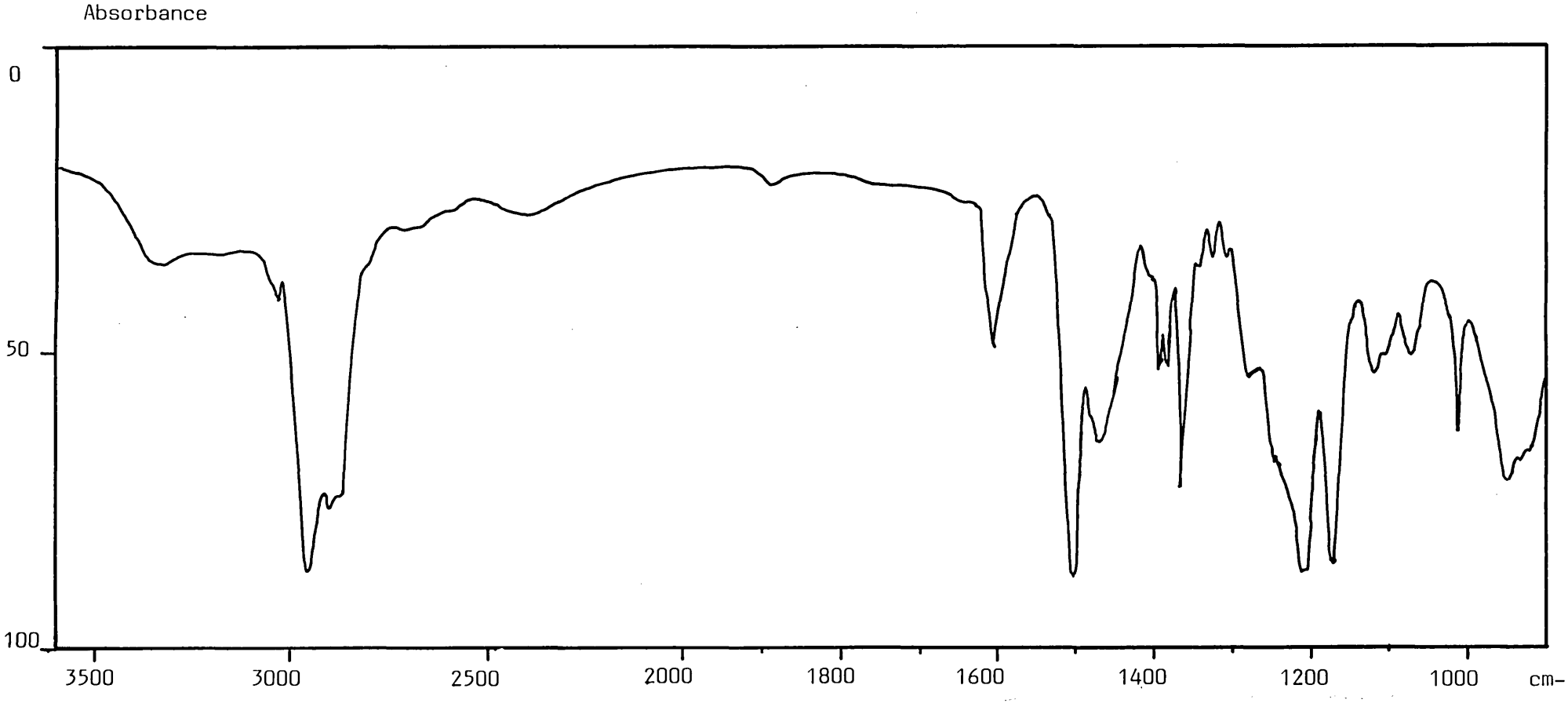


Figure 4.8 Infrared spectrum Bis (4-t-Octyl-phenyl) phosphonate

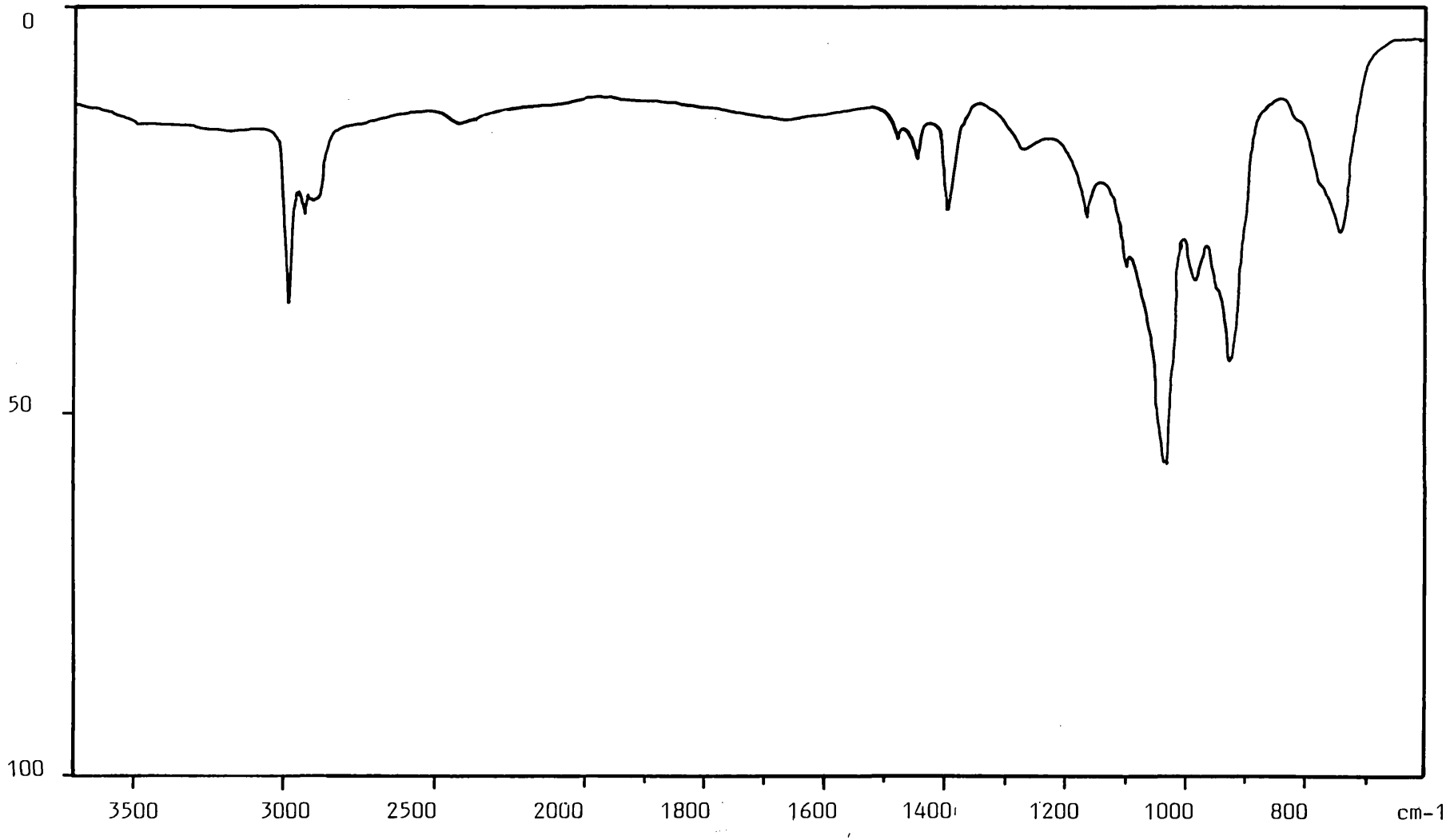


Figure 4.9 Infrared spectrum - tri ethyl phosphite

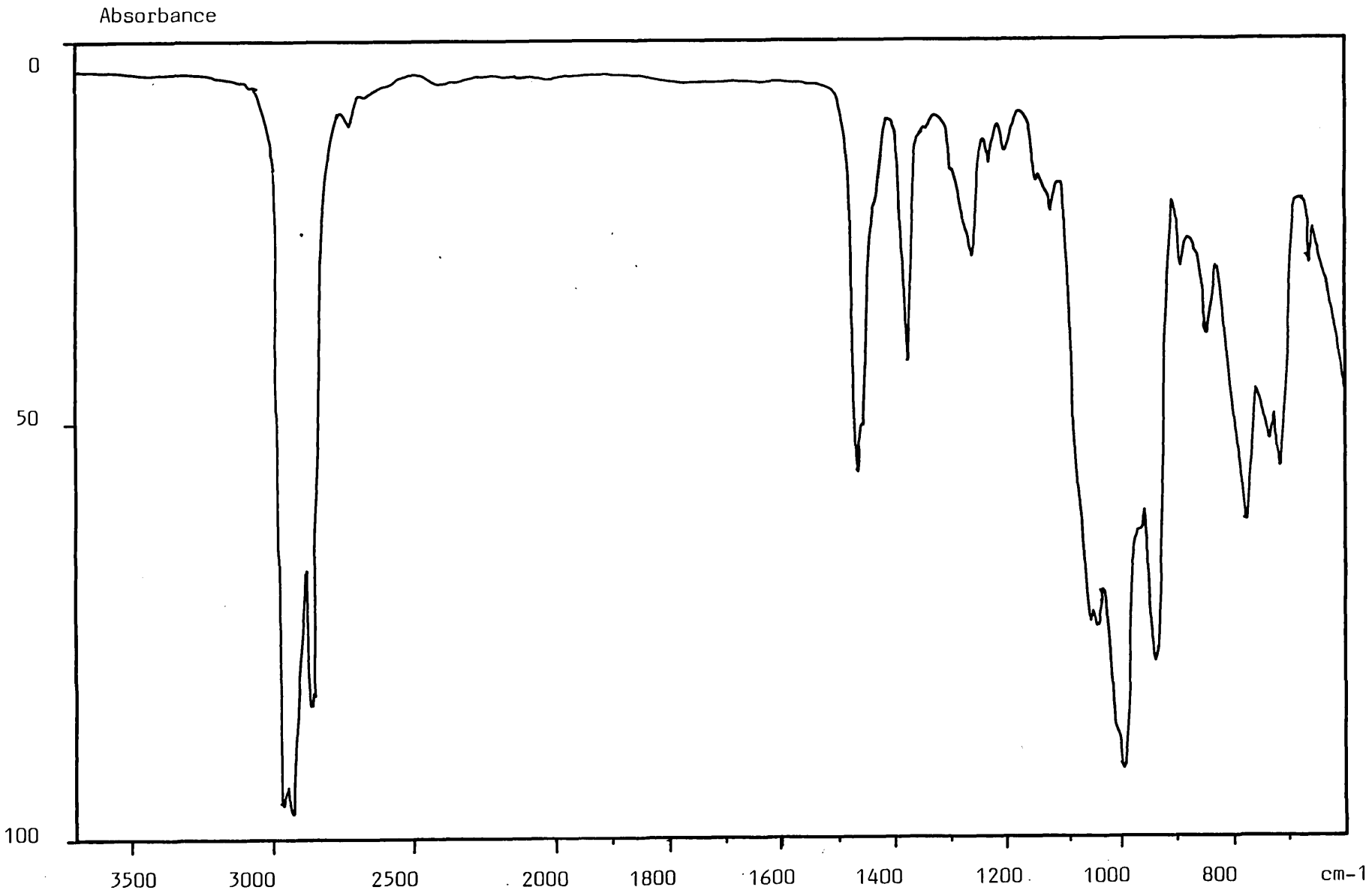


Figure 4.10 Infrared spectrum - tri hexyl phosphite

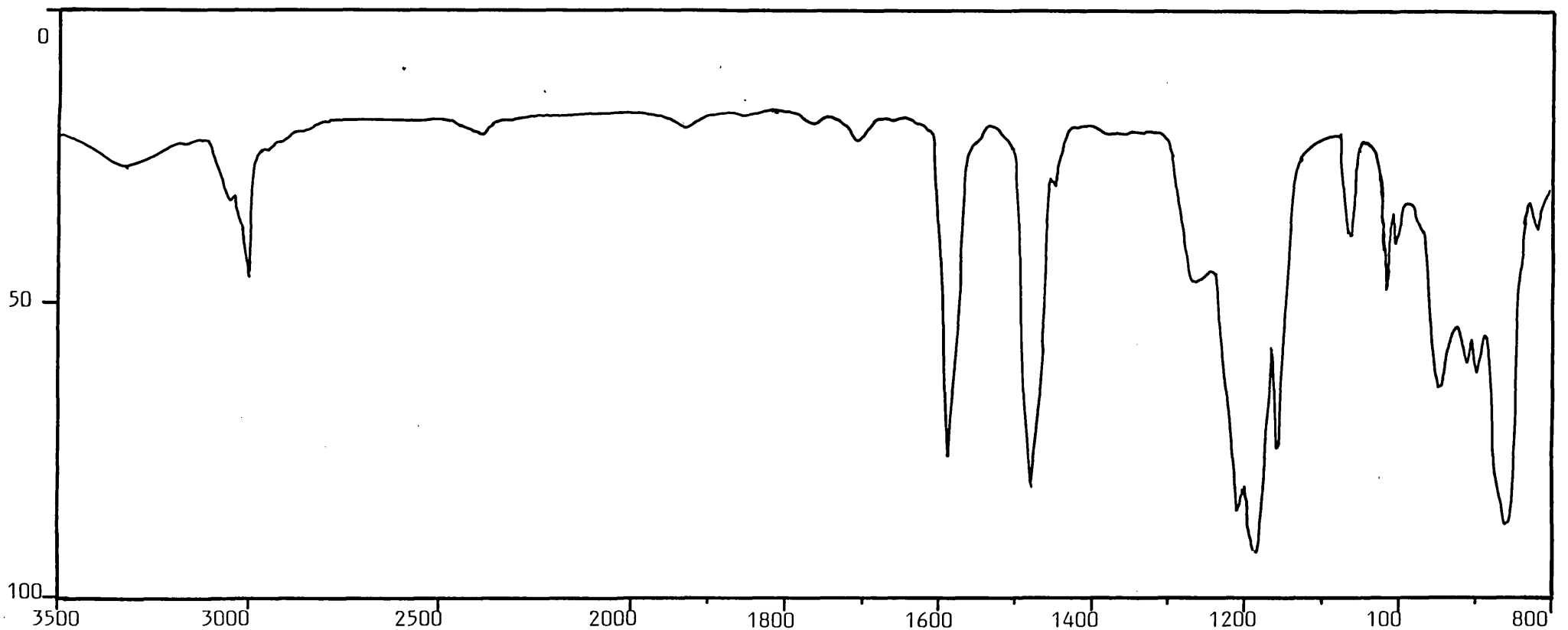


Figure 4.11 Infrared spectrum - tri phenyl phosphite



Figure 4.12 Infrared spectrum - tris (4.t-Octyl phenyl)phosphite

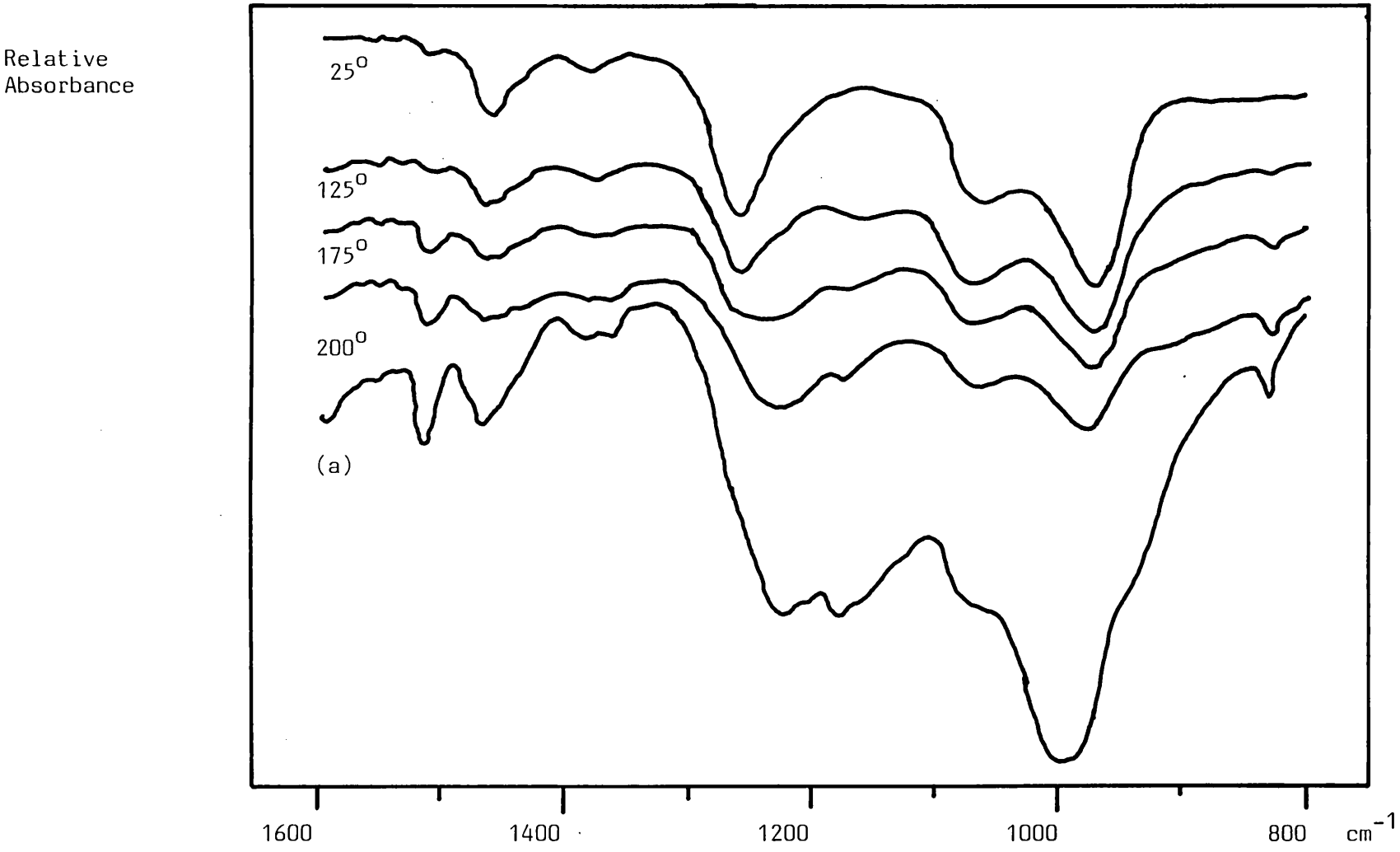


Figure 4.13 Variable temperature infrared spectra - Dihexyl phosphonate

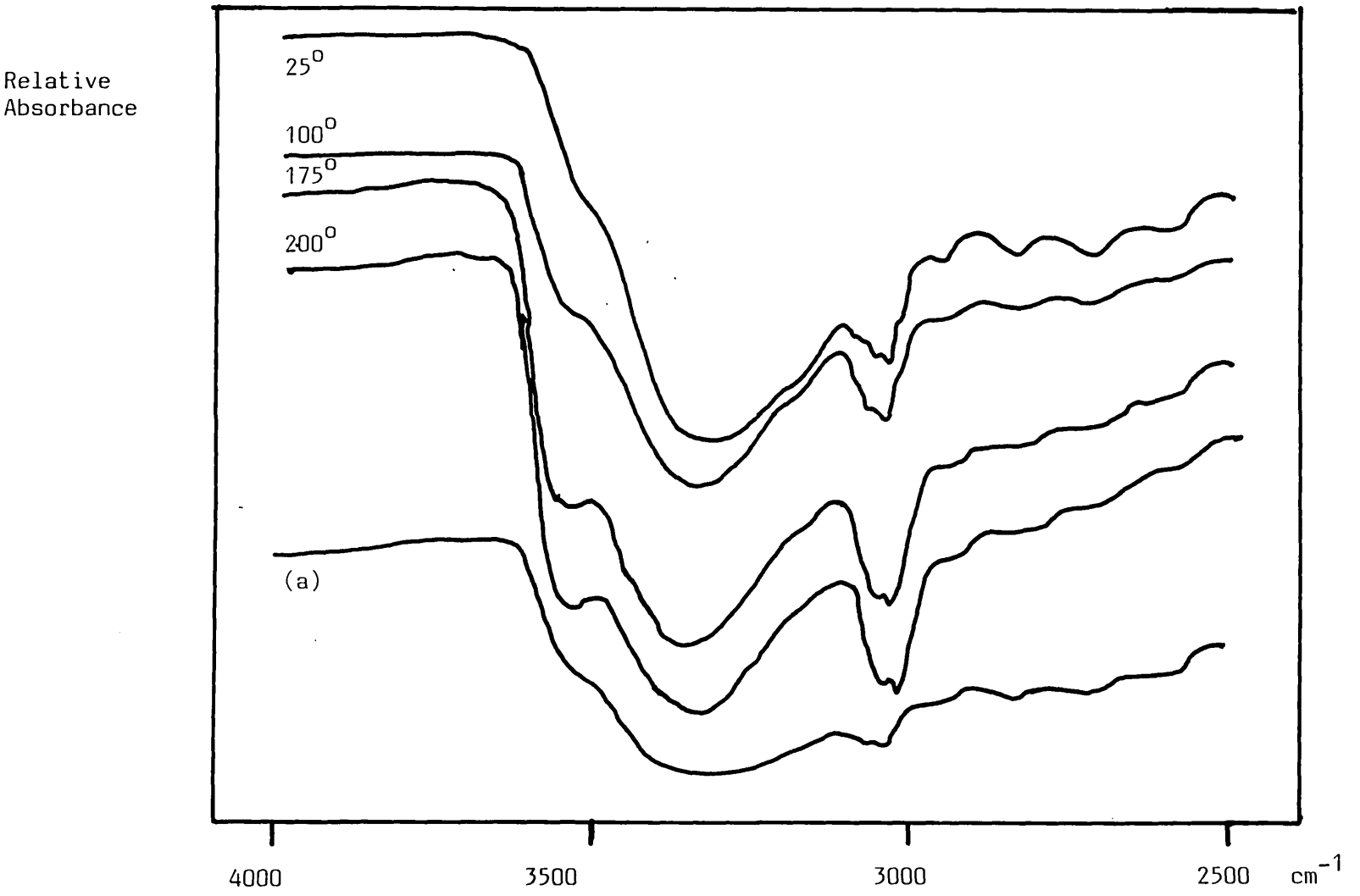


Figure 4.14 Variable temperature infrared spectra - di phenyl phosphonate

Table 4.2

Determined values for the phosphorus group frequencies - di-esters

Ester	frequency (cm^{-1}) P-H	P=O	P-O-C	
$(CH_3O)_2$ PHO	2425	1270	1188	1045
$(C_2H_5O)_2$ PHO	2425	1260	1165	*
$(C_6H_{13}O)_2$ PHO	2430	1250	1150	975
$(C_8H_{17}O)_2$ PHO	2425	1248	1150	980
$(C_{12}H_{25}O)_2$ PHO	2430	1245	*	980
$(C_6H_5O)_2$ PHO	2460	1260	*	955
$(C_8H_{17}C_6H_4O)_2$ PHO	*	1280	*	965

Table 4.3

Determined values for the phosphorus group frequencies - triesters

Ester	frequency (cm^{-1}) P-O-C	
$(C_2H_5O)_3P$	1165	1035
$(C_6H_{13}O)_3P$	1150	980
$(C_6H_5O)_3P$	*	910
$(C_8H_{17}C_6H_4O)_3P$	*	935

* absorbance band not clearly defined in the spectrum

Variable temperature infrared spectra of dihexyl and diphenyl phosphonates are shown in figures 4.13 and 4.14 respectively. On heating, these two phosphonates show different behaviour as shown by changes in their infrared spectra. With dihexyl phosphonate, changes occur in the region 1600 to 600 cm^{-1}, with the P-O-C and P=O bonds affected.

This change is non-reversible as shown by the spectrum 'a' in figure 4.13, which was recorded when the cell had cooled from 200° to 25°C. The changes in the infrared spectrum of diphenyl phosphonate occur in the region 4000 to 3000 cm^{-1} (the region of the spectrum shown in figure 4.14) and are reversible, shown by spectrum 'a' recorded after the cell had cooled to 30°C. The diphenyl phosphonate appears to undergo a dissociation on heating, with a peak appearing at 2250 cm^{-1} which increases in intensity with temperature. This peak is at the position found to be occupied by the phenol peak in impure samples of diphenyl phosphonate.

The behaviour of dihexyl phosphonate on heating is very different. As the temperature was raised above 125°C, a 'shoulder' appeared at 1225 cm^{-1} on the P = O absorbance peak at 1265 cm^{-1}. This 'shoulder' became more pronounced with an increase in temperature and its intensity did not decrease on cooling. Frequency shifts in the P-O-(C) and (P)-O-C absorbances also occurred.

Whilst firm conclusions as to what reaction takes place in dihexyl phosphonate when heated connot be drawn from the infrared spectra alone, it is clear that the behaviour of dialkyl phosphonates and diaryl phosphonates when heated is very different. However as will be shown in Chapter 6, the reactions observed using variable temperature infrared spectroscopy are not those that occur when iron powder is present during heating.

4.2 ^{31}P Nuclear Magnetic Spectra (n.m.r.)

4.21 Introduction to ^{31}P n.m.r.

Nuclear magnetic resonance is a phenomenon exhibited by a relatively small number of atoms for example by ^{1}H, ^{13}C, ^{19}F and ^{31}P. In these atoms the nucleus possesses a non-integral spin and therefore will adopt a particular orientation when placed in a magnetic field. When energy of a suitable frequency is applied, it is possible to observe the transitions which occur between the nuclear energy levels. In n.m.r. this energy corresponds to that of the radio frequency region of the electromagnetic spectrum.

The energies of these transitions are quantised, as they are a function of the angular momentum operator of the nucleus which itself is quantised. The angular momentum operator can have $2I + 1$ values where I is the nuclear spin number, and can have any value which is a multiple of half. Resonance occurs where the nuclear spin is non-zero. In the case of phosphorus ^{31}P, the nuclear spin is half and there are accordingly two nuclear energy levels and resonance can therefore occur.

The frequency at which resonance occurs is dependent upon the magnetic field experienced by the sample, which in turn is a function of the applied magnetic field and the 'internal' magnetic field of the atom. This 'internal' magnetic field depends on the electronic environment of the atom, as the surrounding electrons serve to shield the atom from applied (or 'external') magnetic field. This 'shielding effect' is a function of both the bonding and environment of the atom within the molecule.

Thus it can be seen that the n.m.r. signal for an atom in different compounds will differ. The technique may be used therefore as both a quantitative and qualitative means of analysis.

N.M.R. spectra can be recorded in either of two ways. the sample can be placed in a fixed magnetic field and the radio frequency scanned or the radio frequency can be fixed, and the magnetic field varied. In older instruments the magnetic field tended to be fixed, but in modern instruments the radio frequency is fixed and the magnetic field is scanned through the required range.

The immediate signal received from the spectrometer is one of energy absorbed against magnetic field strength (H). However the magnetic field strength experienced by the sample is a function of the geometry of the particular instrument used. Calibration of the instrument is therefore required in order to compare results from different machines. To do this the resonance signal for a standard substance is recorded. By comparison of the signal from the standard and the sample a non-dimensional parameter δ, termed the 'chemical shift', may be obtained, where δ is defined by:-

$$\delta = \frac{Ho - Hs}{Ho} \times 10^6 \quad ppm$$

where Ho = magnetic field strength (gauss) for standard.

Hs = magnetic field strength (gauss) for sample.

δ = chemical shift in ppm.

The chemical shift thus defined is independent of the particular machine used. In ^{31}P n.m.r. the standard used is 85% Orthophosphoric Acid (H_3PO_4) in water.

A more detailed explanation of the theory of nuclear magnetic resonance may be found in the early chapters of reference (110) for example.

4.2.2. Equipment & Technique

^{31}P n.m.r. spectra were recorded on a Bruker nuclear magnetic spectrometer at Kings College, London.

Samples of the compound to be analysed (typically $\sim$ 150 mg) were dissolved in deuterated chloroform ($CDCl_3$), before being admitted to the instrument. The sample tube is spun within the instrument to improve the homogeneity of the magnetic field experienced by the sample.

The instrument uses a fixed radio-frequency field of 36.4 MHz, and the applied magnetic field is swept across an equivalent 6KHz range.

4.2.3. Spectra

To exemplify the spectra obtained, figure 4.15 shows the ^{31}P n.m.r. spectrum recorded for a sample of dihexyl phosphonate. Chemical shifts recorded for a number of phosphonates and phosphites are listed in table 4.4.

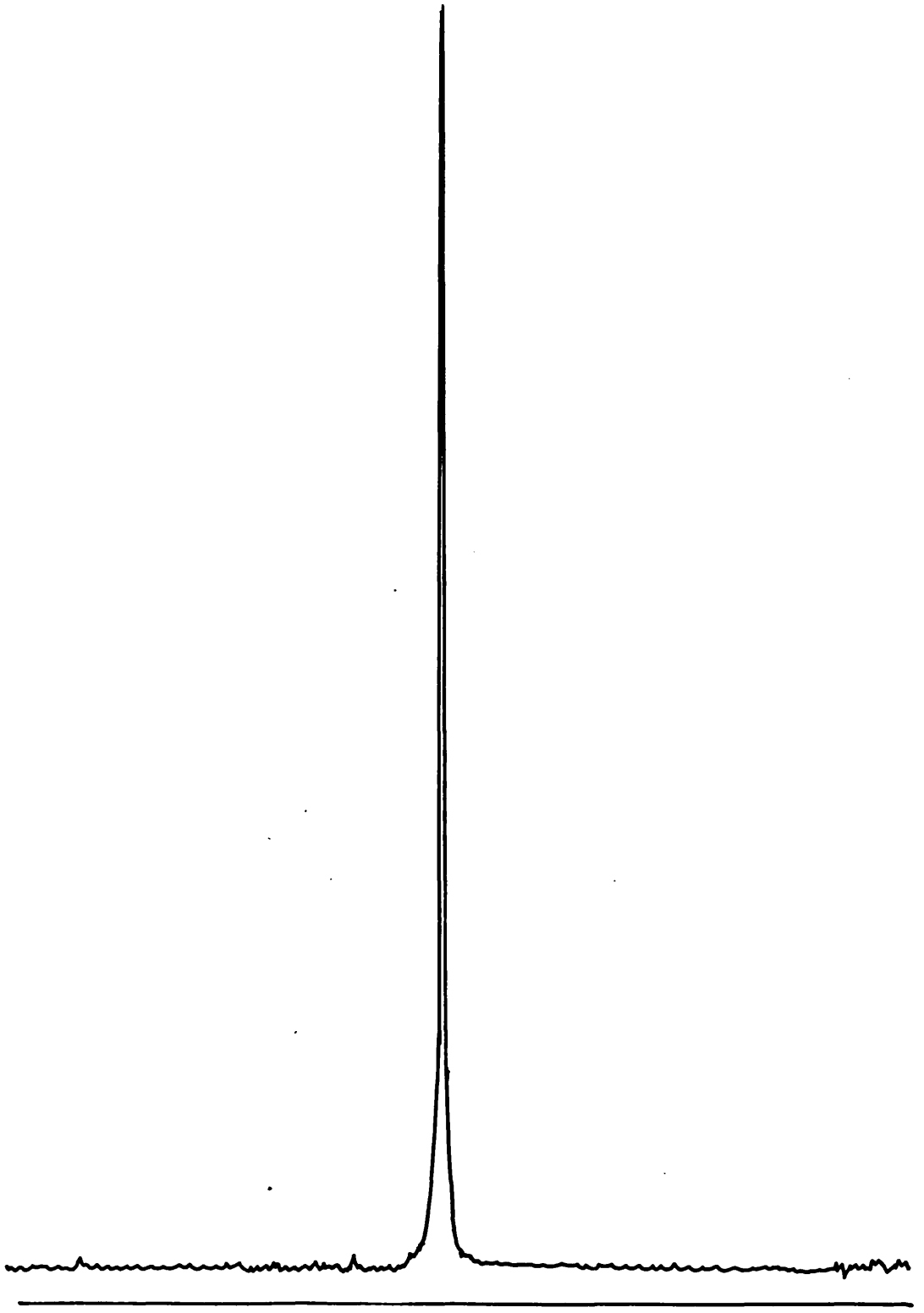


Figure 4.15 Typical ^{31}P n.m.r. spectrum dihexyl phosphonate

Table 4.4

Recorded chemical shifts for several phosphites and phosphonates

Compound	Chemical Shift, δ (p.p.m)
$(C_6H_{13}O)_2$ PHO	7.85
$(C_8H_{17}O)_2$ PHO	7.67
$(C_{12}H_{25}O)_2$ PHO	7.77
$(C_6H_5O)_2$ PHO	0.36
$(C_8H_{17}\text{-}C_6H_4O)_2$ PHO	0.6
$(C_6H_{13}O)_3P$	139.3
$(C_8H_{17}C_6H_4O)_3P$	8.2

4.3 Mass Spectra

4.3.1 Introduction

The molecular weight of organic compounds is often determined using mass spectrometry. The sample (of the order of 0.01g) is volatilised into an evacuated chamber in which it is bombarded by an electron or molecular beam to produce ions of the sample or of fragments of the molecule.

The sample, or fragments of the molecule, becomes electrically charged and can therefore be accelerated by an electrical field.

After acceleration by the electrical field, the ions are deflected by a magnetic field. The greater the mass of the molecule, the less the ion is deflected by the magnetic field from its original path. A signal is obtained for each ion that reaches the detector, the detector recording the number of ions of each ratio of mass to charge (m/e) of the ion.

From the values of m/e obtained, the structure and molecular weight of the compound can be determined. A fuller explanation of mass spectrometry will be found in references 111-114.

The mass spectrum of dihexyl phosphonate was recorded by the Organic Chemistry Section, Department of Chemistry, Imperial College.

4.3.2. Results

One of the more convenient methods of handling the mass spectral data is to convert the spectrum into a "line diagram". In this each m/e ratio is recorded against its relative abundance. The most abundant peak is identified (termed the base peak) and the intensities of the other peaks are measured as a percentage of the base peak intensity (111).

Figure 4.16 shows the line diagram so obtained from the mass spectrum of dihexyl phosphonate, with a septum temperature of 160°. As can be seen from this line diagram, the mass spectrum demonstrates the fragmentation of the $(C_6H_{13}O)_2PHO$ molecule that occurs in the mass spectrometer. For convenience the major m/e ratios are tabulated in table 4.5 together with the assignment of the originating molecular fragment. In this tabulation, the symbol M indicates the molecular ion $(C_6H_{13}O)2^{PHO}$.

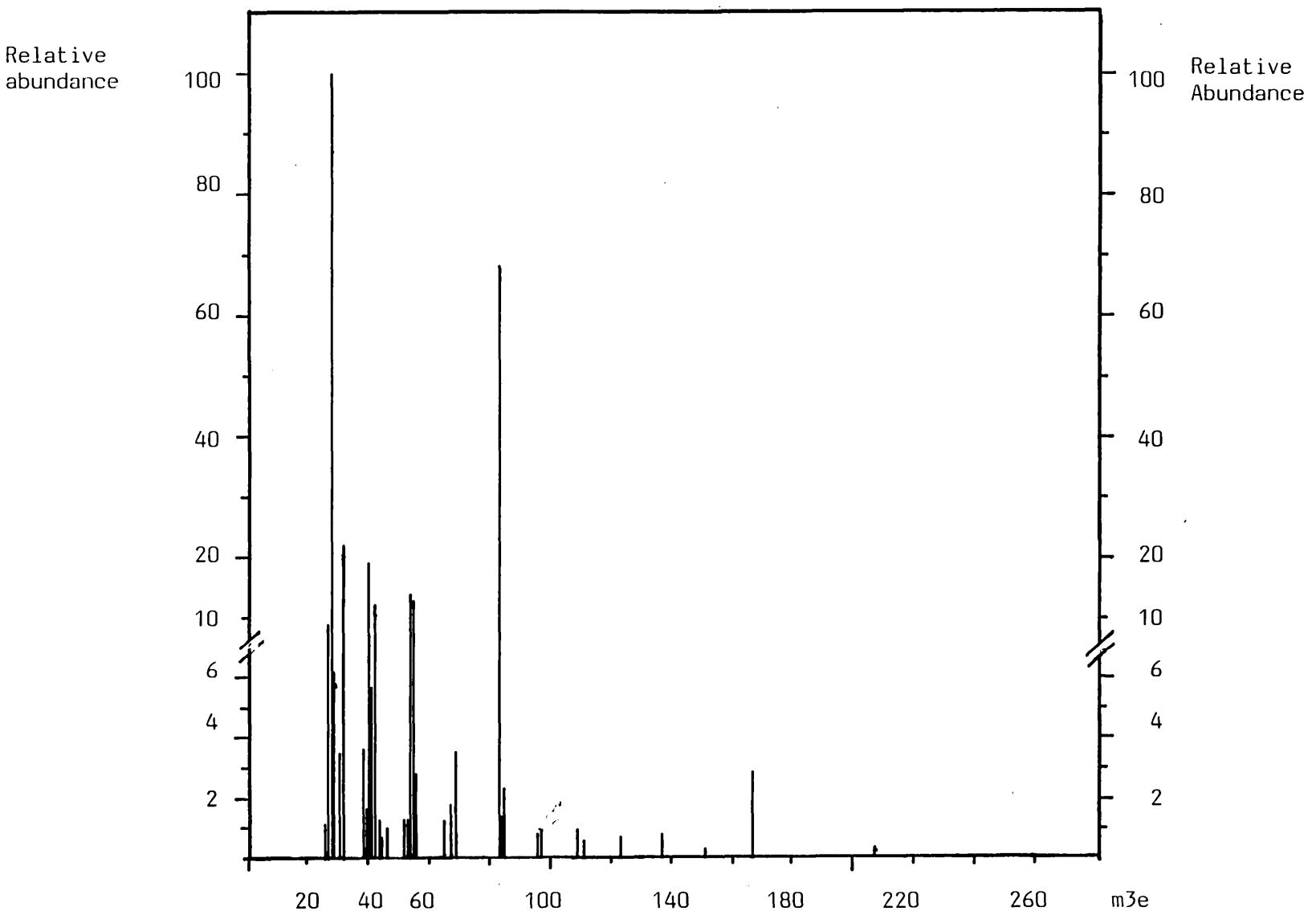


Figure 4.16 Mass spectrum line diagram - di hexyl phosphonate

Table 4.5

Assignment of major m/e ratios in the mass spectrum of dihexyl phosphonate $(C_6H_{13}O)_2$ PHO

m/e ratio	relative abundance %	assignment
207	0.25	$[M - C_3H_9]^+$
167	2.9	$[M - C_6H_{11}]^+$ (McLafferty + 1 rearrangement) (146)
151	0.25	$[(M - C_6H_{12}) - CH_3]^+$
137	0.8	$[(M - C_6H_{12}) - C_2H_5]^+$
123	0.7	$[(M - C_6H_{12}) - C_3H_7]^+$
111		$[(M - C_6H_{12}) - C_4H_7]^+$
109	1.0	$[(M - C_6H_{12}) - C_4H_9]^+$
97	1.0	$[(M-C_6H_{12}) - C_5H_9]^+$
85	2.4	$[C_6H_{13}]^+$
83	68.0	$[C_6H_{11}]^+$ $[M-H]^{3+}$
69	3.65	$[C_5H_9]^+$ $[PO_3]^+$
55	12.08	$[C_4H_7]^+$
54	1.47	$[C_4H_6]^+$ $[PO_2H]^+$
47	1.03	$[PO]^+$
43	21.08	$[C_3H_5]^+$
41	18.0	$[C_3H_5]^+$
32	21.08	$[PH]^+$
29	10.09	$[C_2H_5]^+$
28	100	$[C_2H_4]^+$, $[CH_2O]^+$
27	9.0	$[C_{2H3}]+$, $[CHO]+$

The symbol [M - C_6H_{12} - CH_3] (at m/e 157) indicates fragmentation of the molecular ion by the loss of CH_3 from the hexyl group, after fragmentation by the McLafferty rearrangement (145,146) and loss of C_6H_{12} to form the ion $[(C_6H_{13}O)PO.OH]^+$. This rearrangement is described in Chapter 6.

4.4 Elemental Microanalysis

Elemental microanalysis was carried out on a sample of dihexyl phosphonate, prepared in the laboratory. This analysis was carried out by Elemental Microanalysis Ltd. of Beaworthy, Devon.

4.4.1 Introduction

Quantitative analysis for many elements can be carried out on a microscale (0.005 to 0.05 g) (115,116). Carbon, hydrogen and phosphorus can be readily determined, oxygen can be directly determined but is usually determined by arithmetic difference.

4.4.2 Method

Carbon and hydrogen were determined instrumentally. A weighed sample was oxidised in a helium/oxygen stream and the products of combustion, carbon dioxide and water, were determined automatically by the instrument and compared to values obtained for a standard reference material (117).

Phosphorus was determined by combustion in a sealed flask containing an oxygen atmosphere and an adsorption solution. The phosphorus content was obtained by a spectrophotometric determination of the orthophosphate as molybdovanadophosphoric acid (117).

Oxygen was determined by 'arithmetic difference', the oxygen figure being equated to the difference between the total content of C,H and P and 100%. Determination of oxygen by using an instrumental method was not possible due to the presence of phosphorus which poisons the nickelised carbon catalyst used in such methods. All analysis were made in duplicate.

4.4.3 Results

The results of the elemental microanalysis of a sample of dihexylphosphonate, prepared in the laboratory were C 56.93% H 11.20% P 12.45% O 19.42%.

This compares reasonably with an expected analysis of:-

C 57.6% H 10.8% P 12.4% O 19.2%

4.5 Summary

Analytical methods for the qualitative analysis of phosphonates and phosphites have been established. The methods have been able to show the higher quality of the esters prepared and purified in the laboratory over those obtained commercially. More importantly valuable analytical techniques were established which would be used in later work to study the reaction of dialkyl and diaryl phosphonates with iron.

Chapter 5.

The Reaction of Phosphonates and Iron

In laboratory experiments, alkyl and aryl phosphonates were heated in the presence of iron metal. A polymeric product was formed, which was found to be a ferro-organophosphorus polymer. The nature of this polymer has been studied both by a combination of controlling the conditions of the reaction (and thence observing the effect of these different conditions on the rate of reaction), and by analysis of the reaction product.

5.1 Experimental

The aim was to investigate the reactions which might occur between the alkyl or aryl phosphonates and the metal of the rolling EHD contact. To accomplish this, samples of various di-alkyl and aryl phosphonates were heated in the presence of iron, present as a powder in various states of oxidation. The reaction was monitored by taking and analysing samples at regular intervals.

The analysis methods used, of infrared spectrophotometry and dissolved iron content analysis, are described in section 5.2.

By control of the conditions under which the reactions were carried out, the effect of temperature, oxygen and water were studied. Selective oxidation, reduction and different particle size ranges of the iron powder were used to study the effect of surface oxidation and surface area on the rate of reaction.

5.1.1 General Experimental Method

Samples of the di-alkyl and di-aryl phosphonates were heated with iron powder by weighing the sample into a 6" glass test-tube (15cm by 2.5 cm). To pure phosphonate a known weight of iron powder was added to the test-tube in a heated oil bath. Agitation and an inert atmosphere were provided by introducing nitrogen to the samples at a fixed flow rate through a glass tube drawn to a fine capillary.

The heated oil bath used comprised a thermostatically controlled hot-plate on which an aluminium beaker containing liquid paraffin was placed. The liquid paraffin was stirred using an electric stirrer fitted with a 'screw' or propellor shaped stirrer blade. A 0 to 200°C thermometer was clamped approximately 2.5cm above the base of the beaker to monitor the oil bath temperature. It was found that the system was capable of temperature control to within 1°C.

The time of heating was recorded including the time taken for the sample to warm up to the oil bath temperature. It was found that raising the oil bath temperature by 10°C above the required temperature prior to introduction of the sample test-tube was sufficient to obtain an equilibrium temperature at or close to the required experimental temperature.

The reaction mixture was sampled using a glass teat-pipette. Small samples (approx. 0.5 to 0.75 cm^3) of the reaction mixture were withdrawn at regular intervals, care being taken to minimise the presence of iron powder in the samples. It was important to limit the contamination of samples by iron because of the use of analysis of the dissolved iron content to follow the progress of the reaction.

Furthermore, it was important to avoid contamination by iron powder since the reaction between dihexyl phosphonate and iron was found to occur at low (15°C) temperatures albeit at a very slow rate. This would have continued after sampling. Once a set of samples were obtained, the progress of the reaction was studied usually by analysis of the 'dissolved iron content' although infrared spectro-photometric and ^{31}P nuclear magnetic resonance methods were used to a lesser extent.

Thus a sample of dihexyl phosphonate was weighed into a clean dry test-tube, a weight of 10 to 13 g generally being used weighed to 0.001 g. To this iron powder, sieved into the size fraction range 75 to 53μ, was added an amount equivalent to 8-10 % of the ester weight (weighed to 0.0001 g) being used. Nitrogen was introduced to the sample through the capillary at a steady rate of 100 cm^3/min, and the tube was placed in the heated oil bath. Samples were taken at regular intervals (usually every 20 or 30 minutes) and later analysed.

In a similar manner, the reactions of dioctyl, didodecyl, diphenyl and bis-4-Octyl-phenyl phosphonate with iron powder were investigated.

5.1.2 Heating in a semi-closed system

In the tests in which the dialkyl and diaryl phosphonates were heated with iron powder, condensation was observed on the higher (cooler) parts of the test-tubes. In the case of phenyl and octyl-phenyl phosphonates, a few needle shaped crystals were apparent around the top of the test-tube. Collection of this small amount of material proved difficult under the conditions in which the tests were being carried out. Therefore a modified apparatus was set up to enable collection of this condensate.

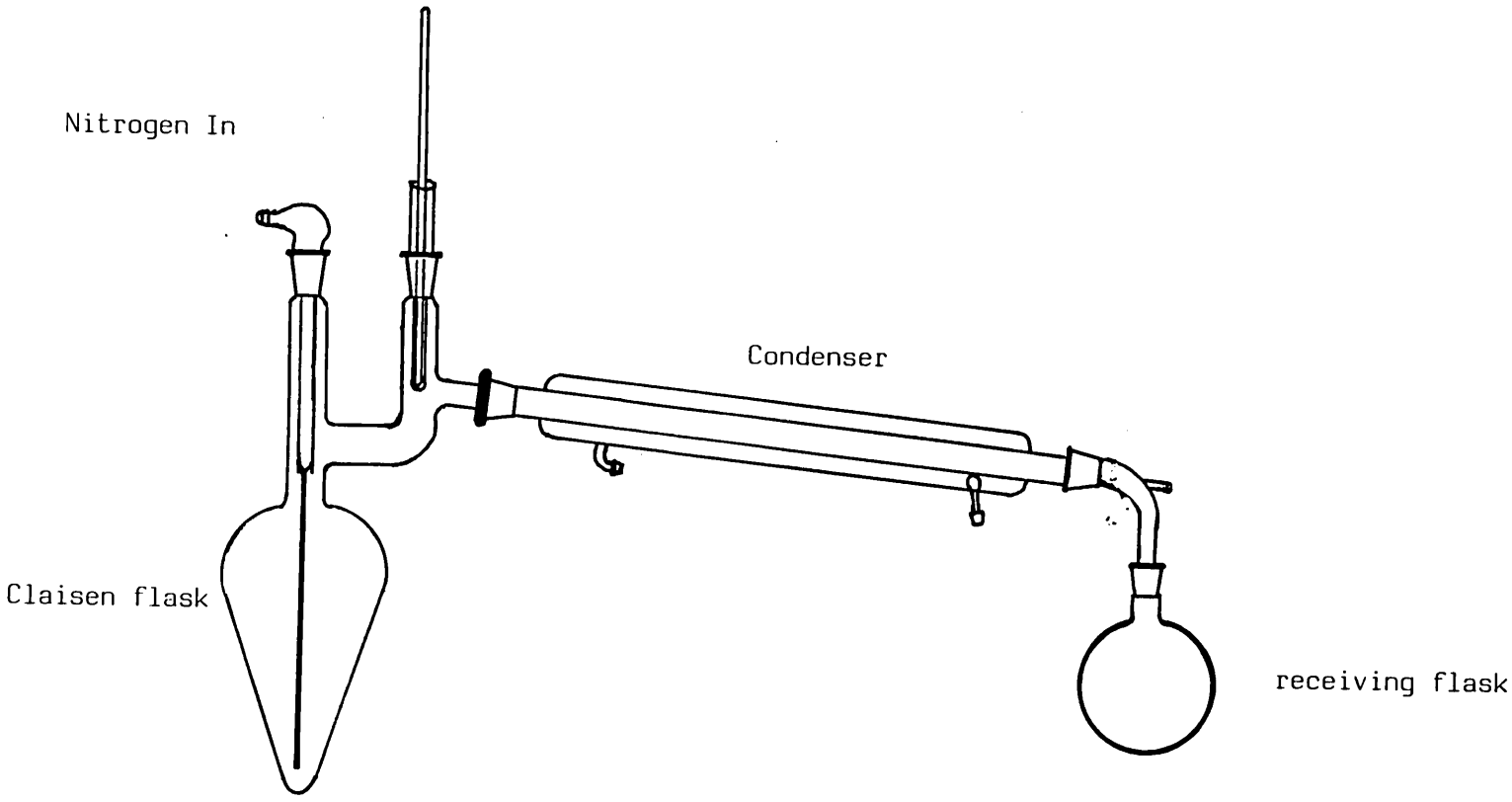


Figure 5.1 Apparatus used for 'Semiclosed' heating tests

The apparatus used comprised a 50 cm^3 pear-shaped 'quick-fit' flask fitted with a 'Claisen Head' and a condenser leading to a collection flask. The apparatus is illustrated in figure 5.1. Nitrogen was admitted to the reaction flask through a capillary tube to provide agitation and an inert atmosphere. Heating was achieved using the heated oil bath described in section 5.1.1.

Dioctyl phosphonate was heated with 10% by weight of iron powder for 12 hours at temperatures of 150-160 ^{o}C. After this time, condensation had collected in the claisen head, condenser and collection flask. This condensate was gathered into one sample and analysed by infrared spectro-photometry.

5.1.3 Effect of temperature

The effect of temperature on the rate of reaction of phosphonates and iron was studied by heating samples of dihexyl phosphonate and iron powder at four different temperatures between 117° and 180°C. The method used was identical to that described in section 5.1.1

A nitrogen blanket was applied in all the tests. Samples were taken every 15 minutes, using a teat-pipette and retained for determination of the dissolved iron content.

5.1.4 Effect of oxygen

To study the effect of oxygen on the rate of reaction of phosphonates and iron, the nitrogen gas used to agitate the reaction mixture was replaced with oxygen flowing at the same rate (100 cm^3/min). The heating of the phosphonates was then carried out as described in section 5.1.1.

A 'control' sample was heated alongside the oxygenated sample, containing near-identical amounts of ester and iron powder, but with nitrogen instead of oxygen as the 'agitator gas'. The comparative rates of reaction in oxygenated and nitrogenated conditions were determined for samples of dihexyl phosphonate and of diphenyl phosphonate in this manner.

5.1.5 The effect of water

To test the effect of water on the rate of the reaction between iron powder and phosphonate diesters, water was weighed into the sample before heating. The rate of reaction was then followed by sampling the reaction mixture and recording the iron concentration against time of sampling.

Samples of dihexyl phosphonate were weighed into a clean, dry test tube and 8-10% by weight of iron powder was added. Using a syringe fitted with a hypodermic needle, distilled water was accurately weighed into the ester sample. Weights of the order of a hundredth of a gram could be introduced by this method, giving rise to water levels of 0.3 to 1.4% in the tests carried out. In each test the 'wet' sample was run against a 'dry' control containing a near identical weight of ester and iron, but with no water. Both samples were heated by placing in an oil bath at 155°C, with Nitrogen passed through each sample via a capillary glass tube. The gas flow to each sample was balanced using needle valves on each flow meter.

The combined effect of oxygen and water was monitored by adding water to both samples and passing oxygen through one, and nitrogen gas through the other.

In addition to dihexyl phosphonate, the effect of water on the reaction of diphenyl phosphonate was also monitored. A problem encountered was the low solubility of water in diphenyl phosphonate. Maximum water levels used in the diphenyl phosphonate tests were approximately 0.3%.

5.1.6 Reaction with oxidised and reduced iron

The introduction of oxygen into the test solution instead of nitrogen, was shown to give rise to a faster reaction. An investigation was carried out to study the difference between the reactivity of phosphonates with oxidised and reduced samples of iron powder.

Iron powder sieved to -75 + 53μ was oxidised by heating at 200°C in air for 72 hours. A similar sample was reduced by heating at 400°C in a stream of hydrogen for 72 hours. Samples of dihexyl phosphonate were then heated at 155°C under nitrogen in the presence of each of these iron samples. Both reactions were regularly sampled and later analysed for iron content. The results obtained were compared to a test carried out using the original 'untreated' iron powder.

5.1.7 Reaction with Iron (III) oxide

In view of the increased rate of reaction of dihexyl phosphonate with iron powder in the presence of oxygen, a study of the reaction of dihexyl phosphonate with iron (III) oxide, Fe_2O_3 or haematite was made. A sample of haematite was dried at 75°C for 24 hours before use. A size fraction in the range 75 to 53 μ was collected and used in the heated tests with dihexyl phosphonate.

As in the tests with iron powder, an ester-iron oxide proportion of 9:1 was used. The reaction mixture was heated in a clean, dry test tube placed in an oil bath at 155°C. Nitrogen was bubbled through the mixture at 100cm^3/min to provide an inert atmosphere and agitation. The reaction was sampled regularly and these samples were later analysed for dissolved iron content.

5.1.8 Effect of surface area of iron

If the rate determining step in the reaction of iron and dihexyl phosphonate involves either the dissolution of the iron or a reaction on the iron surface, then it follows that the surface area of the iron will be important. The effect of surface area may be investigated by using iron powders of different particle size ratios.

Iron powder sized into different size fractions was used in these tests. The size fractions employed together with a median surface area for that size fraction are listed in table 5.1. The median surface area is obtained by assuming spherical shaped particles, and using for calculation the median particle size in each size grouping.

For spheres of diameter 'd' and density 'D', the total surface area A of 1g of particles is derived as follows:

The volume, V, of one particle is given by

$$V = \frac{\pi . d^3}{6}$$

and its mass, m, will be

$$m = \text{density} \times \text{volume} = D \times \frac{\pi . d^3}{6}$$

If 'n' is the number of particles of mass 'm' in 1g, then

$$n = \frac{6}{\pi\, d^3 . D}$$

The surface area, a, of one particle is given by

$$a = \pi\, d^2$$

the total surface area, A, of 1g is therefore

$$A = n . \pi\, d^2$$

and therefore

$$A = \frac{6}{d^3 . D . \pi} \times \pi . d^2$$

$$A = \frac{6}{d . D}$$

for pure iron, the density D is 7870 kg/m^3 (118)

Table 5.1

Iron powder size ranges and estimated surface areas

Particle size range, m x 10^{-6}	Median diameter m x 10^{-6}	'Median surface area per gram m^2 x 10^{-3}
420 - 300	360	2.1
300 - 150	225	3.4
150 - 75	112.5	6.8
75 - 53	64	11.9
53 - 37	45	16.9

The results of these test were inconclusive. The rate of increase in iron concentration with time was found to increase with increasing particle diameter for diameters above 75 x 10^{-6}m, whilst the -37 x 10^{-6}m particles gave a faster rate of reaction than did the 53 - 37 x 10^{-6}m group. As a further means of studying the effect of surface area, reactions with iron foil were carried out using iron foils of different surface areas.

High purity iron foil of thickness 0.025mm was used, and the surface areas were approximated from the mass. The following approximation was used.

For a cuboid of length 'l', breadth 'b' and thickness 'd', the surface area, A, is given by:-

$$A = 2\,(l.b + b.d + l.d)$$

if 'd' $\ll$ b,l then this approximates to

$$A = 2 \times l.b$$

Since the volume V is given by

$$V = \frac{\text{mass}}{\text{density}}$$

and $V = l.b.d$

$$\text{then } l.b = \frac{\text{mass}}{\text{density} \times d}$$

The surface area, A, therefore is given approximately by:-

$$A = \frac{2 \times \text{mass}}{\text{density} \times d}$$

The masses of iron foil used, and their approximate surface areas are listed in table 5.2.

Table 5.2

Masses of iron foils used and calculated surface area

Test no.	Mass of foil used (g)	Surface area ($m^2 x 10^{-4}$)
1	0.1690	17.18
2	0.2709	27.54
3	0.5095	51.79
4	0.9860	100.2

5.1.9. Tests in liquid paraffin solution

All the tests previously outlined have concerned pure phosphonates. Since the esters under test are used as antiwear additives in lubrication oils, it was important to follow the reaction of iron powder and the esters when dissolved in an oil. The oil chosen was liquid paraffin, cleaned by being stored over alumina and passed through fresh alumina immediately before use. This cleaning procedure was used to remove oxidised, and to a lesser extent, 'branched chain' hydrocarbons.

These components, because of their greater polarity than 'straight-chain' hydrocarbons, are more readily absorbed onto the alumina. It was decided to remove these impurities to limit the thermal breakdown of the paraffin oil at the test temperatures used.

Tests in liquid paraffin were carried out using dihexyl phosphonate at 20% and at 3% ester concentrations.

These tests were carried out by dissolving a known weight ($\sim$ 5g) of dihexyl phosphonate in a known weight of liquid paraffin ($\sim$ 20g). This solution was homogenised by passing a stream of nitrogen gas through a capillary tube. To this solution was added a sample of iron powder (0.3g). The solution was agitated by passing nitrogen through the solution. Heating was achieved, as in the tests on the pure ester, by placing the test tube in an oil bath at 155°C.

To test the effect that added water may have on the reaction, a known weight of distilled water was added to the solution using a hypodermic syringe and needle. Once the water could be seen to be completely dispersed (by shaking) into the dihexyl phosphonate, the liquid paraffin solvent was added to the sample.

The effect of oxygen was investigated by using oxygen gas instead of nitrogen as the agitator gas. All the test solutions were sampled regularly during each test using a glass teat-pipette and later analysed for dissolved iron content.

5.1.10 Reaction with chromium powder

Since chromium is used as a surface coating on the discs of the optical EHD lubrication test apparatus, and is also the second most abundant metal in common bearing steels, it was decided to study the reaction, if any, of chromium with dihexyl phosphonate.

The method used was identical to that used for studying the reaction of dihexyl phosphonate with iron powder. A heating temperature of 162°C was used for this test.

Chromium (1.11g) sized into the range 75-53 x 10^{-6}m, was added to a sample of dihexyl phosphonate (9.98g) under a nitrogen atmosphere. The mixture was heated for 5 hours samples being taken every half hour.

The samples collected were analysed for dissolved chromium content by chemical digestion of a known weight of sample (0.05 - 0.1g), followed by atomic absorption spectroscopic analysis.

5.1.11 Reaction of trihexyl phosphite and iron powder

Samples of trihexyl phosphite were heated in the presence of iron to investigate what, if any, reaction occurred.

Thus 1.03g of trihexyl phosphite, was heated at 175°C for 4 hours under N_2 with 0.3g iron powder. After this time the liquid was decanted from the iron powder and analysed by infrared spectrophotometry.

In a similar manner trihexyl phosphite to which distilled water (2.7% by weight) had been added was heated with iron powder. After decanting of the sample, infrared analysis was carried out on the remaining liquid.

In both tests, a control sample containing only the ester (and water for the 'wet' test) was heated under the same conditions.

5.2 Monitoring of the reaction progress

Three methods of monitoring the progress of the phosphonate-iron reactions were used. Of these, two were wholly instrumental, i.e. infrared absorption spectrometry and ^{31}P n.m.r. whilst the third was a combination of wet chemical and instrumental analysis being the method used for the analysis of the iron content.

Whilst it was found that each of these methods could be used to follow the progress of the reactions, in the later experimental work only the analysis for iron content was employed. Both the infrared and ^{31}P n.m.r. suffered from a fairly involved preparative stage. Obtaining the data from the infrared spectra was, as will be seen, a time consuming task. The necessity of despatching the samples to a different site (Kings College, London) for ^{31}P n.m.r. analysis would have introduced a long delay in obtaining the data for each experiment had this method been chosen. Although the chemical digestion of the samples for iron analysis took a few hours, batch processing meant that this corresponded to only 10 minutes per sample analysed. Accordingly the experimental reactions of phosphonates with iron were monitored by measurement of the dissolved iron content.

5.2.1 Measurement of dissolved iron content

As outlined above iron content analysis was found to be the most convenient method of following the reaction progress.

The analysis was carried out by chemical digestion of the sample followed by atomic absorption spectrometry to measure the iron content.

A sample of the reaction product (0.05 to 0.1g) was accurately weighed (±0.0001g) into a 250 cm^3 Erlenmeyer Flask, 15 cm^3 'Analar' nitric acid and 5 cm^3 60% 'Analar' perchloric acid were added and the sample heated for 2-3 hours, at a gentle boil on a hotplate. The solutions were then allowed to cool, transferred to a 100cm^3 volumetric flask and diluted to volume with distilled water. A 'blank' solution was prepared with each set of samples, by heating together the acids alone.

To analyse the samples taken from the tests carried out in liquid paraffin solutions a larger sample was required. Therefore for a 20% ester solution in paraffin a sample weight of 0.25 to 0.5g was taken. These oil solutions were digested using 50cm^3 of 'Analar' nitric acid and 5cm^3 of 72% 'Analar' perchloric acid.

Analysis of the iron content of these solutions was made using Baird Alpha 1 and Alpha 3 atomic absorption spectrometers. For each set of samples analysed, a series of concentrations in the range 0.25 to 10ppm Fe were prepared by dilution of a 1000 ppm 'Analar' spectrometric standard solution. The concentration range used is the optimum range for the analysis of iron on the spectrometers employed.

(The sample weight range used was also fixed by the need to have the iron concentration within this optimum range). The spectrometers were fitted with iron element hollow cathode lamps thus making the absorbances selective for iron. The light output of these lamps is the emission from excited iron atoms, corresponding to the frequency of light absorbed by the iron atoms introduced from the sample into the flame of the spectrophotometer.

The standards, test samples and blanks were introduced to the flame through a sampling tube. The absorbances obtained were recorded from the digital readout once a steady reading had been obtained. Distilled water was run between each sample to purge the machine of any contaminant and also to check if any "zero-drift" had occured.

Using the absorbances obtained for the standard solutions, calibration graphs of absorbance against iron concentration (in ppm) were produced. A typical example of this is shown in Figure 5.2. Using these calibration graphs, the absorbances obtained for the samples were converted to concentrations of iron in p.p.m. From these figures, the iron concentration of the original sample, expressed as a percentage, was obtained as follows:-

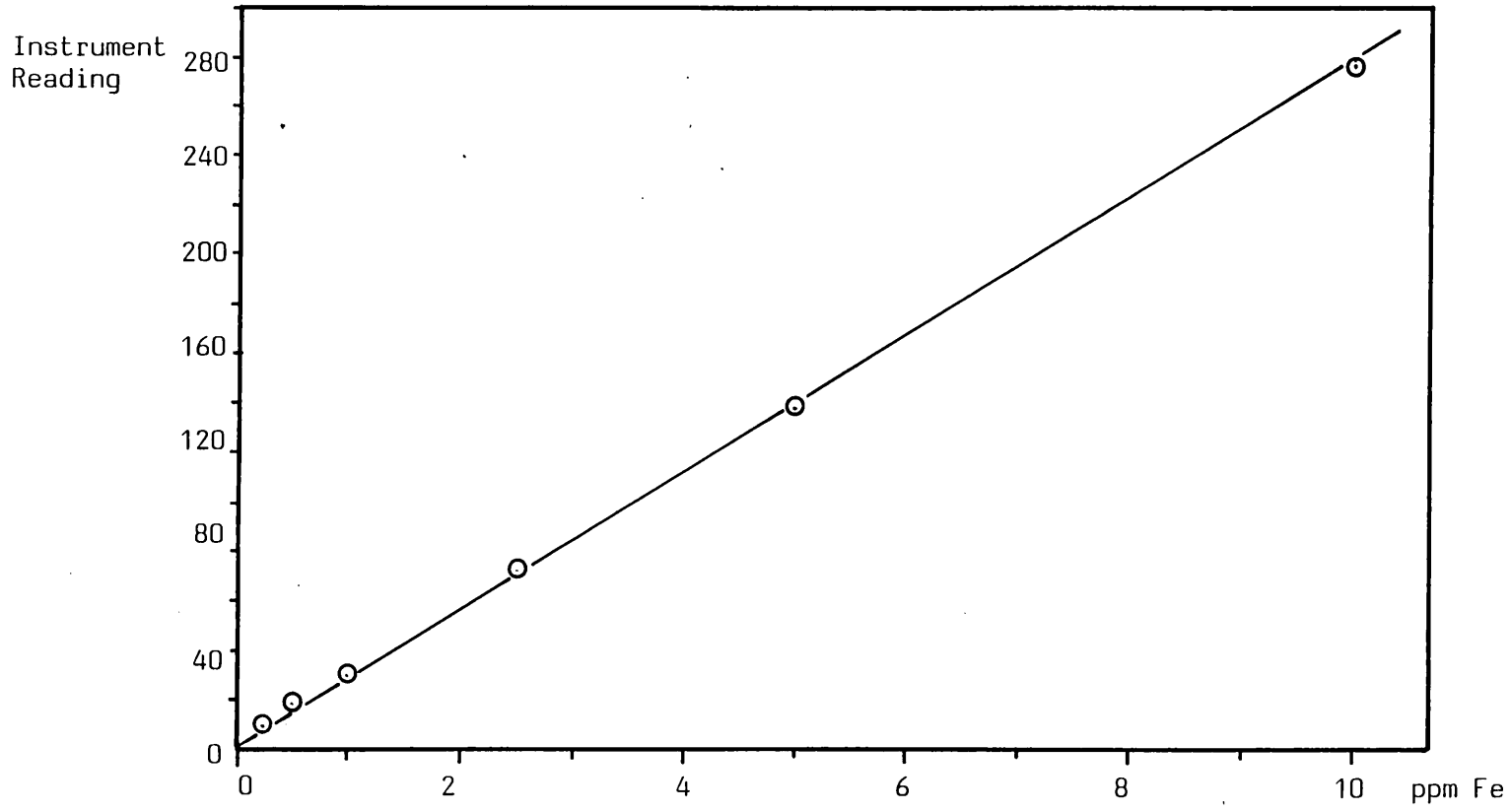


Figure 5.2 Typical calibration graph - Iron by Atomic Absorption Spectrophotometry

The concentration obtained from the calibration graph is in p.p.m. (mg/l). A concentration of 1 ppm (100 mgl^{-1}) represents 1 x 10^{-4}g of iron present in the 100 cm^3 solutions to which each digested sample is diluted. The iron concentration (expressed as a percentage) of the original sample is thus obtained by dividing the weight of iron in the $100cm^3$ flask by the sample weight and multiplying by 100:-

$$\% \text{ Fe} = \frac{\text{ppm} \times 10^{-4}}{w} \times 100$$

$$\% \text{ Fe} = \frac{\text{ppm}}{w \times 100}$$

where % Fe = iron concentration expressed as a percentage of the original sample.

ppm = concentration of iron in ppm

w = weight of digested sample

The method described above for the analysis of iron was based on a commercially used method for the quantitative analysis of tin in di-, tri- and tetra-butyl tin esters (119). It has also been found to be effective for the determination of calcium, magnesium and zinc in formulated oils.

5.2.2 Infrared spectrophotometry

In the infrared spectra of the products obtained from the reaction of the phosphonates and iron powder, a strong absorbance can be seen at 1160 cm^{-1}. The amount of this absorbance increases with the time of heating.

Figure 5.3 shows the infrared spectra recorded for a sample of dihexyl phosphonate after heating in the presence of iron powder at 180°C for 180 minutes, and for a sample of (unheated) dihexyl phosphonate. The increased absorbance at 1160 cm^{-1} can be clearly seen in the upper spectrum. The significance and origin of this absorbance will be discussed further in chapter 6.

To use infrared absorption spectrometry as a means of following the progress of the reaction, the absorbance must be first obtained from the spectrum. The absorbance at a wavenumber is a measure of the concentration of the species under observation (or more precisely of the number of bonds vibrating by absorption of the incident radiation). Absorbances are related to the concentration of absorbing species by the Broguer-Beer law (120) which may be written as:

$$A = a.b.c$$

where A is the absorbance

a is the absorbitivity of the species

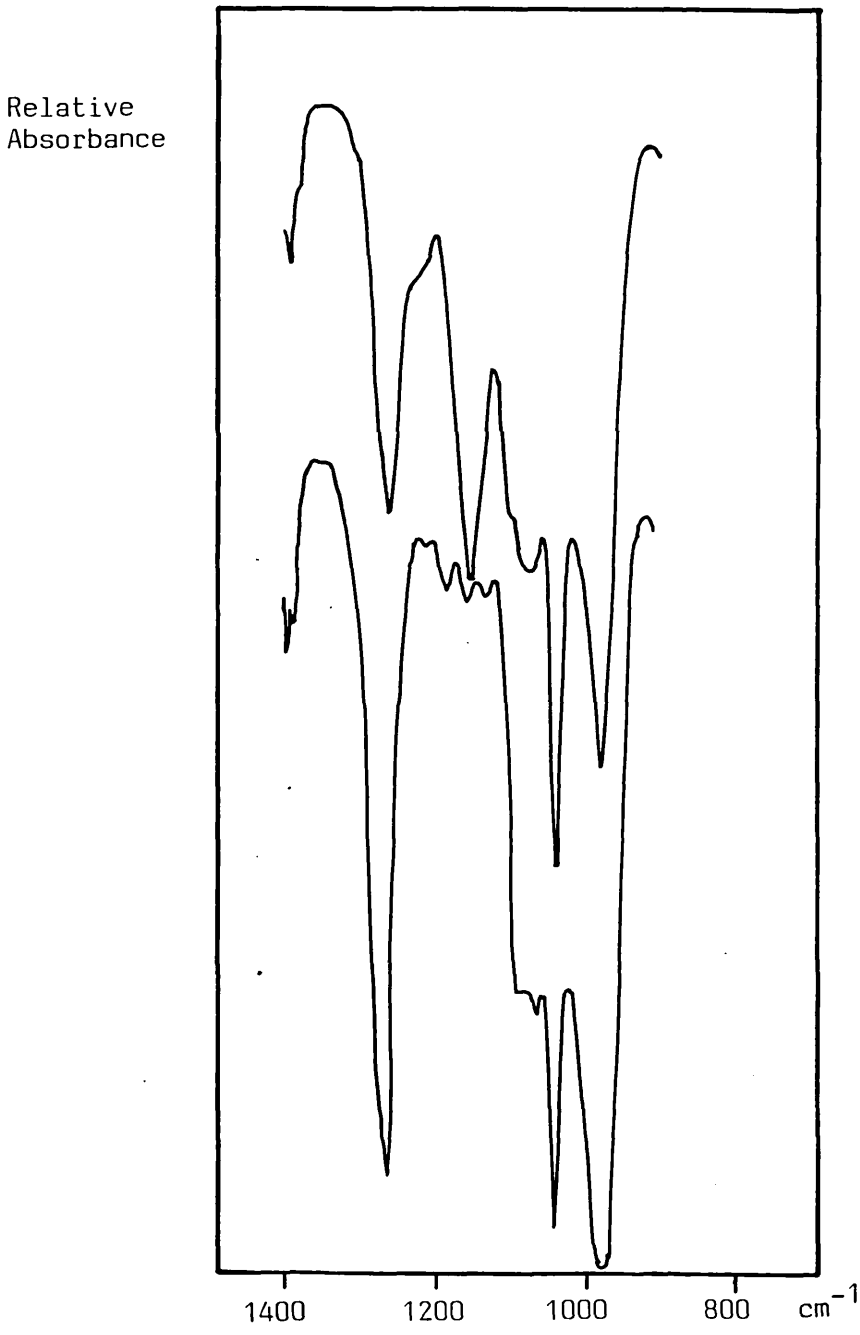
b is the constant related to the optional path length

c is the concentration of the species

The absorbance cannot usually, however, be directly measured from the spectrum obtained. The absorbance is defined as the logarithm of the reciprocal of the transmittance, where

$$A = \log \frac{Io}{I}$$

Figure 5.3 Infrared spectrum of dihexyl phosphonate after heating with iron (upper spectrum) and unheated dihexyl phosphonate (lower spectrum)



The term Io/I is the transmittance, where Io is the intensity of incident radiation, and I is the intensity of radiation transmitted by the sample. However the PE599, in common with many infrared spectrophotometers, presents the data in the form of percent transmission. Absorbances are obtained by measuring the incident radiation intensity Io and the transmitted light intensity I as shown in figure 5.4, and then taking the logarithm of the ratio Io/I (121).

In order to use this method of analysis in a quantitative manner, the absorbance of this vibration at 1160 cm^{-1} was measured for a series of samples taken at different heating times. In recording the infrared spectra of the different samples, it was apparent that a variation in the absolute absorbance (at 1160 cm^{-1}) was occuring due to a variation in the film thickness of the sample cell. Consequently a measuring technique independent of the film thickness was developed.

To measure the absorbances, a baseline was constructed by drawing a line from the minima on either side of the absorbance peak. This standard quantitative technique (121) is shown in figure 5.5. By measuring the absorbance and comparing it with an absorbance which remained constant throughout the set of samples, a relative absorbance was obtained. Absorbances obtained at 1160 cm^{-1} were thus compared with those obtained at 2950 cm^{-1} (P-H) 2410 cm^{-1} (C-H) and 1260 cm^{-1} (P=O).

All spectra were recorded for 25% (w/w) solutions of the samples in benzene. This method was chosen because the samples were found to be increasingly viscous and rheopectic with increased heating times.

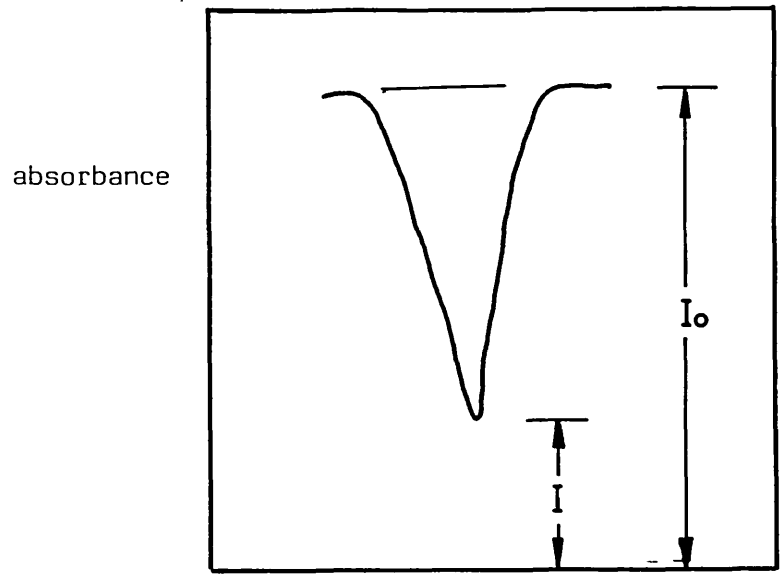


Figure 5.4 Method of measuring absorbances directly from the spectrum

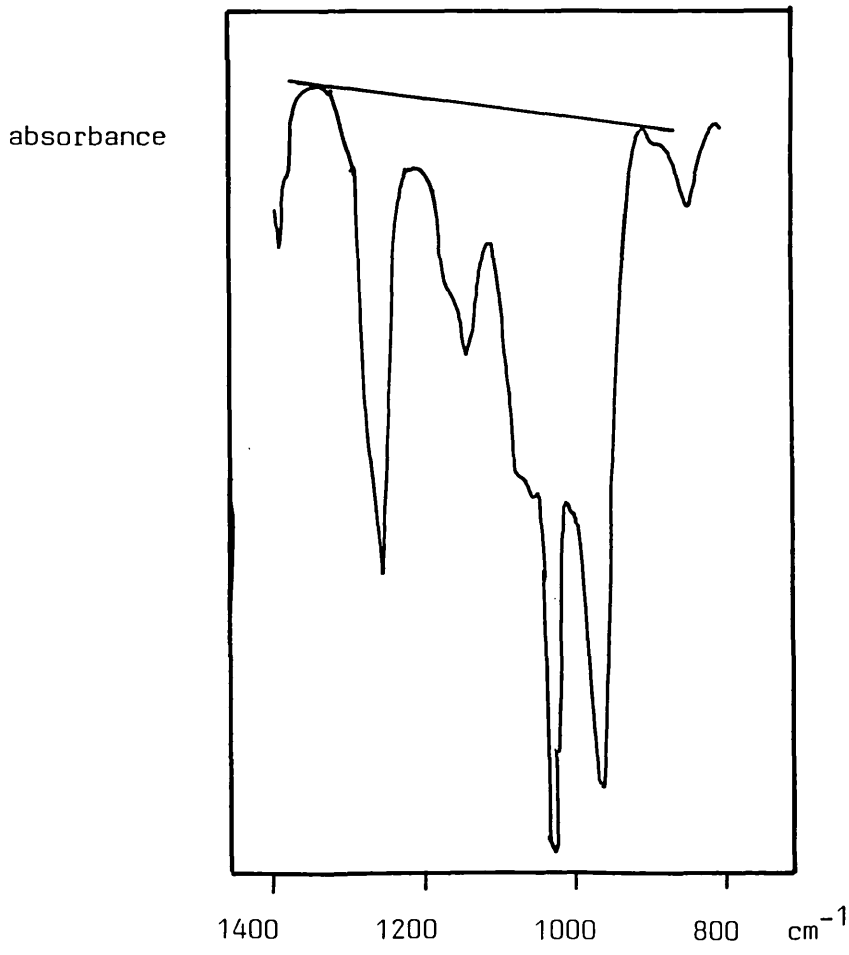


Figure 5.5 Method of construction of the spectral baselines for measuring absorbances in the dihexyl phosphonate-iron reaction product spectra

Thus injection of the later samples into an infrared cell was not possible, and preparation of good films of these later samples was made difficult by their rheopecticity, i.e. the sample solidified between the sodium chloride plates when these were squeezed together to produce a capillary film.

To prepare the solutions 0.5g of the sample was accurately weighed into the sample tube, benzene was accurately weighed into the sample tube, sufficient to prepare a 25% (w/w) solution. Once homogeneity of the sample was achieved, the solution was injected into an infrared liquid cell fitted with a 0.25mm teflon spacer (thereby giving a sample cell of path length approx. 0.25mm). Infrared spectra were than recorded for each sample in the range 4000 to 600 cm^{-1}. The absorbances were measured as described above.

5.2.3 ^{31}P n.m.r. spectra

^{31}P n.m.r. spectra were recorded for both selected samples of the ester-iron powder reaction products and for a series of samples of a dihexyl phosphonate iron powder reaction product. The spectra were recorded at King's College, London. Further details of n.m.r. and the equipment may be found in section 4.2. Each signal in the ^{31}P n.m.r. indicates the presence of a phosphorus atom in its own characteristic electronic environment.

To use ^{31}P n.m.r. as a semi-quantitative technique, spectra were recorded for a series of samples obtained by heating dihexyl phosphonate with iron powder, and the absorbance of each signal measured. The samples were prepared by heating 10.5g of dihexyl phosphonate with 1.4g of iron powder under a nitrogen blanket/agitation. The samples were taken every 20 minutes for 6 hours.

Each sample was allowed to cool, and a smaller sample (0.250g) was transferred to a clean sample tube. This smaller sample was despatched for ^{31}P n.m.r. analysis.

Since the signal obtained is proportional to the number of nuclei giving rise to that signal, by comparing the 'new' signal obtained in the spectrum with the signal due to the phosphorus atom of dihexyl phosphonate, a measure of the proportion of the species giving rise to the 'new' signal is obtained. Measurement of the signals was made initially be obtaining the ratio of the peak heights printed out by the signal analyser. A problem with this method is that no peak height is printed out for the spectra of the earlier samples. To counter this, the peak heights on the printed spectra were measured using a ruler and the ratio of these peak heights was used. Both peak heights were plotted against the time of sampling.

5.3.4 Summary

Of the three methods used to follow the progress of the reaction, only one, the analysis of dissolved iron content, proved to be convenient for regular analysis of the samples obtained. Both infrared absorption spectrophotometry and ^{31}P n.m.r. techniques proved too involved and open to greater inaccuracies than did the analysis for iron content. They were however, used to provide further insight into the reaction that occurred.

5.3 Results and Discussion

5.3.1 General reaction result

The heating of dialkyl and diaryl phosphonates in the presence of iron powder was found to give rise to a wax-like product. Samples of the reaction mixture show increasing viscosity and rheopecticity as the time of heating increases. (A rheopectic fluid is one in which the viscosity rises as stress is applied, for example by stirring, (122)).

From the methods of analysis used to follow the progress of the reaction and observations made on the samples taken, the reaction product was shown to be a ferro-organophosphorus polymer. As the sampling time increased the iron content rose and the sample became more viscous. This rise in vicosity is in itself indicative of the polymeric nature of the reaction product. Furthermore, when infrared spectra of successive samples were recorded it was found that the later samples took increasingly long times to dissolve in the benzene solvent. A characteristic of polymers is their slow rate of dissolution. The organic nature of the reaction product is clearly illustrated by the solubility in organic solvents (e.g. benzene, toluene and chloroform). The presence of phosphorus in a different chemical environment to that of the original phosphonate, is shown by the new signal obtained in the ^{31}P n.m.r. spectrum.

This polymerisation reaction was observed for samples of dihexyl, dioctyl, didodecyl, diphenyl, and bis Octyl-phenyl phosphonates. The rate of reaction, as measured by determining the increase in iron content with time of heating, was found to be dependent on the organic portion of the ester.

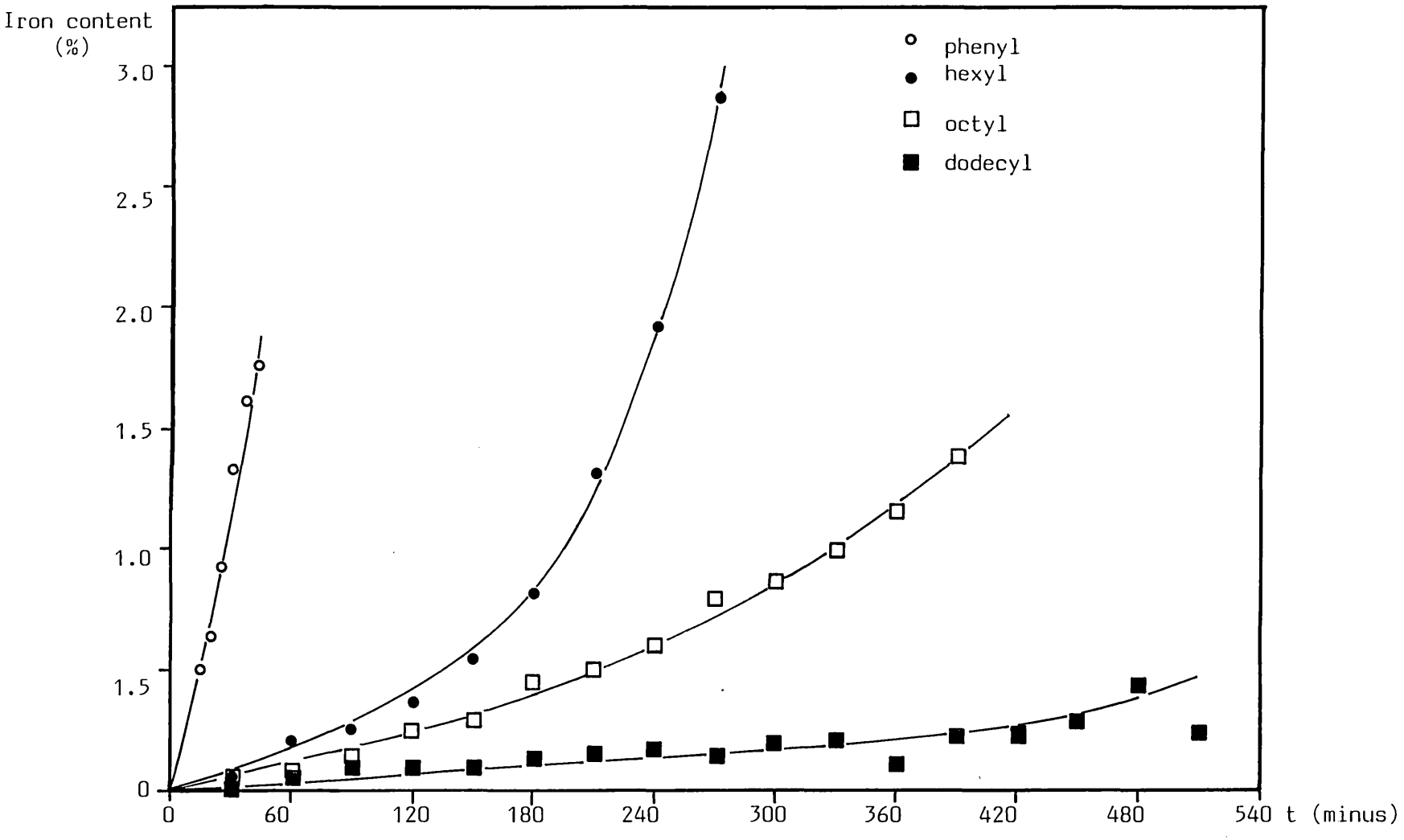


Figure 5.6 Iron concentration with time for four disubstituted phosphonates on heating with iron under nitrogen at 157°C

Figure 5.6 shows the difference in reactivities for these phosphonates. The iron content of samples from the reaction mixtures, heated under nitrogen, at 155°C are plotted against the time of heating (i.e. sampling). It can be seen from these results that the order of reactivity is:

phenyl > hexyl > octyl > dodecyl

5.3.2 Reactions in a semi-closed vessel

Figure 5.7 shows the infrared absorption spectrum recorded for the condensate obtained by heating dioctyl phosphonate in the presence of iron powder at 150°C. For comparison figure 5.7 also shows the infrared spectra recorded for samples of octan-1-ol and dioctyl phosphonate.

Visual comparison of the spectra indicates that the 'condensate' spectrum has absorptions in common with each of the others. (It should be realised that the absorptions common to both the octan-1-ol and the dioctyl phosphonate, arise from the octyl group present in both compounds). Table 5.3 lists and assigns the absorbances for all three spectra.

It can be seen from table 5.3 that the spectrum of the condensate has absorbances in common with both the octanol and dioctyl phosphonate, other than those absorbances common to all three spectra. The condensate would appear to be a mixture of dioctylphosphonate and octanol. Comparison of the 'shape' of some of the absorbance peaks further points to this conclusion.

Figure 5.7 Infrared spectra of dioctyl phosphonate (DOP) Octanol (O) and condensate (C) of semi-closed heating tests

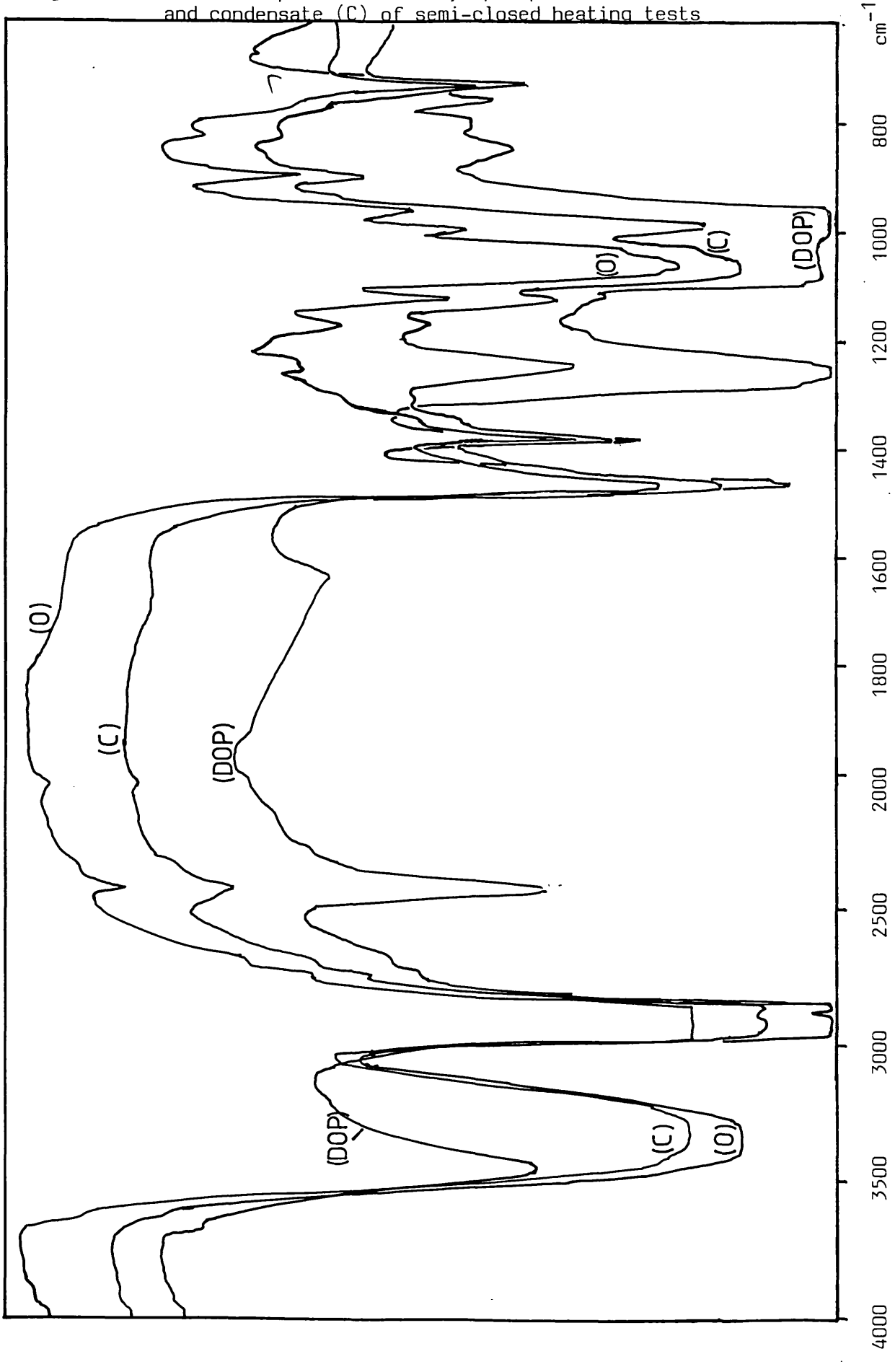


Table 5.3

Infrared absorbances for Octanol, Dioctylphosphonate and "reaction condensate"

Octanol	DOP	Condensate	Assignment
3370 - 3260	3280	3380 - 3280	H- bonding
2960 - 2840	2960 - 2840	2960 - 2840	C-H stretch
	2420	2420	P-H
	1648		
1468	1468	1468	C-H deformation
1380	1380	1380	C-O stretch
	1255	1245	P-O
1168		1170	O-H deformation
1120	1120	1120	
1055		1065 - 1050	
	1070		P-O-C
990	980	985	P-O-C (in DOP)
958			
890		892	
	850		
820		820	
	800		
	760	770	
725	725	725	
660-590			
	560	565	
530		530	

The hydrogen bonding absorption in the condensate has a similar shape to that found in the octanol spectrum, whereas in the 1100 - 900 cm^{-1} regron, a double absorbance is recorded, similar to the two P-O-C vibrations recorded in the dioctyl phosphonate spectrum. All three spectra have absorbances in common at 1470, 1380 and 1120 cm^{-1} and the relative absorbances are fairly constant in all three spectra. The main difference between octanol and dop in this region is the strong P = O absorbance present in the dop spectrum at 1255 cm^{-1}, this absorbance appears in the condensate spectrum, but is a much weaker absorbance relative to the absorbances at 1470, 1380 and 1120 cm^{-1}.

The polymerisation reaction of phosphonates and iron would appear to proceed with the evolution of the parent alcohol. This is supported by the observation that in the tests involving diphenyl and bis Octyl-phenyl phosphonate (where the parent alcohols are solids) a crystaline material collected on the upper (cooler) parts of the test-tubes.

5.3.3 The effect of temperature

The polymerisation reaction, which was found to occur between phosphonates and iron powder, increased in rate as the temperature was raised.

Figure 5.8 illustrates the higher rates of reaction encountered at elevated temperatures. The iron content was measured for samples taken from reaction mixtures of dihexyl phosphonate and iron powder heated at 117°, 140°, 160° and 180°C under nitrogen.

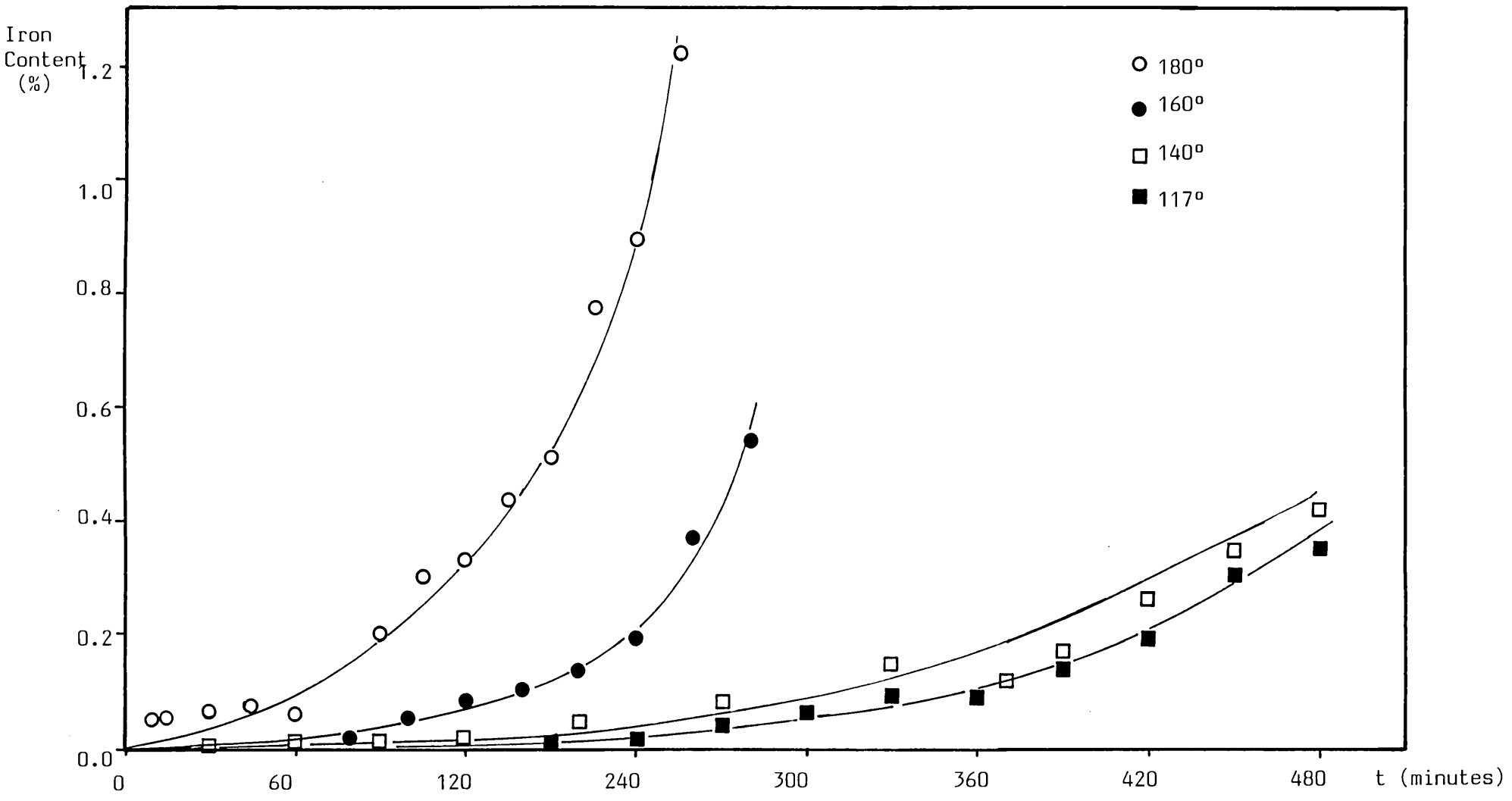


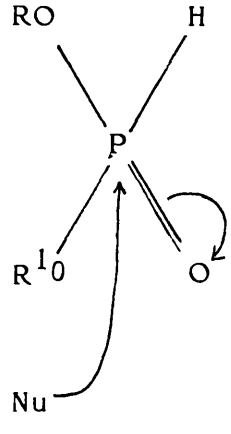
Figure 5.8 Effect of temperature on the rate of the dihexyl phosphonate-iron reaction

5.3.4 The effect of oxygen

The use of oxygen as agitator gas instead of nitrogen, leads to higher rates of reaction. This was seen both by measurement of the iron content and by observation of the increased viscosity of samples from the oxygenated reaction compared to those taken from the nitrogenated reaction. This increase in reactivity was observed for both dihexyl and diphenyl phosphonates.

Figures 5.9 and 5.10 compare the rise in iron content with time for nitrogen or oxygenated samples of dihexyl phosphonate and diphenyl phosphonate respectively.

The role of oxygen in the enhancement of the reaction rate indicates that an oxidation step is involved, in the mechanism of the reaction. Further, it indicates that the oxidative process is rate-determining (i.e. the slowest 'step' of the reaction sequence). Dialkyl and diaryl phosphonates have a high stability to oxidation compared to the tri substituted ester (54,55). Their reactions are characterised by nucleophilic attack (124) at the phosphorus atom (125) as illustrated below:-



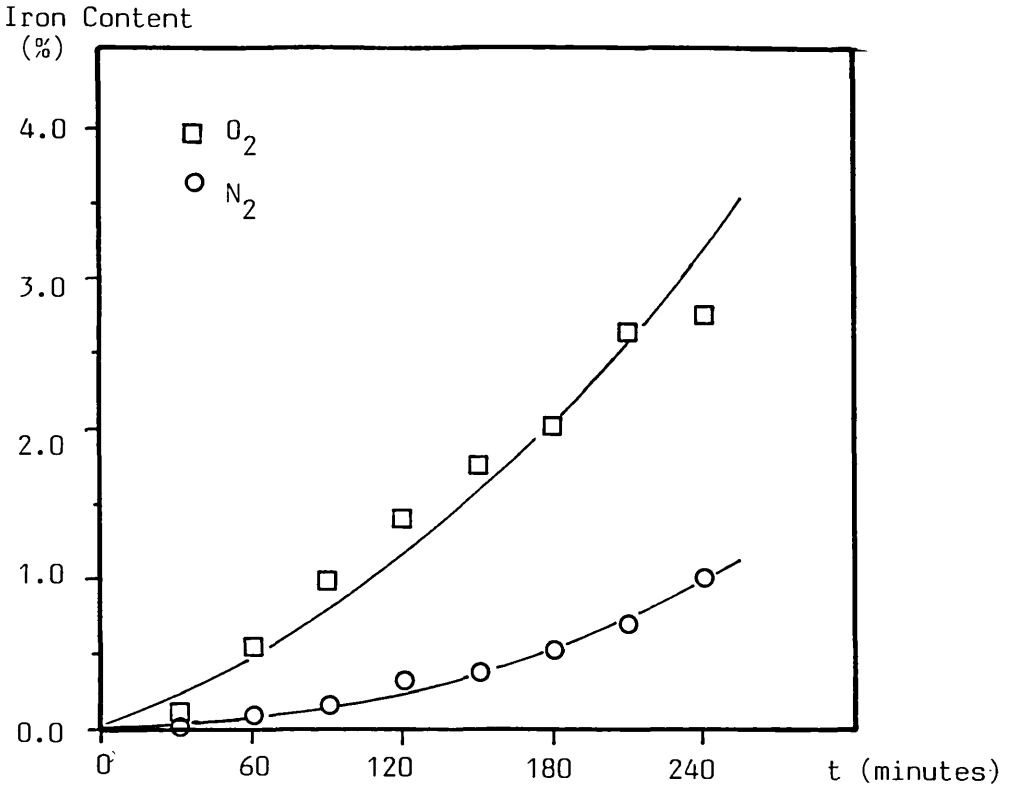


Figure 5.9 Effect of oxygen on the rate of the dihexyl phosphonate-iron reaction

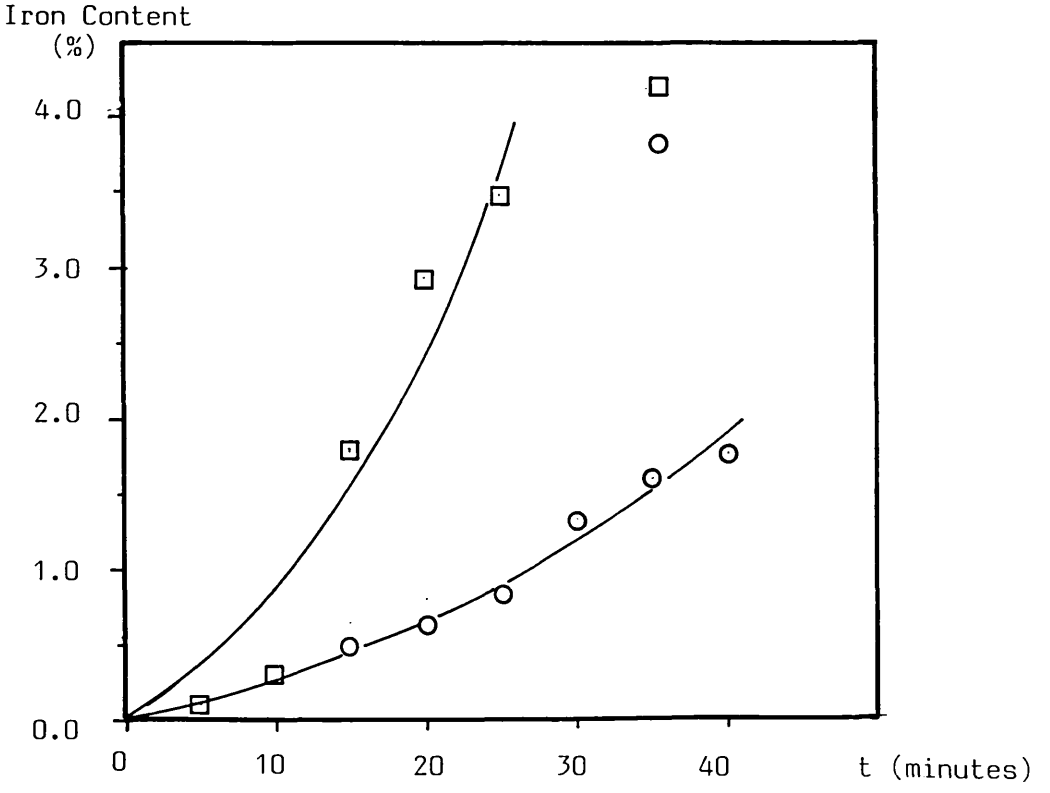


Figure 5.10 Effect of oxygen on the rate of the diphenyl phosphonate-iron reaction

In this sense, the phosphonates may be considered as being similar to ketones, the typical reactions of which are nucleophilic addition (126).

The oxidation of iron proceeds readily, especially in the presence of oxygen and/or water (127). In particular iron (II) is oxidised in neutral solutions to iron (III) when molecular oxygen is present (128) although the mechanism is far from resolved (129).

5.3.5 Effect of water

The addition of water to the phosphonate-iron reaction was found to increase the rate of reaction. This increase in reactivity was found to be dependent upon the amount of water present.

Figure 5.11 compares the rise in iron content for reaction mixtures of dihexyl phosphonate and iron powder under 'wet' and 'dry' conditions. The effect of varying the amount of water present can be seen by comparing the reactivities for the two 'wet' conditions. A faster rise in iron content is observed in the high (1.37%) water content sample compared to the low (0.25%) water content sample.

Similarly the addition of water to the reaction of diphenyl phosphonate and iron, was found to enhance the rate of reaction. The relative rates of reaction for 'dry' and 'wet' (0.3%) samples of diphenyl phosphonate heated under nitrogen at 157°C are shown in figure 5.12.

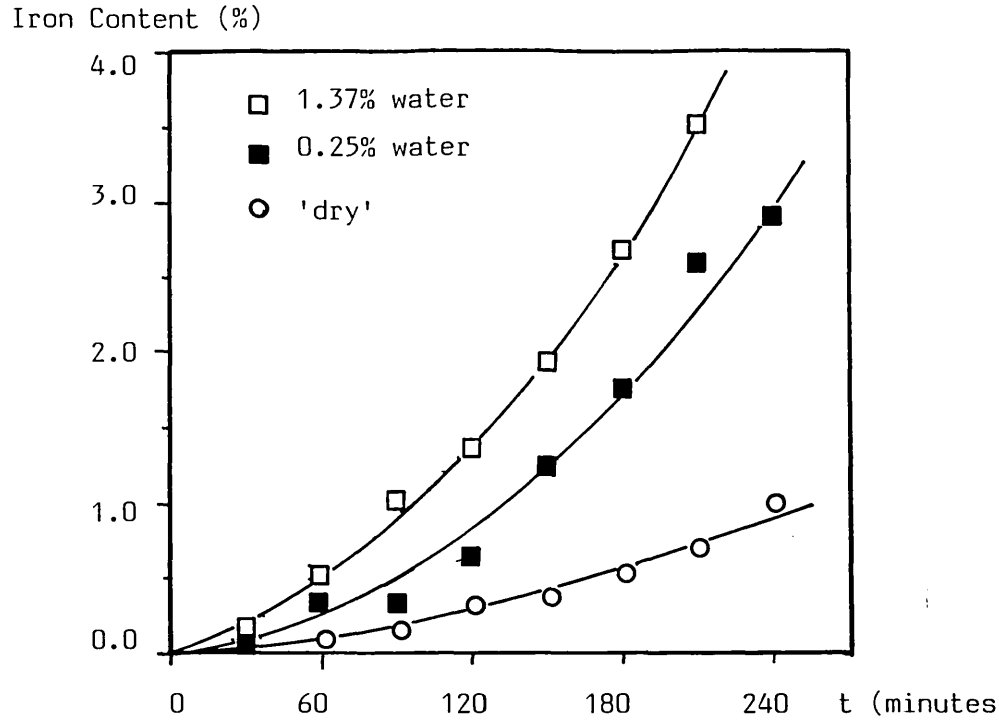


Figure 5.11 The Effect of water on the dihexylphosphonate - iron reaction

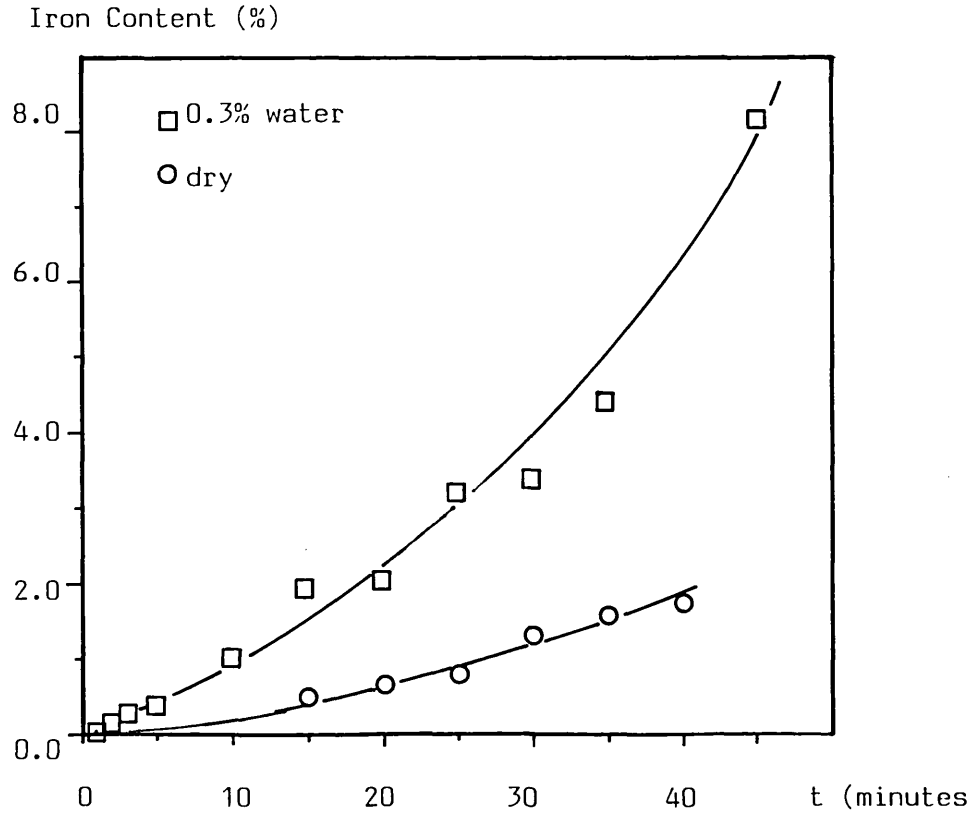


Figure 5.12 The Effect of water on the rate of the diphenyl phosphonate-iron reaction

In the preceding section it was shown that the presence of oxygen gave rise to faster rates of reaction, for 'dry' samples of both dihexyl and diphenyl phosphonates. The presence of oxygen was found to further increase the rate of rise of iron content in 'wet' samples of dihexyl phosphonate and diphenyl phosphonate. Figure 5.13 shows the rise in content with time for samples of dihexyl phosphonate containing 0.26% water under nitrogenated and oxygenated conditions. The results for diphenyl phosphonate are shown in figure 5.14.

In view of the results obtained when oxygen is present, it is not surprising that the presence of water also gave rise to higher rates of reaction. The mechanism by which water enhances the rate of reaction is however not so clear. There are two distinct mechanisms by which water may enhance the rate of reaction, either or both of which may be involved.

The presence of water will favour the oxidation of the iron metal to Fe^{II} and Fe^{III} (127). The oxidation of Fe^{II} to Fe^{III} readily occurs in the presence of water and oxygen even in neutral solutions (128, 129).

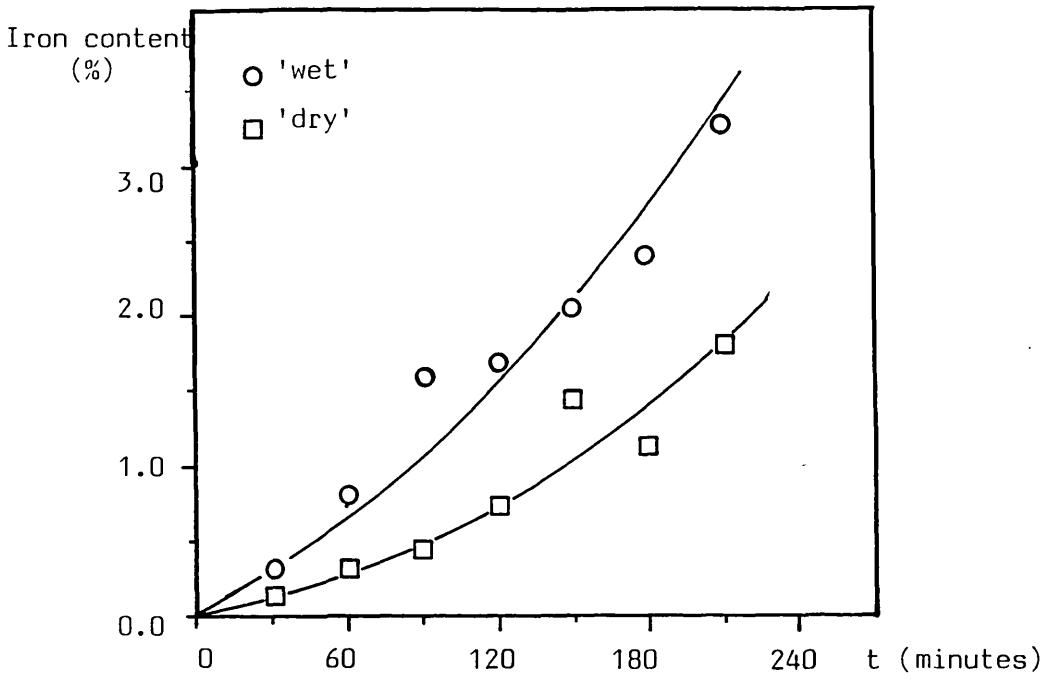


Figure 5.13 The Effect of oxygen and water on the rate of the dihexyl phosphonate-iron reaction

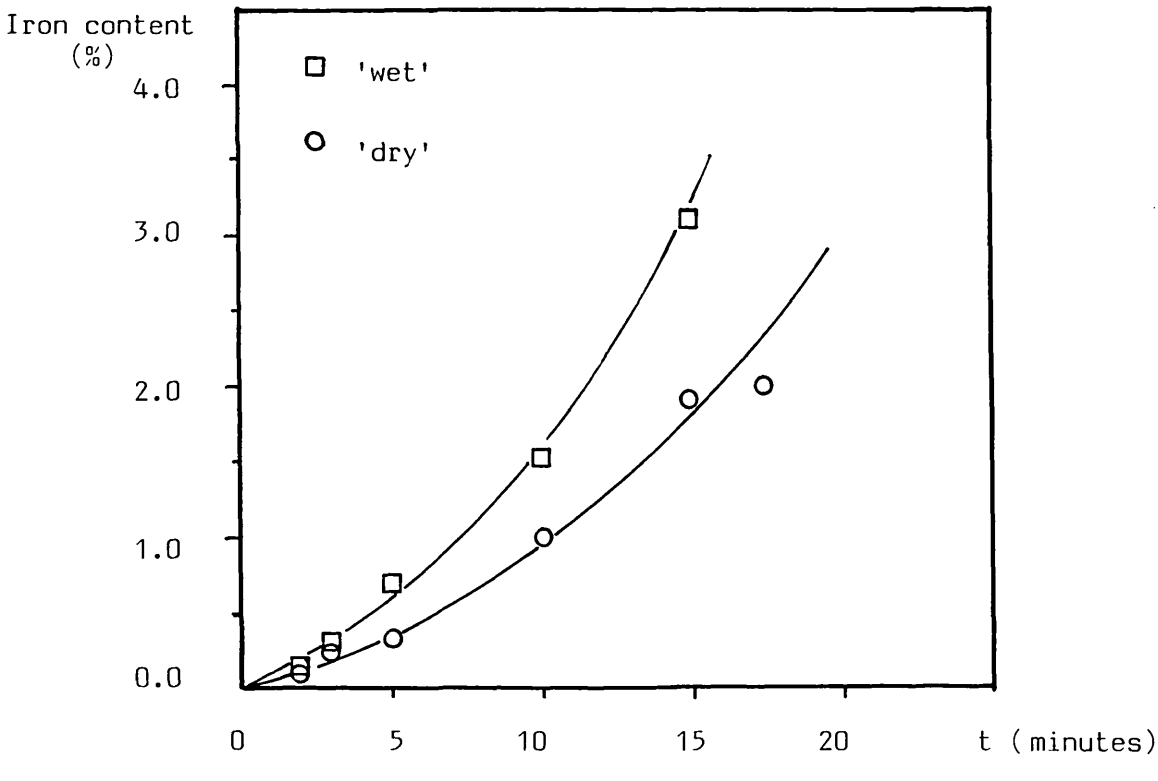
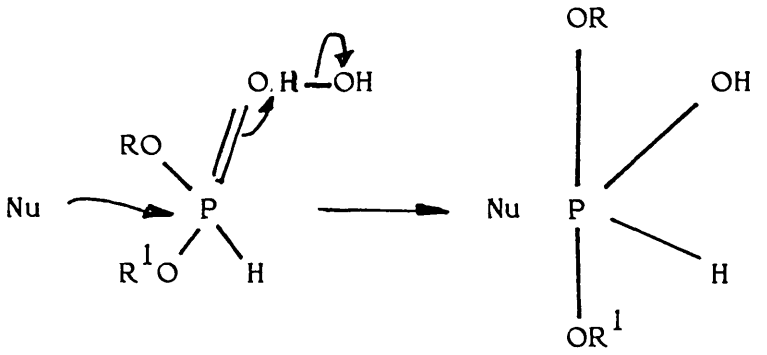


Figure 5.14 The effect of oxygen and water on the rate of the diphenyl phosphonate-iron reaction

Another mechanism of involvement for water is via its ability to behave as a 'Lewis Acid' (i.e. an electron acceptor) (130) thus aiding nucleophilic attack on the phosphonate, as shown below.



Since the reactions were carried out at above 100°C and the increase was observed throughout, it is reasonable to conclude that the water molecules are firmly bound. This would most likely involve co-ordination to the iron, readily forming stable hexa aquo ions $[Fe(H_2O)_6]^{2+}$ and $[Fe(H_2O)_6]^{3+}$ (131).

5.3.6 Reaction with oxidised and reduced iron

The results of the reactions of dihexyl phosphonate with specifically oxidised and reduced samples of iron powder gave further insight into the mechanism by which oxygen increases the rate of reaction. Oxidation of the iron powder by heating in air gave a relatively faster rate of reaction than was obtained for a 'normal' (i.e. as received) iron sample. Reduction of the iron by hydrogen was found to give a relatively lower rate of reaction. These results are illustrated in figure 5.15.

The results show that the presence of a surface oxide is influential on the rate of reaction.

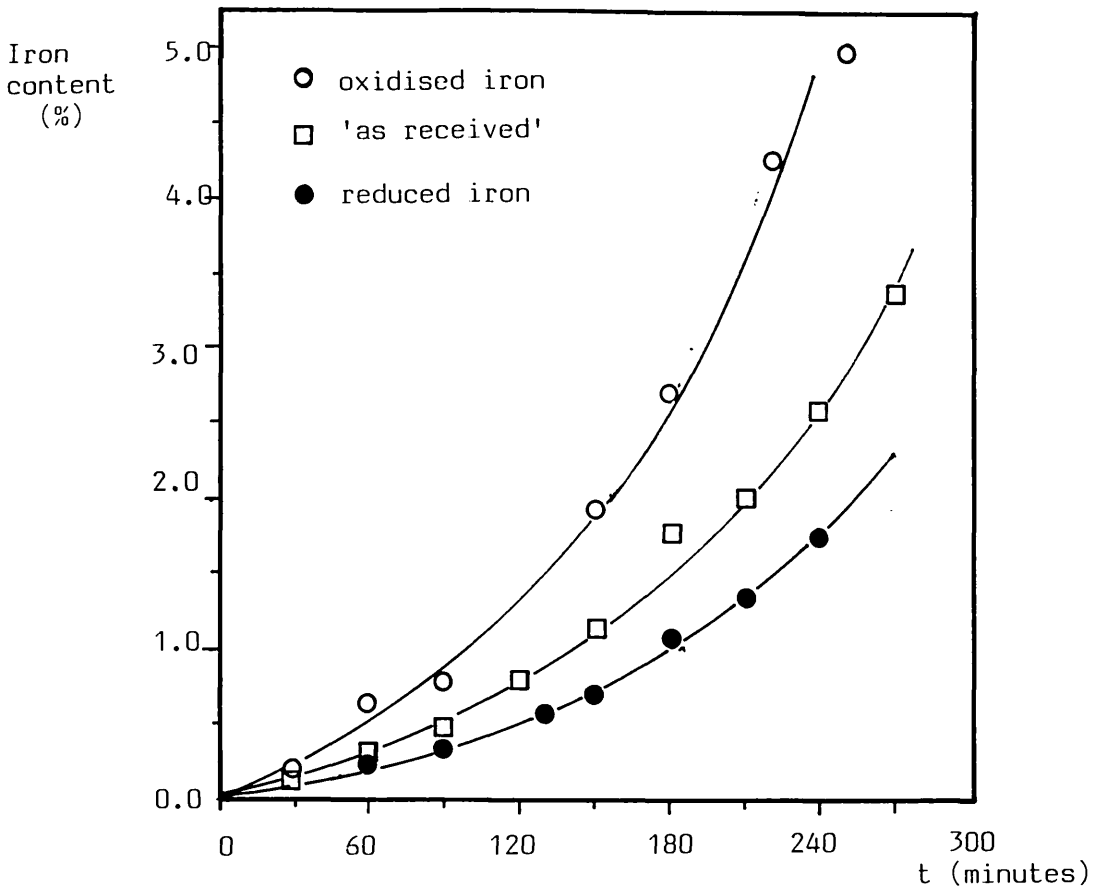


Figure 5.15 Effect of oxidation and reduction of the iron on the rate of the dihexyl phosphonate-iron reaction

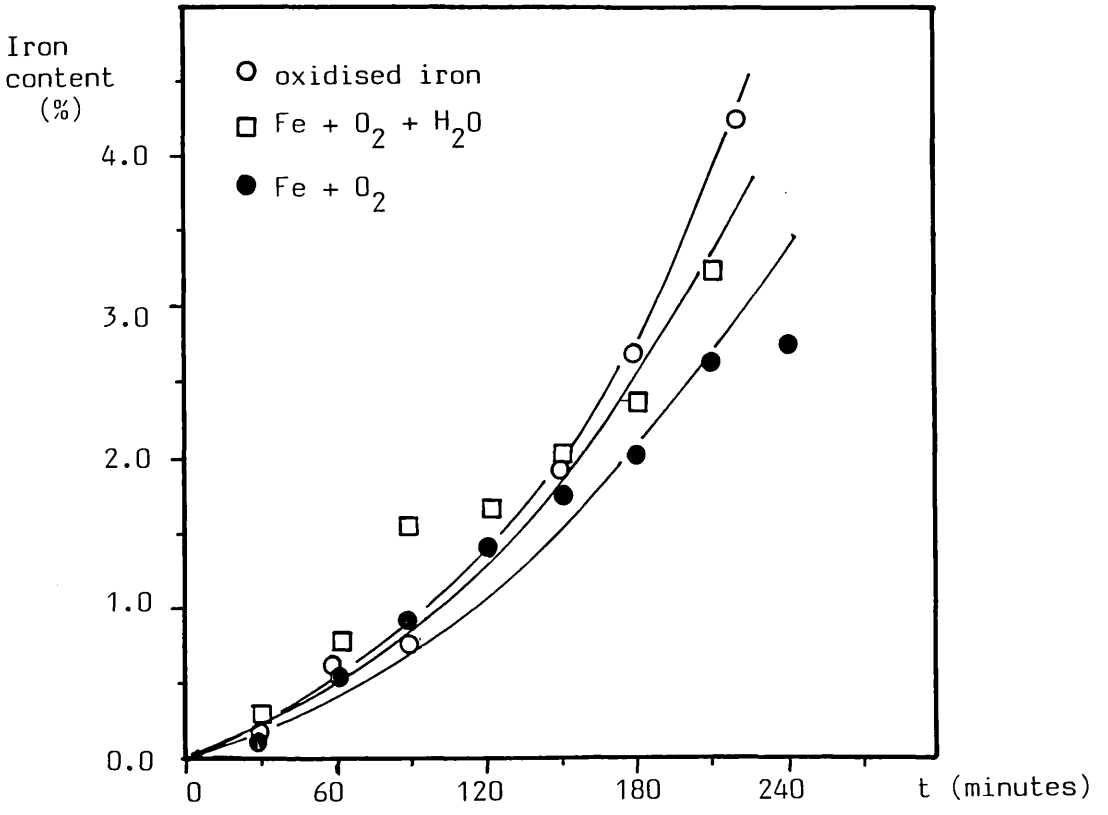


Figure 5.16 Comparison of the rates of reaction of dihexyl phosphonate with oxidised iron and with 'as received' iron in the presence of oxygen and/or water

The results obtained on the infuence of oxygen and water on the rate of reaction indicate that the mechanism of reaction involves oxidation of the metal. A comparison of the reaction rates of dihexyl phosphonate with the oxidised iron sample, and with iron (as received) in the presence of oxygen and of oxygen and water is made in figure 5.16. The oxidised iron has a similar rate of reaction to that obtained under oxygenated conditions. The rate determining steps in both these reactions involves the reaction of an oxidised iron species. The method of preparation of the oxidised iron sample (section 5.1.6) would be expected to produce an oxide layer consisting largely of hydrous iron (III) oxide FeO (OH) (123). Since the presence of oxygen gives rise to a similar rate of reaction to that obtained with an oxidised iron sample, the role of the oxygen must be to oxidise the iron metal and not the phosphonate.

The higher reactivity observed for a 'wet' oxygenated phosphonate-iron reaction mixture would appear to indicate that the water raises the reaction rate by acting as a 'Lewis Acid' and not by aiding the oxidation of the iron.

5.3.7 Reaction with Iron (III) oxide

Dihexyl phosphonate was found to undergo a similar reaction with iron (III) oxide, Fe_2O_3 as occurred with iron (metal) powder. The rate of reaction observed was found to be between those recorded for an 'oxidised' iron sample and for an 'untreated' iron sample.

Figure 5.17 shows the rise in iron content with time for samples of dihexyl phosphonate heated at 157°C in the presence of iron (III) oxide and with iron powder. The faster rate of reaction of 'oxidised' iron compared to iron (III) oxide is shown in figure 5.18.

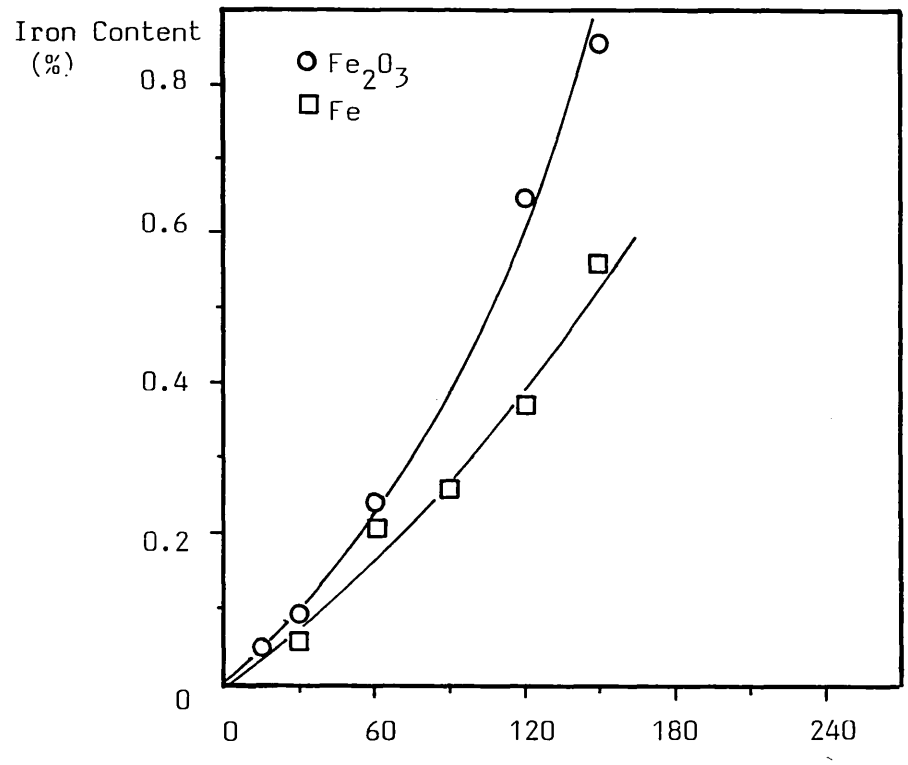


Figure 5.17 A comparison of the rates of reaction of dihexyl phosphonate with Fe_2O_3 and with Fe

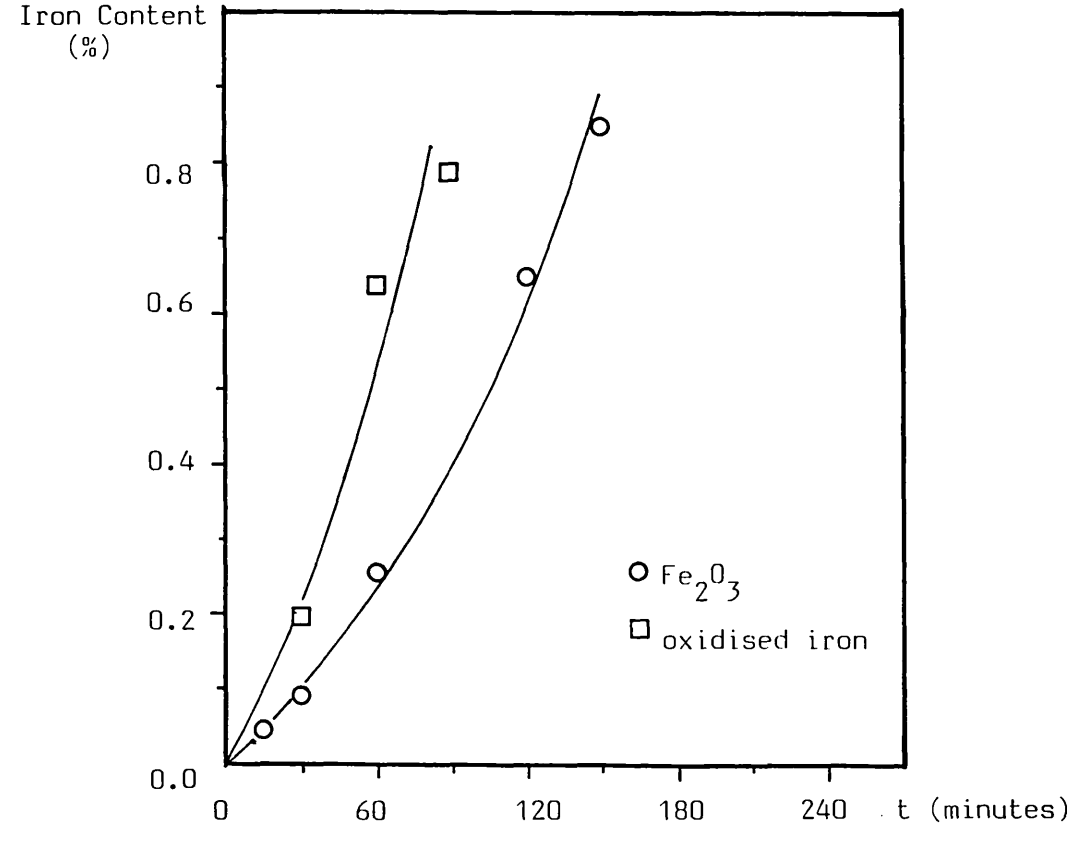


Figure 5.18 A comprison of the rates of reaction of dihexyl phsphonate with Fe_2O_3 and with oxidised iron

From these results, it is clear that the reaction of iron and phosphonates does not proceed through the anhydrous iron (III) oxide Fe_2O_3. The greater reactivity of this oxide, however, compared to 'untreated' iron would seem to indicate that iron (III) is involved in the reaction (but not as Fe_2O_3).

5.3.8 Effect of surface area

The reaction of dihexyl phosphonate with iron powders of different size fractions gave unexpected results. From the results obtained for the effect of oxygen and prior oxidation of the iron surface, it would be expected that reaction at the iron surface is important to the reaction kinetics. However as shown in figure 5.19 reactivity was found to increase with increasing particle size, that is with decreasing surface area.

To test these results, tests were carried out using iron foil in place of the different sizes of iron powder. Figure 5.20 compares the rise in iron content for samples of dihexyl phosphonate heated at 157°C in the presence of iron foils of different surface areas. Here the results are almost as expected, with reactivity increasing with an increase in surface area.

The explanation may rest with the assumption that the particles are spherical. It has been reported (132) that because of surface roughness effects, the actual surface can be over 18 times larger than the assumed surface area, for ilmenite particles in the size range 100-250 μ. Consequently the surface areas assumed for the iron powders may be considerably greater than the true surface area.

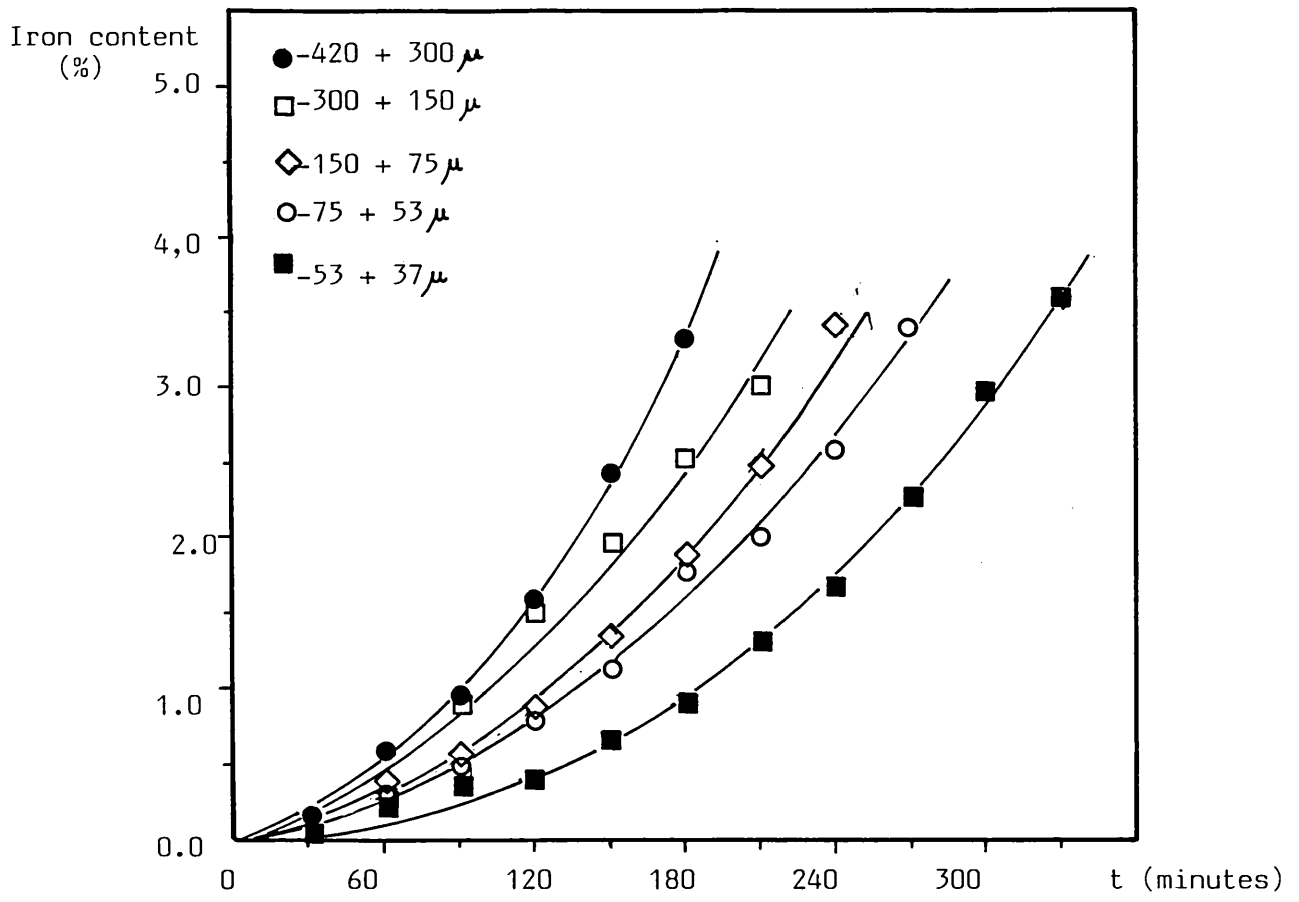


Figure 5.19 Effect of particle size of the iron powder on the rate of the dihexyl phosphonate-iron reaction

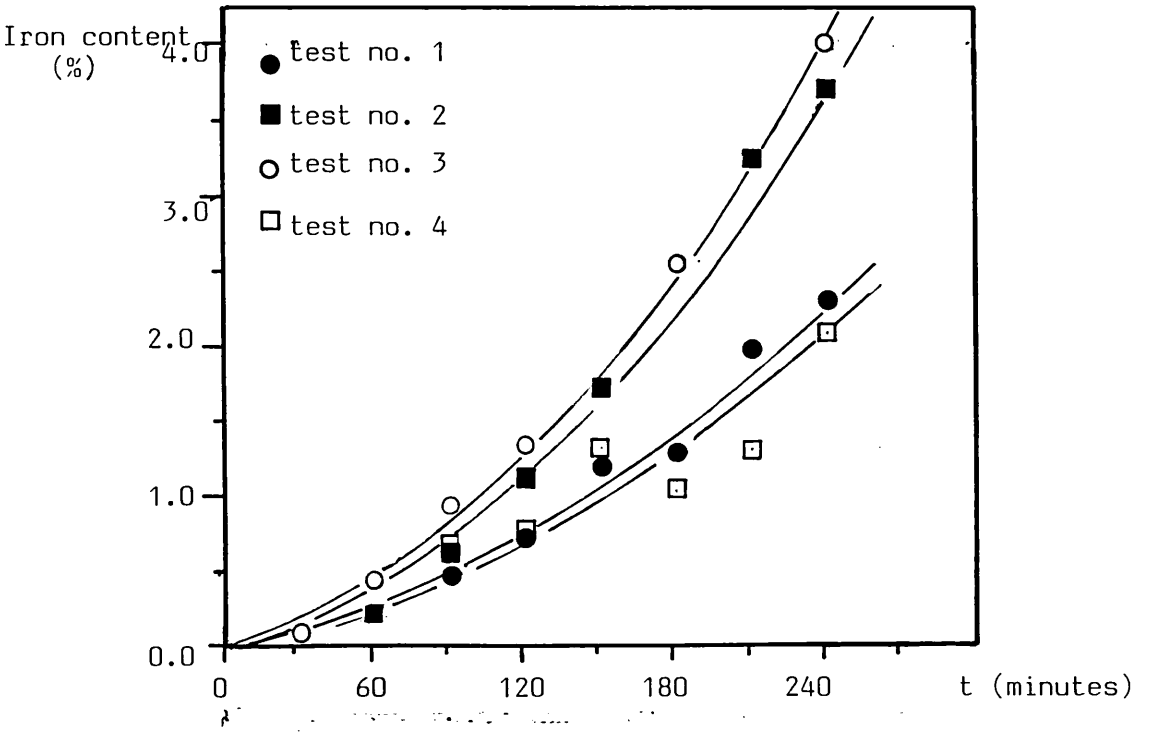


Figure 5.20 Effect of surface area of iron foil on the rate of the dihexyl phosphonate-iron reaction

5.3.9 Tests in liquid paraffin solution

Dihexyl phosphonate dissolved in liquid paraffin on being heated with iron powder undergoes a similar reaction to that recorded for those tests carried out with no liquid paraffin present. A major difference, however, was seen after approximately 120 minutes, when in all the tests in liquid paraffin, the iron concentration was seen to fall. Furthermore if the concentration of iron recorded is corrected by the dilution factor, the solutions of dihexyl phosphonate would appear to react faster than do 'neat' samples of the ester.

Figure 5.21 shows the rise in relative iron content (corrected by dilution factor) for 3% and 20% solutions of dihexyl phosphonate heated with iron at 155°C. These results can be explained by considering the nature of the ferro-organophosphorus polymer that is formed. In the early stages of the reaction the polymeric molecules will be fairly small (only a few monomer units) and will be soluble in the liquid paraffin, however as the reaction proceeds and the polymer units increase in length, their solubility will decrease and less polymer and correspondingly less iron will be present in the samples taken. In all the tests carried out, a viscous liquid residue was found in the test-tube at the end of the test, from which the liquid paraffin could easily be decanted. As no such residue was visible in the samples, the conclusion drawn was that the samples taken became increasingly unrepresentative of the true state of reaction towards the end of the test.

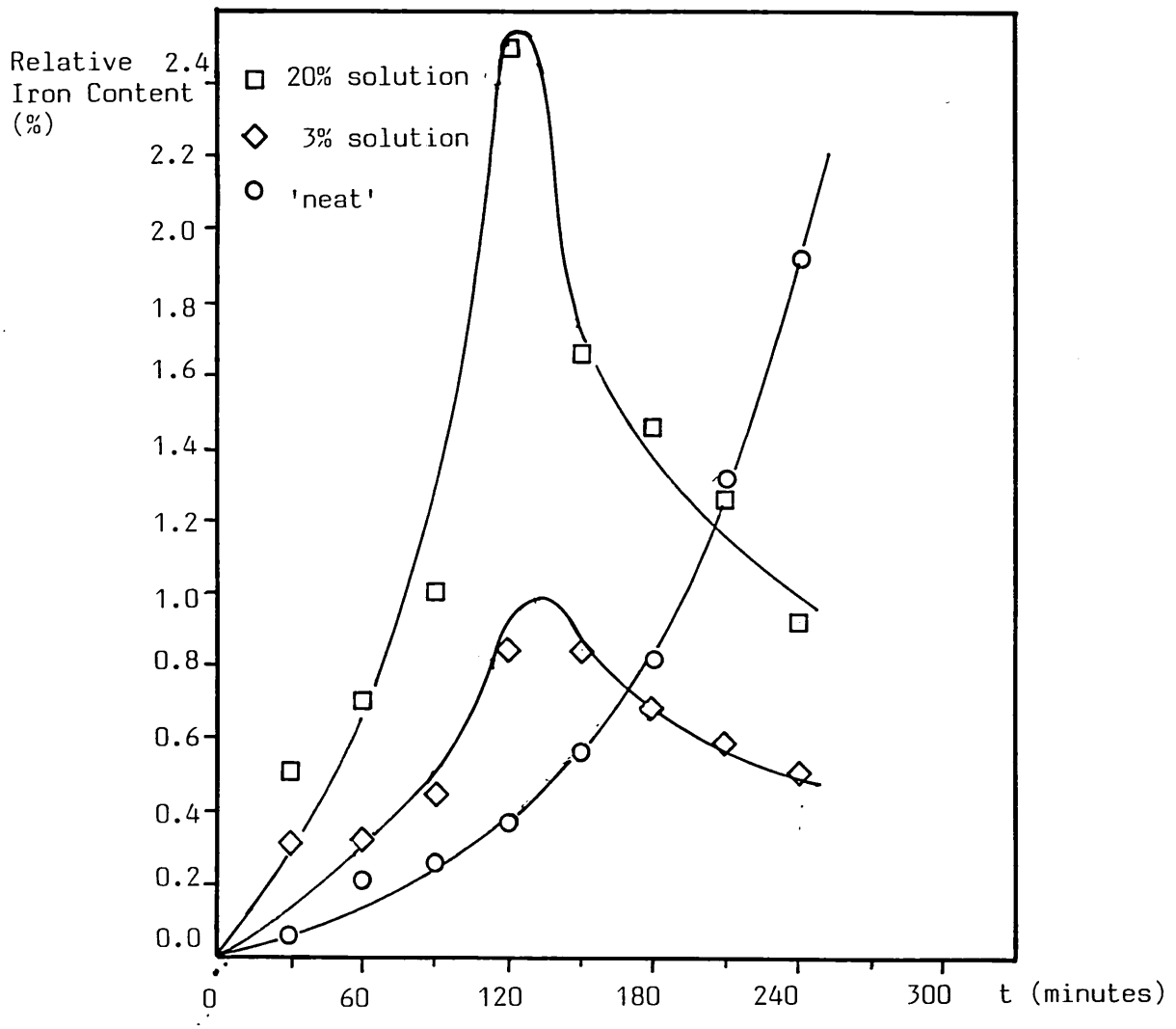


Figure 5.21 A Comparison of the rate of reaction of dihexyl phosphonate with iron in liquid paraffin solutions and in 100% concentration

The disparity between the 'corrected' iron contents of the 'neat' ester and the 3% and 20% solutions may also be a result of the insolubility of the polymer. Iron compounds usually have a co-ordination number of 6 (127), and it would seem reasonable to assume that a sample taken from the reaction of ester and iron contains some iron atoms in which the co-ordination to monomer groups is incomplete.

Those polymer molecules in which the iron atom is fully co-ordinated would be expected to be of lower solubility in the liquid paraffin. Samples taken therefore would, it is assumed, not be a measure of the average iron content, but that of the paraffin soluble fraction, which not being fully co-ordinated by monomer groups would have a higher iron content than the true average. Since the liquid paraffin solvent used was low in content polar of polar compounds, it is reasonable to assume that the 20% dihexyl phosphonate solutions were more polar than the 3% solutions. Accordingly a lower fraction of the dissolved iron would be expected to be present in the 3% solutions than in the 20% solutions, and lower 'corrected' iron contents would be recorded.

As in the pure ester tests, the presence of oxygen gives rise to faster rates of reaction for liquid paraffin solutions. However it would appear that the rates of reaction measured are again not wholly representative, since higher iron contents are recorded but the discontinuity in rise of iron content appears at the same point for both oxygenated and nitrogenated samples. Figure 5.22 illustrates the rises in iron contents for 20% solutions of dihexyl phosphonate heated with iron with oxygen present and with nitrogen present. The effect of oxygen cannot be regarded as simply an increase in the rate of reaction.

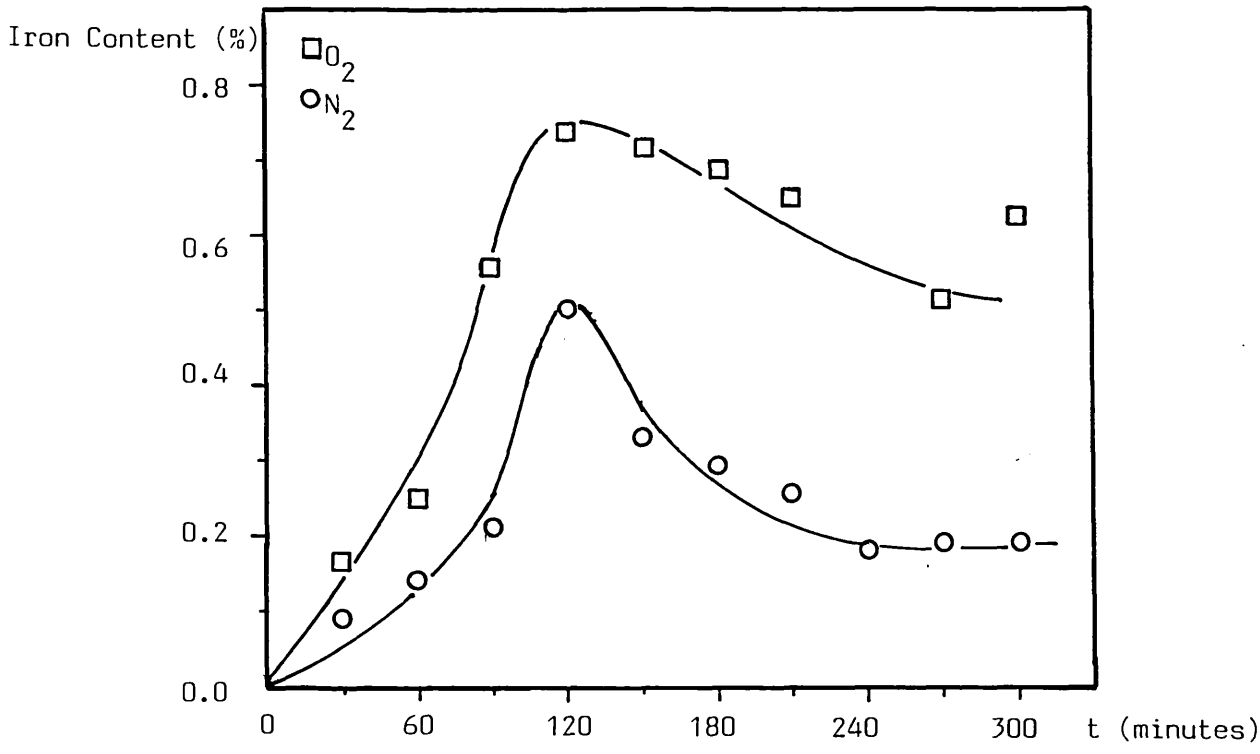


Figure 5.22 Effect of oxygen on the rate of the dihexyl phosphonate-iron reaction in liquid paraffin conditions

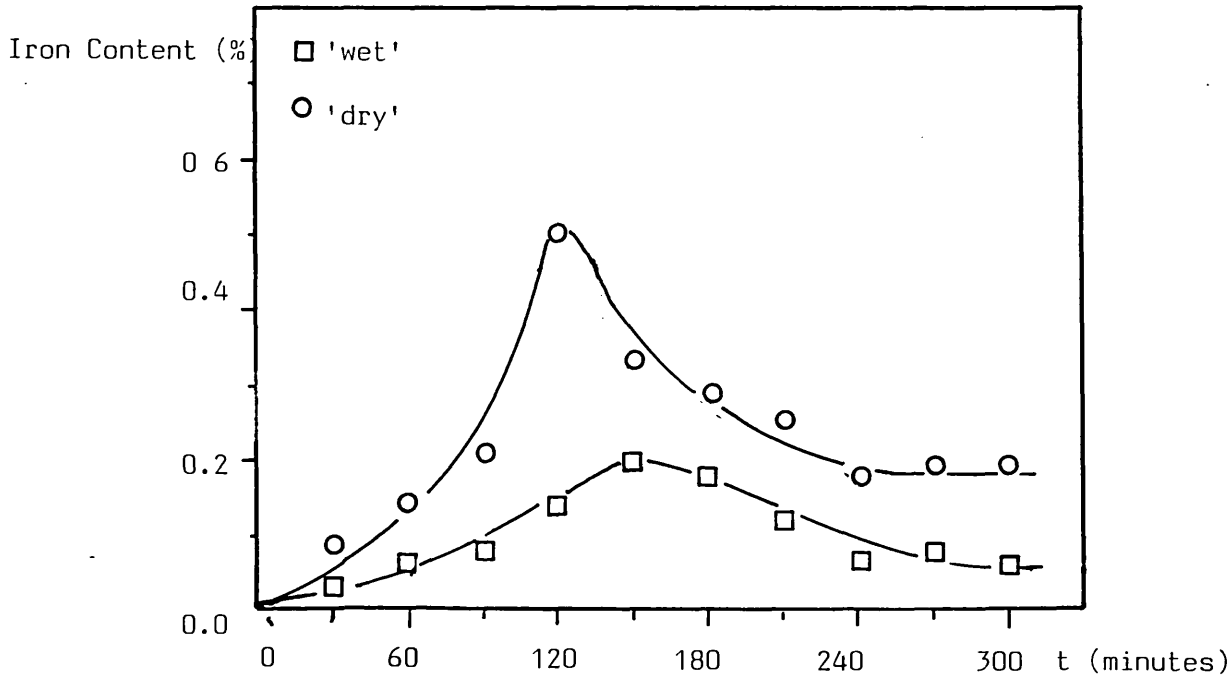


Figure 5.23 Effect of water on the rate of the dihexyl phosphonate -iron reaction in liquid paraffin conditions

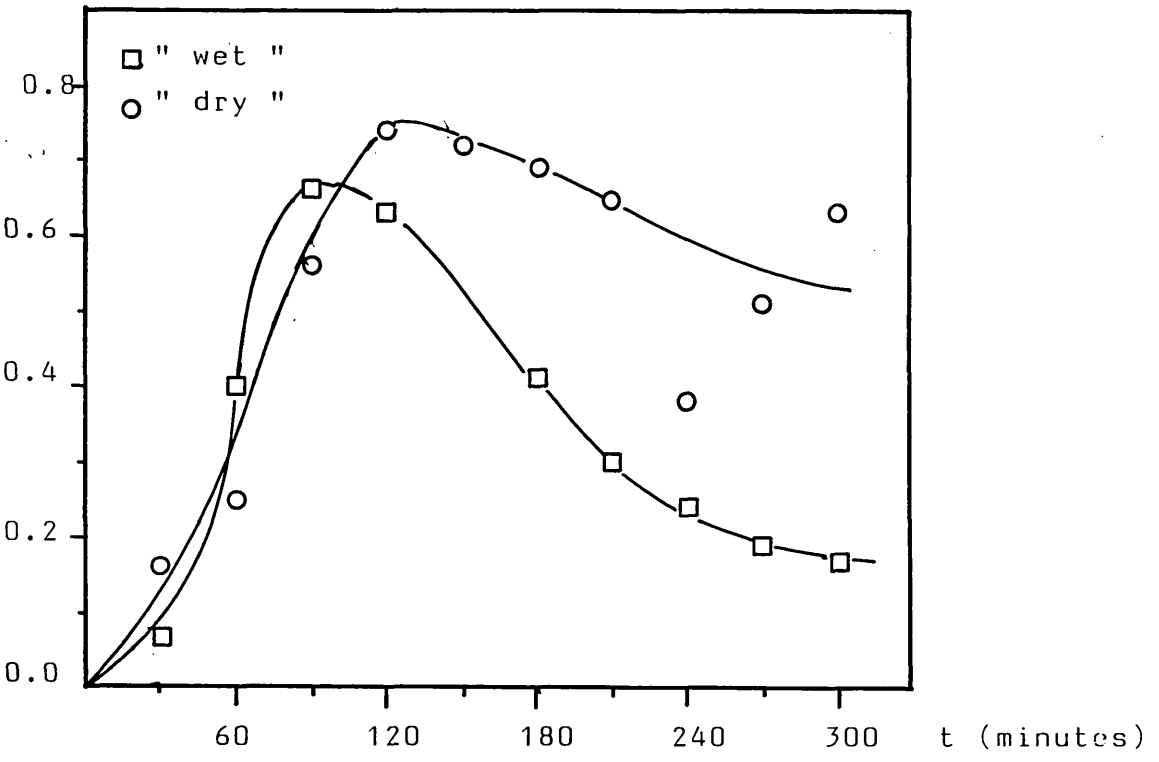


Figure 5.24 Effect of water on the rate of reaction of dihexhl phosphonate and iron in liquid paraffin solution in the presence of oxygen

The discontinuity in rise in iron content occurs at a similar time, but at a higher iron content, to that observed for the nitrogenated sample. A rise in reaction rate should cause the discontinuity to arise earlier, but the iron contents of both samples at and after the discontinuity should be similar. Observation of the samples taken showed a much greater colour change in the samples of the oxygenated solution compared to the nitrogenated solution. It may be that oxidation of the liquid paraffin solvent takes place, as a result of which, it becomes a better solvent for the polymer produced.

The role of water is even less clear. In the tests which involved the heating of pure esters with iron powder, the presence of water gave rise to increased rates of reaction. In tests using liquid paraffin solutions, a lowered rate of reaction is observed. This effect is illustrated in figures 5.23 and 5.24 for 20% solutions of dihexyl phosphonate heated with water and iron powder under nitrogen and oxygen respectively. The decrease in the measured rate of reaction is unexpected. If the effect of water on the reaction is negated by the liquid paraffin solution then no difference between 'wet' and 'dry' samples would be observed. However a 'negative' effect is recorded. The presence of water in these liquid paraffin tests may therefore be inhibiting the reaction.

Such inhibition may involve adsorption onto the iron powder, desorption being limited by the non-polar nature of the solvent. It may be that an aquated iron species would not react as readily with the phosphonate ester. This would arise if the stability constant of the initiating stage of the polymerisation was lower than the hexaquo iron species, in the presence of the non-polar liquid paraffin solvent.

An alternative approach is to consider that the method of determining rates is not valid when wet and dry conditions are compared. For example, the presence of water, acting as a 'Lewis Acid' may encourage a faster rate of reaction, but instead of initiating the reaction, it enhances polymer growth. Thus an increase in iron occurs but because polymer growth is enhanced, the fraction of iron species dissolved in the liquid paraffin is a lower proportion of the total dissolved iron content than was the case under dry conditions.

From the results obtained, it is not clear which is the correct approach. From the tests under nitrogen a slower reaction is indicated by the longer time taken to reach the 'discontinuity point'. However a lower iron concentration is obtained throughout, which might support the presence of the dissolved iron as less soluble species, i.e. of a higher degree of co-ordination, than in the 'dry' test. When oxygen and water were present the discontinuity appears earlier, indicating a faster reaction rate. Lower iron concentrations obtained under the 'wet' conditions, as in the nitrogenated tests, appear to indicate that the iron is present in a less soluble form.

Clearly the reactions of dihexyl phosphonate and iron in liquid paraffin are complicated by the solvent presence. However it has been shown that a reaction occurs to produce a polymeric adduct. Importantly it has been found that the product is of low solubility in the paraffin, and this may well prove to be of vital importance under rolling contact conditions.

5.3.10 Reaction with Chromium Powder

Using both similar methods of reaction and of analysis of the samples taken, no discernable reaction was observed between dihexyl phosphonate and chromium powder.

Samples were analysed by atomic absorption spectroscopy, and gave signals equivalent to the noise levels obtained on the instrument. If converted to values for chromium content, these gave chromium contents of 0.02% for samples taken at 300 minutes. Under similar conditions using iron powder, an iron content of greater than 3.0% would have been obtained.

Unlike iron, chromium metal has a high resistance to attack by corrosive agents (133).

5.3.11 Reaction of trihexyl phosphite and iron powder

The heating of trihexyl phosphite with iron gave rise to no apparent reaction. No obvious polymerisation or colour change was observed even after 4 hours heating at 175°C. This may be compared with the results obtained for dihexyl phosphonate when after a similar period samples had developed a dark brown colour and were of a distinctly 'wax-like' consistency.

Examination of the samples remaining at the end of the test using infrared absorption spectrophotemtry showed no appreciable differences in the spectra of the test or control samples. These spectra are shown in figures 5.25 (dry conditions) and 5.26 ('wet' conditions).

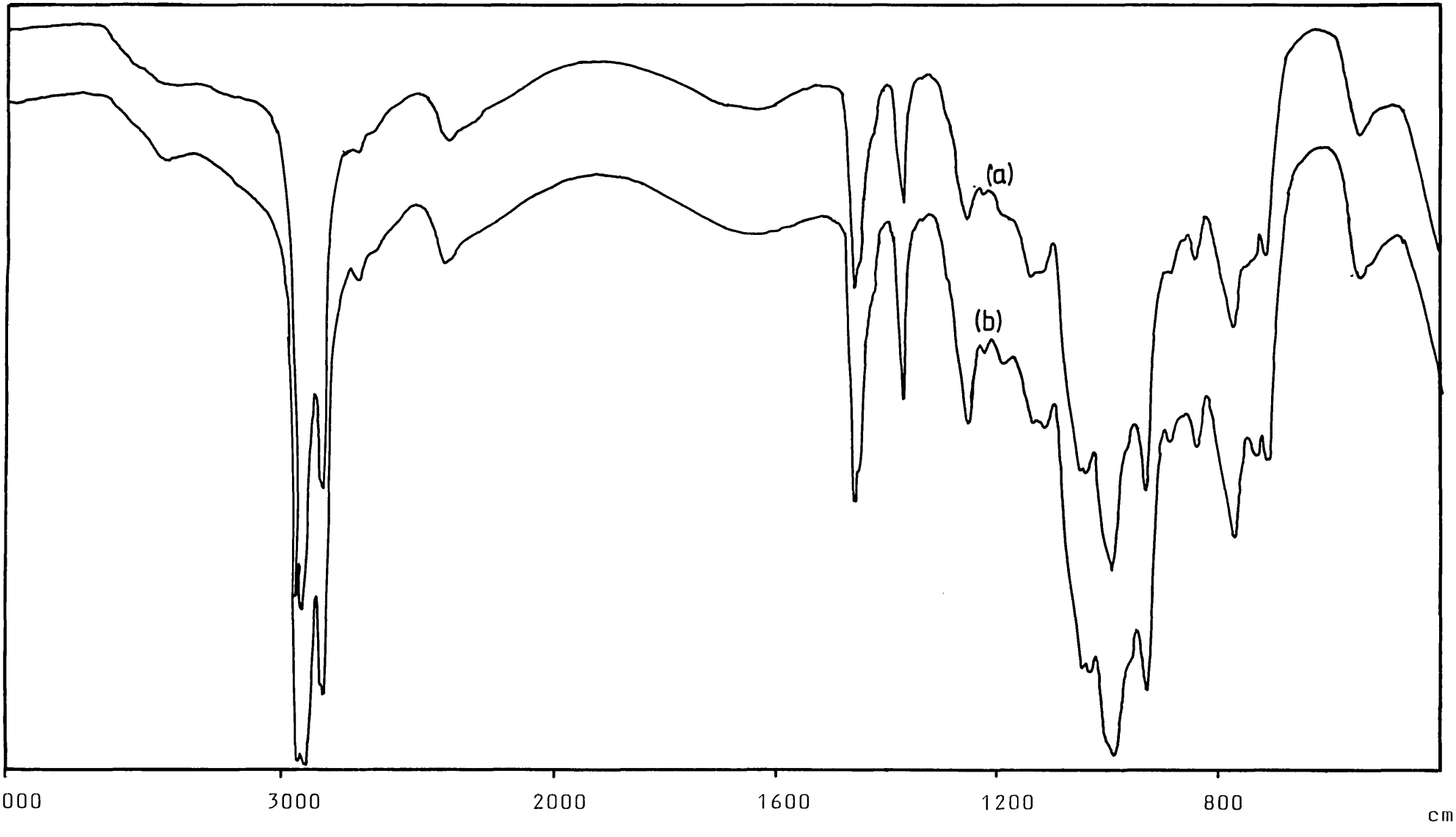


Figure 5.25 Infrared spectra of trihexyl phosphite before (spectrum(a)) and after (spectrum(b)) heating with iron.

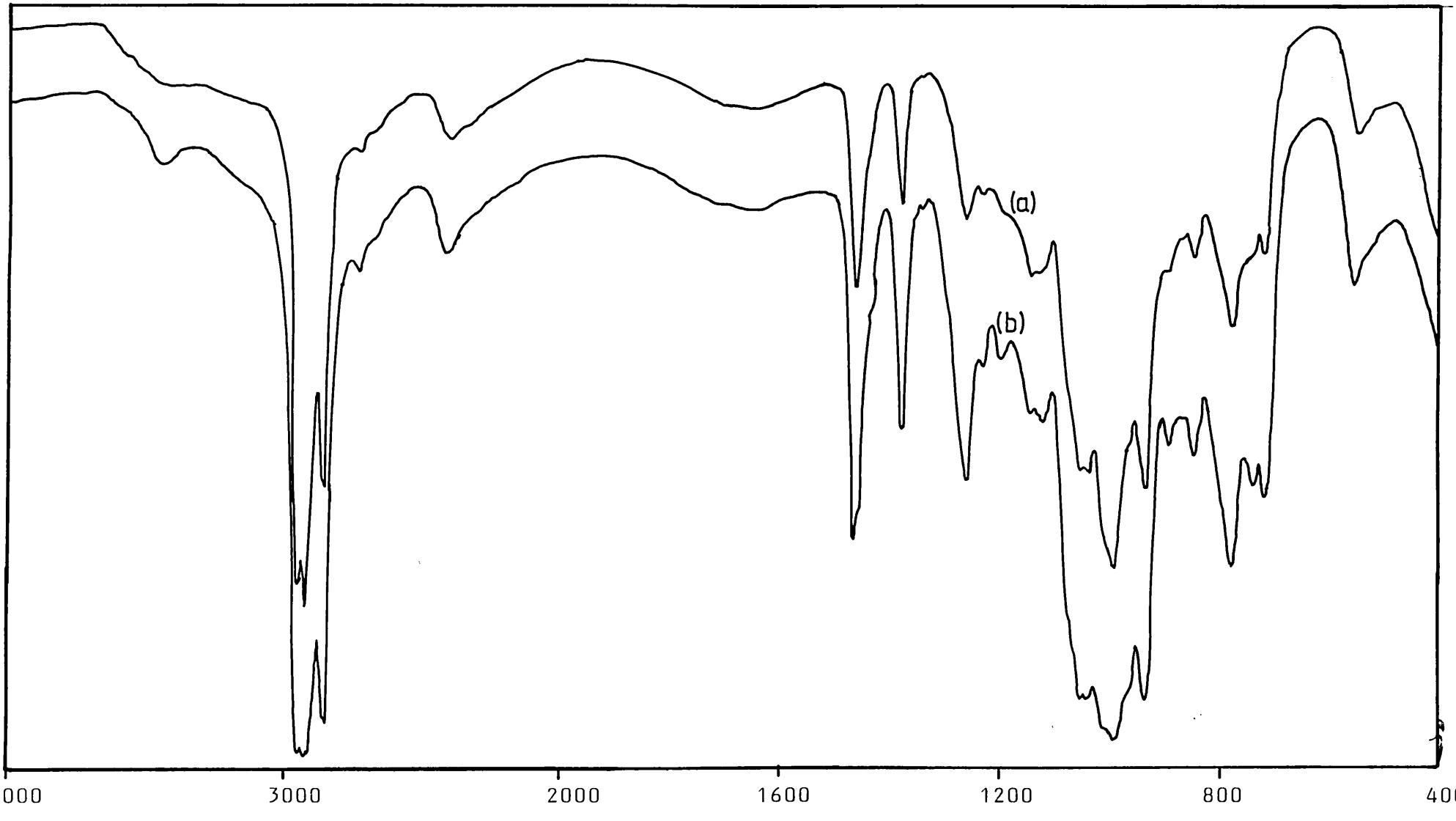
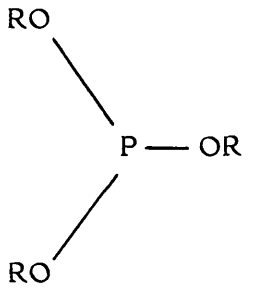
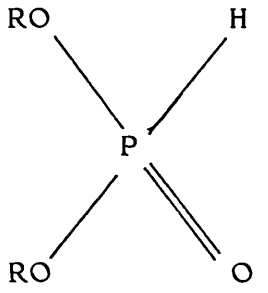


Figure 5.26 Infrared spectra of trihexyl phosphite (spectrum(a)) and after (spectrum(b)) heating with iron in the presence of water.

This non-reactivity between trihexyl phosphite and iron powder compared to that found for dihexyl phosphonate, is explained by comparing the chemical structures of the two esters. Tri esters adopt the phosphorous acid form (I) whereas diesters occur as the phosphonic acid form (II).

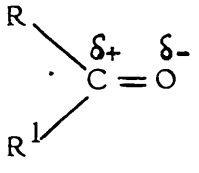


I

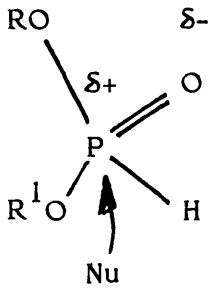


II

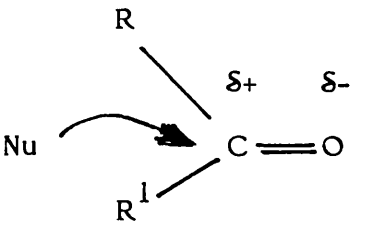
As outlined in Chapter 2 this difference in structure leads to considerable differences in chemical reactions. In particular susceptibility to oxidation and reduction (54,55). The presence of the lone pair of electrons in the phosphite structure (I) makes for a higher susceptibility to oxidation than exists for the phosphonates. The phosphonate structure (II) bears a similarity to the carbonyl structure (III) in its susceptibility to reduction by nucleophilic attack (124) because of electron displacement along the phosphoryl (P = O) bond, as illustrated below (IV and V).



(III)



IV



V

5.4 Summary

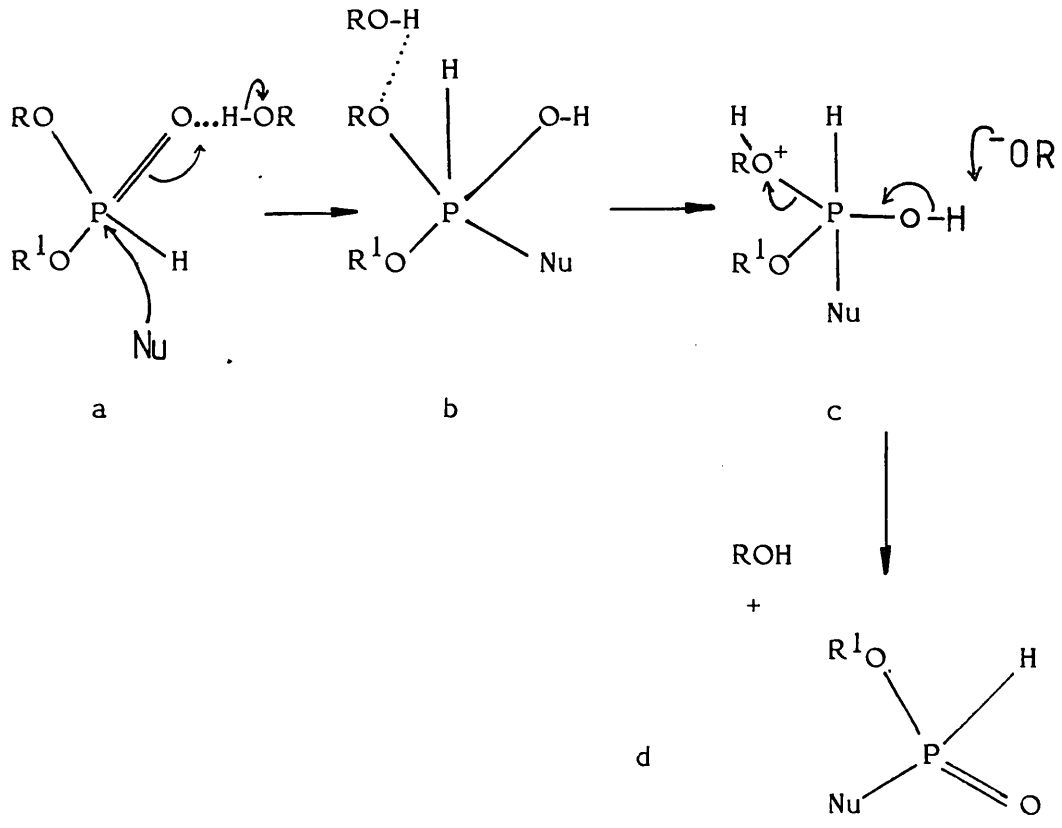
The reaction of several di-alkyl and -aryl phosphonates with iron has been investigated under a range of conditions. The products of these reactions are ferro-organophosphorus polymers, which with increasing heating times assume a wax-like consistency. The formation of a reaction product between phosphonates and iron powder was reported by Barber (26) although the product was not considered to be polymeric.

Control of the reaction conditions has given considerable insight into the mechanism of the reaction. The reaction clearly involves an oxidation step as was shown by the increase in rate when oxygen is present. Prior oxidation of the iron powder also led to an increased reactivity indicating that the oxidation step involved oxidation of the iron and not of the phosphonate. This is further supported by the observed non-reactivity of tri-hexyl phosphite, which as previously discussed has a greater susceptibility to oxidation than dihexyl phosphonate.

It has been found that the complete oxidation of iron to iron (III) oxide is not as favourable to the reaction rate as is partial oxidation. Thus it would appear that both Fe^{II} and Fe^{III} species are involved in the reaction process.

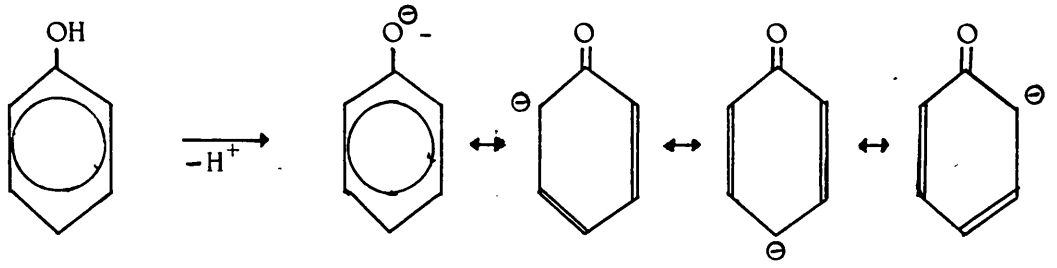
The influence of water on the reaction, would appear to be that of a 'Lewis acid', aiding thereby nucleophilic attack on the phosphorus atom. From the results obtained and the known differences in reactivities of phosphonates and of phosphites, nucleophilic attack on the phosphorus appears to be involved.

The presence of the alcohols in the condensates of the reaction is supportive of this. The presence of alcohols in the reaction solution when dialkyl phosphonates were heated with iron has been reported previously (10). Nucleophilic attack may be considered to follow the following scheme:-



Transfer of alkoxy groups by a similar mechanism to that outlined above is known (134). The presence of water, acting as Lewis acid in steps (a) or (b) would increase the rate of reaction, comparable to the effect encountered in carboxylate ester hydrolysis (135).

The higher reactivity of diphenyl phosphonate compared to dihexyl phosphonate is in keeping with the above mechanism. Phenol (C_6H_5OH) is a much stronger acid than hexanol ($C_6H_{13}OH$). This is due to resonance stabilisation of the electron charge around the molecule (136) as shown below:



This increased acidity of the phenols over alcohols is responsible for the increased tendency shown by the phenols to undergo acyl-oxygen fission in the hydrolysis of esters (137). The stronger the acidity, the weaker the base and the better the group is at leaving under nucleophilic attack (135). A greater tendency for the '-OR' group to leave, the greater the tendency for phosphoryl-oxygen fission to take place (compare this with acyl-oxygen fission in carboxylate ester hydrolysis). This will therefore promote step c to d in the above reaction scheme.

The next chapter describes the various analytical methods used to determine the structure of the phosphonate-iron product. From the results obtained from these analytical methods a possible structure of the polymer is developed.

Chapter 6.

The Analysis of the Phosphonate-Iron Reaction Product

The products of heating dihexyl and other phosphonates with iron metal have been subjected to a number of methods of analysis in order to determine the nature of the product formed. Some of these methods have previously been described in Chapter 5 (Infrared and ^{31}P n.m.r. spectroscopy) as a means of following the progress of the reaction. Elemental micro analysis and mass spectroscopic analysis have been used to study the composition of the polymer and these methods have been described in Chapter 4. Two other methods of analysis have been used. These were electron spin resonance spectroscopy and Mossbauer spectroscopy and are both concerned with the determination of the electronic environment of the iron atoms present in the polymer.

6.1 Infrared spectroscopy

The principles and practice of infrared spectroscopy as related to organophosphorus esters have already been described (Chapters 4 and 5). The essential difference between the recording of spectra of the phosphonate-iron reaction product as described in Chapter 5, and the work described in this section is the use of undiluted samples. In addition variable temperature infrared spectroscopy has been carried out on a sample of the reaction product to examine the effect of heat on the phosphonate-iron reaction product when no iron was present.

6.1.1. Method

To obtain the infrared spectra of the phosphonate-iron reaction products, each of the esters (di-hexyl, -octyl, -dodecyl, -phenyl and bis octyl-phenyl phosphonates) were heated at 155°C in the presence of iron powder. Samples taken from these reactions, in which polymerisation could be seen to have taken place (i.e. when a sample of significantly greater viscosity than the parent phosphonate was produced) were used for the analyses. Each sample was placed between two KBr or NaCl infrared cell plates. The infrared spectrum of the capillary film of the sample thus formed was then recorded over the range 4000 - 400 cm^{-1} (to 650 cm^{-1} with NaCl plates).

Variable temperature infrared spectroscopy of a sample of the dihexyl phosphonate - iron reaction product was carried out using a Specac 21000 Variable Temperature cell, previously described in section 4.1.2. The sample for this test was taken from the reaction of dihexyl phosphonate and iron powder at 185°C after heating for 135 minutes. These spectra were recorded with a sample film thickness of 0.025mm. Spectra were recorded at temperatures of 25° to 175°C.

6.1.2. Infrared Spectra

In section 5.2.2. the change in the infrared spectrum of dihexyl phosphonate on heating with iron was briefly described. This change, the appearance of an absorbance at 1160 cm^{-1} which increases in intensity with time, is apparent in the spectra of the reaction products obtained by heating other phosphonates with iron powder.

Figures 6.1 to 6.5 show the infrared spectra of the phosphonate-iron reaction products for dihexyl, dioctyl, didodecyl, diphenyl and bis octyl-phenyl phosphonates, each compared with those of the original phosphonate.

In figure 6.6 the infrared spectra of a sample of dihexyl phosphonate-iron reaction product recorded, using a variable temperature infrared cell, at temperatures of 25° to 175° are shown.

6.1.3. Discussion

The infrared spectra of the phosphonate-iron reaction products share a common change in the spectra compared to the original esters. This change is the appearance of a new absorbance at approximately $1160cm^{-1}$. Table 6.1 lists the frequency of this new absorbance for each of the phosphonate-iron reaction products.

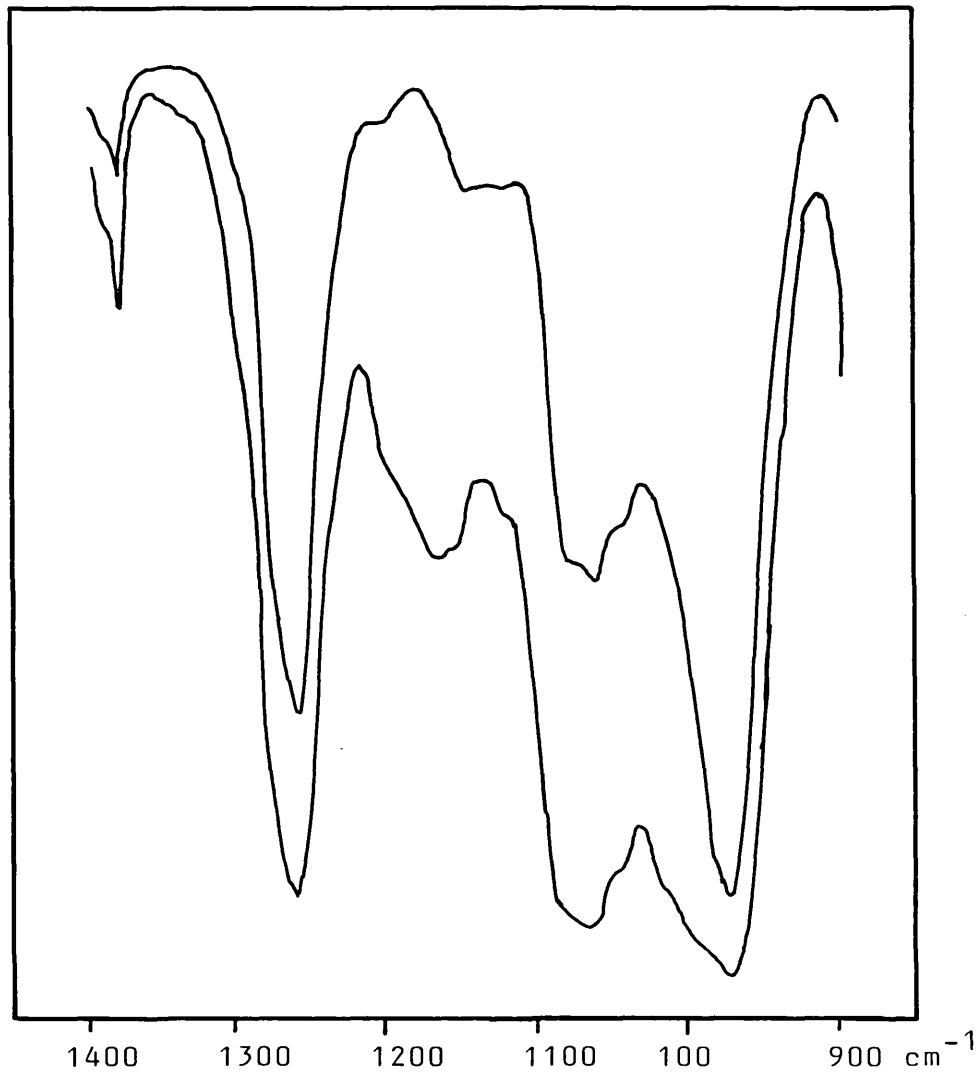


Figure 6.1 Infrared spectra of the dihexyl phosphonate iron reaction product (lower spectrum) and of dihexyl phosphonate (upper spectrum)

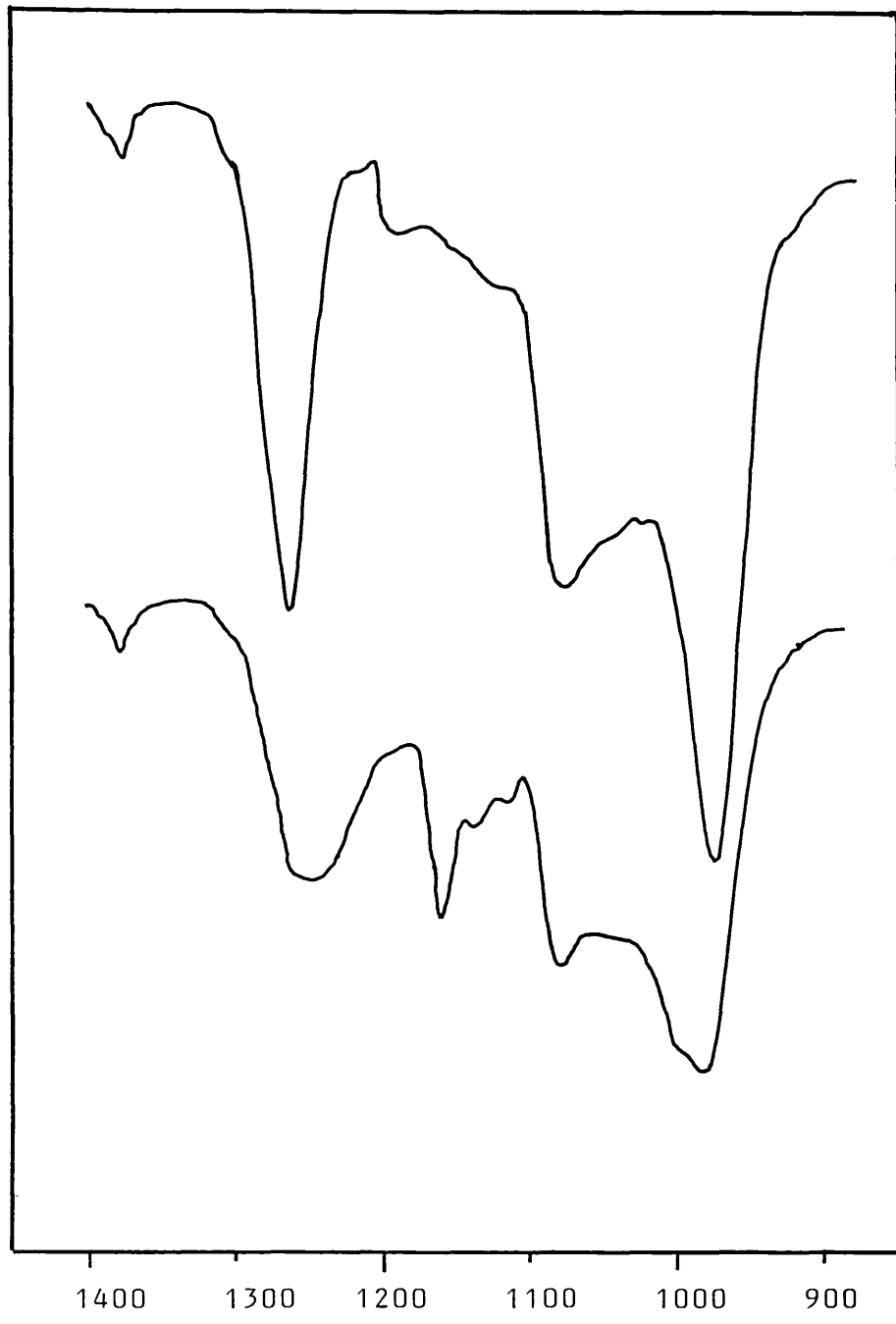


Figure 6.2 Infrared spectra of the dioctyl phosphonate iron reaction product (lower Spectrum) and of dihexyl phosphonate (upper spectrum)

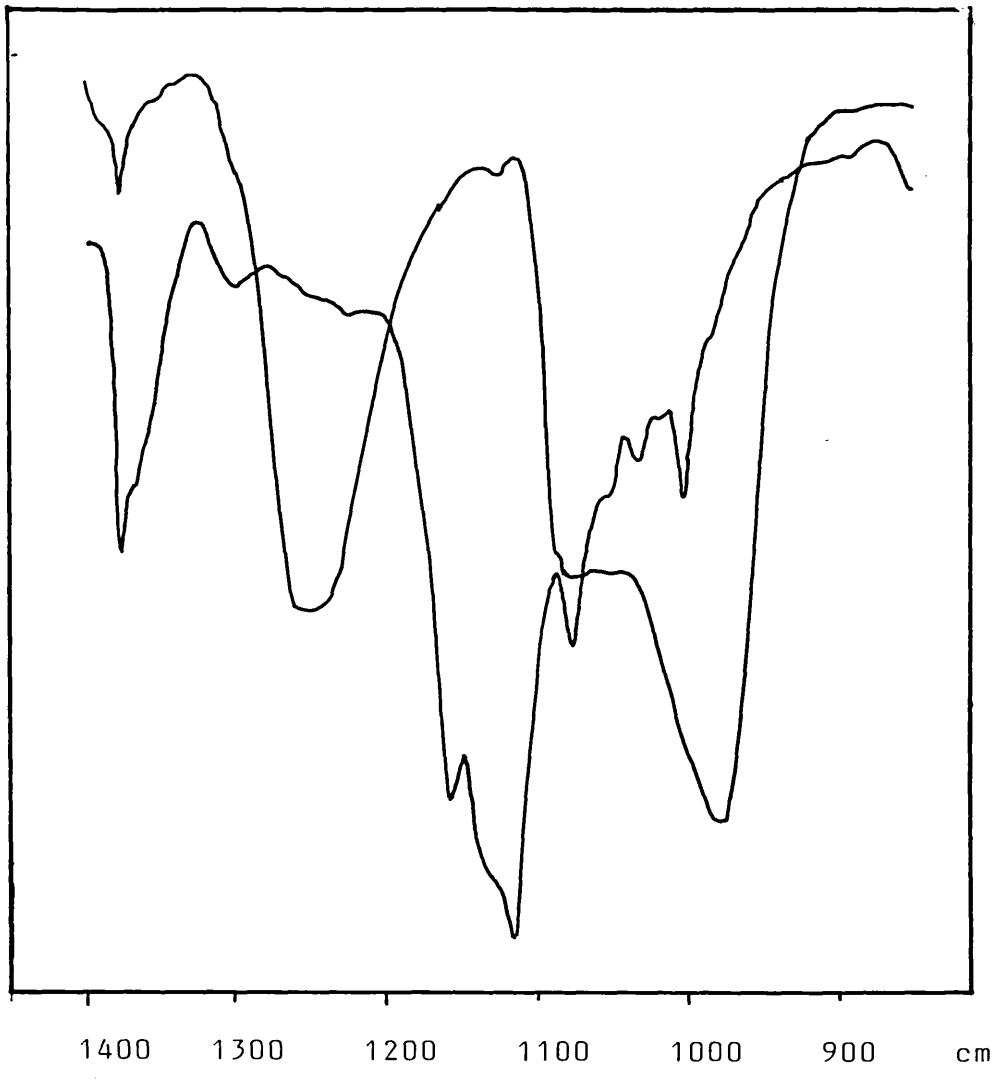


Figure 6.3 Infrared spectrum of the didodecyl phosphonate-iron reaction product (lower spectrum) and of didodecyl phosphonate (upper spectrum).

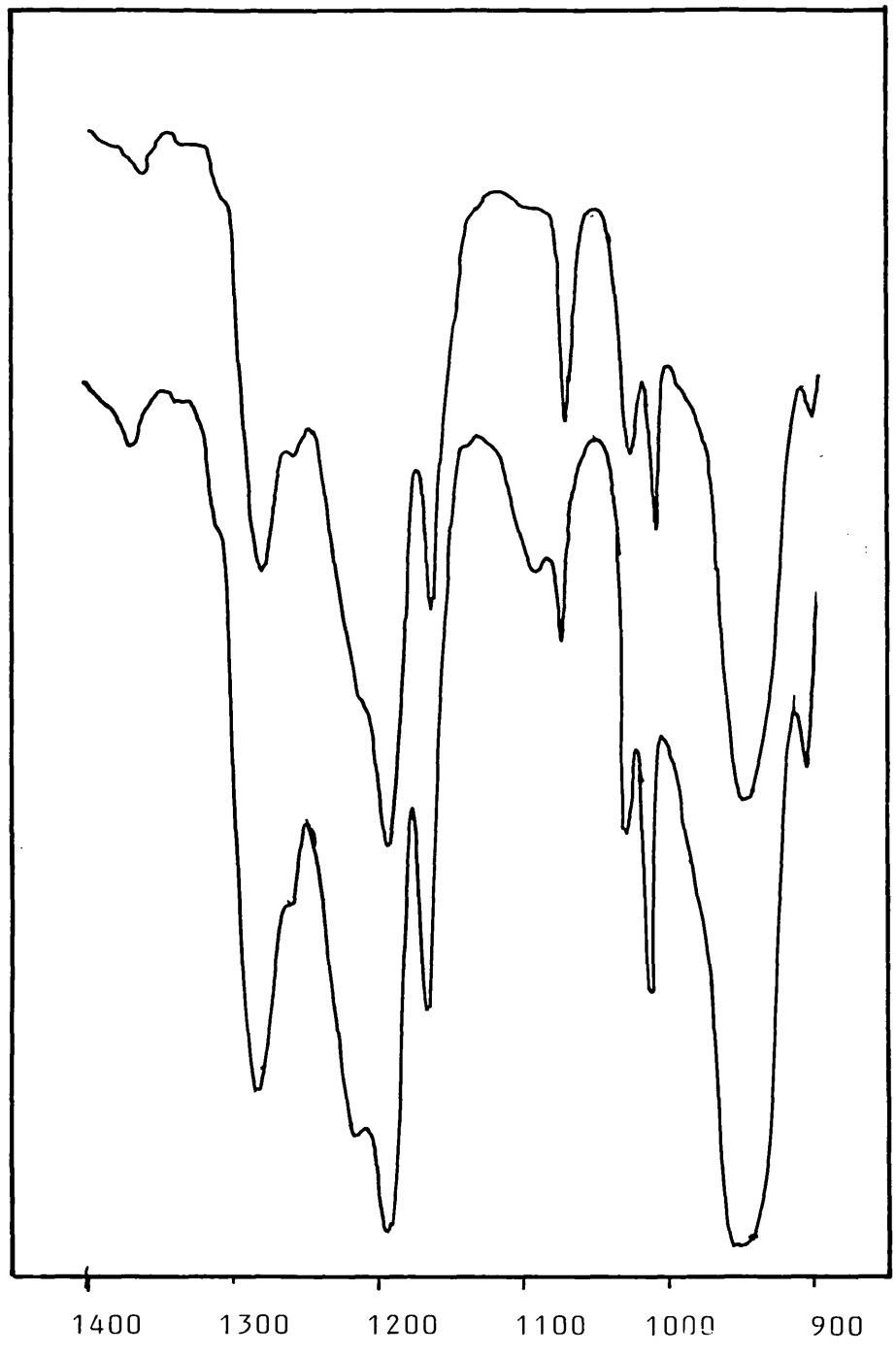


Figure 6.4 Infrared spectrum of the diphenyl phosphonate iron reaction product (lower spectrum) and of diphenyl phosphonate (upper spectrum).

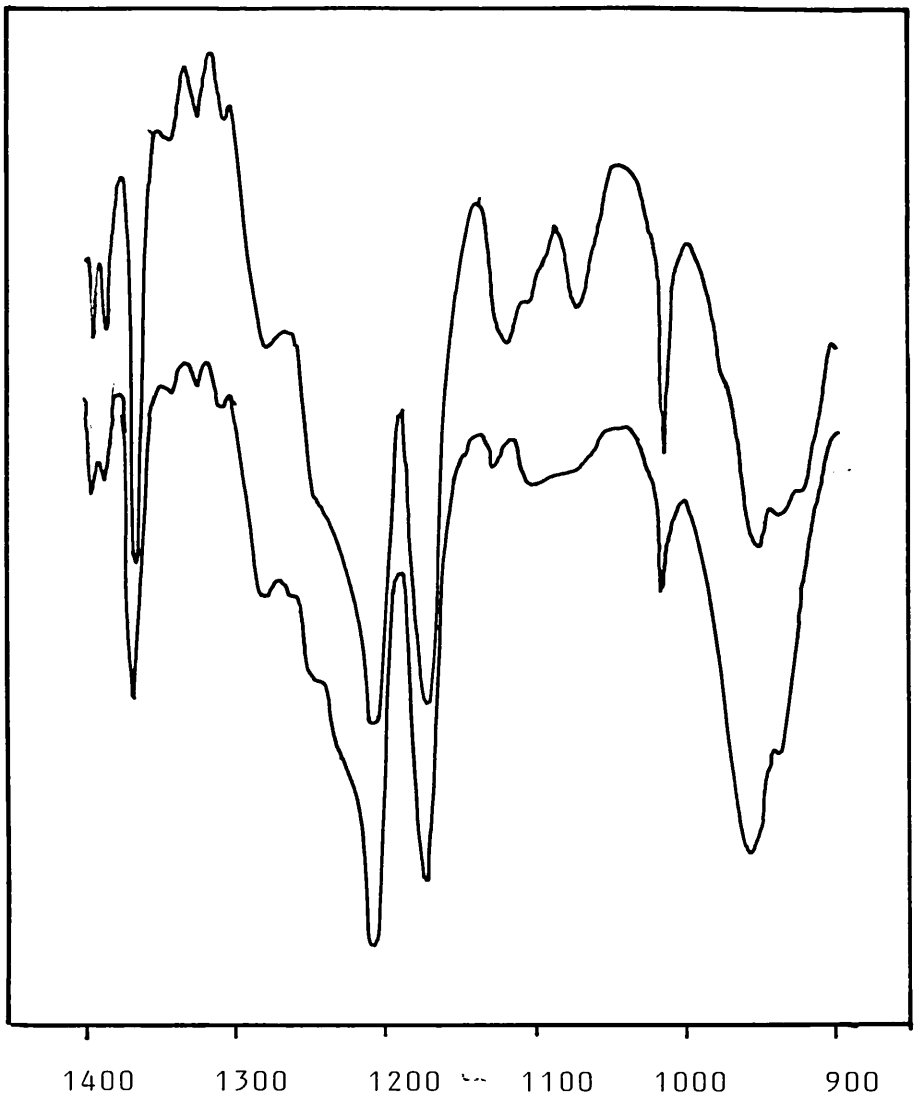


Figure 6.5 Infrared spectrum of the bis(octyl-phenyl) phosphonate-iron reaction product (lower spectrum) and of bis(octyl-phenyl) phosphonate.

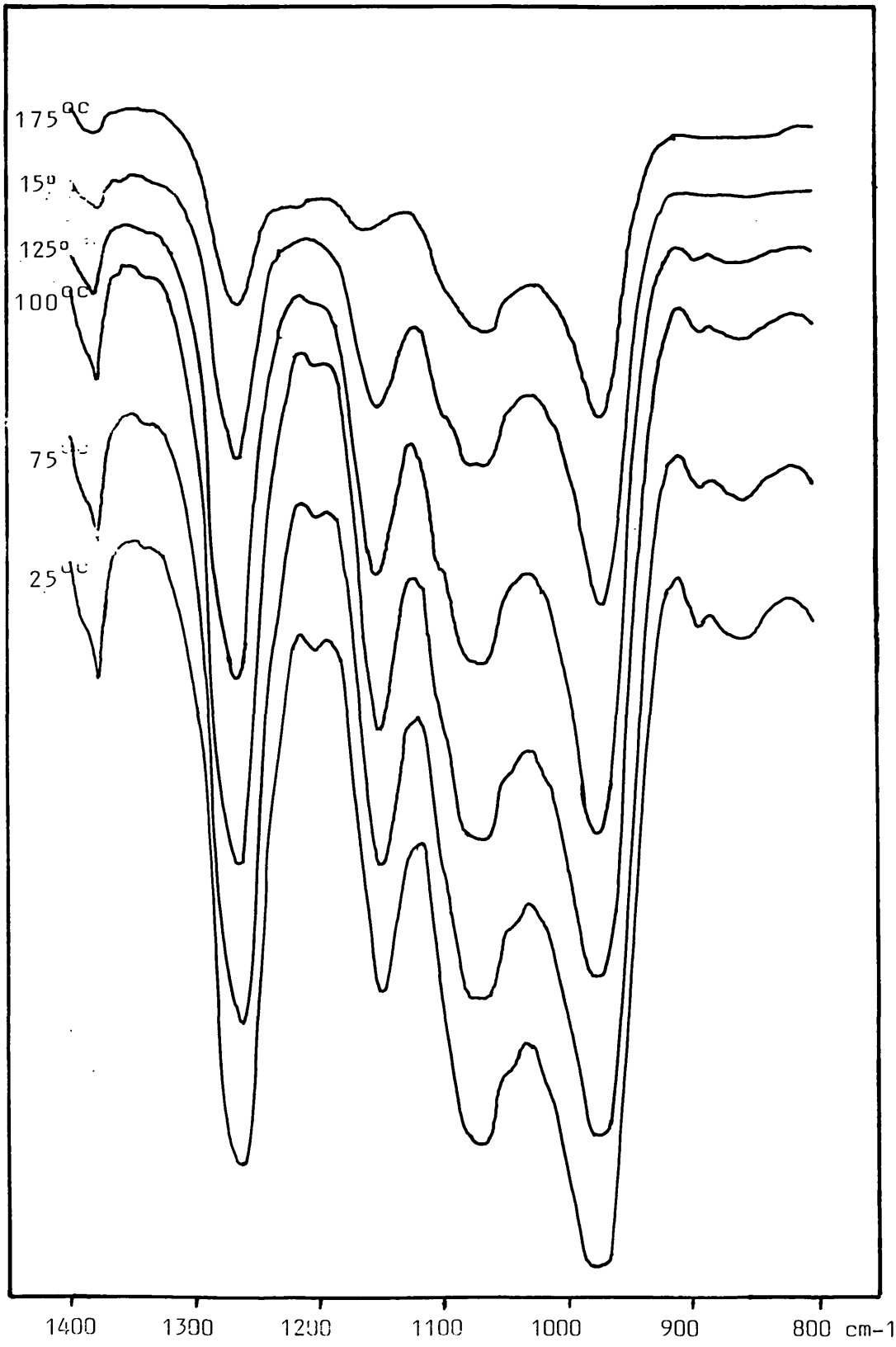


Figure 6.6. Infrared spectra of the dihexyl phosphonate-iron reaction product 25° - 175°C.

Table 6.1

"New absorbance" Frequencies for the Phosphonate-Iron Reaction Products

Parent phosphonate	(cm^{-1})
hexyl	1153
octyl	1159
dodecyl	1160
phenyl	1164
Octyl-phenyl	1171

As has already been noted (section 5.2), the rise in the intensity of the absorbance is comparable to and coincidental with the rise in the dissolved iron content. The absorption falls within the limits of the P = O absorbance frequency (104,138). The phosphoryl bond in di-alkyl and -aryl phosphonates usually has an infrared absorbance at approximately 1260 - 1250 cm^{-1}. The phosphonates tested show absorbances due to the phosphoryl bonds, in this narrow region.

The 'new' absorbance occurs in the region of the infrared spectrum of organophosphorus compounds where absorbances arising from 'donor' phosphoryl bonds (P=O) stretching vibrations occur (139). Often these arise as a result of hydrogen bonding to the oxygen (104,138), usually where the P - OH group is present in the molecule. Absorbances at this frequency can also be due to the phosphoryl bond vibration in the group 'P=O-M', where M is a metal atom forming a co-ordinate bond with this oxygen (138,140,141). Correct assignment of an absorbance in this region can be made since the hydrogen bonded phosphoryl vibration, usually results in a broad absorbance (138) whilst the metal coordinated phosphoryl absorbance is sharp (141).

Compounds containing the group P-OH with a phosphoryl bond present are further differentiated by the presence of five absorption bands not found in compounds containing the group 'P=O-M'. These absorbances are in the regions 2525 - 2725 cm^{-1}, 2080 - 2350 cm^{-1}, 1600 - 1740 cm^{-1}, 917 - 1040 cm^{-1} and 450 - 540 cm^{-1}, which are the group frequencies resulting from the various vibrational modes of the P - OH group. All five absorbances are present when the P- OH group is present (137). Examination of the spectra recorded for the phosphonate-iron reaction products shows that these absorbances are not present.

Support for the assignment of the 'new' vibration as being due to the P=O-M group comes from work by three groups of workers. In chemisorption experiments of di-isopropyl methyl phosphonate ($(^{i}C_3H_7O)_2PO\,CH_3$) on different transition metal salts (141) an absorbance, assigned to being due to the phosphoryl bond vibration of the P=O-M group, was recorded in the region 1167 to 1232 cm^{-1}, the frequency depending on the electronegativity of the metal ion.

With iron (III) salts, the frequency of the P=O bond was lowered to 1167 cm^{-1}. A lowering of the phosphoryl bond absorbance to 1118 - 1136 cm^{-1} was reported to occur in phosphinate ($R_2P(O)OH$) polymers involving donor bonding of the phosphoryl bond to cobalt (142). A similar lowering of the phosphoryl bond frequency was reported (143) in stannyl phosphinates, again reported to contain P=O-M bonding.

The 'new' absorbance present in the infrared spectra of the phosphonate-iron reaction products is clearly due, therefore, to the presence in the polymeric product of a donor phosphoryl bond to the iron atom (depicted as P=O→Fe).

This bond possesses a high thermal stability. The results obtained from the variable temperature infrared spectra show no change in the spectra as the polymer is heated. Figure 6.6 shows the infrared spectra recorded at temperatures between 25° and 175°C for a sample of the dihexyl phosphonate-iron reaction product. Even at 175°C, little change, other than a lowering in intensity throughout the spectrum, can be seen in the relative intensities or positions of the P=O P=O Fe and P-O-C bonds.

In Chapter 4, the use of variable temperature infrared spectroscopy to investigate the effect of heat on dihexyl and diphenyl phosphonates was described. A comparison of these variable temperature spectra (figures 4.14 and 4.15) with the infrared spectra recorded for the phosphonate-iron reaction samples (figures 6.1 to 6.5) shows that the reaction that takes place when phosphonates are heated with iron is not the same as when these esters are heated alone.

6.2 ^{31}P n.m.r. Spectroscopy

The principles of ^{31}P nuclear magnetic resonance (^{31}P n.m.r.) spectroscopy have been outlined in section 4.2. In Chapter 5, the use of ^{31}P n.m.r. to follow the progress of the phosphonate-iron reaction, was described. In this section ^{31}P n.m.r. is used to investigate the nature of the organophosphorus polymers formed by dihexyl and other dialkyl and diaryl phosphonates on being heated with iron.

6.2.1. Method

The method used was identical to that described in Chapter 4. The ^{31}P n.m.r. spectra were recorded of samples of the reaction products formed with iron by di-hexyl, -octyl, -dodecyl, -phenyl and bis Octyl-phenyl phosphonates. Additionally spectra were recorded of samples of the dihexyl and diphenyl phosphonate-iron reaction products obtained when water and/or oxygen were present during heating.

Samples used to obtain these spectra, were obtained from those experiments described in Chapter 5.

6.2.2. ^{31}P n.m.r. Spectra

The ^{31}P n.m.r. spectra recorded for the phosphonate-iron reaction products of the four phosphonates are similar in appearance, each showing two peaks in the spectrum. To illustrate their appearance, figure 6.7 shows the spectrum recorded for the dihexyl phosphonate-iron reaction product.

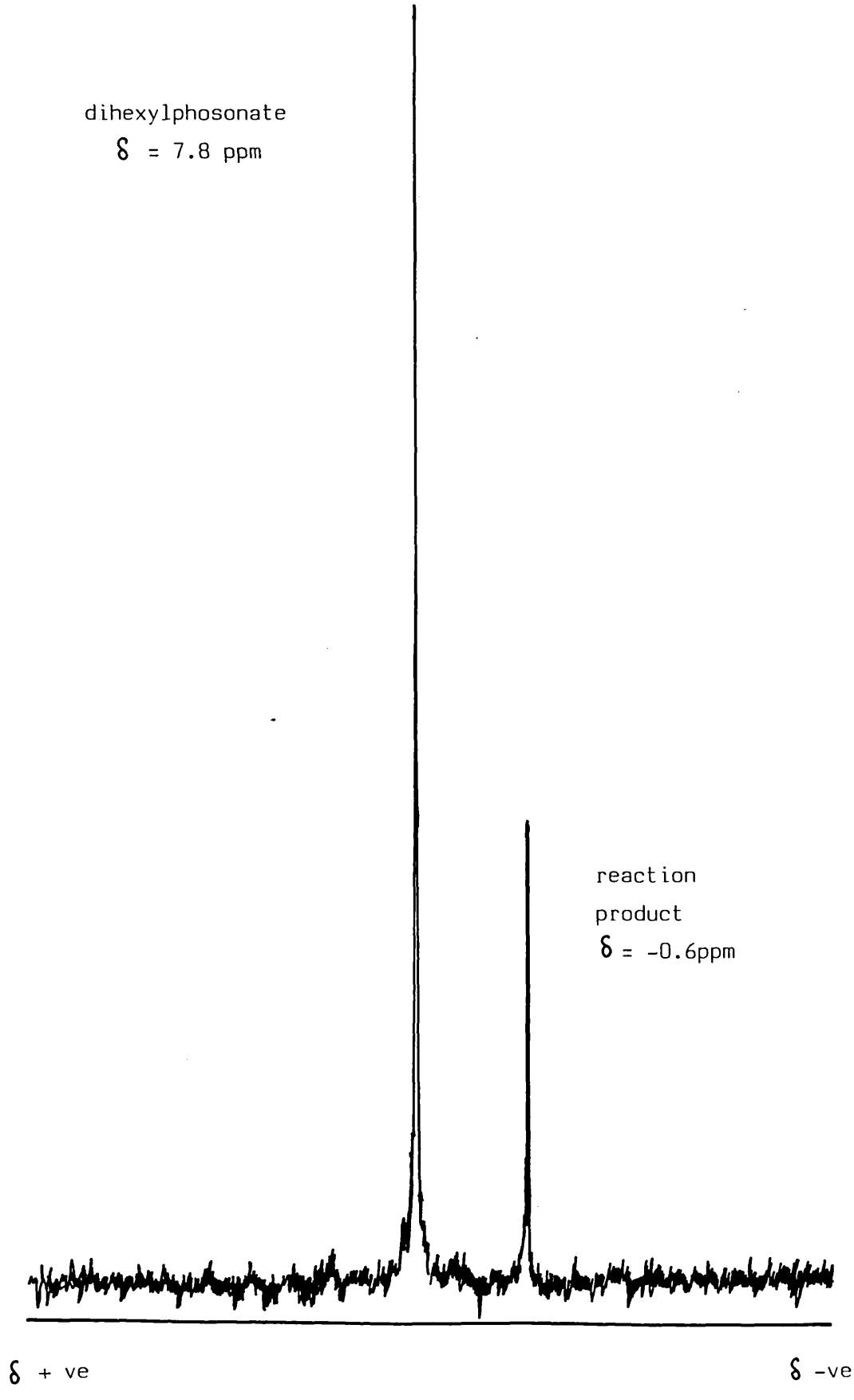


Figure 6.7 ^{31}P n.m.r. spectrum of the dihexyl phosphonate-iron reaction product.

6.2.3. Results and Discussion

The reaction products of the dialkyl and diaryl phosphonates with iron show similar responses in their ^{31}P n.m.r. spectra. Table 6.2. lists the chemical shifts recorded for the phosphonate-iron reaction products, together with the chemical shift recorded for the original phosphonate.

Table 6.2.

^{31}P n.m.r. Chemical Shifts for the Phosphonate-Iron Reaction Products

Parent Phosphonate	Chemical Shifts (in p.p.m.) δ	
	phosphonate	phosphonate-iron product
Hexyl	7.8	-0.6
Octyl	7.7	-0.7
Phenyl	0.4	128
Octyl-phenyl	0.65	129

The ^{31}P n.m.r. spectrum of the didodecyl phosphonate-iron reaction product showed no signal, other than that of the original ester, although the measured iron content of the sample used was 0.25% and a significant difference could be seen in the infrared spectrum. This is unsuprising since ^{31}P n.m.r. is generally less sensitive for the determination of trace levels of organophosphorus compounds than is infrared spectrometry (144). Also the reaction of didodecyl phosphonate with iron powder proceeds at a much slower rate than the corresponding dihexyl phosphonate reaction, as was shown in section 5.3.1. In Chapter 5 it was reported that ^{31}P n.m.r. was not suitable for following the progress of the earlier stages of the reaction of dihexyl phosphonate with iron.

The similarity of the chemical shifts recorded for dihexyl and dioctyl phosphonates and for diphenyl and bis octyl phenyl phosphonates has already been observed (section 4.2.). The similarity of the chemical shifts recorded for the phosphonate-iron reaction products indicates that the reactions with iron undergone by dihexyl and dioctyl phosphonates and by diphenyl and bis octyl-phenyl phosphonates give rise to similar products. The dissimilar signals from diaryl phosphonate-iron and dialkyl phosphonate-iron reaction products may be linked to the large difference in the inductive effect that the organic group has through the oxygen on the phosphorus atom (145). Chemical shifts for aromatic organophosphorus compounds are often higher than for the corresponding aliphatic compounds (144). It is not possible to determine directly from the ^{31}P n.m.r. spectrum whether the electronic environment of the phosphorus atom in the dialkyl phosphonate-iron reaction products is the same as that in the diaryl phosphonate-iron reaction products.

The effect of oxygen and water on the reaction of phosphonates with iron was studied using ^{31}P n.m.r. The samples used were obtained from tests described in section 5.1, for samples of dihexyl phosphonate and diphenyl phosphonate heated with iron in the presence of nitrogen or oxygen with and without water being present. The results are tabulated in table 6.3.

It can be seen that there is no difference in the chemical shifts recorded in the ^{31}P n.m.r. spectra. It can therefore be concluded that there is no difference in the electronic environment of the phosphorus atom between the reaction products formed in the absence of oxygen and water, and those produced when either or both are present.

Table 6.3.

^{31}P n.m.r. Chemical Shifts for the Phosphonate-Iron Reaction Products obtained in the presence of oxygen and water

Conditions	Chemical Shifts (in p.p.m.)			
	dihexyl		diphenyl	
N_2	7.75	-0.73	0.27	128.06
N_2, H_2O	7.67	-0.73	0.33	128.13
O_2	7.79	-0.81	0.27	128.13
O_2, H_2O	7.83	-0.69	0.27	128.13

The small variation in the chemical shifts is due to the digitised manner in which the data was recorded. Chemical shifts (in p.p.m.) were calculated from the cursor position at the maximum absorbance, and not by direct measurement. The position of the cursor was effectively 'quantised'.

In conclusion, therefore, the ^{31}P n.m.r. spectra have shown that each of the phosphonate-iron reaction products contains phosphorus atoms in one of two chemical environments. Of these two environments one is identical to that found in the parent phosphonate, and would appear to be due to the presence in the sample of the parent phosphonate. The other phosphorus environment is that of the reaction product. No difference in the chemical environment of this 'new' phosphorus atom occurs when oxygen or water are introduced to the reaction during heating.

6.3. Mass Spectrometry

The Mass Spectra of a number of the phosphonate-iron reaction products have been recorded in order to study the composition of the reaction products. The technique has already been described in Chapter 4.

6.3.1. Method

Mass spectra of samples of the dialkyl phosphonate-iron reaction products were recorded, using samples taken from the reaction tests described in Chapter 5. These samples consisted of the reaction products formed by dihexyl, dioctyl and didodecyl phosphonates on heating with iron.

In recording the mass spectra, the best results were obtained using septum temperatures of 300° to 400°C. Spectra recorded with these higher septum temperatures gave signals at higher m/e (Mass/charge) ratios.

The spectra obtained showed the fragmentation pattern of the polymeric phosphonate-iron products. Using three reaction products in which the alkyl chain length alone varied, comparison of the spectra helped identify the "building blocks" of the polymers.

6.3.2 Spectra

The mass spectra recorded for the dialkyl phosphonate-iron reaction products show a complex pattern of signals. A large number of peaks is present in each spectrum and analaysis of all these peaks is impractical. Figure 6.8, which shows part of a typical spectrum recorded for a sample of the dihexyl phosphonate-iron reaction product illustrates this.

From a visual inspection of the spectra it can be seen that a pattern is present. This pattern is of a two-fold nature, and consists of a few high intensity peaks, regularly spaced (the "primary" pattern) interspersed with several lower intensity peaks (the "secondary" pattern). The frequency of the primary pattern differs between the hexyl, octyl and dodecyl phosphonate-iron reaction products. The frequency of the secondary pattern, however, does not alter with the change in organic group.

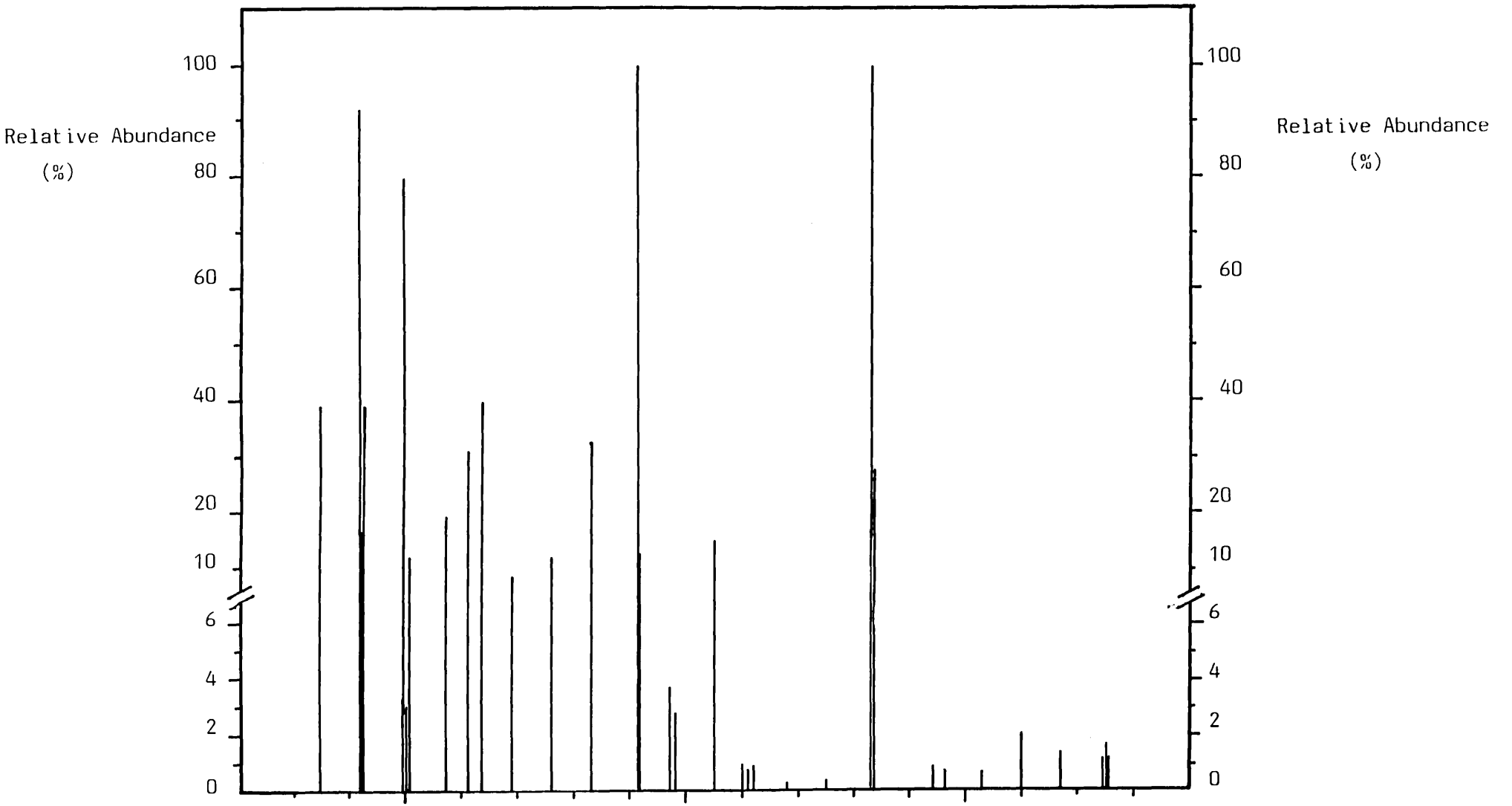


Figure 6.8. Mass spectrum line diagram of the dihexyl phosphonate-iron reaction product.

The mass spectra, as recorded, can be converted into a more useable form by converting them into line diagrams. In these the abundance of each of the most prominent peaks, expressed as a percentage of the most abundant peak is plotted against the mass/charge ratio (111). The line diagrams are shown in figures 6.9 to 6.11 for the dihexyl, dioctyl and didodecyl phosphonate-iron reaction products respectively. These line diagrams are in effect simplified versions of the mass spectra.

Using these line diagrams, a comparison was made of the mass spectra of the hexyl, octyl and dodecyl homologues of the phosphonate-iron reaction products.

6.3.3. Results and Discussion

The line diagrams derived from the mass spectra of the phosphonate-iron reaction products (figures 6.9 to 6.11) allowed measurement of the intervals of the "primary" pattern. These intervals differ for the three dialkyl phosphonate-iron reaction products. There are two possible deductions that may be drawn from this difference in the intervals of the primary patterns. That is, either the polymers derived from hexyl, octyl and dodecyl phosphonates are not comparable, or the polymers formed differ only in the size of the alkyl groups.

If the polymers are not comparable, then the difference in intervals observed in the mass spectrum should bear no relationship to the difference in mass units between the alkyl groups. Furthermore there should be no similarity between the mass spectral pattern for the three polymers.

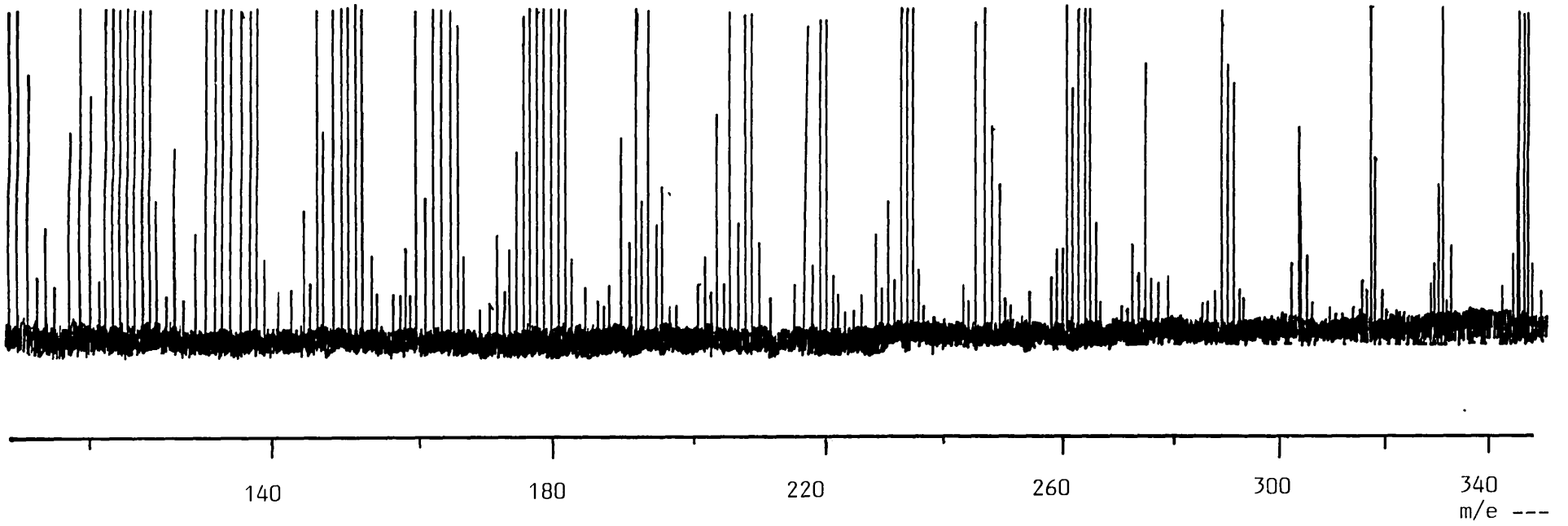


Figure 6.8b Representation of a portion of the mass spectrum obtained from a sample of the dihexyl phosphonate-iron reaction product (obtained from the maximum sensitivity trace).

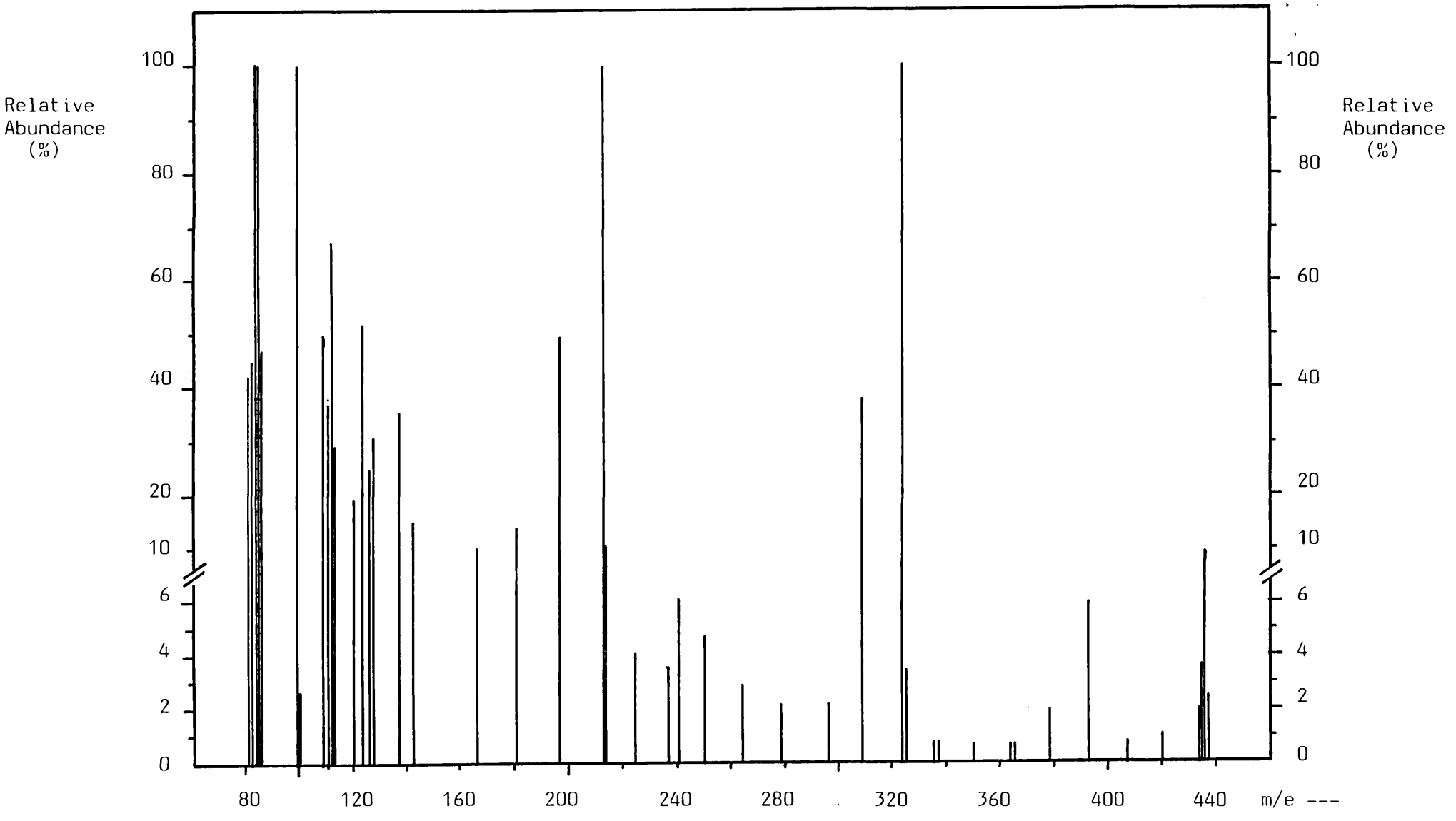


Figure 6.9. Mass spectrum line diagram for the dioctyl phosphonate-iron reaction product.

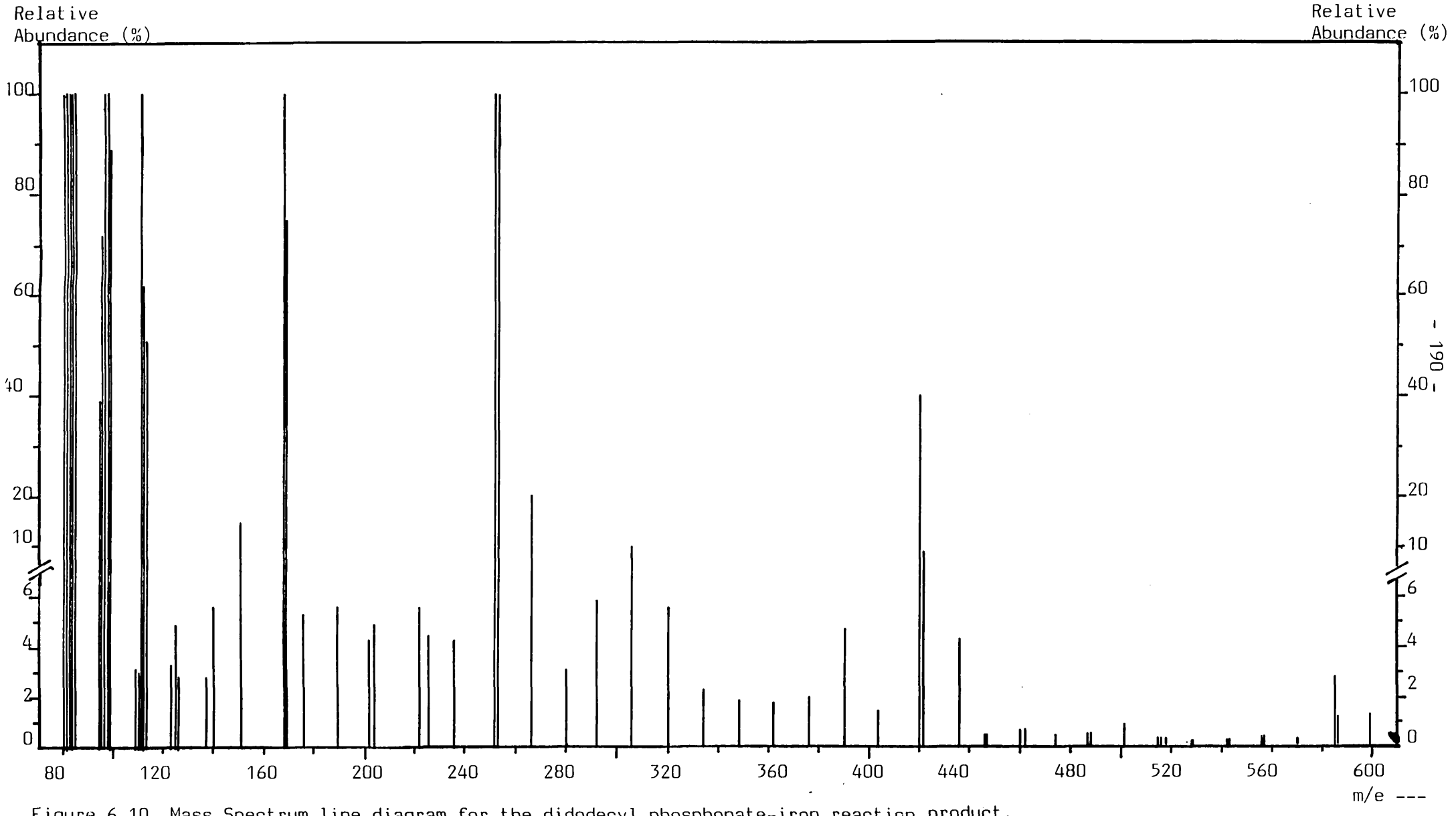


Figure 6.10 Mass Spectrum line diagram for the didodecyl phosphonate-iron reaction product.

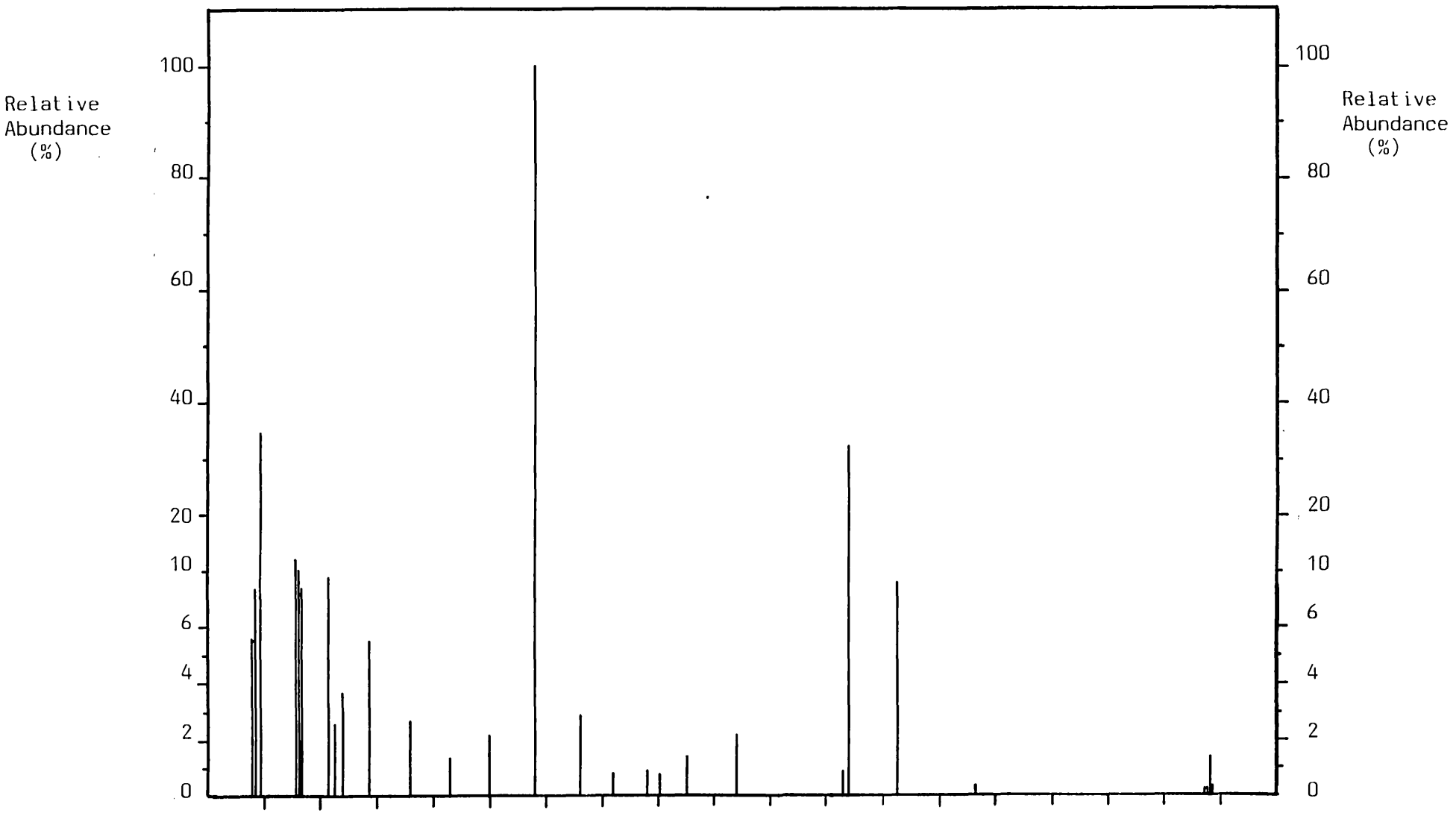


Figure 6.11 Mass spectrum line diagram for the dioctyl phosphonate-iron reaction product recorded at lower (300°C) septum temperature.

On the other hand if the hexyl, octyl and dodecyl homologues of the phosphonate-iron are similar in structure (excepting the alkyl chain length) then a relationship would be found between the difference in intervals and the difference in alkyl group masses. In this case, the general pattern in the mass spectra of the three polymers will be similar.

The primary peaks are marked on each of the line diagrams, in order of increasing mass/charge ratio as A, B and C. The mass/charge ratios of these peaks are listed in table 6.4 for the hexyl, octyl and dodecyl polymers.

Table 6.4

m/e ratios for "primary" mass spectrum pattern peaks

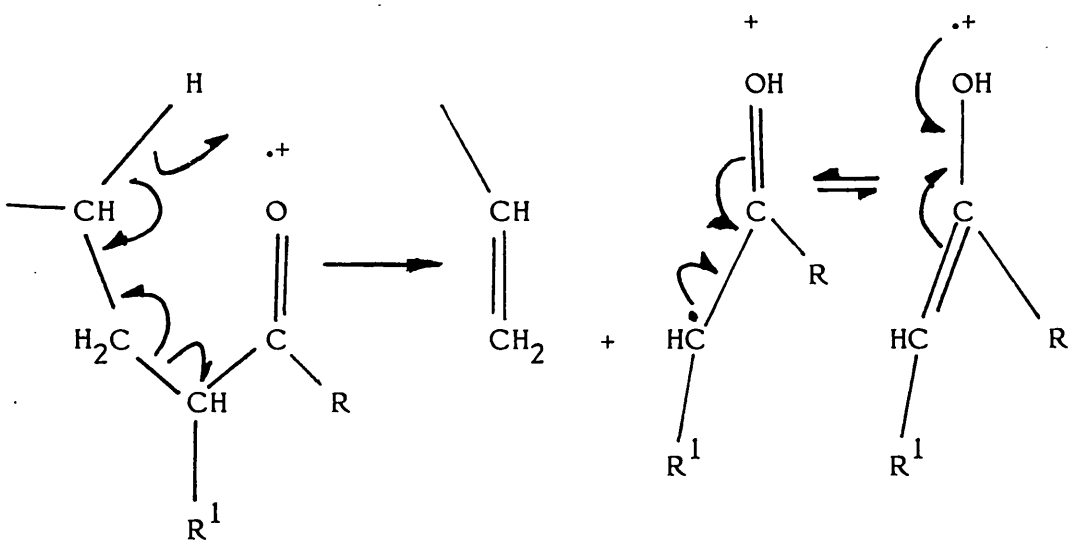
Peak	m/e ratio		
	hexyl	octyl	dodecyl
A	182	212	252
B	266	324	420
C	350	436	588

The intervals between primary peaks are therefore 84, 112 and 168 for hexyl, octyl and dodecyl respectively. The differences between the intervals are therefore 28 (Octyl-Hexyl) and 56 (Dodecyl-Octyl). These interval differences are exactly equal to the difference in molecular weights between the octyl and hexyl groups and between dodecyl and octyl groups. From the observed similarity in the mass spectra, it may be concluded that the polymers formed by di-hexyl, -octyl and -dodecyl phosphonates are similar. The equality observed between the mass differences and the interval differences supports this, indicating as it does that those differences present in the mass spectra arise from differences in the alkyl chain length. In addition it may be concluded that the difference between peaks A, B and C involves one alkyl group per step. If the molecular ions involved in peaks A to C differed by two alkyl groups, the interval difference between hexyl and octyl would be 56 (= 2 x C_2H_4). This assumption does depend on the ions A - C being single charged. If these ions were, for example, doubly charged the molecular weights would be double the mass/charge value obtained. The interval differences would then be 56 and 112 mass units for octyl-hexyl and for dodecyl-octyl respectively. In such circumstances the ions A to C would differ by 2 alkyl groups.

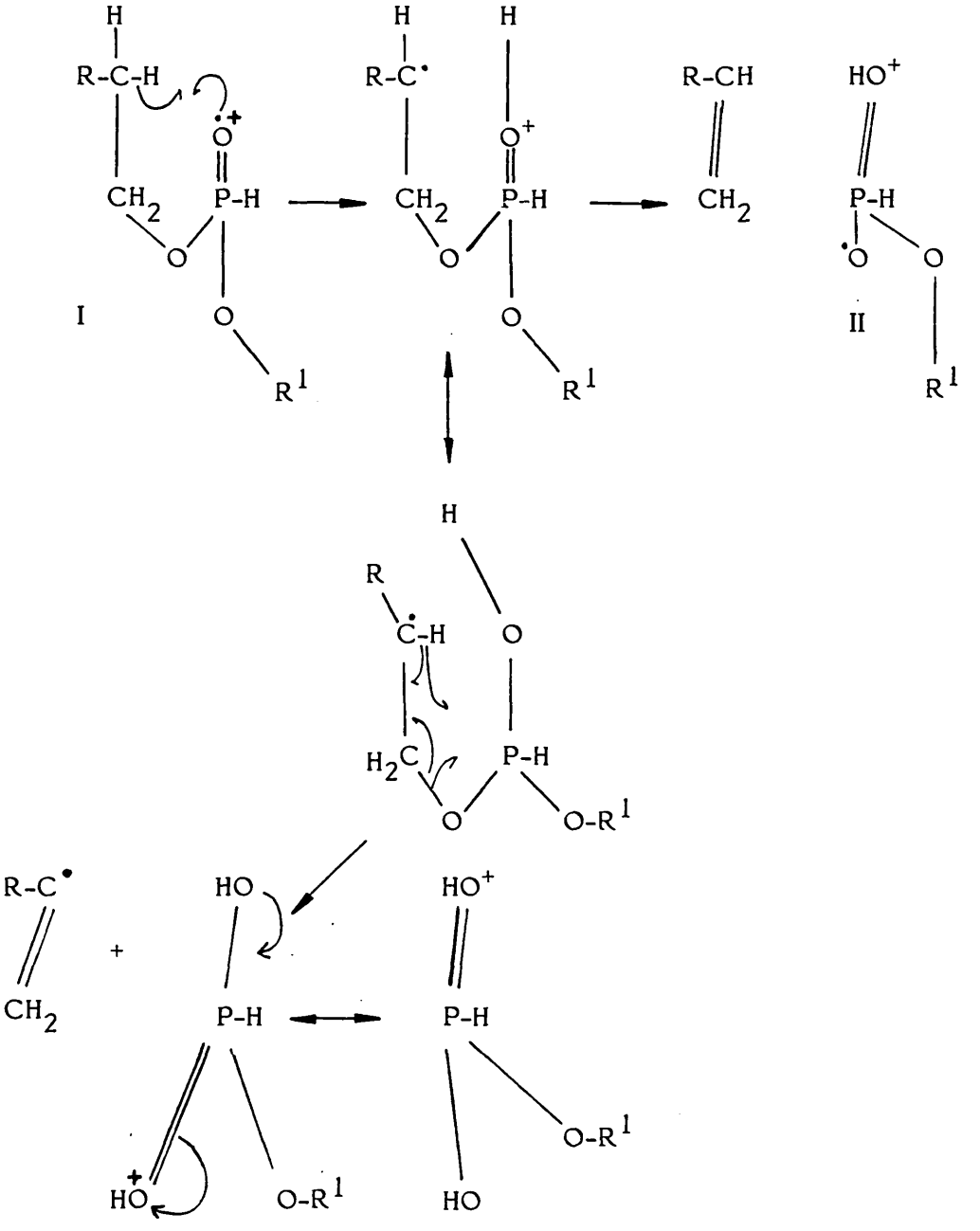
Thus there is one alkyl group involved in the difference between each of the ions A to C. By a comparison of the molecular weights of the alkyl groups and the intervals observed, the difference in molecular structure of these ions can be identified. The alkyl groups involved, hexyl (C_6H_{13}), octyl (C_8H_{17}) and dodecyl ($C_{12}H_{25}$) have molecular weights 85, 113 and 169 respectively. That is, the alkyl groups are one mass unit higher than the "primary" intervals observed in the mass spectra.

Thus the difference, in terms of molecular structure, between ions A, B, and C corresponds to the groups C_6H_{12}, C_8H_{16} and $C_{12}H_{24}$ respectively for the hexyl, octyl and dodecyl polymers.

This fragmentation by the loss of an alkene (C_6H_{12}, C_8H_{12} or $C_{12}H_{24}$) implies that the compounds are fragmenting in a manner similar to that found to occur with ketones, aldehydes and carboxylic acids. This is the "McLafferty rearrangement" (111,146) shown below for a ketone:-



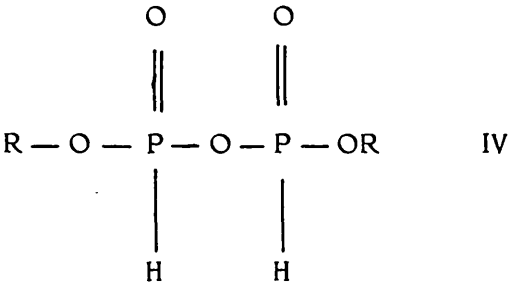
Both this rearrangement and a second rearrangement known as the "McLafferty + 1" rearrangement are characteristic rearrangements of phosphates (146) and presumably also of phosphonates since a phosphoryl bond is present in both. These two rearrangements are shown below for a phosphonate ester:-



III

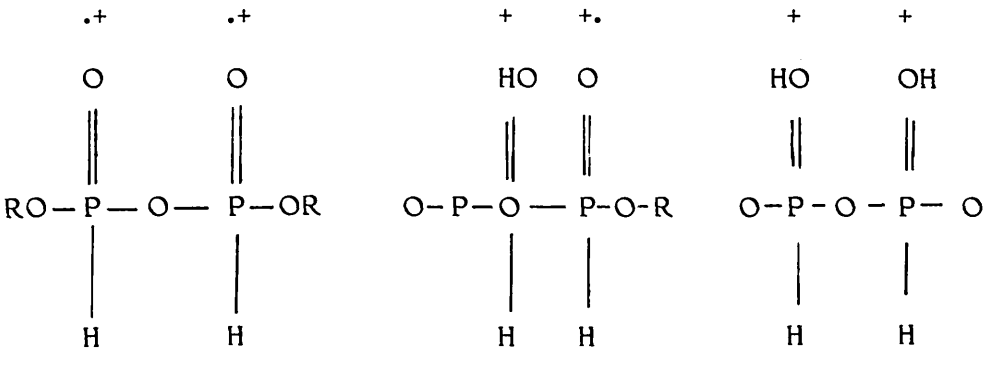
The "McLafferty + 1" rearrangement (above) results in the presence in the spectrum of m/e ratios that differ by C_nH_{2n} (I and II) and by C_nH_{2n-1} (I and III). This is shown in the mass spectra by, for example, the ions C,B+1 and B.

The products of the above rearrangement, cannot undergo a second such rearrangement, since no phosphoryl bond remains in the structure. If another phosphoryl bond were present in the molecule, as in IV below, a second rearrangement could occur:-



IV

However in order for this to occur, both phosphoryl oxygens will need to carry a charge, thus the parent ion and the daughter ions would be doubly charged. Although the parent ion and the two daughter ions (IVa, IVb and IVc below) would differ in mass by the mass of the alkene "R - H" (C_nH_{2n} where R = C_nH_{2n+1}), this would be shown in the mass spectra by m/e ratios differing by half the mass of C_nH_{2n}.



IVa IVb IVc

Consequently the series of peaks C to A do not arise as a result of consecutive "McLafferty + 1" rearrangements of the same parent ion. A proportion of each of the ions C to A must result either as the result of different fragmentations, or must themselves be "parent" ions.

Analysis of the likely composition of the m/e ratios leads to the same structures for the peaks C to A in the mass spectra of the dihexyl and dioctyl polymers.

C = $(RO)_3PO$

B = $(RO)_2\ P(O)OH$

A = $(RO)\ P(O)(OH)_2$

The didodecyl phosphonate mass spectrum has peaks 16 mass units lower than required for the above structures, which correspond to the presence of phosphites and phosphonates rather than phosphates. In the dodecyl mass spectrum, peaks were recorded at the m/e ratios corresponding to the phosphates but at a lower intensity. The peaks are marked in the line diagram (figure 6.11) as A_1, B_1 and C_1. This unexpected difference in the spectra would appear to be associated with a lack of volatility of the polymer-bound molecules. It can be seen that the mass spectra of the dihexyl and dioctyl polymers (figures 6.9 and 6.10) show peaks corresponding to the phosphonates but at lower intensities. However when the mass spectrum of the same dioctyl polymer sample was recorded at a lower (300^oC) septum temperature the ratio of the intensities of the phosphate/phosphonate peaks were reversed. The line diagram for this mass spectrum is shown in figure 6.12.

The intensities of these peaks reflects both a contribution from a "parent ion" and from rearrangement/fragmention reactions as outlined above. Clear evidence that rearrangement reactions occur, in this case the "McLafferty + 1" rearrangement, is shown by the presence of strong peaks at a m/e ratio of 99 in all three spectra, resolution of which yields the formula H_4PO_4, which is the "McLafferty + 1" rearrangement product of $(RO)P(OH)_2O$. Further evidence is given by the m/e ratios one greater than each of A and B. These again are the products of the "McLafferty + 1" rearrangement of C and B respectively. Isotopic effects, i.e. the presence of ^2D, ^{17}O and ^{13}C in the molecule, can be excluded since those "M + 1" peaks are present at too high an intensity (111).

A study of the intensities of the "major" peaks does not indicate the relative abundances, since the signals at m/e ratio A and B are 'off scale' in the dihexyl and dioctyl mass spectra even on the lowest sensitivity. In the dodecyl mass spectrum, the intensities are in the order A > B (also $A_1 > B_1$). Of more use is the "minor" pattern present between the "major" peaks. This "minor" pattern arises as the result of partial fragmentation of the alkyl chain. An examination of the line diagrams shows that the first peak (not including the phosphite/phosphonate peak at 16 mass units lower than the A, B, or C peak (dihexyl and dioctyl polymers only) is 30 mass units below the major peak, and the pattern continues at intervals of 14 mass units. These peaks correspond to the loss of C_2H_6 (mass = 30) and higher alkanes from the alkyl chain (111). It can be seen from the line diagrams that the relative abundances of the minor pattern below A are greater than those below B. It follows therefore that the most abundant component of the sample is A, that is, the monoalkyl phosphate $(RO)P(O)(OH)_2$.

In conclusion therefore, mass spectrometry of the dialkyl phosphonate-iron polymers has shown the following:-

a) The polymers formed by dihexyl, dioctyl and didodecyl phosphonate on being heated with iron are similar compounds, which give rise to comparable fragmentation patterns in their mass spectra.

b) The mass spectra show the presence of phosphate esters, and in particular the mono-alkyl phosphate $(RO)P(OH)_2O$.

c) Changes in the septum temperature appear to indicate that the phosphate esters are more firmly bound to the iron than are the phosphonate molecules. Thus it would follow that these phosphonate molecules are loosely bound to the polymer as for example terminating groups on the end iron atom, or are trapped in the polymer sample

6.4 Elemental Analysis

Elemental microanalysis was carried out on a series of samples of the dihexyl phosphonate-iron reaction product to study the changes in elemental composition that occurred in the reaction.

6.4.1 Method

The methods of elemental microanalysis have been detailed in section 4.5. The analysis described in this section was carried out by Elemental Microanalysis Ltd. The samples used for these analyses were prepared by heating dihexyl phosphonate with iron powder at $155^{o}C$ under nitrogen.

Samples were withdrawn from the reaction mixture, using a glass teat pipette, at 30 minutes intervals over 3 hours. These samples were despatched to EMA Ltd. for carbon, hydrogen and phosphorus analysis. Analysis of iron content was carried out in the laboratory as described in section 5.2.1. The oxygen content was determined by arithmetic difference.

6.4.2 Results and Discussion

The results obtained are in the form of percentage content of each element. From these percentages the oxygen content was determined by arithmetic difference. These results are listed in table 6.5.

Table 6.5

Elemental compositions for a series of dihexyl phosphonate-iron reaction samples

Sample Heating time	percentage content				
	C	H	P	Fe	O
30	55.895	11.3	12.265	0.29	20.25
60	48.235	9.725	12.465	0.61	28.965
90	54.05	10.715	12.485	1.74	21.01
120	53.25	10.39	13.005	2.42	20.935
150	51.715	10.35	14.10	2.91	20.92
180	51.34	10.22	13.39	4.54	20.51

Division of these figures by the respective atomic weights, gives the proportion of each atom present. By dividing throughout by the phosphorus figure, so obtained for each sample, gives the number of atoms of each element, relative to one phosphorus atom, that are present. This data is presented in Table 6.6.

Table 6.6

Elemental ratios for a series of dihexyl phosphonate-iron reaction samples

Sample Heating time (mins)	atomic ratios				
	C	H	O	Fe	P
30	11.8	28.5	3.2	0.013	1
60	10.05	24.2	4.5	0.027	1
90	11.2	26.6	3.25	0.077	1
120	10.6	24.7	3.12	0.103	1
150	9.5	22.7	2.87	0.114	1
180	9.9	23.6	2.96	0.308	1

If the results for the 60 and 150 minutes are assumed to be erroneous, then the remaining results show a clear trend. A decrease in the ratios of carbon, hydrogen and oxygen to phosphorus is seen with increasing times of heating. The decrease in the oxygen-phosphorus, in proportion to the original ratio, is significantly less than the decrease in the carbon-phosphorus and hydrogen-phosphorus ratios. This anomaly is discussed below.

The reactions between the phosphonates and iron powder were shown to involve the elimination of the parent alcohol (or phenol). A comparison of the '30 minute' and '180 minute' samples shows the decreases in the elemental ratios occurred in the approximate ratios $C_6H_{15}O_{0.75}$ that is approximately the ratio as the elements occur in the parent alcohol, hexanol $C_6H_{13}OH$. However if the elimination of hexanol occurs, the oxygen contents of the samples are too high. The "180 minute" sample has the composition $C_{10}H_{23}O_3Fe_{0.3}P$ assuming that all the carbon is present at the hexyl group, then this composition is equivalent to $(C_6H_{13})_{5/3}\ PO_3H\ Fe_{0.3}$. In this sample, then, one hexyl (C_6H_{13}) group has been eliminated for every three phosphorus atoms. This is in conflict with the 'alcohol elimination' mechanism and supports an "alkane-elimination" mechanism, a mechanism which has been previously proposed (10,26). However both the infrared analysis and the observations of the reactions, especially the diphenyl phosphonate reaction, do not support this latter mechanism.

In Chapter 5 it was seen how oxygen and the oxidation of iron samples enhanced the rate of the reaction of phosphonates and iron powder. The higher than expected oxygen figures shown in table 6.6 for all the samples would appear to result from a contribution to the elemental ratios by oxygen from surface iron oxides.

The sample used for these analyses are of necessity impure, since the intention was to observe the changes that occurred in the elemental ratios rather than to determine the elemental composition of the reaction product. It must therefore be assumed that the samples contained both unreacted dihexyl phosphonate and eliminated, but 'trapped' hexanol. This assumption will be of importance later, when possible structures of the polymer are discussed.

Evidence that the samples do contain a certain amount of unreacted ester and alcohol was provided by comparing the results of microanalysis of two identical samples of dihexyl phosphonate-iron reaction product, one sample of which was heated (to 100°C) under high vacuum before analysis. A significantly lower proportion of alkyl groups (as C_6H_{13}) and of oxygen relative to phosphorus, was found in the vacuum "stripped" sample compared to the "non-stripped" sample.

6.5 Electron Spin Resonance Spectroscopy

The electron spin resonance spectrum of a sample of the dihexyl phosphonate-iron reaction product was recorded in order to examine the electronic nature of the iron atoms present in the polymer. Electron spin resonance (e.s.r.) or as it is also known, electron paramagnetic resonance (e.p.r.), is a phenomenon associated with unpaired electrons.

The oxidation state of an atom, which may have unpaired electrons in one oxidation state, and none in another, may be determined by the presence (or absence) of an e.s.r. signal.

The spectra were recorded in the Department of Chemistry, Imperial College.

6.5.1. Introduction

Molecules or ions containing unpaired electrons show a marked difference in behaviour to those in which all the electrons are spin-paired when both types of molecules are placed in a magnetic field. In molecules with unpaired electrons one or more of the orbitals contain one electron only.

These orbitals therefore possess a net spin momentum. (In filled orbitals, the two electrons are spin-paired, consequently there is no net spin momentum). The result of this net spin momentum is that the electron possesses a net magnetic moment. When the molecule or ion is placed in a magnetic field an interaction occurs between the magnetic field generated by the electron and the applied external field. This interaction causes the energy of the electron to be split into two levels.

At room temperature, the lower energy level is more highly populated, but when radiation of the correct frequency is supplied, excitation of the electron to the higher energy occurs. Relaxation to the lower energy levels takes place mainly through a non-radiative transfer and a net absorbance of energy is thus observed.

A mathematical treatment of the phenomenon (148,149) shows that the energy difference between the two electron energy states is equal to gBH, where g is the gyromagnetic ratio (150), that is the ratio of the magnetic moment to the angular momentum, B is the Bohr magneton (150) and H is the magnetic field strength. Thus when radiation of frequency given by $h\nu = gBH$ is supplied, resonance occurs. In e.s.r. this radiation is in the microwave region.

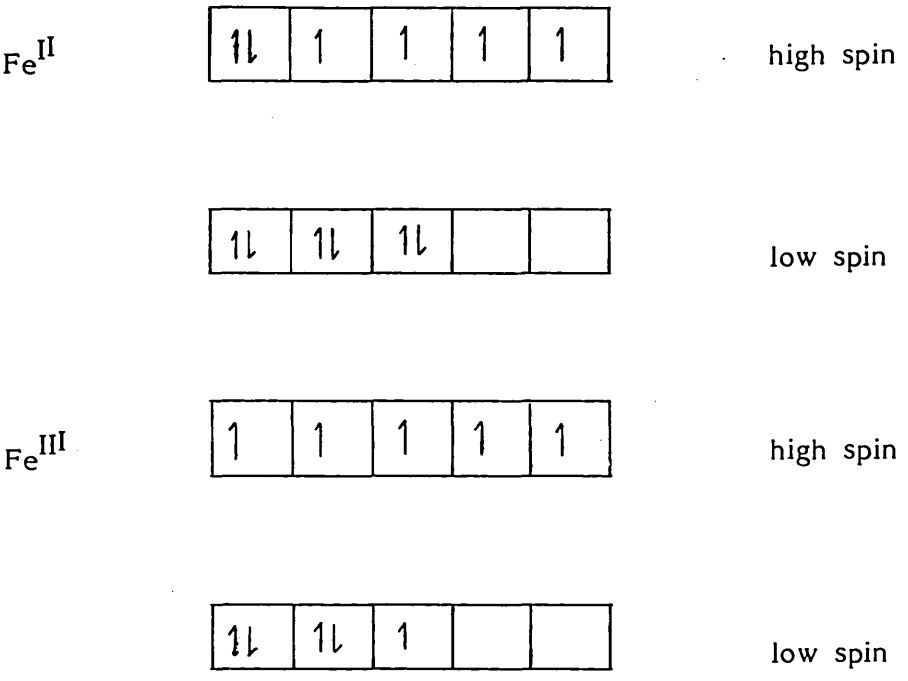
To record the spectrum, the sample is placed in one of the arms of a cross-shaped microwave resonator cavity. One of the arms contains the microwave oscillator and detectors occupy the remaining two arms - one opposite the source (to measure the in-phase radiation) the other at 90° to the source that is opposite the sample arm (to measure the out of phase signal). A powerful (fixed) magnet provides the external magnetic field.

The resonator cavity, acts as a microwave equivalent of a Wheatstone bridge, "null" signals being returned by both detectors until resonance occurs. A small a.c. modulation is applied to the magnetic field. When, the amplitude of this modulation is smaller than the line width of the resonance signal, it can be shown (158) that the output of the resonator is proportional to the in-phase (X') and out-of-phase (X') signals of the detectors.

Resonance is observed by sweeping the oscillator across the microwave region and recording the output of either the inphase or out of phase detectors (as $dX'/d\nu$ or $dX''/d\nu$) against the microwave frequency. A more detailed description of the instrumentation and methods of recording the spectra may be found in references (151), (152), (153).

In considering the applicability of e.s.r. to the study of iron compounds, it is necessary to examine the electronic states of the iron (II) and iron (III) species. The neutral iron has the electronic structure [Ar] $3d^6\ 4s^2$ (where [Ar] represents the electronic configuration of argon, completely filled 1s, 2s, 2p, 3s and 3p sub-shells). The electronic structures of Fe^{II} and Fe^{III} compounds are therefore Fe^{II} [Ar] $3d^6\ 4s^o$ and Fe^{III} $3d^5\ 4s^o$. The distribution of these d electrons within the five d orbitals is governed by a number of factors, noticeably Hund's rule (154). Hund's rule states that the pairing of electrons is an unfavourable process. In competition with this is the increase in energy of some of the orbitals when the geometric distribution of ligands around the ion is considered.

The net result is that there are two electron configurations possible for Fe^{II} and Fe^{III} which depend on the relative energies of electron pairing and ligand effects (154). These configurations are termed high spin (maximum number of unpaired electrons) and low spin (maximum electron spin pairing), and for Fe^{II} and Fe^{III} are:-



Of these configurations, two spin Fe^{II} possesses no unpaired electrons and is therefore diamagnetic. Low-spin Fe^{II} compounds therefore do not give rise to a signal in the e.s.r. spectrum. High spin Fe^{II}, although paramagnetic, does not give rise to e.s.r. signals except in a very few cases (155). E.s.r. signals in compounds with an even number of unpaired electrons are very difficult to obtain (156). In contrast, both low spin and high spin Fe^{III} compounds possess unpaired electrons and, therefore, give an e.s.r. signal.

6.5.2. Spectra

The e.s.r. spectrum of the dihexyl phosphonate-iron reaction product was recorded. The sample used for this spectrum was prepared by heating dihexyl phosphonate with iron powder for 18 hours at 125°C, under nitrogen. The spectrum obtained is shown in figure 6.13.

6.5.3 Results and Discussion

The dihexyl phosphonate reaction product was shown to give rise to a signal in the e.s.r. spectrum. It can therefore be concluded that the iron present is in the +3 oxidation state (155).

The value obtained for g (g = 2.0054) is close to the theoretical value g = 2.00. Although this does not yield any positive information, it does indicate that the system under examination is showing simple behaviour. This may well indicate that all the iron atoms are equivalent (156).

The spectrum recorded shows no hyperfine splitting, i.e. splitting due to a magnetic dipole interaction between the electronic magnetic moments and the nuclear magnetic moment of the paramagnetic ion (157, 158). The absence of hyperfine structure indicates that there is no other paramagnetic atom present (including iron in a different environment) (159). Thus all the iron atoms are equivalent.

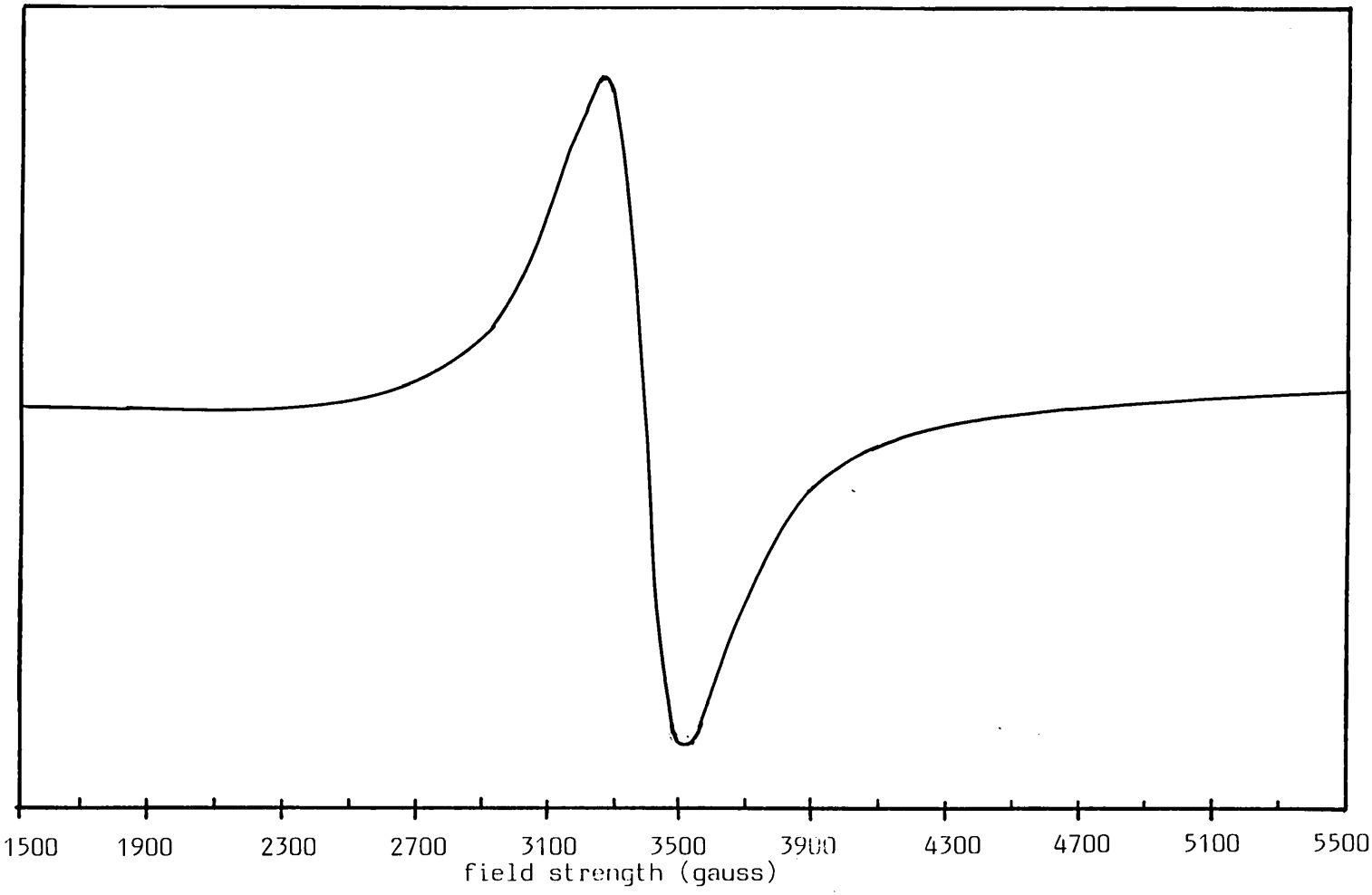


Figure 6.12 Electron Spin resonance spectrum of the dihexyl phosphonate-iron reaction product.

6.6. Mossbauer Spectroscopy

Mossbauer spectroscopy is a phenomenon, which, although found in many nuclei, is chiefly exploited for studying iron and tin compounds. The effect relies on the excitation of the nucleus to a higher energy state by the absorption of a gamma ray of the appropriate energy. The excited nucleus will decay to the ground state by emission of a gamma ray but not necessarily in the same direction as the incident gamma ray. Mossbauer spectroscopy is therefore a type of nuclear fluoresence spectroscopy.

6.6.1. Introduction

The radioactive decay of ^{57}Co, proceeds by electron capture ($p + e \rightarrow n$), forming a daughter nuclide ^{57}Fe in an excited state. This nucleus decays to the ground state by the loss of a gamma ray. When this radiation falls on an absorber in which the iron nuclei are in an identical chemical environment, some of this radiation will be absorbed. If the iron atoms are in a different chemical environment, no resonance and hence no absorbance of energy, occurs.

The energy difference between the ground and excited nuclear states is dependent on the chemical environment and oxidation state of the ion, since a major influence is the electronic shielding of the nucleus by the inner-most orbitals. In order to measure this energy difference, the energy of the incident gamma ray, as seen by the sample, must be able to be varied. To accomplish this the absorber is vibrated slightly towards and away from the source. The small Doppler energies induced by these vibrations, alter the energy "seen" by the absorber.

The nuclear resonance is therefore observed at a doppler speed particular to the environment of the absorber nuclei. This doppler speed, expressed in mm/sec. is usually termed the "chemical" or "isomer shift" (δ).

In the Mossbauer spectrometer, the absorber (sample) is placed between the source and the detector, a Geiger-Muller tube. The detector is connected to a multi-channel analyser each channel of which is dedicated to a particular vibration speed. The spectrum is recorded by scanning the vibration speed (from 0 to 3 mm/sec), the detector-analyser recording the transmitted radiation at each vibration speed.

The Mossbauer resonance is subject to a number of competing effects, which degrade the energy of the incident gamma ray. The main effects are nuclear recoil and thermal energy effects. These effects are limited by carrying out the analysis at low temperatures (77 K) and by using a solid sample in which the absorber atom is firmly held in a lattice.

The spectra are recorded over a relatively long counting period (hours rather than minutes). This is a consequence of the health hazard associated with high energy radioisotopes and their high cost of production. Low photon flux densities are therefore used to achieve an acceptable resolution.

A more detailed explanation of the theory and practice of Mossbauer spectroscopy is given in references (161), (162), (163).

6.6.2 Spectra

The Mossbauer spectrum of the dihexyl phosphonate-iron reaction product was recorded at eight temperatures between 77K and 298K. These spectra were recorded in the Department of Chemistry, Imperial College. The sample used for these spectra was prepared by heating dihexyl phosphonate with iron powder for 18 hours at 125°C under nitrogen.

The Mossbauer spectrum is shown in figure 6.14 for four different temperatures.

6.6.3. Results and Discussion

Several useful parameters are obtainable from Mossbauer spectra. These are the chemical (or isomer) shift, the quadrupole splitting and its temperature dependance, if any, and the presence and nature of any hyperfine splitting.

Examination of the spectra recorded (figure 6.14) shows a narrow split doublet. This doublet is the quadrupole splitting (164, 165) and the isomer shift is determined from the centroid of these doublets (164). Figure 6.15 shows the isomer shifts plotted against the temperature at which the spectrum was recorded. These isomer shifts range from 0.55 mm/sec at 77K to 0.44 mm/sec at 298K. These values do not of themselves provide any definitive evidence of the oxidation state of the iron atom. The values obtained fall within the normal limits for high spin Fe(III) and diamagnetic covalent Fe(II) and just outside the limits for Fe(II) (low and high spin) and for low spin Fe(III) (166). Further guidance is given by the quadrupole splitting.

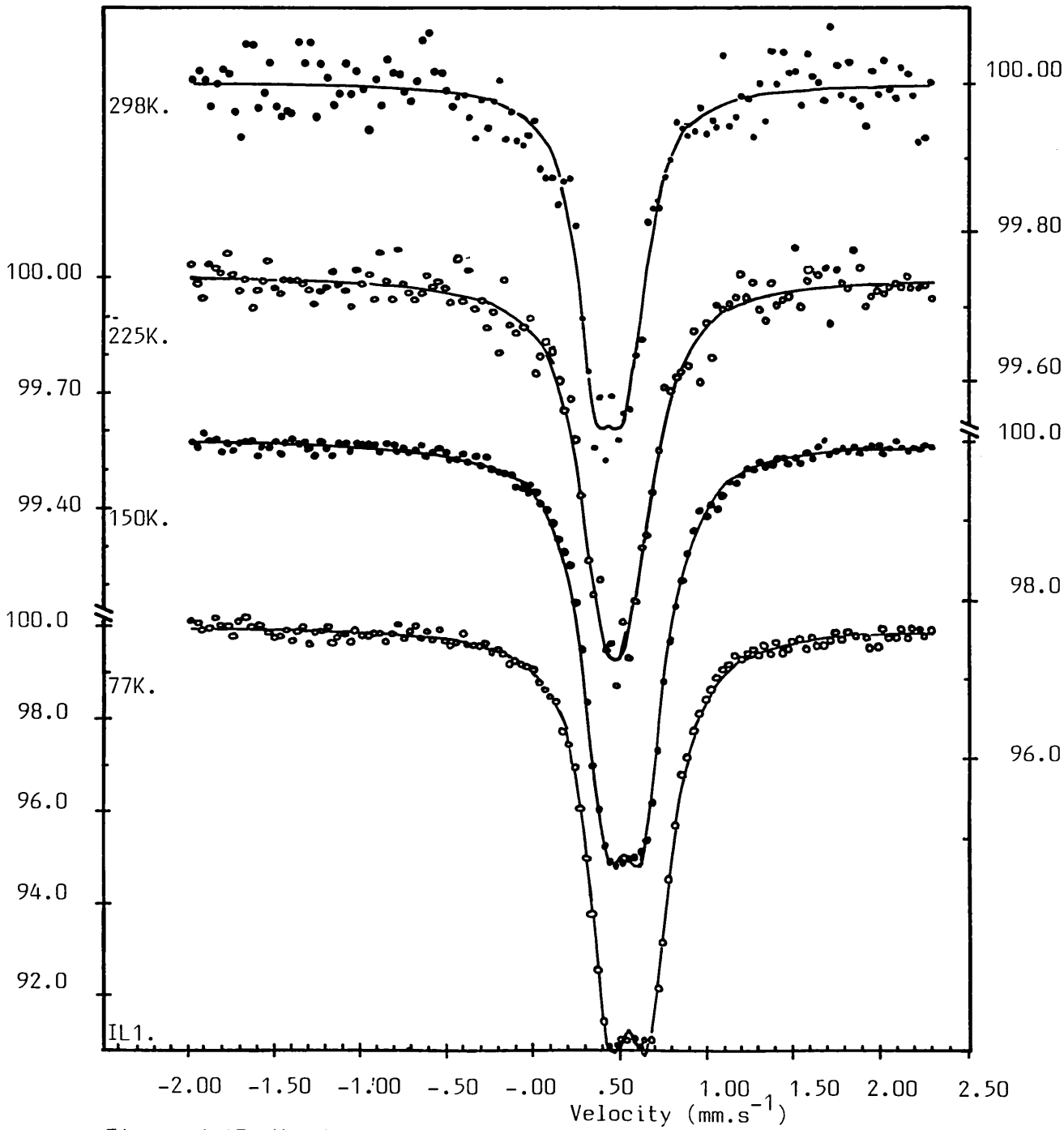


Figure 6.13 Mossbauer spectrum of the dihexyl phosphonate-iron reaction product.

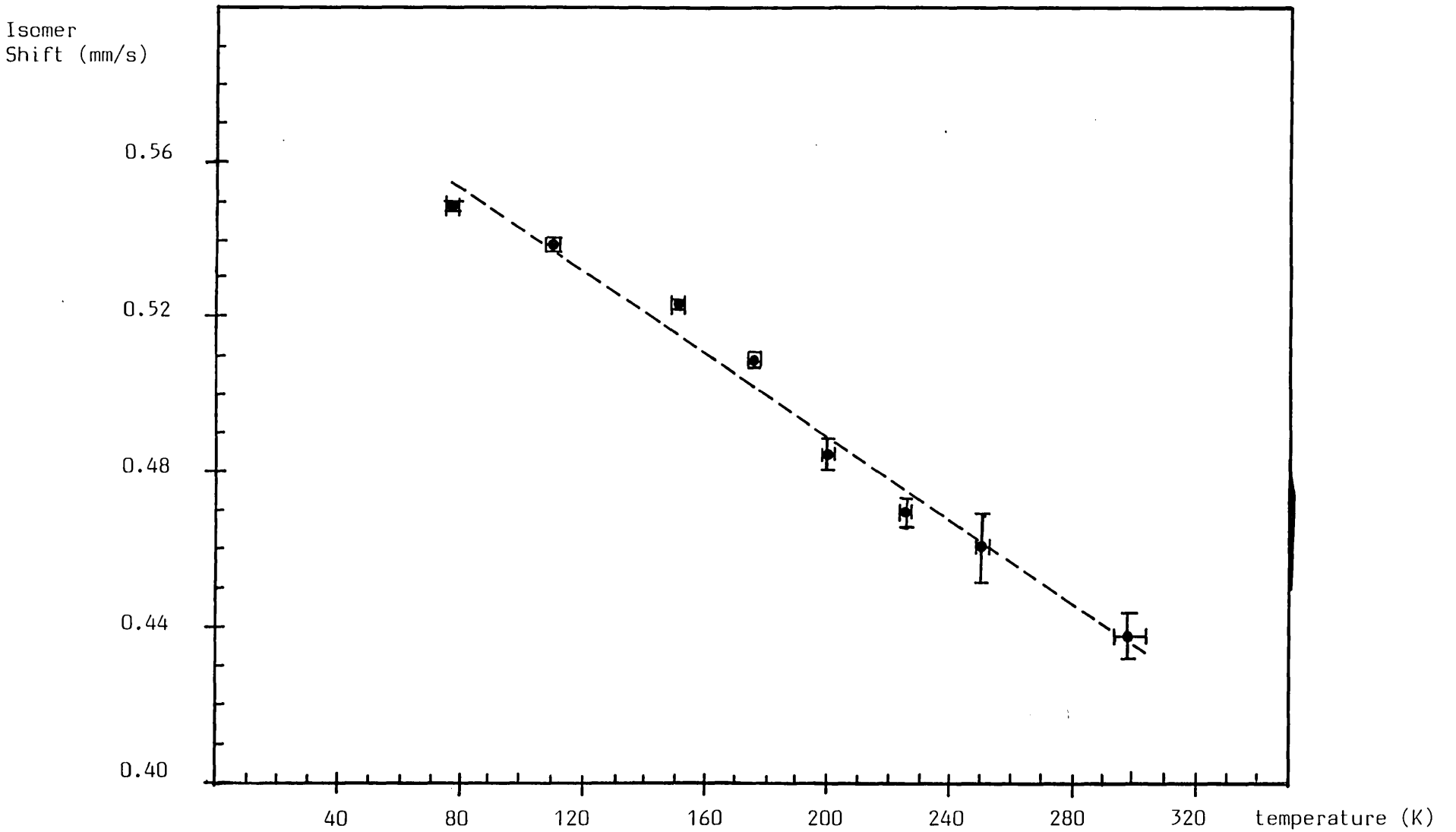


Figure 6.14 Temperature dependence of the Mossbauer Isomer shift for the dihexyl phosphonate-iron reaction product.

The quadrupole splitting arises from an interaction of the nuclear quadrupole moment and the electric field gradient. The nuclear quadrupole moment is a measure of the non-sphericity of the nuclear charge distribution. In a nucleus of spin $I > {}^{1}/_{2}$, a non-spherical charge distribution results, and therefore in ^{57}Fe, the higher nuclear spin state $I = {}^{3}/_{2}$ results in a non-zero quadrupole moment. In the ground state $I = {}^{1}/_{2}$ so there is no quadrupole interaction arising from the ground state, and only that arising from the excited ($I = {}^{3}/_{2}$) state needs to be considered. For ^{57}Fe the spectrum shows a doublet, centred around the isomer shift (164,165,168,169,170). The electric field gradient is a resultant of the non-symmetrical distribution of ligands around the nucleus. If a symmetrical distribution exists there the elctric field is zero. When the electric field gradient is non-zero, then a quadrupole splitting is observed, with those nuclear states of spin quantum $I > {}^{1}/_{2}$ (170). Nuclear spins are quantized, and the nuclear spin number with respect to the principal axis z, Iz can take (2I + 1) values of +I,I-1,....,. For $I = {}^{3}/_{2}$ the spin of the nucleus has four values $I_z = {}^{3}/_{2}, {}^{1}/_{2}, -{}^{1}/_{2}, -{}^{3}/_{2}$ with the $\pm$ Iz values equal. There are therefore two energy levels associated with the nuclear spin quantum number $I = {}^{3}/_{2}$ viz $Iz = \pm {}^{3}/_{2}$ and $Iz = \pm {}^{1}/_{2}$ (164,171). The value of the quadrupole splitting cannot be used directly to determine the oxidation state (169). The observed quadrupole splitting of 0.23 to 0.17 mm sec are comparatively small, which is in keeping with iron (III) (172). However quadrupole splitting energies for Fe(II) can vary from 0.0 to 3.6 $mm.s^{-1}$ and for Fe(III) from 0.0 to 0.7 mm s^{1} (169), and an absolute decision cannot be made on this evidence alone.

The quadrupole splitting observed varies with temperature, and this temperature dependence is a characteristic of paramagnetic compounds (172,173). In paramagnetic compounds the energy of the first excited electronic state is close to kT above the ground state (where k is the Boltzmann constant and T is the absolute temperature). The orbital occupation becomes temperature dependent, and this affects the quadrupole splitting. The paramagnetic species are Fe(II) high spin and Fe(III) high and low spin, all possessing unpaired electrons. High spin Fe(III) has a symmetrical electronic distribution, and consequently no inherent electric field gradient. Quadrupole splitting in Fe(III) arises from charges external to the atom, and no temperature dependance is observed (172,173).

In the previous section (6.5) the recording of the e.s.r. spectrum was described. It was reported that very few high spin Fe(II) compounds give rise to e.s.r. signals. Consequently it was concluded that the iron species present was Fe(III). From the thermal dependency observed in the quadrupole splitting it follows that the iron is present is low-spin iron (III).

The isomer shift 0.55 to 0.44 $mm.s^{-1}$ is just beyond the limits given by Gibb for low spin Fe(III) compounds (-0.17 to 0.4 mm s^{-1}) (166) but falls within the limits given by Danon (174) of 0.0 to 0.7 $mm.s^{-1}$ for iron complexes. Danon (174) also reports that practically all organo-iron complexes are low spin.

6.7 Discussion of the Analytical Results

The results of the various methods of analysis described in this chapter allow further insight into the nature of the products of the reaction of dialkyl and diaryl phosphonates. From earlier discussions it was concluded that a ferro organophosphorus polymer was produced by these reactions.

The work reported in this chapter gives information about certain features of the polymer and enables further aspects to be deduced.

6.7.1 Similarity

The different phosphonate-iron products obtained show distinct indications of being similar compounds. The three dialkyl phosphonates give comparable results in their mass spectra and in their ^{31}P nmr spectra. Likewise the two diaryl phosphonates (diphenyl and bis octylphenyl) show similar changes in their ^{31}P nmr spectra and it may be concluded that these two reaction products are similar.

From the similarity of their reactions, the comparable changes in their ^{31}P nmr spectra and the similar change that occurs in the infrared spectra it is reasonable to assume that the products of the reactions of iron with dialkyl and diaryl phosphonates are similar.

6.7.2 Polymeric Nature

All the phosphonate-iron reaction products show the same trend of increasing viscosity and rheopecticity and an decreasing rate of solution. This trend indicates that the products are polymeric and become increasingly more so with time.

6.7.3 Oxidation State of the Iron

The combined results from the Mossbauer and e.s.r. spectra indicate that only one type of iron is present. The results indicate that these iron atoms are present as Fe(III) low-spin, that is covalently bonded, atoms.

6.7.4. Bonding State of the Phosphorus Atom

The infrared spectra of the phosphonate-iron polymers show that the phosphorus atom is bound through a donor phosphoryl bond (P=O→) to the iron atom. The presence of P-O-C bonds and of P-H bonds is also shown by the infrared spectra. Unlike the donor phosphoryl bonds however, these bonds were present in the parent phosphonate and the relative contribution, if any, to these absorbances, by the polymer molecules could not be determined.

The infrared spectra of the polymers show that phosphorus-oxygen-phosphorus (P-O-P) bridges are not present in the polymer. The spectra do not provide either direct evidence of P-O-P bonds by the presence of a new absorbance band at 900 to 1000 cm^{-1} (105,136) or indirect evidence by the appearance of a new phosphoryl absorbance at a frequency of 1200-1300 cm^{-1} (104). No evidence of P-O-P groups is provided by the mass spectra of the polymers. None of the m/e ratios in these spectra can be resolved into structures which include the P-O-P group.

The most information about the bonding state of the phosphorus was given by the mass spectra. These spectra show the presence of the phosphate group in the polymer. The mass spectra showed that the polymer consisted largely of the monoalkyl phosphate, with a significant amount of the dialkyl phosphate present. At first sight this would appear to conflict with the results obtained from the ^{31}P n.m.r. spectra, which indicated that the phosphorus atoms in the polymers were present in only two different environments.

Two signals were obtained in the n.m.r. spectra, of which one was at the same value of chemical shift as recorded for the parent phosphonate. The existence in the polymer of a donor phosphoryl bond was discussed above, as shown by the appearance of a new absorbance at 1160 cm^{-1}. The difference in these two absorbance frequencies results from a relative weakening of the donor phosphoryl bond. This weakening of the bond is caused by the "donation" of a lone pair of electrons from the oxygen atom to form the bond with the iron. This in turn causes a displacement of electron density away from the phosphorus, and a reduction of the formal bond order to approximately 1.5 (144). This electron displacement will greatly affect the electronic environment of the phosphorus atom and hence the ^{31}P n.m.r. chemical shift. However it has been shown that the environment of phosphorus atom in the polymer is that of the phosphate group. The ^{31}P n.m.r. chemical shifts of phosphates and phosphonates are substantially different (145) and a 'new' signal would be expected in the spectrum arising from the increasing proportion of phosphate present. Since only one 'new' signal is obtained, it follows that all the phosphate groups are donor bonded to the iron atoms. It must also follow that the parent phosphonate is not donor bonded to the iron.

The mass spectra showed the presence of both dialkyl and monoalkyl phosphate in the polymer. With two different compounds it might be expected that two 'new' signals would be recorded in the ^{31}P n.m.r. spectrum instead of only the one new signal recorded. However the electronic environment of the phosphorus is affected most by those atoms bonded directly to it and less by the atoms or goups bonded to the adjoining atoms (144). This may be seen by the similarity of the chemical shifts recorded for the dihexyl, dioctyl and didodecyl phosphonates and their polymers formed with iron.

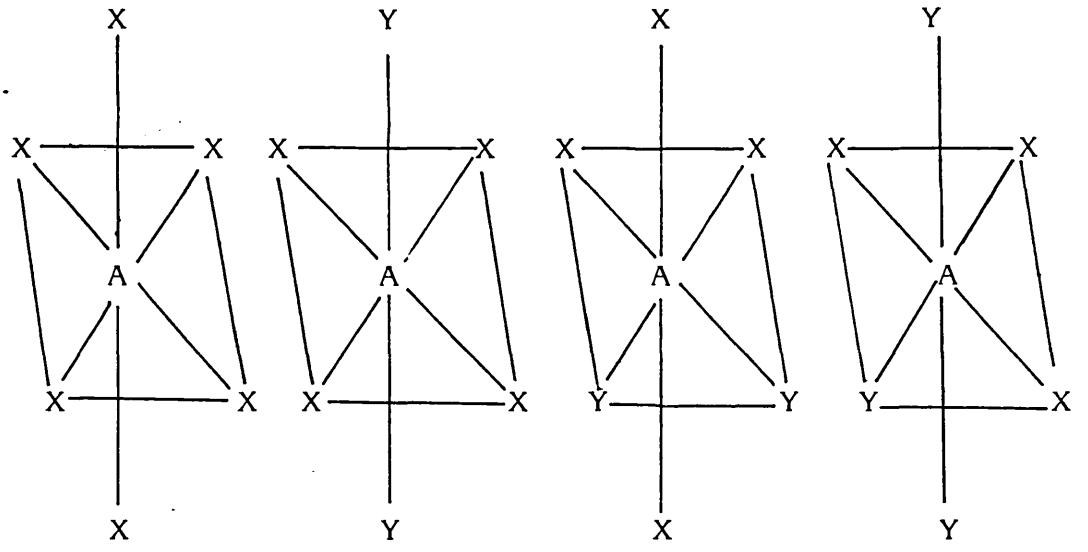
It has been reported that the average value of the chemical shift for five trialkyl phosphates was 1.07 $\pm$ 1.0 ppm relative to phosphoric acid at 0.00 ppm (144). The effect of the donor phosphoryl bond is likely to negate any small differences in the chemical environment of the phosphorus atom between the mono and di-alkyl phosphates.

From the evidence obtained, therefore, it can be concluded that the phosphorus in the polymer bound molecules is present as a phosphate, donor bonded through the phosphoryl oxygen to the iron atom. The phosphate group present is largely the monoalkyl phosphate, but a proportion of dialkyl phosphate is also present.

6.7.5. Co-ordination around the Iron Atoms

From the deduction that the iron is present as Fe(III) low spin, it follows that the co-ordination around the iron atoms is almost certainly octahedral as no tetrahedral low spin Fe^{III} compounds are known (172,175).

Both the e.s.r. and Mossbauer spectra indicate that the iron is present in only one type of site. The same groups must be co-ordinated, therefore, around each of the iron atoms. The Mossbauer spectrum showed a low quadrupole splitting, which implies a considerable degree of symmetry is present in the co-ordination around the iron. There are four octrahedral co-ordinations of the ligands X and Y around an atom A, which are illustrated below.



a b c d

Of these arrangement 'a', having perfect or near perfect symmetry, possesses a zero or near zero electric field gradient. With no electric field gradient to interact with the nuclear quadrupole moment, no quadrupole splitting will be observed in the Mossbauer spectrum (170). For this reason alone this arrangement may be discounted.

Arrangements 'b', 'c', and 'd' possess non-zero electric field gradients, a quadrupole split would therefore be expected from each of them.

A simple analysis of the elemental analysis results shows that the phosphorus-iron atomic ratio falls to at least 1:0.308 or nearly 3:1. In the '180 minute' sample an iron content of 4.5% was recorded. The sample used for the Mossbauer and e.s.r. spectra has a higher iron content of 5.5.%. A comparison of these iron contents indicates a likely phosphorus-iron ration of 2.7:1 in the Mossbauer/e.s.r. sample. Each phosphorus atom implies one phosphoryl bond, since there is one present in the orginal ester and there is infrared evidence for its continuing presence. As no phosphorus compounds are known in which the phosphorus atom has two double bonds to oxygen (176), it follows that each phosphorus atom must imply the presence of one and only one phosphoryl bond.

Since only one iron site is implied by both the Mossbauer and the e.s.r. spectra, the phosphorus : iron ratio of 2.7:1 must indicate an excess of phosphorus atoms over that number required to fully co-ordinate the iron atom, rather than some of the iron atoms being partly co-ordinated. The co-ordination of the iron must therefore involve two phosphoryl groups. Three or more phosphoryl groups would not agree with the observed ratios of phosphorus to iron, nor with the observation that there is substantially only one site. Only one phosphoryl group would involve a molecule of low symmetry, not supported therefore by the Mossbauer spectroscopy.

6.7.6 Molecular Formula

The elemental microanalysis of the "180 minute" sample (section 6.4) resulted in an elemental composition of $C_{10}\ H_{23}\ PO_3\ Fe_{0.3}$, which assuming that all the carbon is present as the hexyl (C_6H_{13}) group reduces to:

$$(C_6H_{13}O)_{\frac{5}{3}}\ PO_{\frac{4}{3}}\ H_2\ Fe_{\frac{3}{10}}$$

This composition does not, however, represent the molecular formula of the polymer since the sample analysed was not purified before use. It should be expected therefore that this composition also represents the inclusion of an amount of dihexyl phosphonate and hexanol. In addition, the mass spectra showed the presence of mono, di and trialkyl phosphates together with the phosphonates.

Resolution of this composition, based on the iron to phosphorus ratio of 1:2 deduced in the previous section and the evidence from the mass spectra of the composition being largely monoalkyl phosphate does not produce a result which can easily be rationalised into a mixture of several components.

6.7.7. Possible Structures

The physical properties of the phosphonate-iron reaction products (as discussed in section 6.7.2) indicate that a polymer is formed by these reactions. Furthermore the lack of hyperfine splitting in the e.s.r. spectrum (section 6.5) indicates that the iron atoms are coupled to each other through the polymer. One of the bonds formed to the iron atom has been shown (section 6.2) to be a donor phosphoryl bond. These bonds alone are not sufficient to complete the co-ordination of the iron atom, and some other type of bond must exist to complete the co-ordination and assist in the formation of the polymer chain. There are a number of conceivable linking groups, which are shown below:-

a. M-O-M

b. M-O-P-M

c. M-O-P-O-M

d. M-O-P-O-P-O-M

e. M-P-M

f. M-P-P-M

g. M-O-P-P-M

h. M-O-P-P-O-M

i. M-P-O-P-M

j. M-O-P-O-P-M

Chain 'a.' suggests a polymeric oxide chain, with the phosphoryl donor bonds completing the co-ordination. Iron oxides are crystaline materials and it is difficult to see how an oxide bridge provides the physical properties observed.

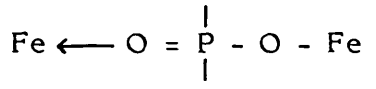
Chain 'b' requires a metal-phosphorus bond. In metallo-organophosphorus compounds in which metal-phosphorus bonds are found, the metal-phosphorus bond is easily hydrolysed and oxidised (142). A metal-phosphorus bond is not in keeping with the method of preparation and the observed thermal stability of the reaction products. For the same reasons, chains e,f,g,i and j can be excluded.

Polymers using bridges of type 'c' exist for transition metal complexes with phosphinates ($R_2P(O)OH$) (177,178) and with phosphates ($(RO)_2P(O)OH$) (179). Chain 'd' includes a P-O-P lingage, which, as was discussed earlier, is not indicated either directly or indirectly by the infrared spectra.

Chain 'h' has a phosphorus to phosphorus bond. With the exception of elemental phosphorus, few such compounds are known (180).

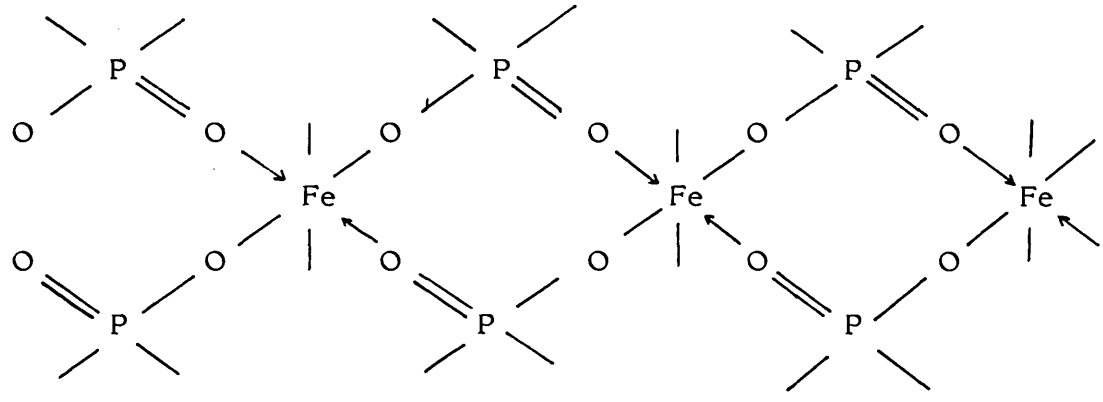
Thus only chain 'c' remains as a likely bridging group. These linkages M-O-P-O-M are known to exist in the many polymeric metal phosphinate and phosphate complexes that have been prepared (177,178,179). In both complexes the presence of donor phosphoryl bonds is reported (143,179). Based on these complexes, a similar model may be developed for the phosphonate-iron polymers.

The "bridging" group is 'O-P-O' as in (I)



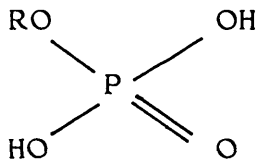
(I)

Based on the structure of the phosphinate and phosphate polymers a 'partial' structure (II) is obtained:

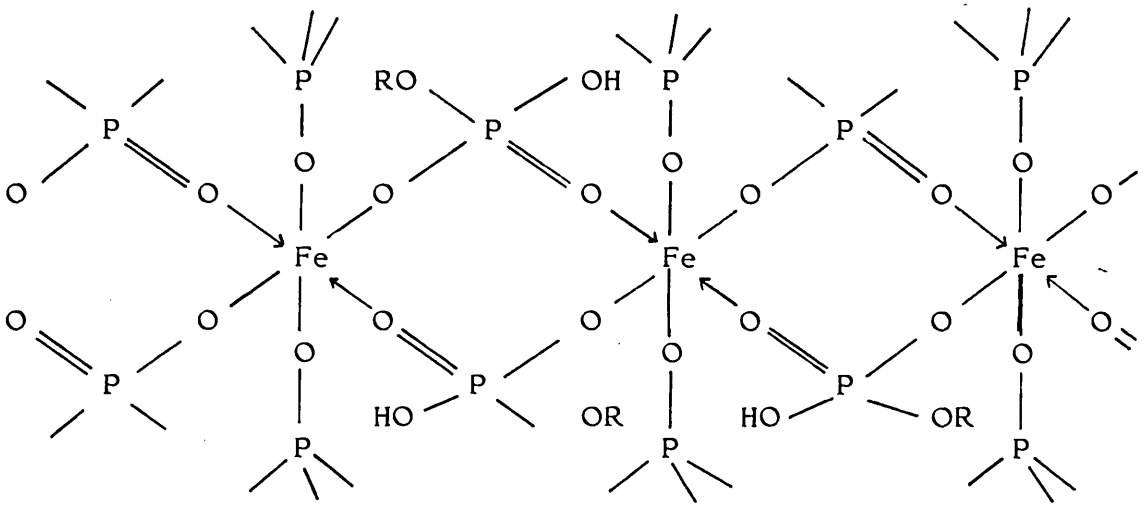


(II)

In this structure (II) the co-ordination of the iron atom is incomplete, in addition the structure around the phosphorus atom has not been completed. The mass spectra of the polymers showed that the polymer structure consisted largely of the monoalkyl phosphate. The ^{31}P n.m.r. spectra indicated that the phosphoryl oxygen of this molecule was donor bonded. It has been shown that the limiting iron : phosphorus ratio is 1:2, the phosphate group must therefore be triply co-ordinated to the iron atom. The monoalkyl phosphonate molecule has the structure:



It is reasonable to assume, therefore, on steric grounds alone that three fold co-ordination of this molecule around the iron atom would utilise, in addition to the donor phosphoryl bond formed, the oxygen of the hydroxyl groups. A completely co-ordinated structure can therefore be proposed (III).



In the next chapter, the EHD film forming properties of these additives under rolling conditions are investigated.

Chapter 7.

Optical Interferometric Study of EHD Film Thickness

The EHD film forming abilities of the dialkyl and diaryl phosphonates prepared in the laboratory, were tested under dynamic (rolling) conditions. These tests were carried out using a heated optical interferometry EHD test rig, the oils for each test being prepared by dissolving the phosphonates in a synthetic hydrocarbon fluid. Control of the heating allowed steady temperatures in excess of 100°C to be obtained during the tests. The effect of temperature on the EHD film forming ability could therefore be monitored.

The design of the test apparatus allowed both the ball and disc to be driven against each other or for the ball to be freely rolling, the glass plate only being driven. By alteration of the ratio at which the ball and disc were driven against each other, either pure rolling or mixed rolling/sliding conditions could be maintained.

The surface films formed on the ball were analysed by infrared spectroscopy, Mass spectrometry and Scanning Electron Microscopy (SEM).

7.1 Elastohydrodynamic lubrication

There are many examples of lubricated contacts where the surfaces are non-conformal, and the load is spread over a small contact area. Examples of these contacts are ball and roller bearings, spur gears and cams. In such examples, the classical application of the Reynold's equation alone predicts film thicknesses of only molecular dimensions, because of the high contact pressures encountered in the contact, often 1 - 5 GPa.

However, the high contact pressures have two beneficial effects which result in a greater film thickness than those obtained from the elementary application of the Reynold's Equation. The two effects are the increasing of the oil viscosity within the contact and the elastic deformation of the contacting surfaces. This lubrication regime is known as elastohydrodynamic lubrication (EHD or EHL), and the mechanism is well described by Wedeven (181).

Theoretical solutions of EHD have been developed by several authors (182-192) and two important ones are those of Grubin (183) and Dowson and Hamrock (191,192). Experimental results obtained by various workers have shown a correlation between theoretical and experimental values of the film thickness.

The typical film profile of a rolling point contact is shown in figure 7.1. The characteristic "horseshoe" shape is clearly illustrated surrounding a central "plateau" of greater and almost uniform thickness. An elevation view of the contact (figure 7.2) shows the elastic deformation of the contacting surface that occurs in the contact zone (for clarity deformation is shown on one surface only). This film profile can be observed using optical interferometry, and plate 7.1 is a photomicrograph of the contact zone obtained using this method.

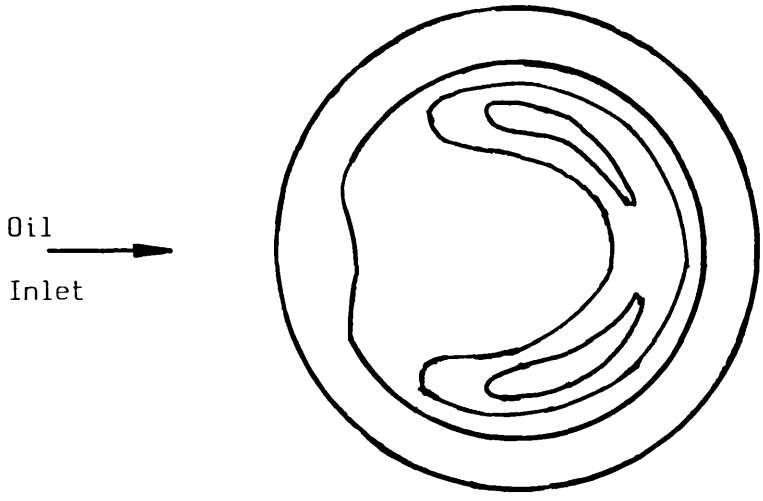


Figure 7.1 Film profile of a rolling point contact under EHD conditions (plan view).

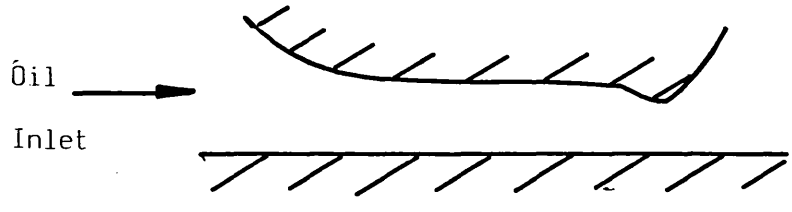


Figure 7.2 Film profile of a rolling point contact under EHD conditions. (Side elevation) (vertical scale greatly exagerated).

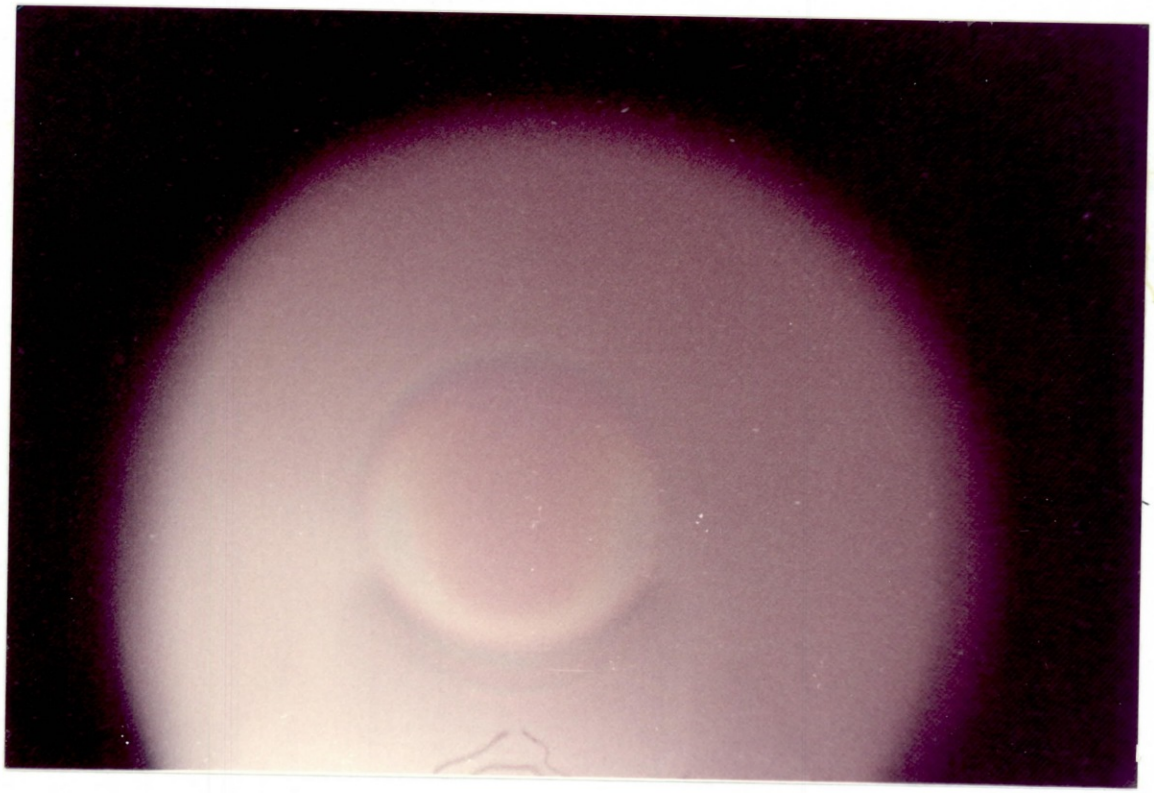


Plate 7.1 Typical EHD point contact interferogram

7.2 EHD Film Thickness measurement by Optical Interferometry

7.2.1 Introduction

Optical interferometry is now a commonly used method of measuring the EHD film thicknesses obtained in experimental studies. The earliest significant work was carried out by Cameron and Gohar (53,193), using a high refractive index (1.93) glass disc and a steel ball to produce a detailed map of the contact area and values of the oil film thickness from the Newtonian ring pattern obtained.

Improvements have since been made to this basic technique. The use of sapphire and diamond surfaces has enabled the use of higher pressures than those possible with glass discs (193). Poor fringe quality in early work has been improved by the sputtering of a thin layer (20nm) of chromium as a semireflective coating on the transparent disc, and by the use of metallic balls of a very fine surface finish (0.025 um c.l.a.) which give 60% reflectivity in oil (195,196).

Two forms of optical interferometry have been used, Monochromatic interferometry using light of a single wavelength and chromatic interferometry, using white light. The principles of both methods are similar and they differ in the means of illumination and the image obtained. In both forms a beam of light is directed through the glass disc and reflected off the surface of the ball. A part of the incident light does not strike the ball but instead is reflected from the semi-reflective layer on the disc as shown in figure 7.3. These two reflected beams have a phase difference between them, the amount of which depends on the separation of the ball and the disc.

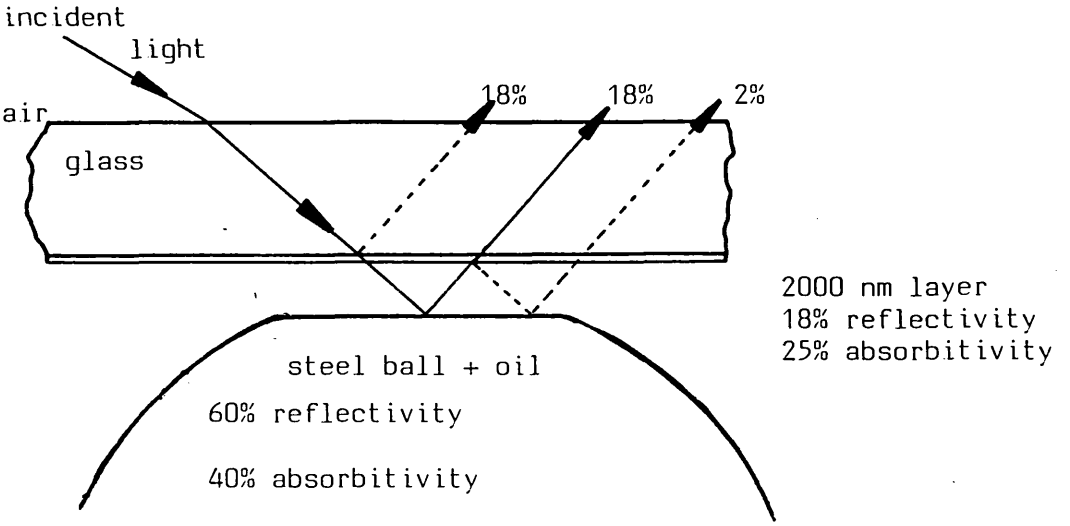


Figure 7.3 Two beam interferometry

In monochromatic interferometry an image is obtained which varies in intensity depending on the phase difference of the two beams. When the two beams are in phase a light-fringe is obtained and when out of phase a dark fringe results. The phase difference depends on the optical path length which in turn is a function of the refractive index of the oil and the physical separation of the ball and the disc. A detailed, theoretical explanation may be found in references (196) and (197).

In chromatic interferometry the phase difference between the two reflected beams results in the formation of coloured interference bands. The different wavelengths of which the white light is composed give rise to different phase differences from the same optical path length. As the optical path length increases a definite order of colours is seen. The advantage of white light interferometry over monochromatic interferometry is largely one of sensitivity. A small change in film thickness will produce a significant change in the colour of the interference band, which with monochromatic light may not be sufficient to produce a change from a dark fringe to a bright fringe. Chromatic (white light) interferometry was used in all the optical EHD work presented in this thesis.

7.2.2. Chromatic Interferometry

In both forms of optical interferometry (monochromatic and chromatic) use is made of the constructive or destructive interference arising from the in-phase or out of phase combination of the two reflected light rays. The condition for bright interference fringes is that the optical path difference(S) is equal to an integral number of wavelengths, that is

$$S = N\lambda \qquad \text{.....7.1}$$

The optical path length is 2nh, for a ray at normal incidence, where n is the refractive index of the oil and h is the physical separation of the disc and the ball. Because of anomalous phase changes on reflection at the metallic surfaces a correction factor $\not{\emptyset}$ has to be introduced. By substitution in 7.1 the condition for bright fringes is

$$N.\lambda = 2n.h + \not{\emptyset} \qquad \text{.....7.2}$$

With chromatic or white light interferometry the interference bands appear as different colours and not bright and dark bands as found in monochromatic interferometry. The colour of the interference band is dictated by which wavelength has its maximum intensity at the optical path difference obtained.

Accurate calibration, however, is not possible for two reasons (198). The colour of the central plateau is very much the subjective choice of the observer and the value of the phase change factor $\not{\emptyset}$ is difficult to determine and an inherent inaccuracy in the value of h would result if this was neglected. To counter this problem calibration of the interference colours is necessary. Two methods of calibration have principally been used.

The earlier method used (53,195) utilised the principle used by Newton, who placed a convex lens on a plane mirror. A series of concentric coloured rings (Newton's rings) were obtained, and from the radius of curvature of the lens, and the radii of each ring, the separation, h, could be calculated. If the radius of the fringe r is much less than the radius of curvature of the lens then the separation h is given by:-

$$h = \frac{r2}{2R} \qquad \text{.....7.3}$$

This method is subject to two inaccuracies, which both arise from the difficulty of obtaining a zero-load contact. Wedeven (197) pointed out that inaccuracies may arise by deformation of the glass plate due to a small but finite load being imposed in an attempt to obtain a good contact. The radii of the rings being increased by an amount equal to the contact radius. Alternately if the contact is too lightly loaded, it may not be complete and dust or surface asperities will separate the two surfaces.

Gentle (198) overcame these two problems by loading the ball and plate in air so as to obtain a good contact. The resultant deformation of the surfaces was compensated for, using the Hertz equation:

$$h = \frac{a\ Pmax}{E^1} \left\{ - (2-r^2/a^2) \cos^{-1} \frac{a}{r} + (r^2/a^2 - 1)^{1/2} \right\} \qquad \text{.....7.4}$$

where h = separation of surfaces

E^1 = reduced Young's Modulus

r = radial distance from centre

a = Hertz contact radius

$Pmax = 3/2\ W/\pi a^2$ = maximum Hertz contact pressure

W = load

The separations obtained in air are tabulated in table 7.1. These values of surface separations are used in this thesis. The values obtained by this method may be taken as the optical thicknesses. The relationship between the optical and the actual distances is given by:

$$h_{optical} = h_{actual} \times n\ (p,T) \qquad \text{.....7.5}$$

and the refractive index, n, of air is virtually unity

Table 7.1

Surface separations against colour (from ref. (198))

Order	Colour	Separation (nm)
1	Yellow	200
	Red	270
	Blue	340
	Green	430
2	Yellow	470
	Red	560
	Blue	610
	Green	670
3	Yellow	760
	Red	860
	Blue	900
	Green	960
4	Yellow	1050
	Red	1150
	Green	1250

7.2.3 Refractive Index

To obtain the separation of the surfaces when a fluid other than air is in the gap, the refractive index of the fluid is substituted into equation 7.5 above. Strictly speaking the refractive index to be used is that of the medium at the fluid hertz pressure and temperature in the contact, since the refractive index is a function of temperature and pressure.

The refractive index normally increases with pressure and falls with temperature. Using a conventional refractometer the refractive index of the fluid can be measured at different temperatures. The refractive index of the oil was found not to fall rapidly with temperature and consequently the refractive index obtained from the known inlet temperature may be used as a close approximation to that in the contact. The measurement of refractive indices under the high pressures found in an EHD contact is a more difficult task. A technique has been developed (199) to measure the refractive index within a lubricated point contact. The effect of pressure on the refractive index was shown to be less than 10% from atmospheric pressure to 1 GPa. Nagaraj (in ref. (200)) reported a similar result.

Since the work in this thesis is largely comparative, relative rather than absolute values of the film thickness are used. The absolute value of the refractive index is therefore not required. Since the work was carried out under identical load and temperature conditions for each test the values obtained for the refractive indices at the inlet temperature and at atmospheric pressure may safely be compared. From the discussions above it is clear that the resultant errors in film thicknesses will be second order and can be neglected.

7.3 The Optical EHD Test Apparatus

The Optical EHD test apparatus used to carry out the work described in this chapter was a ball-on-disc apparatus, in which both the ball and the disc, or the disc alone could be driven. It was therefore possible to study the effect of sliding on the formation and stability of the EHD film formed. The test rig could be heated to temperatures in excess of 140°C, although in the work described here, a maximum temperature of 100°C was used. Thermocouples at the inlet zone allowed the temperature to be both monitored and controlled.

The detailed description of the test rig is divided into appropriate sections, e.g. power train, temperature control, for clarity.

7.3.1 General Description

As stated above, the test rig employed a "ball-on-plate" as used by previous workers. A 25.4mm (1") diameter steel ball is loaded vertically onto a glass disc coated with a semi-reflective coating on the upper surface. A microscope, placed directly underneath the contact of the ball and disc, allowed the contact zone to be observed using white light interferometry. A general view of the test rig is shown in plate 7.2.

The glass disc, ball and loading arm are enclosed within a lagged and electrically heated retaining tank fitted with a lid. Figure 7.4 shows a cross-section through the middle of the test chamber, and the relative positions of the disc and retaining tank. The retaining tank consisted of two parts, a base fastened to the base plate, and the side wall, which fastened to the base by means of two bolts.

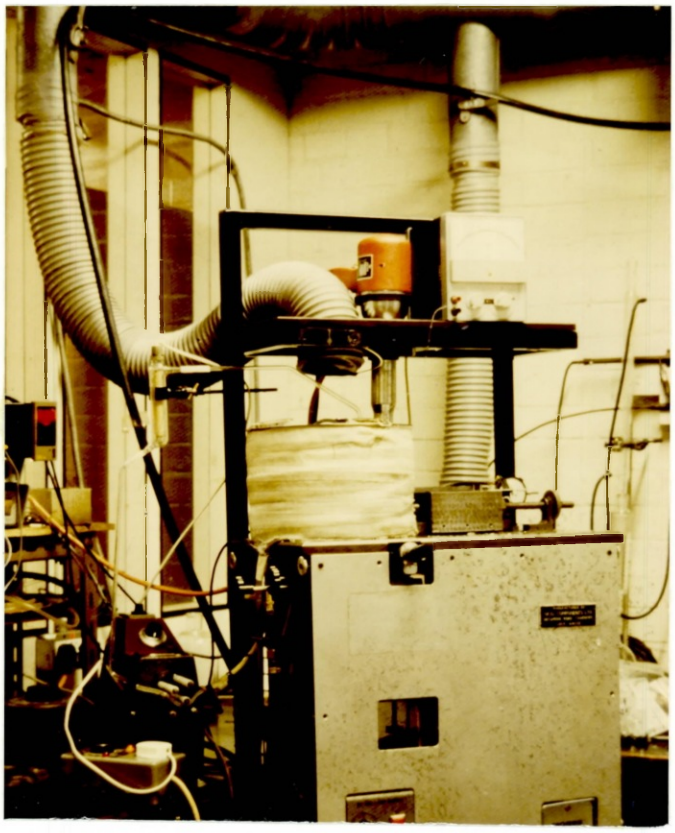


Plate 7.2 Front view of EHD Test rig

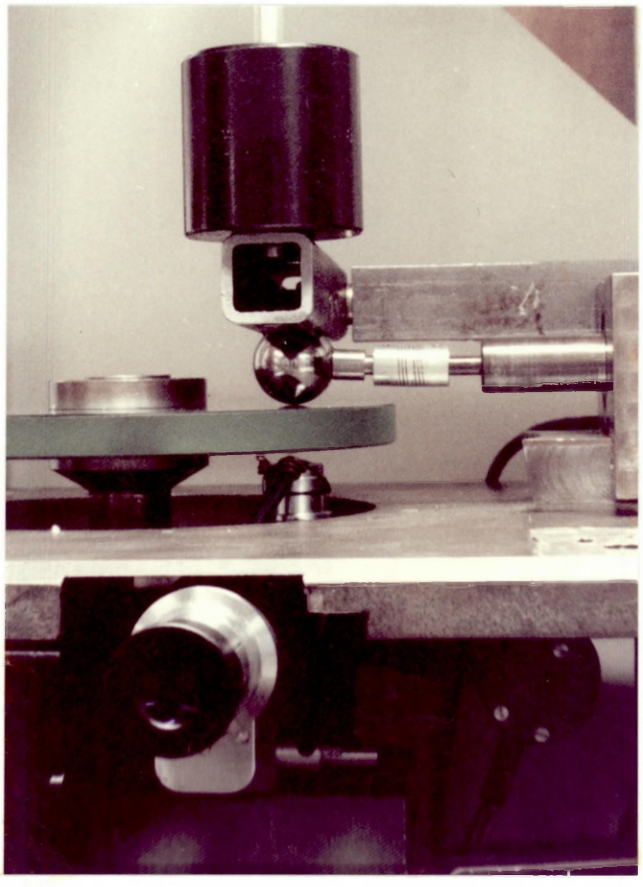


Plate 7.3 Microscope Position

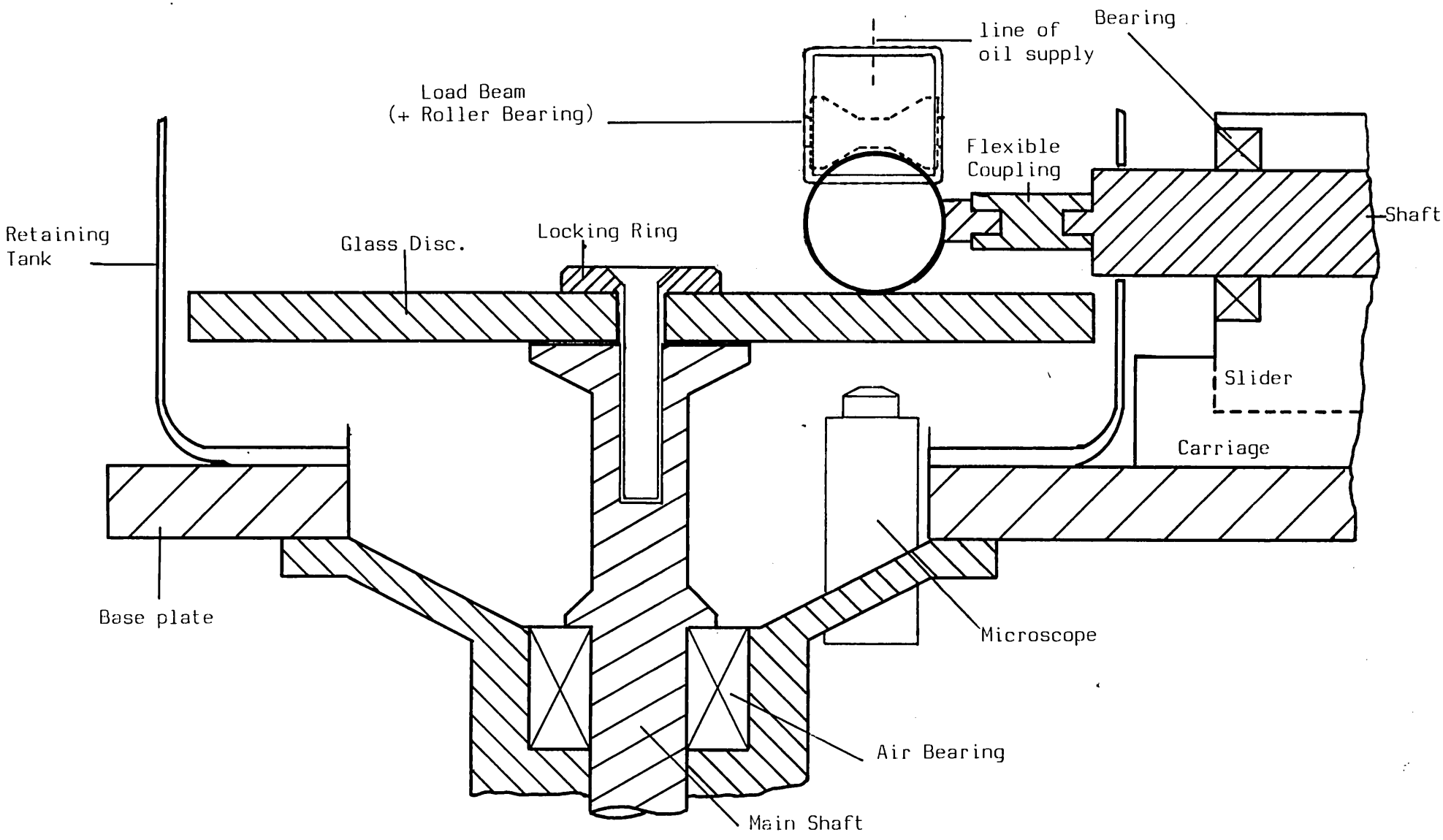


Figure 7.4 Sectional View of EHD Test rig.

The base was sealed to the base plate using a waxed paper gasket and a silicone rubber sealing compound. The lip between the base and side wall was also sealed with the silicone rubber compound. A drain hole through the base and the base plate allowed oil thrown from the disc by its rotation to be collected for recirculation or disposal as required. Drainage was aided by adjustment of the levelling feet on the base so as to lower the drain point.

The glass disc is supported by an air bearing, and the 25.4mm (1") steel ball is loaded against the upper surface of the glass disc to obtain the EHD contact. The original design of the rig used a 133mm (5 1/4") diameter glass disc, coated on the upper surface with a semi-reflective coating. The rig was later modified to accept 152mm (6") and 165mm (6 1/2") diameter discs, to lessen oil losses due to "under-running" of oil droplets at slow rotational speeds.

Loading of the ball was achieved by placing weights on a loading arm above the ball, contact with the ball being made through two roller bearings. The loading arrangement is shown in figure 7.4, and also in plate 7.3 which shows the front elevation of the ball and loading arm.

Both the glass disc and steel ball were driven by the same electric motor. The ratio of their respective speeds was controlled by a planetary gearbox on the drive train of the ball. The overall speed of the disc and the ball was governed by a speed controller. In most of the work, conditions of pure rolling were used. The ball was then driven by contact with the disc, the coupling shown in plate 7.3 not being attached.

To induce sliding a drive was applied to the ball to rotate it at a speed slightly (typically 5 - 10%), below or above that of the disc. Both drive shafts were fitted with speed sensing devices. These are described in section 7.3.3, in which the drive trains to both the ball and the disc are described in greater detail.

The ball, loading arm and ball-drive pulley could be moved radially across the disc by means of a sliding carriage. This carriage allowed the ball to be moved to a new 'track' on the disc when loss of the chromium coating caused a deterioration of image quality. The radius of each rolling track on the disc was indicated by a dial gauge micrometer attached to the sliding carriage.

The position of the microscope can be seen in plate 7.3. The objective lens is positioned directly under the contact. An aluminium block into which this lens is threaded holds a mirror at an angle of 45° to the direction of the light beam. The light beam is thus deflected through a right angle into the body of the microscope to the eyepiece. Illumination of the contact was provided by 6V light source attached to the side of the microscope. A semi-reflective coated glass disc in the microscope housing reflected the light from the source onto the mirror and thence the contact, but allowed the light reflected from the contact to arrive at the eyepiece. Movement of the microscope, so as to accurately position it under the contact, and focussing were achieved by using three travelling microscope mounts one each in the X, Y (to position the objective lens) and Z planes (to focus the microscope). The microscope was fitted with a x3 objective lens and a x10 eyepiece lens.

To protect the objective lens against the condensation of oil mist and splashes of oil a stream of compressed air was passed over the face of the lens. The position of the air pipe can be seen attached to the objective lens in plate 7.3. An improved method of protection used in later work was achieved by fitting a guard around the objective lens. This guard tube was conveniently made of a strip of paper approx. 2.75 cm wide, fastened around the lens using 'sellotape'.

7.3.2 Speed control and measurement

As was mentioned above a single electric motor provided a drive to both the disc and the ball when the rig was operated with a degree of sliding at the contact. A schematic diagram of the power train layout is shown in figure 7.5.

The drive was supplied by a variable speed d.c. motor of 1.1. Kw power. The motor speed was controlled by a d.c. motor speed control unit (Morse-Chain Ltd.) and a quoted range for this controller-motor combination was 0 to 3000 rpm, although in practice a speed of about 2,500 rpm was found to be the maximum obtainable before severe vibrations developed.

The speed range, as originally designed, was too high for the work described in this thesis. The output of the motor was decreased using a 10:1 reducing gearbox before the drive was split to the disc and ball drive shafts. The disc drive was taken from this gear box output shaft by a 2:1 increasing belt drive using 28 and 14 tooth pulleys on the gearbox and disc drive shafts respectively. A (theoretical) maximum shaft speed of 600 rpm could then be supplied to the disc.

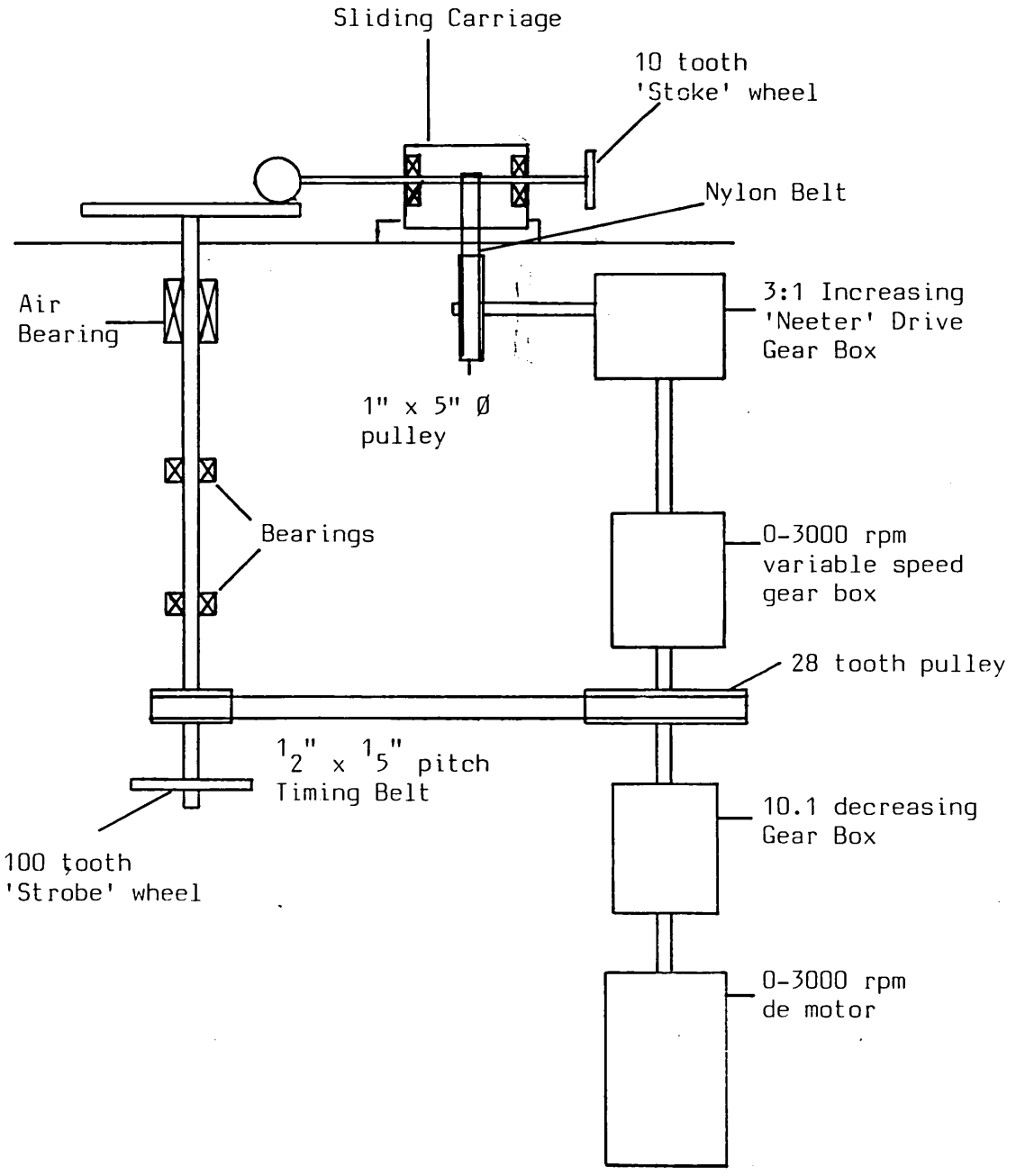


Figure 7.5 Schematic diagram of power train layout for EHD rig.

The drive to the ball was taken vertically upwards coupling the output shaft of the 10:1 reducing gearbox to the input shaft of a planetary gearbox the ratio of which could be continuously varied from 1.36:1 increasing to 8.24:1 increasing. A right angled 3:1 increasing helical gearbox and 5:1 increasing pulley belt drive completed the ball drive train. A maximum (theoretical) ball speed of 3307 rpm was possible by this arrangement, variable down to 546 rpm, at maximum motor speed.

A comparison of the disc and ball speeds will show that the arrangement described above, allows the ball to be driven at pure rolling at a maximum disc track diameter of 5.5" (13.97 cm). The speed of each shaft was measured from a digital counter using an optical switch system. The optical switch was composed of a phototransistor, mounted opposite an infrared light source. The tachometer discs, mounted on the disc and ball drive shafts, ran between the switches, operating them by regularly breaking the light beam. Each optical switch was operated at 15 volts, and was connected in a Schmidt trigger electronic circuit, details of which may be found in reference (201).

The digital counter could display the shaft speed of either the disc or the ball, or the ratio of the one to the other.

7.3.3 Temperature Control and Measurement

Three independent methods of heating were used to maintain the rig and oil supply at the required temperature. A hot air blower (1200 W power) controlled by a CAL 7300 proportional and derivative controller (Controls and Automation Ltd.) heated the test chamber of the rig. The blower motor was operated continuously during the test, the heater element being switched by the CAL 7300. Temperature sensing for this controller was by an Iron/Constantan thermocouple fitted to the loading arm, sited 1cm from the ball.

Loss of heat from the test chamber was limited by lagging the chamber wall with insulating material, and by heating this wall with a heating tape. The element has a maximum rating of 1700W (@ 240V). Operated at 60V the element uses approximately 100W, which was sufficient power to provide a wall temperature of 100°C. Voltage control was provided by a 'Variac' a.c. voltage variable transformer.

The third method of heating employed was a small heated oil sump in the recirculating oil circuit. In commissioning the rig, it was found that when operated at a temperature of 100°C, the oil cooled by 30° on re-entering the test chamber. A small all-glass heated sump was placed in the recirculating line. This heater consisted of a double glass-walled cylinder, with a lower inlet and an upper outlet to allow the oil to circulate between the two walls. Heating was provided by a 200W aquarium-type heater within the inner wall. Heating control was provided by a thyristor power controller (Gallenkamp Ltd.).

A setting of 3.5 was found to suffice to reheat the oil to a temperature of 100°C as measured at the oil inlet. Measurement of the oil inlet temperature was by an iron-constantan thermocouple inserted into the end of the oil inlet tube, the temperature being displayed by an electronic thermometer.

7.3.3 Oil circulating system

In all the work described in this thesis the oil sample was recirculated around the rig. Oil was thrown from the disc by centrifugal force and collected in the base of the retaining tank.

From here the oil was pumped by a peristaltic pump upwards, through the heated sump (section 7.3.2) and returned to the test chamber. The oil inlet was directly above the ball, oil being fed from the inlet tube through the hole in the top of the loading arm, onto the top of the ball.

The circuit tubing consisted of a 13cm length of silicone rubber tubing used in the peristaltic pump and a similar length of polythene tubing from the drainage hole to the pump, the tubing from the pump to the oil heater and from there to the ball was of 7mm O.D. glass tubing connected to the heater by PTFE sleeving. In early work it was found that a rapid degradation of the silicone rubber tubing occurred in the hotter parts of the oil circuit. Therefore as much tubing as possible was replaced by glass.

7.4. Experimental Work

7.4.1. Materials

Both base oils used for the EHD lubrication tests were synthetic hydrocarbon fluids. In the tests came out at 75° and 100°C, the base oil used was Gargoyle Arctic SHC 234 (Mobil Oil Company Ltd). For the 25°C tests, another (less viscous) synthetic hydrocarbon fluid RTS 3521 (Mobil Oil Company Ltd) was used.

The phosphonates used in these base stocks were dihexyl, dioctyl, didodecyl, diphenyl and bis-octylphenyl phosphonates. These were prepared and distilled in the laboratory. Their preparation and characterisation are described in Chapters 3 and 4.

Two corrosion inhibitors were used in conjunction with the phosphonate additives. These were NA-Sul BSN (RT Vanderbilt Company Inc.) a Barium dinonylnaphthalene sulphonate and a sodium based corrosion inhibitor (B.P. Oil Ltd.).

7.4.2. Preparation of fluids

Test fluids were prepared by dissolving 3% by weight of phosphonate into the synthetic lubricant base stock, immediately prior to use. The sample phosphonate (approx. 2g) and lubricant (approximately 64.6g) were weighed together, and dispersion was achieved by combination of stirring and use of an ultrasonic bath.

7.4.3. Test Procedure

General Procedure

The rig was cleaned before use with first toluene and then acetone, the peristaltic pump being used to pump the toluene or acetone around the oil circuit. All surfaces were wiped with a paper tissue ('Kimwipe') soaked in the solvent. Three cleanings with toluene, followed by one or two with acetone were found to be generally sufficient. The glass disc was removed after these cleanings in order to clean the underside of the rig of any oil which had spilled under during the previous test. The microscope objective lens was cleaned using toluene and acetone if necessary, and a new shield fitted.

A new ball was used for each test. These 1" (2.54 cm) steel balls of EN31 steel, were cleaned before use in toluene and acetone using an ultrasonic bath. A loading weight of 761g was used in all the tests.

Once assembled, the compressed air and power to the rig were turned on and the required temperature set on the 'CAL' temperature controller. The hot air blower and heating jacket were switched on and allowed to reach equilibrium temperature.

When the rig had equilibrated at the required temperature (this was assumed to have happened after this temperature had been maintained for 10 minutes), the oil sample was poured into the base of the retaining tank directly above the drainage hole. The oil pump was started, and when the oil had filled the sump heater, that heater was switched on. The drive motor was started once the oil started to be delivered to the contact.

The speed was adjusted to give the required central fringe colour and the speed of rotation, time and inlet temperature were recorded. After periodic time intervals, the speed was readjusted to re-obtain the original fringe colour. As the film built up, a slower speed was needed. The test was halted when the disc speed was too slow for the motor to give steady running or when a poor image was obtained due either to contamination of the microscope or poor optical qualities of the film.

Procedure for tests with sliding

For the tests involving sliding of the ball against the disc a coupling was attached to the ball. The coupling was centred on to the ball by clamping the coupling into the chuck of a lathe, and supporting the ball in the headstock of the lathe. A fast-setting iso-cyanate "superglue" was used to attach the ball to the coupling.

Before the ball and coupling were attached to the ball drive train, the ratio of the disc and ball was set to give the required amount of sliding at the track diameter being used. The ball and coupling were then attached and the test procedure described above was then used.

7.4.4 Measurement of Refractive Index

Refractive indices of the base stock and samples of the formulated lubricants were measured using an "Abbe 60" refractometer (degree scale model). The refractometer was heated by circulating a polyglycol fluid from a thermostatically controlled heating bath. Refractive indices of the base stock were measured at temperatures of 25° to $110^{o}C$ and those of the formulated oils were measured at $100^{o}C$.

The refractive index of the SHC 234 oil was found to vary from 1.46877 at 25°C to 1.44035 at 110°C with a value of 1.44398 at 100°C. The average refractive index of 16 formulated oils was found to be 1.4440 ± 0.0002 at 100°C. In all conversions of optical film thicknesses at 100°C to actual film thickness a value for the refractive index of 1.444 was used. A value of 1.4526 was measured for SHC 234 at 75°C.

7.4.5 Calibration of Rolling Track Diameter

The diameter of the rolling track is needed to determine the rolling speed of the ball, and the ratio of the disc and ball drive shaft speeds for the tests with sliding. The measure of calibration was as follows.

The rig was assembled as for a 'sliding test' with the exception of the loading arm which was omitted. The mean position of the disc locking ring was determined using a dial gauge. The disc was turned so as to align this 'mean position' of the locking ring opposite the ball. The separation of the locking ring and the ball was then measured using a set of slip gauges. A micrometer guage was used to measure the locking ring diameter and that of the ball. The radius of the rolling track is given by the sum of the radii of the ball and the locking ring and the separation of the two. A schematic diagram of which measurements were taken is shown in figure 7.6.

From this diagram it can be seen that the radius of the rolling track R is given by

$$R = R_{L_R} + R_B + d$$

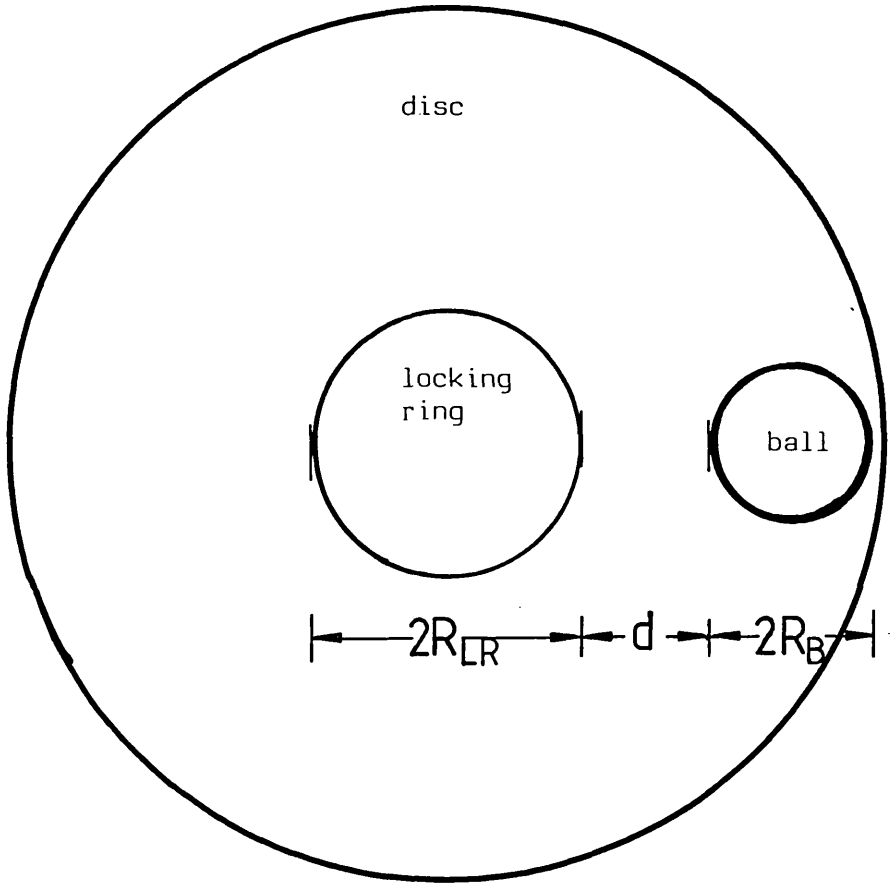


Figure 7.6 Calibration of the rolling track radius

From the reading of the dial gauge at this track radius, the track radius at a dial gauge reading of zero was determined. The radius of any new track could then be determined from the track radius at zero dial gauge reading and the new dial gauge reading. Since the dial gauge used to indicate the carriage (and hence ball) position was marked in inches, all measurements of track radii were initially determined in inches.

Recalibration was carried out whenever the dial gauge or carriage were moved. As an example of the calibration method, the following measurements were obtained for the locking ring and ball radii and the ring-ball separation at a dial gauge reading of 0.1000 inches.

R_{LR} = 0.9865"

R_B = 0.500"

d = 0.6417"

Track radius R = 2.1002"

At a dial gauge reading of 0.0000", the track radius R_o is therefore 2.0002".

The track radius on this setting is therefore equal to 2.0002" + dial gauge reading.

7.5 Results and Discussion

All the phosphonates, with the exception of diphenyl phosphonate, were found to give rise to the build-up of a chemical film in the EHD rolling contact. Diphenyl phosphonate was found to be either too corrosive or too reactive for the film build-up to be monitored using the optical EHD test rig.

7.5.1 'Pure' rolling tests

Chemical film build-up was found to occur for 3% w/w solutions of dihexyl, dioctyl, didodecyl and bis-octyl phenyl phosphonates in a synthetic hydrocarbon base stock at at test temperature of 100°C. In addition, slower film build up was found to occur for didodecyl phosphonate and bis Octyl phenyl phosphonate at a temperature of 75°C, and for BOPP at 25°C. The film build-up was monitored in two ways. The preferred method was to set the rig running so as to give a particular central fringe colour and as the film built up, the speed was reduced to maintain a constant film thickness. The alternative method was to set the rig at a constant speed, noting the colour of the central fringe at regular time intervals. This method suffers from having less data points. Film thicknesses are only given for four colours per spectrum order in (719).

Figures 7.7 to 7.10 show the film build up as a function of a reduction in rolling speed for BOPP, DHP, DOP and DDDP respectively. Figure 7.11 shows the film build-up as measured by the increase in optical film thickness against time at constant rolling speed for DDDP.

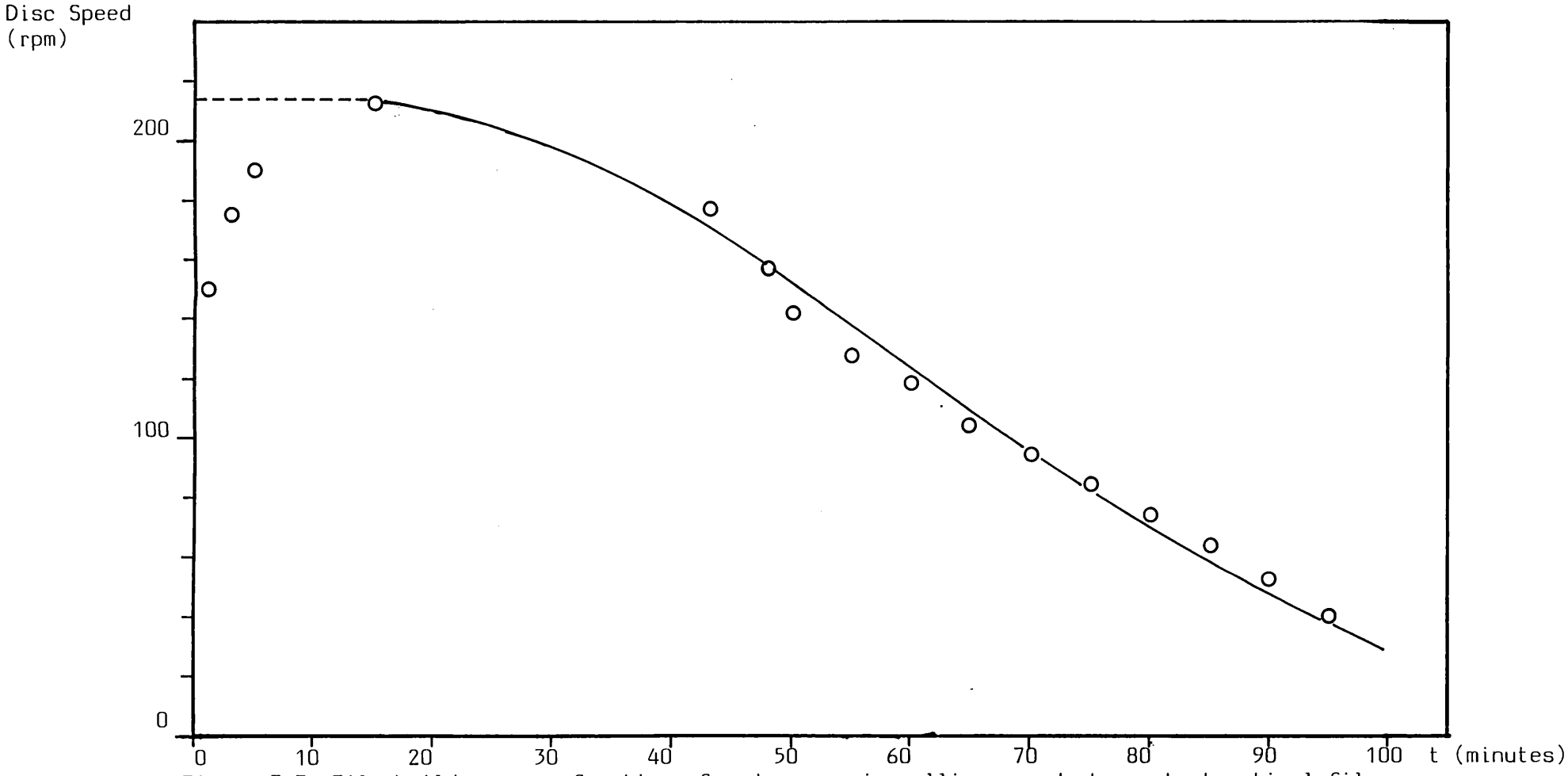


Figure 7.7 Film build-up as a function of a decrease in rolling speed at constant optical film thickness using bis (octyl phenyl) phosphonate in SHC 234. at 100°C. h_0 = 235 nm

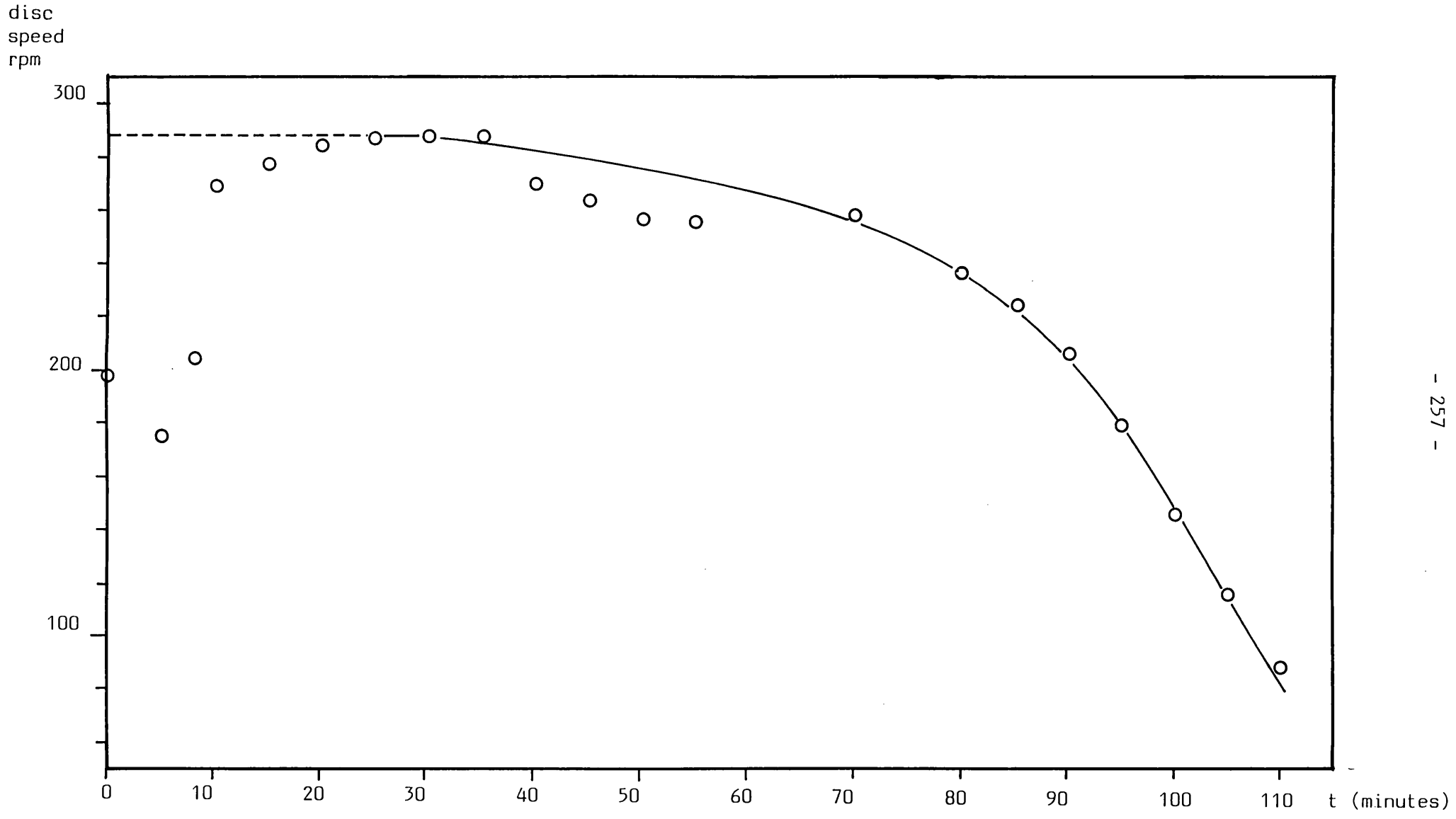


Figure 7.8 Film build up as a function of a decrease in rolling speed at constant optical film thickness using dihexyl phosphonate in SHC 234 at 100°C. (h = 235 nm)

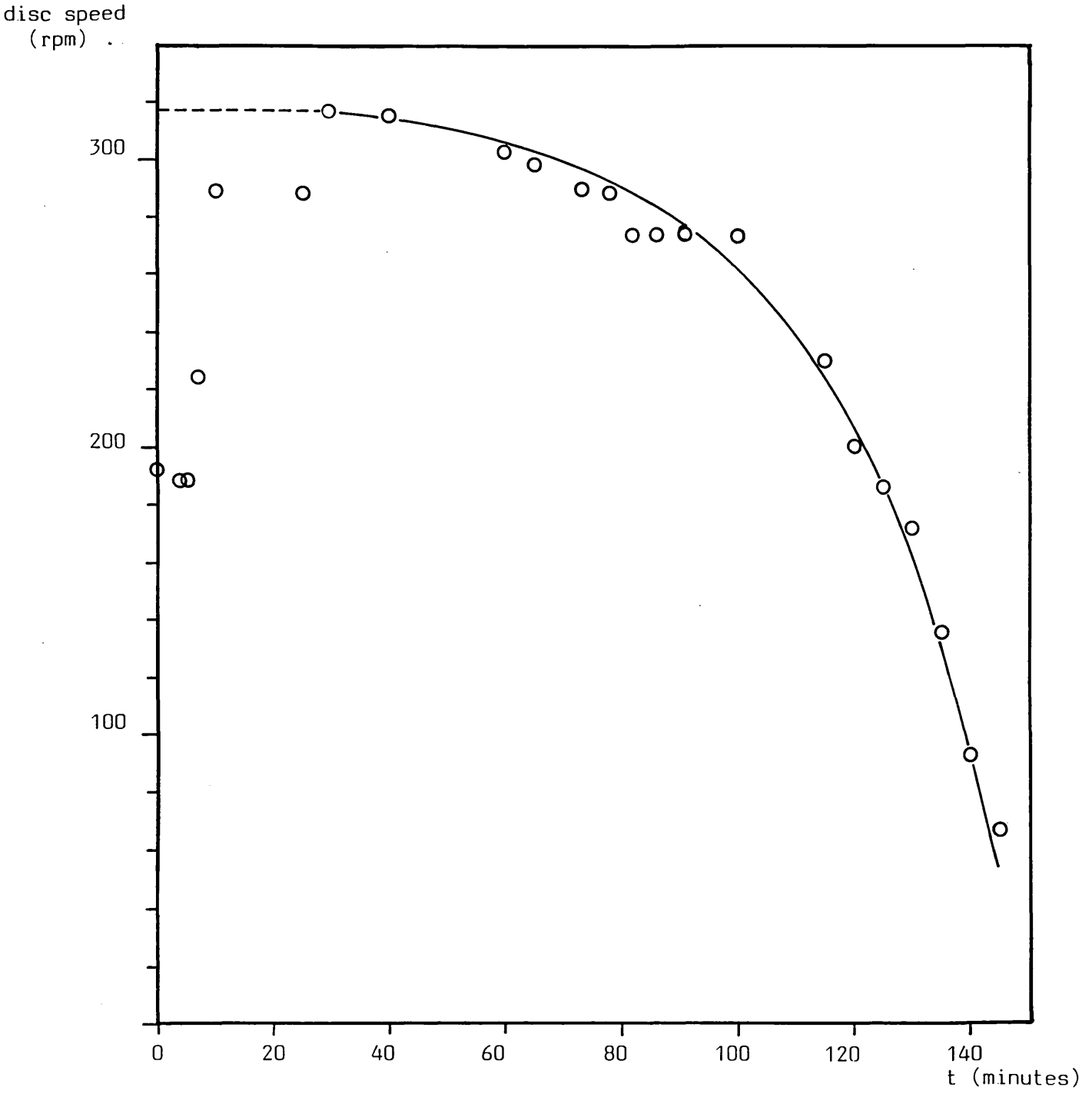


Figure 7.9 Film build up as a function of a decrease in rolling speed at constant optical film thickness using dioctyl phosphonate in SHC 234 at 100°C.
h = 235 nm

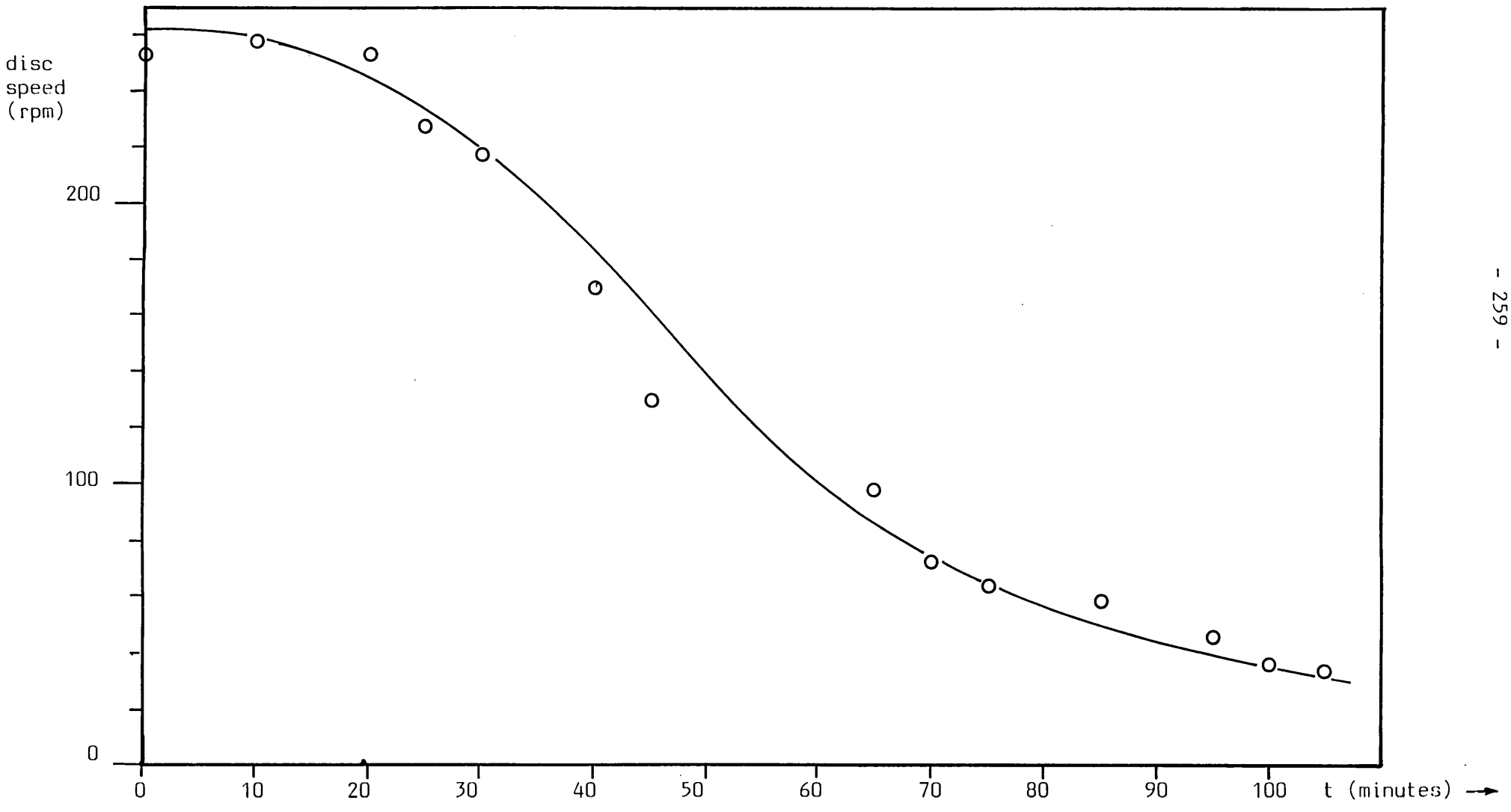


Figure 7.10 Film build-up as a function of a decrease in rolling speed at constant optical film thickness using didodecyl phosphonate in SHC 234 at 100°C. (h = 235 nm)

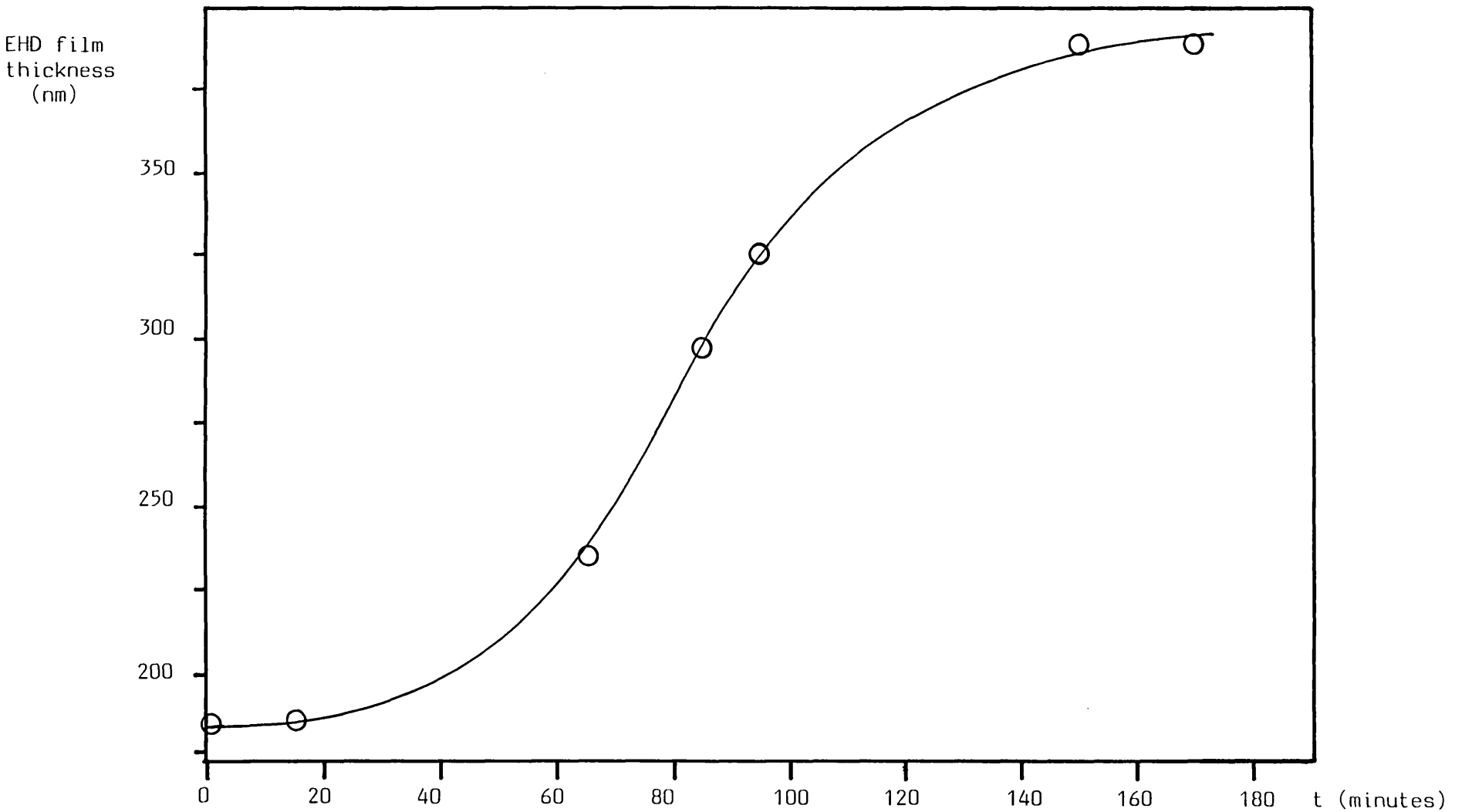


Figure 7.11 Film build-up as a function of an increase in EHD film thickness at constant rolling speed using didodecyl phosphonate in SHC 234 at 100°C. (u = 1. 15 M/S)

In. all the tests the assumption is made that the refractive index of the oil does not change significantly during the test, and that the refractive index of the chemical film formed on the ball surface is similar to that of the oil. Measurements of the refractive indices of several oil samples taken at the end of tests showed only a very small variation in the refractive index compared to the newly prepared oil samples. An increase in the actual film thickness must therefore be taking place, due to an adsorbed film on the surface of the ball. By assuming that the chemical film has the same refractive index as the oil, a straight correlation between optical and actual film thicknesses remains. This assumption was also made by Fowles et al (2) in their work on chemical film formation in EHD contacts.

The thickness of the built up chemical film can be determined from either method of following the film formation. With the constant rolling speed tests, a direct indication of the chemical film thickness is obtained from the increase in the optical film thickness, by dividing the optical film thickness by the refractive index. For the tests conducted at a constant (optical) film thickness, use must be made of one of the equations which relates the central film thickness (h_o) with the rolling speed (u). A suitable equation to use is that of Dowson and Hamrock (191,192) from which the following relationship (equation 7.5) can be obtained.

$$ho \propto (u)^{0.67} \qquad \text{.....7.5}$$

Assuming that there are no changes in the bulk oil properties (viscosity, pressure-viscosity index) during the test then this relationship can be used to determine the "EHD component" of the film thickness at reduced running speeds, since

$$\frac{h_o^1}{h_o} = \frac{(u^1)^{0.67}}{(u)} \qquad \text{.....7.6}$$

where h_o^1 is the film thickness in the centre of the contact at a running speed of u^1, and h_o is the central film thickness at a lower running speed u.

Figure 7.11 shows the increase in optical film thickness with time at a constant rolling speed of 1.15m/sec, with DDDP as antiwear additive. An increase in the optical film thickness of 290 nm occurs, equivalent to an increase in the actual film thickness of 200 nm. (This figure was calculated using a value for the refractive index of the oil of 1.444 at 100°C determined as described in section 7.4.4).

Using equation 7.6, data collected under conditions of constant film thickness could be converted to obtain the contribution to the film thickness due to the chemical film. Use of equation 7.6 determines the EHD contribution to the film thickness at the reduced rolling speed. The chemical film thickness is thus the difference between the EHD "contribution" and the observed film thickness. Thus chemical film thicknesses of 120-173 nm were calculated from the data presented in figures 7.7 to 7.10.

A comparison between the two methods shows them to be in close agreement. After 110 minutes a chemical film thickness of 173 nm is indicated in the constant film thickness test (figure 7.10). The constant rolling speed test (figure 7.11) shows an increase in the optical film thickness of 240nm, equivalent to a chemical film thickness of 166nm after the same time.

The formation of chemical films was observed with lower test temperatures. At 75°C the formation of a 100nm thick film was observed with BOPP. This film built up over 60 minutes, a slightly slower rate than that found to occur at 100°C. A similar film thickness was observed with DDDP at 75°C again at a slightly slower rate that that recorded at 100°C. At 25°C, a very much reduced rate of film formation was recorded. Using BOPP in RTS 3521 a chemical film of only 35 nm was observed after 200 minutes.

The build up of the chemical film in the rolling contact can be seen by the presence of fringes in the hot stationary contact at the end of the test (plate 7.4). These fringes remained even after the ball was slightly rotated, and are not therefore due to trapping of oil. Also they do not show the motion typically shown by oil globules trapped in an EHD contact due to being squeezed out of the contact by the load. At the beginning of these tests a more typical stationary Hertzian contact is seen. These contacts are either dark or bright but are monochromatic, a typical example is shown in plate 7.5 which shows the view seen of the contact at the start of a test.

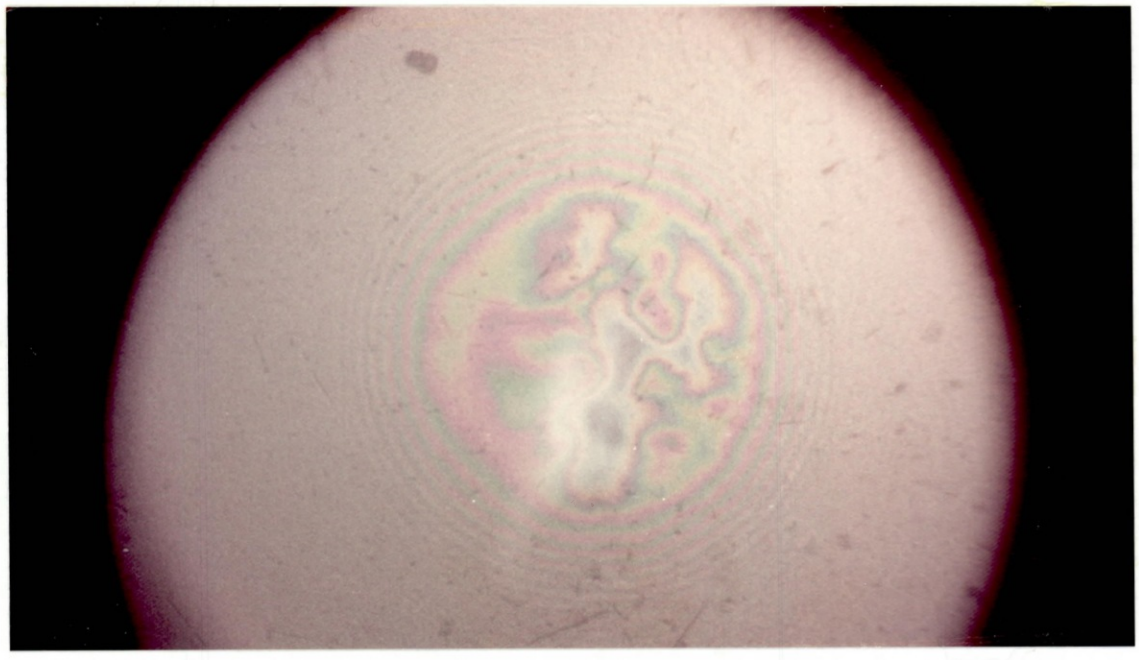


Plate 7.4. Stationary contact after 'growth' of a chemical film

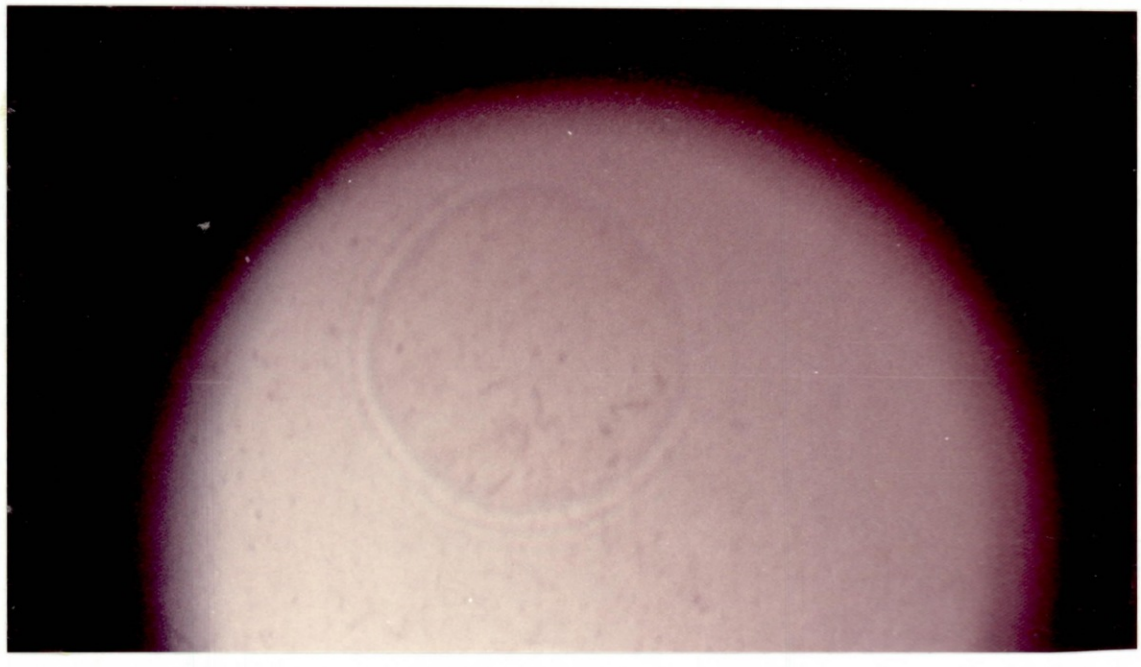


Plate 7.5. Stationary contact at start of test.

The build up of the chemical film was shown to be due to the added phosphonate and not the lubricant base stock. Using the SHC234 base stock alone, no change in optical film thickness occurred after running at constant speed for one hour. On adding BOPP (3% by weight) to the base oil while the rig was running, an increase in optical film thickness was observed after 10 minutes, which continued to the end of the test.

From Figures 7.7 to 7.12 it appears that the film growth slows down after some hours running. This effect was further investigated by adding fresh phosphonate solution to a test where film thickness had stabilised. Upon addition, film growth resumed and continued for several hours to reach a film thickness approximately twice that formed previously. The stabilisation of film thickness can thus be ascribed to depletion of a film-building component in the circulating lubricant rather than to a mechanical effect.

The rate of formation of these films varies from test to test, and a comparison of the different phosphonates was not possible from the results of the limited number of tests carried out. In a few tests no film formation was observed, either by a change in optical film thickness or by the appearance of fringes in the stationary contact at the end of the test. This was despite similar conditions being used to those used in other tests with the same additive in which film formation was observed. The reasons for this variance in the rates of formation are not clear, but a significant factor may be the presence of polymer remaining from a previous test as a result of inadequate cleaning.

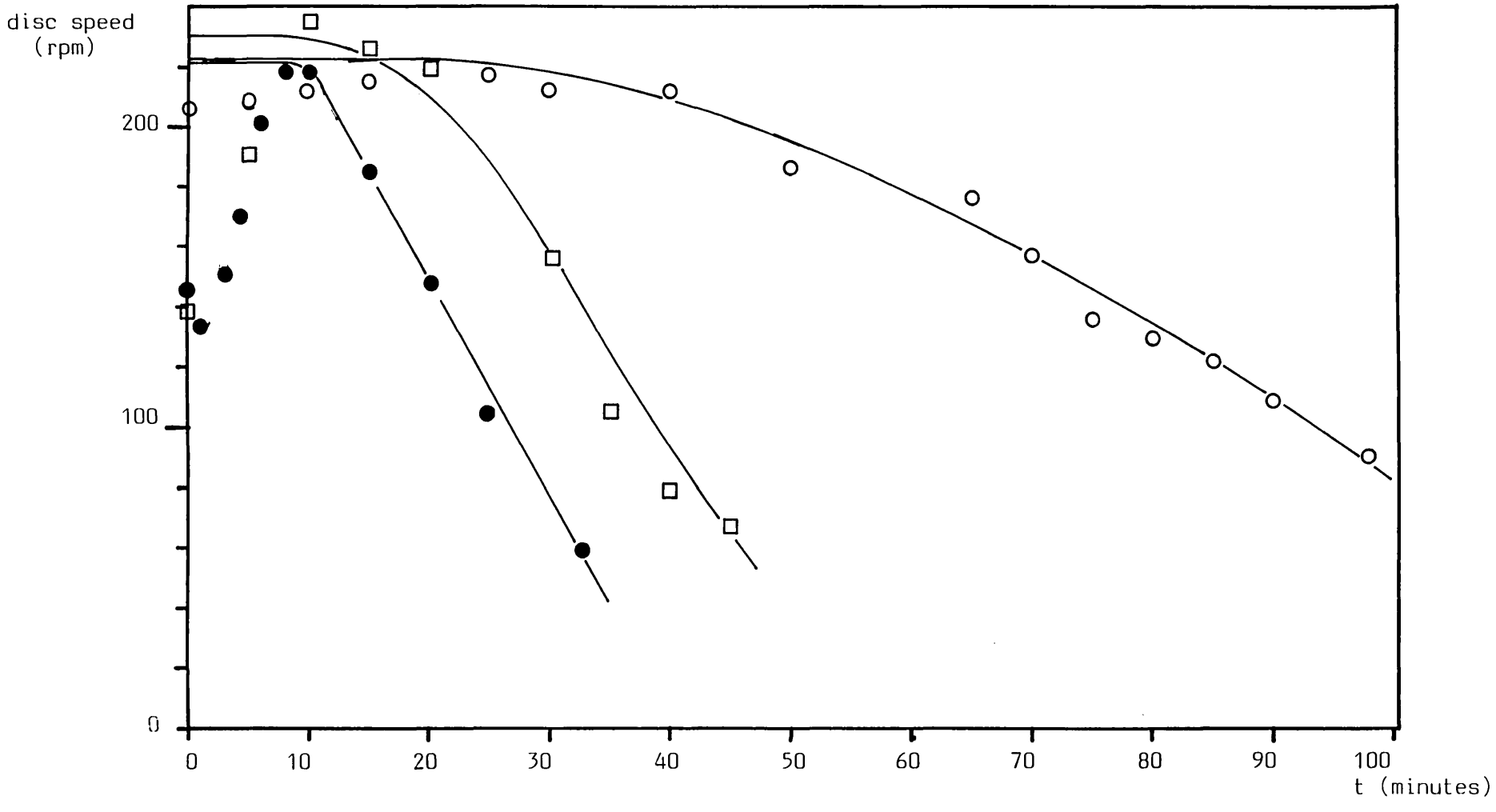


Figure 7.12 Effect of inadequate cleaning on the rate of film build-up in three successive tests using bis (octyl phenyl) phosphonate in SHC 234 at 100°C. (h = 235 nm)

In cleaning the rig and the disc it was found that a film remained on most surfaces which was not removed by several wipings with a toluene soaked tissue. Successful removal was achieved only with a tissue soaked in acetone. In three successive tests on which only toluene had been used to clean the rig between tests, the rate of film formation became progressively faster. The difference in rates can be seen from figure 7.12, in which the rolling speeds needed to maintain the same optical film thickness are plotted against the time of running.

This enhancement of the film formation by the presence of a film remaining from a previous test does not appear to be caused by transfer of this film onto the clean metal of the rolling contact. This was shown by changing the ball after a film had formed, and restarting the test. Initially a steady decrease in the rolling speed had been needed to maintain a constant optical film thickness. After changing the ball, a rolling speed approaching that used at the start of the test was needed to obtain a similar optical film thickness. No change in this optical film thickness was then observed after 30 minutes running. When further BOPP was added, an increase in the film thickness was apparent within 5 minutes and a steady reduction in rolling speed was required throughout the remainder of the test, to maintain the same film thickness.

This chemical film could be seen on the surface of the ball after removal from the test and cleaning using toluene or heptane, as a colouration (interference film) or in extreme cases a white deposit. In some instances physical removal of this film was possible by 'scratching' it from the surface. Analysis of the surface film is described in section 7.6.

7.5.2 "Sliding" Tests

The effect of mixed sliding/rolling was studied using both BOPP and DDDP as additives. Both of these additives were found to form thick chemical films in such situations. Film build-up was observed with up to 9% sliding applied. Sliding percentage is defined as 100 $(U_B-U_D)/UD$, where U_B and U_D are the surface speeds of the ball and glass disc respectively. The ball was always faster than the disc.

All the sliding tests were, for convenience, carried out at a constant rolling speed. It had been found that the ratio of the ball and disc speeds varied slightly as the speed of the motor was changed. The constant rolling speed technique, although giving less data points, avoided this problem. Changes in the film thickness were followed by observation of the colour of the central fringe.

Using this method, the formation of a 200nm thick chemical film was observed when up to 6% sliding was applied using BOPP in SHC 234 lubricant at 100°C. Using DDDP the formation of a 140nm chemical film was observed at up to 9% sliding. Evidence of film formation at 9% sliding with BOPP as additive was given by the presence of interference fringes in the stationary contact at the end of the test. Direct observation was not possible due to loss of the optical image (for reasons which are not clear). All the "sliding tests" gave rise to interference fringes in the stationary hot contact as were found in the pure rolling tests (see plate 7.4). Figures 7.13 and 7.14 show the change in film thickness with time for BOPP (6% sliding) and DDDP (9% sliding) dissolved in SHC 234 at 100°C respectively.

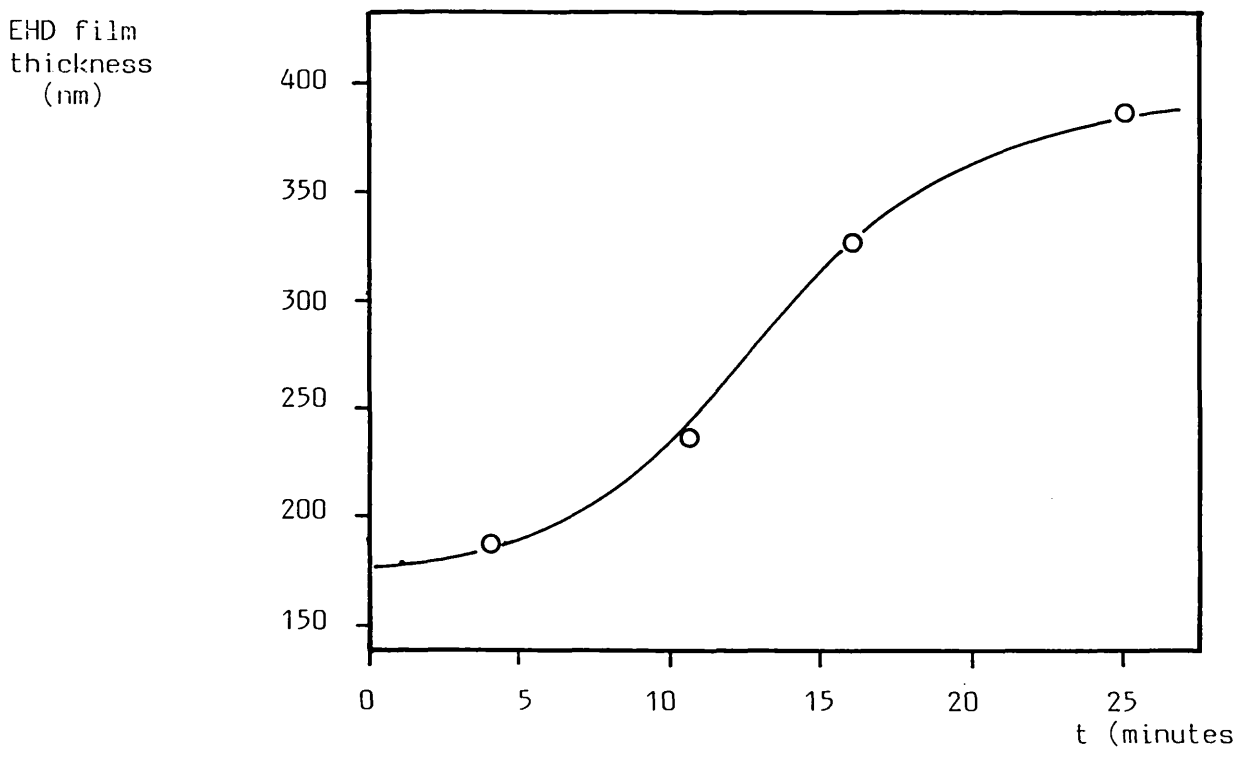


Figure 7.13 Film build-up at constant rolling speed under mixed rolling/ sliding conditions using bis Octyl Phenyl phosphonate in SHC 234 at 100°C. (U = 1.25 M/S)

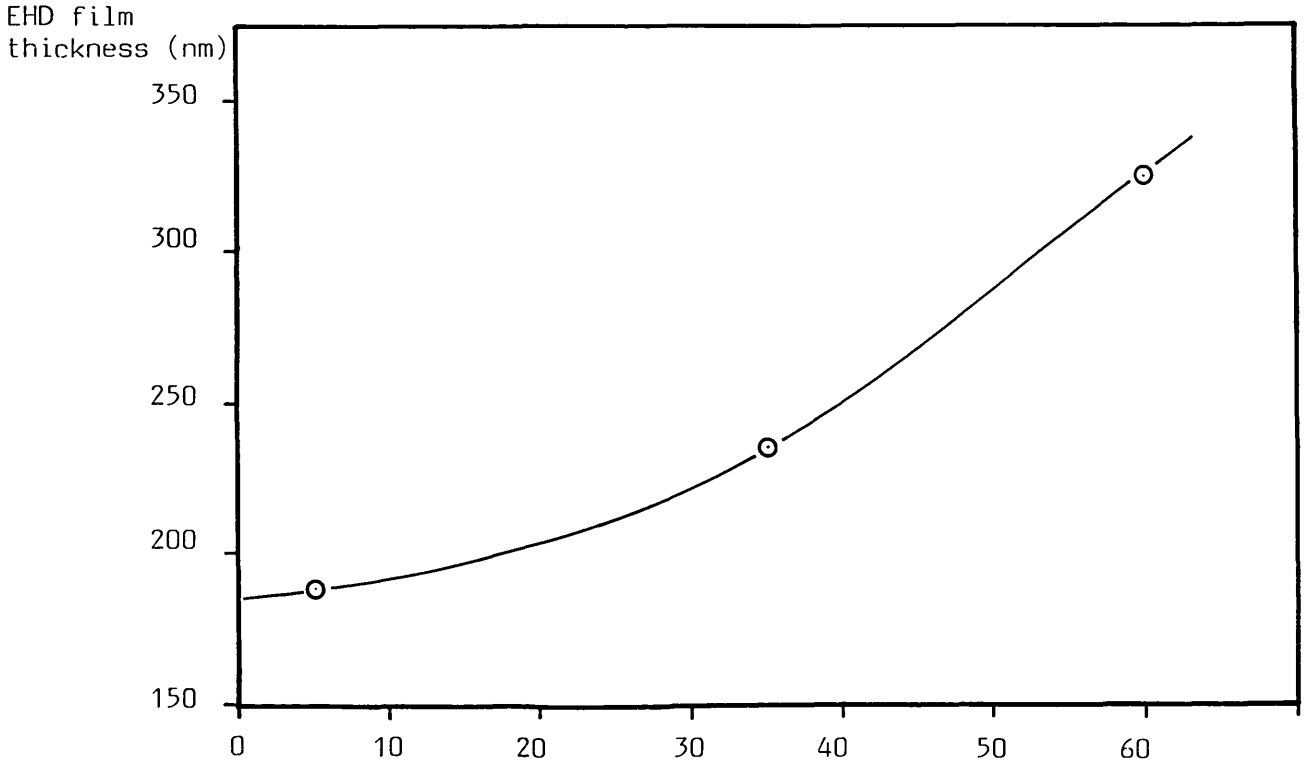


Figure 7.14 Film build-up at constant rolling speed under mixed rolling/ sliding conditions using didodecyl phosphonate in SHC 234 at 100°C. (U = 1.2 M/S)

No effect on the central fringe colour was observed when the amount of sliding was altered by adjustment of the planetary gearbox through which drive was supplied to the ball. The chemical films formed are therefore of a sufficient mechanical strength to not be removed by an increase in the amount of sliding.

The amount of sliding present has an apparent effect on the rate of film formation, with faster rates of build-up being found with greater amounts of sliding. Using BOPP as the additive an increase in film thickness of 160nm was obtained after 95 minutes running at 100°C with pure rolling. With 4% sliding the same increase in film thickness was observed after 32 minutes. With 6% sliding a similar increase in film thickness occurred after only 17 minutes. This effect may be the result of the rheopecticity observed with the phosphonate-iron reaction products discussed in Chapter 5.

The appearance of the balls after the test were similar to those obtained from the pure rolling. A film was visible as colours on the surface, or in extreme cases as a solid material, after cleaning with toluene and acetone.

7.5.3 Effect of Corrosion Inhibitors

The effect of the presence of oil based commercial oil inhibitors on the formation of chemical films was studied using BOPP as additive in SHC 234 synthetic hydrocarbon oil. Two corrosion inhibitors were investigated, NA-SUL BSN, a neutral Barium dinonyl naphthalene sulphonate (RT Vanderbilt Company Inc.) and an unspecified neutral sodium based corrosion inhibitor (BP Oil Ltd.)

Successful monitoring of the build-up of a chemical film was only achieved with the BP corrosion inhibitor. Addition of 1% by weight of NA-SUL BSN to the BOPP/SHC 234 mixture produced a viscous "congealed" precipitate. A feature of 'SHC's' which are very non-polar is their inability to dissolve very polar additives satisfactorily.

This mixture would not easily homgenise and presented serious problems in respect of distribution of the oil. Optical measurement was not possible with this oil, and film formation could not be monitored by the conventional method. This precipitation would seem to be an adduct of the phosphonate and the barium dinonyl naphthalene suphonate (the level of usage of NA-SUL BSN was based on published recommended usages (202)). This precipitation may not interfere with the film growth since after 20 minutes running, interference colours were observed in the stationary contact and the ball was coated with a film not soluble in toluene or acetone. Both of these were observed when film formation had occurred with no corrosion inhibitor present (described in sections 7.5.1 and 7.6.1 respectively).

With the BP corrosion inhibitor, optical monitoring of the chemical film was possible. This corrosion inhibitor was used at 0.4% weight of lubricant and no 'coagulation' of the oil sample was observed. An increase in the film thickness of 54nm was observed after 60 minutes running, which was a similar rate of film formation to that found when no corrosion inhibitor was present. As with the "NA-SUL" corrosion inhibitor and the "phosphonate only" tests, interference colours were observed of the stationary contact and a film (visible as interference colours) was observed on the cleaned ball after the completion of the test.

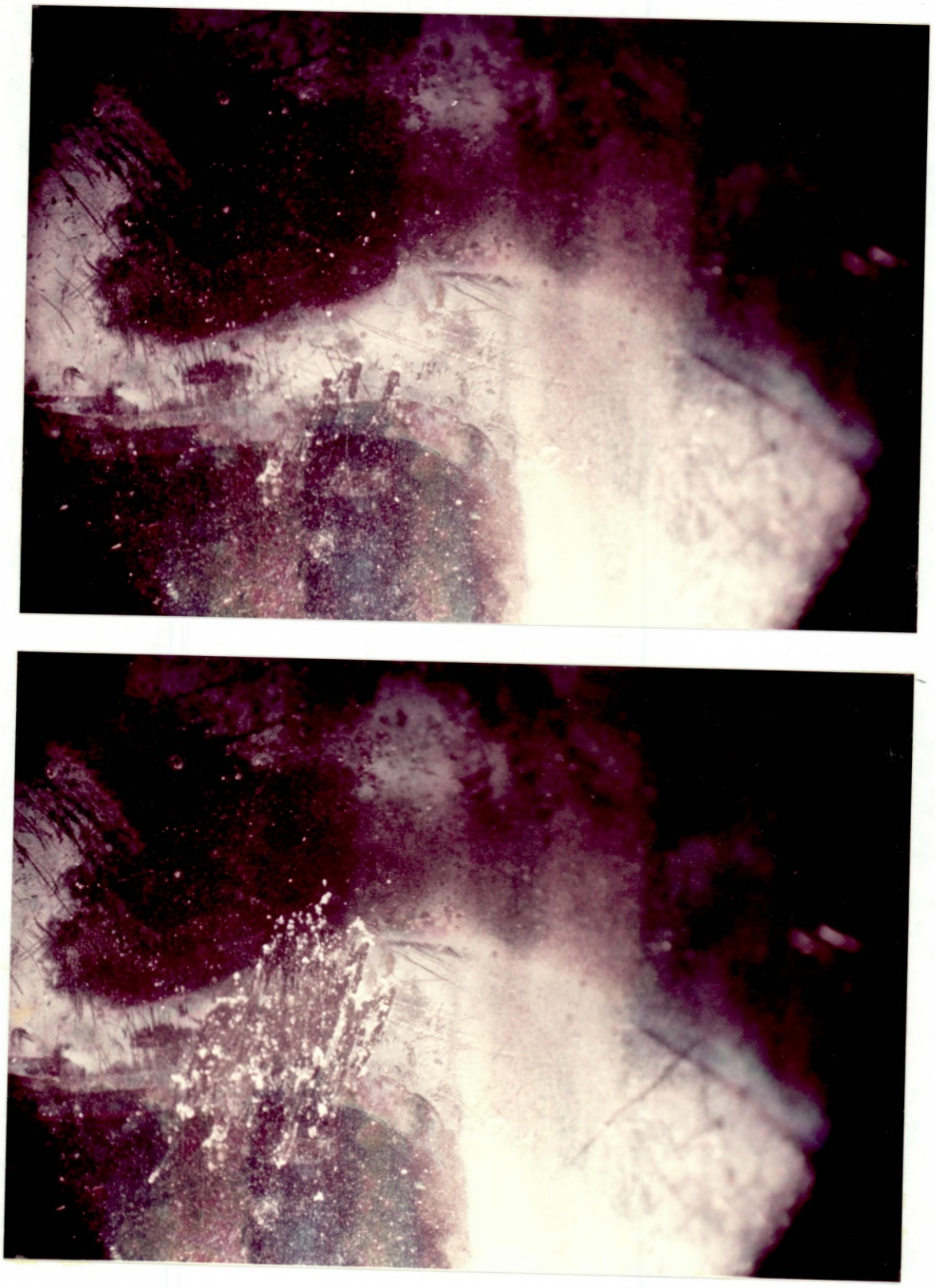
7.6 Analysis of the Surface Film

When the steel balls were removed after completion of each lubrication test and cleaned using toluene and acetone, a film could be seen on the surface. This film was generally seen as interference colours visible under normal laboratory lighting. The surface film was analysed by Scanning Electron Microscopy (SEM), Infrared Spectroscopy and Mass Spectrometry.

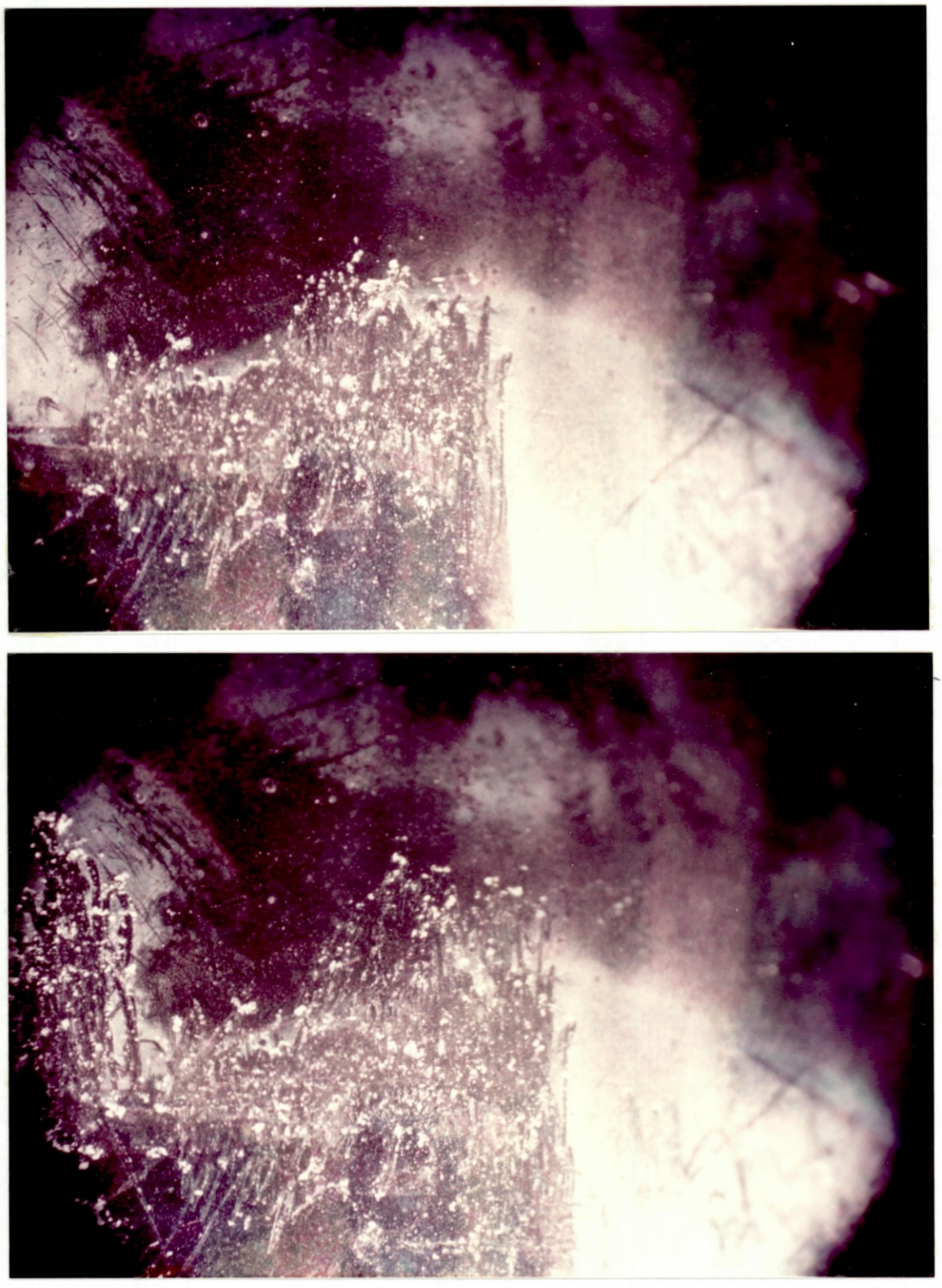
7.6.1 Appearance of the Film

After cleaning with toluene and acetone, a series of coloured bands could be seen on the surface of the ball which ran parallel to the rolling track. When viewed under the microscope (20x magnification) this surface-coating could be seen to be irregularly deposited over the surface, which was shown by the variation in the surface colouration. On parts of the surface the film was sufficiently thickly deposited to appear as white "patches". These thicker deposits could be scraped from the surface using a glass rod drawn to a fine point.

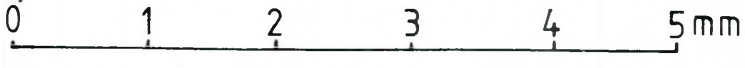
Photomicrographs of the surface film are shown in plates 7.6-7.9. The bands of colour on the surface can be clearly seen in plates 7.6 and 7.7 which are photomicrographs of a cleaned 'dioctyl phosphonate ball" and of a cleaned "bis octyl-phenyl phosphonate ball" respectively. The rolling track in each case is parallel with the horizontal axis of the photograph. A thick deposit of surface film can be seen in plates 7.8 and 7.9. Plate 7.8 shows the deposit as first observed on the surface of the ball. This deposit was sufficiently thick to be 'scratched' and in plate 7.9 the effect of this 'scratching' can be seen.



Plates 7.6 and 7.7 Photomicrographs of the surface film



Plates 7.8 and 7.9 Photomicrographs of the surface film



7.6.2 Scanning Electron Microscopic Analysis

A Scanning Electron Microscope (SEM) was used to analyse the surface of the balls removed after completion of the lubrication tests. The SEM was used to detect the presence of phosphorus in the surface film. This was accomplished using the "EDAX" (Energy Dispersive Analysis of X-Rays) facility attached to a JEOL JSM T-200 SEM.

In addition to providing a magnified image of the sample, the incident electron beam produces X-rays. The energy of these X-rays is characteristic of the element struck by the electron beam. An analysis of the energy distribution of the X-rays produced allows a determination of which elements are present at the surface. This energy distribution analysis is performed by the 'EDAX' facility. A detailed description of SEM and Energy Dispersive X-ray analysis may be found in references (203) and (204).

The output of the detector is processed so as to give a measure of the number of X-rays counted against the energy distribution. Since the energy of the X-rays is constant for each element, the axis of the output display is marked in KeV and is labelled to identify the elements giving rise to a particular peak.

A major drawback of the system used was that the technique only worked for elements of atomic number 11 (sodium) or higher. This is a limitation imposed by the detector (205). Thus the technique could not be used for hydrogen, carbon or oxygen, atomic numbers 1, 6 and 8 respectively. Counting of the X-rays was automatically halted when a preset number of counts had been recorded for a set peak or background region (termed a "window").

The conditions used for the analysis were as follows:

Magnification	x1000
Electron Beam Energy	10 KeV
Preset Count Total	25000
Preset Window	2.68 - 3.2 KeV
Resolution	20 eV/channel

Analysis was made of three randomly selected areas within the rolling track of balls used in lubrication tests with dihexyl, dioctyl, didodecyl and bis octyl-phenyl phosphonates. An unused ball was analysed to provide a comparison with the used balls. In addition analysis of 3 areas on the side of the dihexyl phosphonate ball well outside the rolling track was carried out.

The used and the unused balls were cleaned in an ultrasonic bath before analysis using toluene, followed by rinsing with acetone. It was found not to be necessary to coat the surface with carbon in order to obtain the SEM image. Electrical contact to the balls was made by painting a small amount of silver loaded paint onto the sample staging and placing the ball onto this before closing and evacuating the sample chamber.

Figures 7.15 to 7.20 show the X-ray spectra obtained. These show respectively the spectra obtained from a clean unused ball, from the rolling tracks of balls used in dihexyl, dioctyl, didodecyl and bis octyl phenyl phosphonate lubrication tests, and from the side of the dihexyl phosphonate ball.

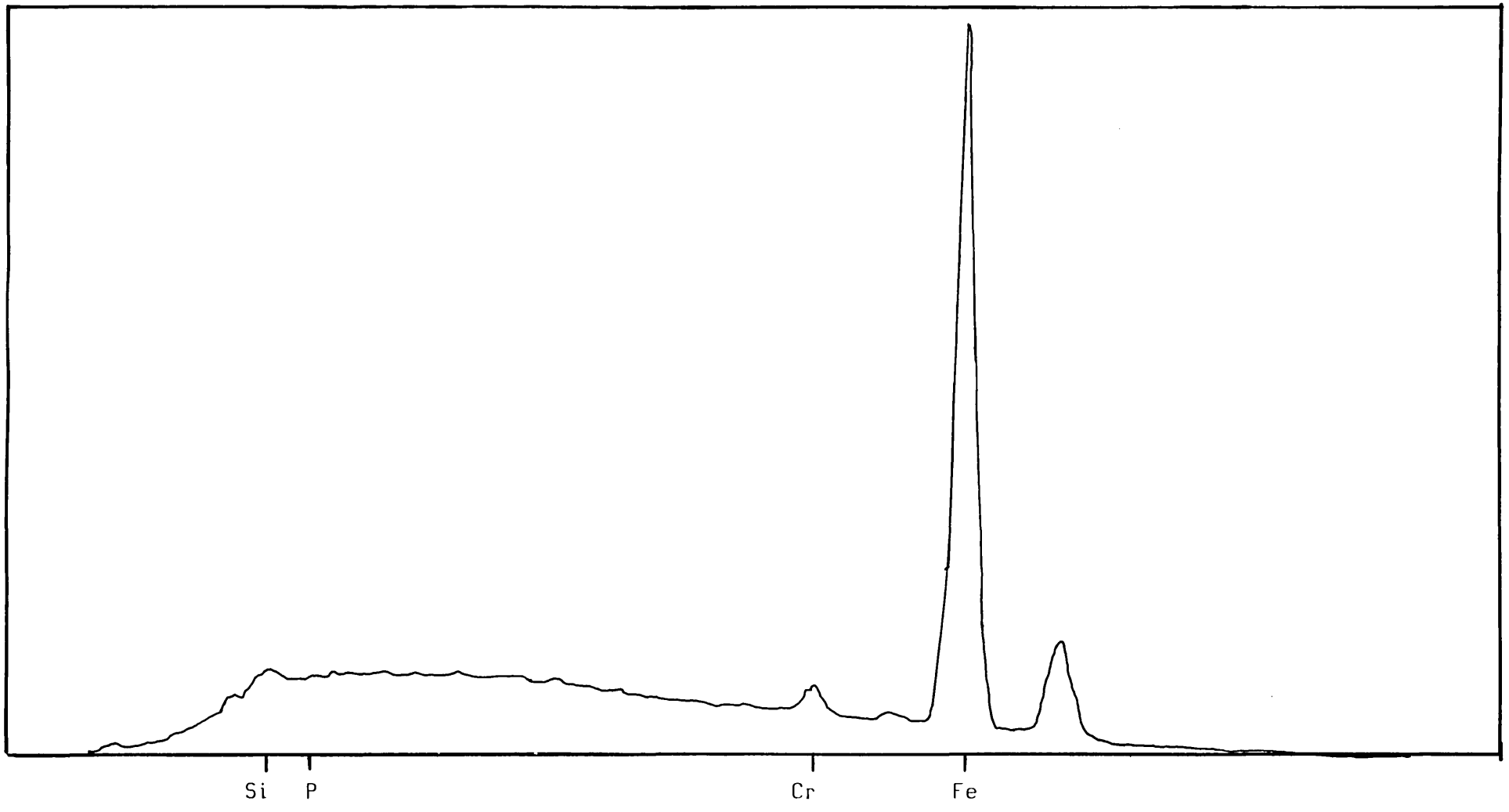


Figure 7.15 EDAX/X ray emission spectrum of the surface of a clean (unused) ball.

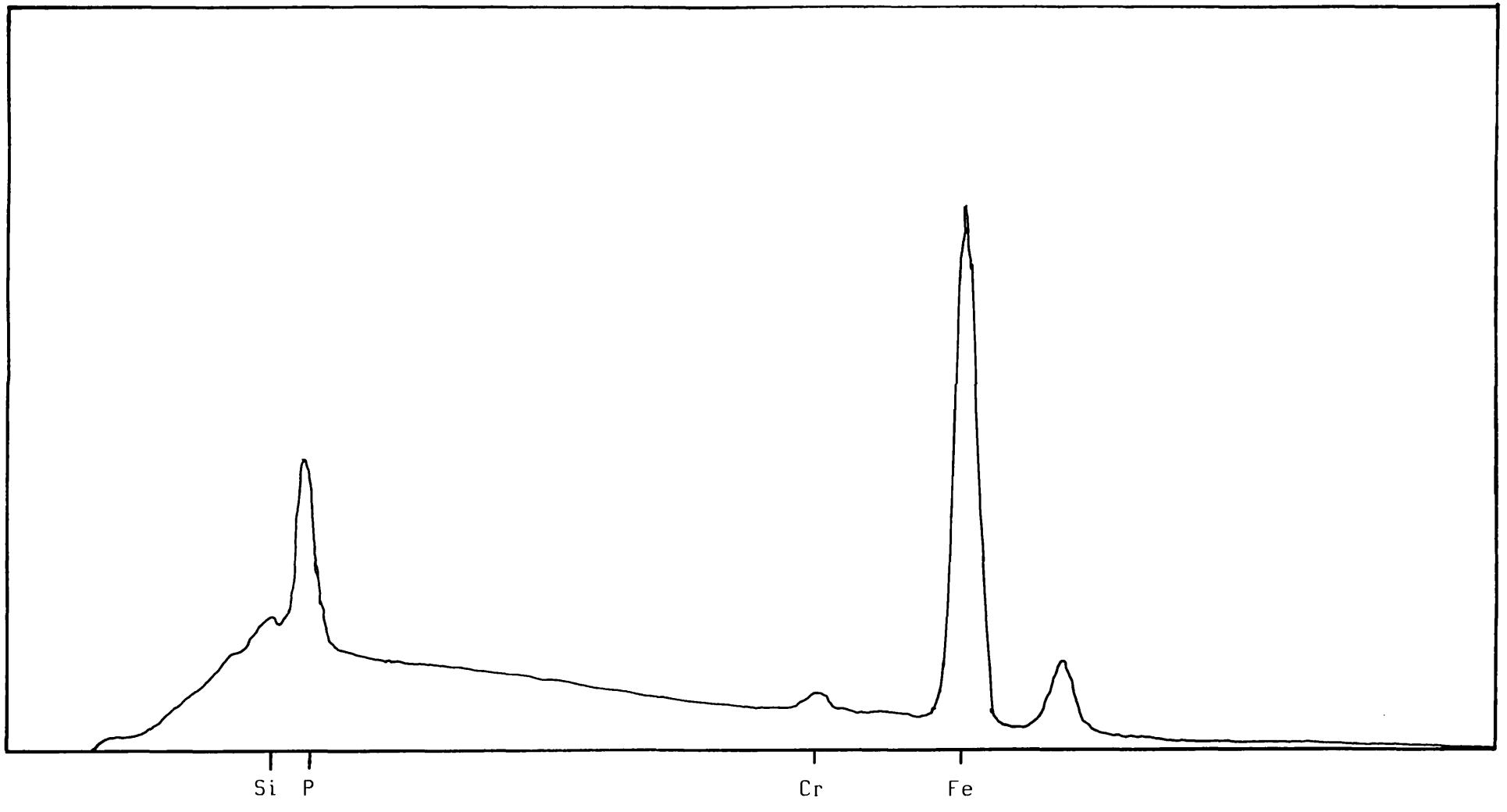


Figure 7.16 EDAX/X ray emission spectrum of the surface of a ball from a dihexyl phosphonate/SHC 234 lubrication test at 100°C.

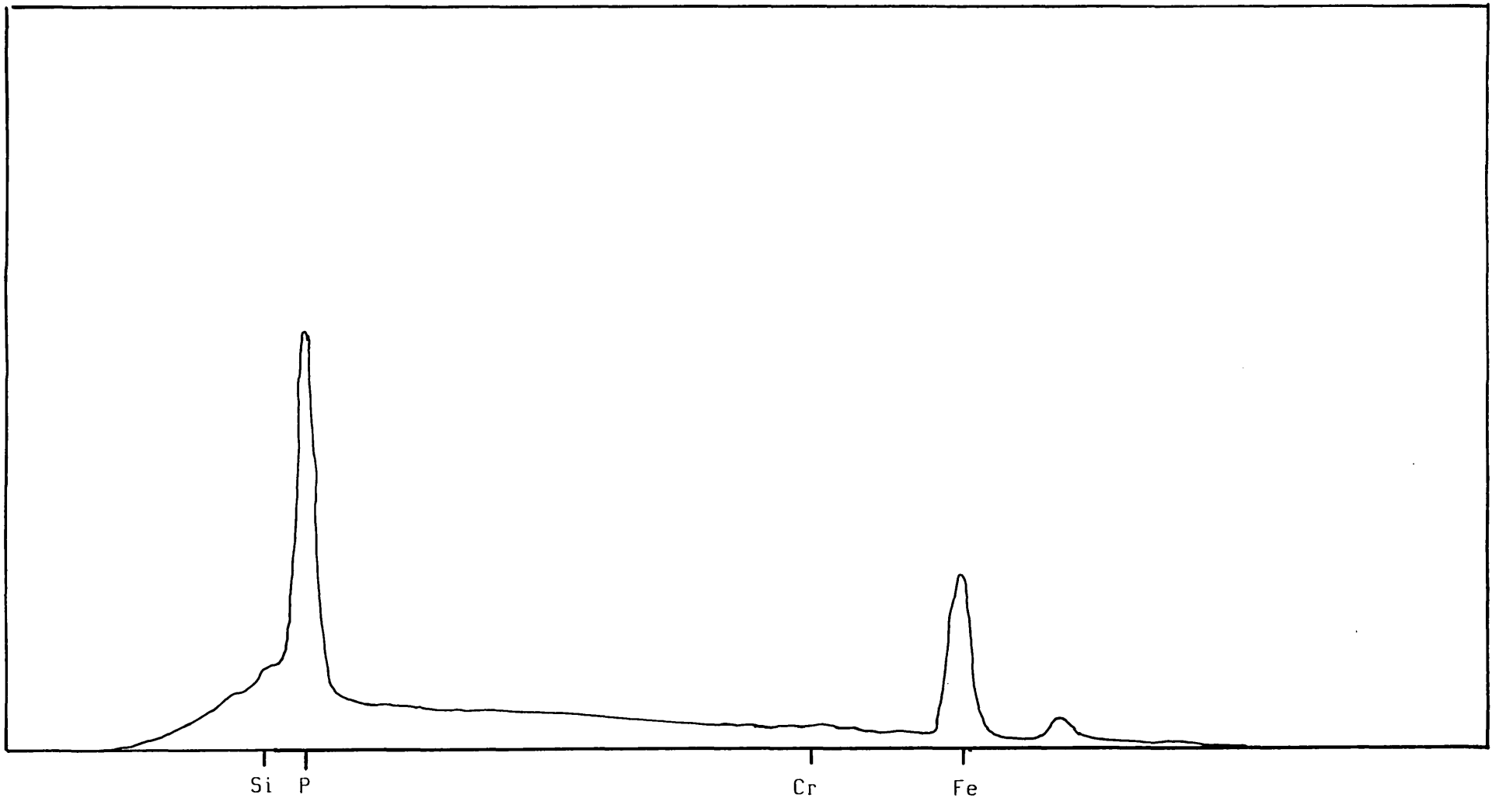


Figure 7.17 EDAX/X ray emission spectrum of the surface of a ball from a dioctyl phosphonate /SHC 234 lubrication test at 100°C.

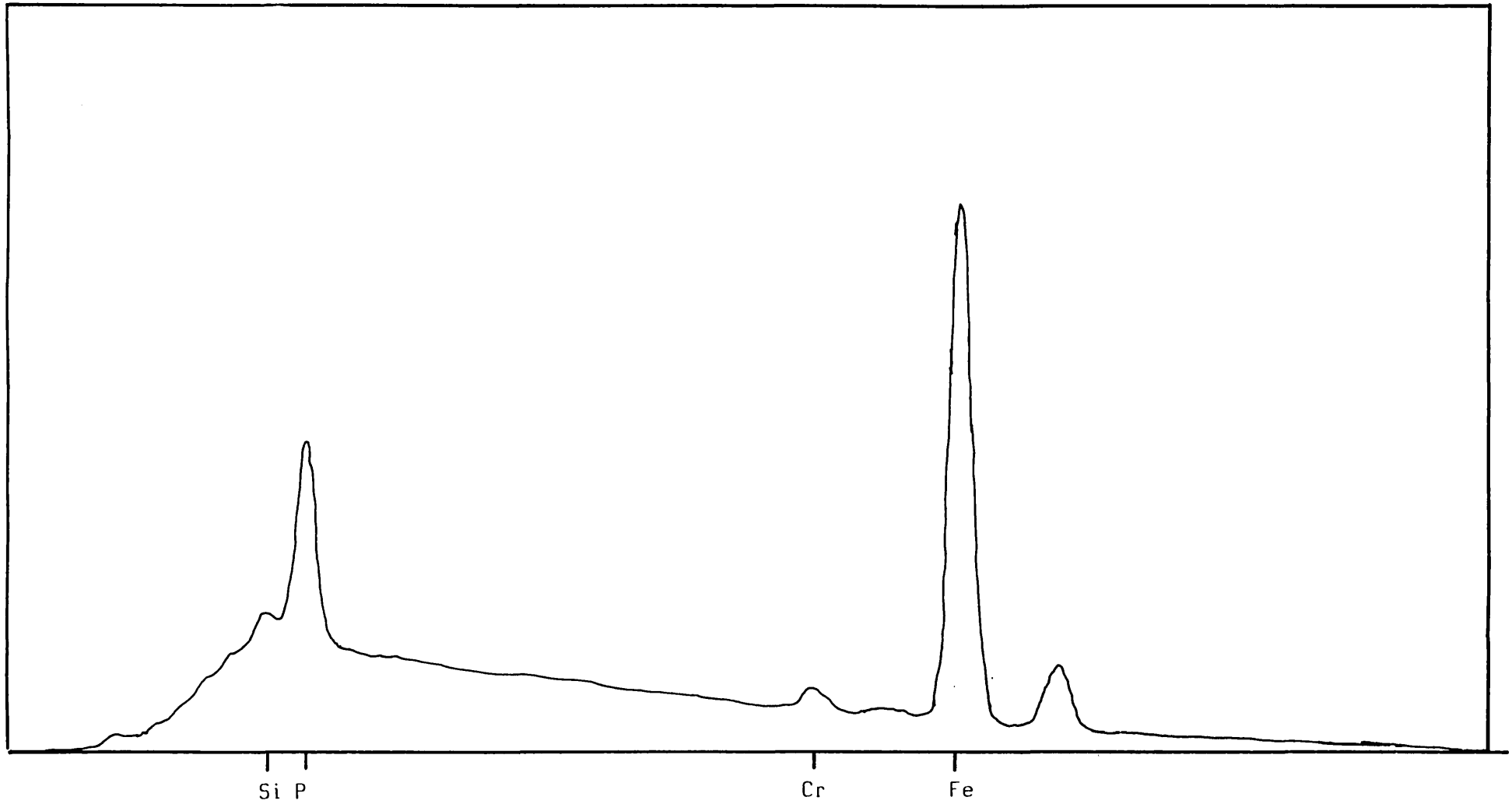


Figure 7.18 EDAX/ X ray emission spectrum of the surface of a ball from a didodecyl phosphonate/ SHC 234 lubrication test at 100°C.

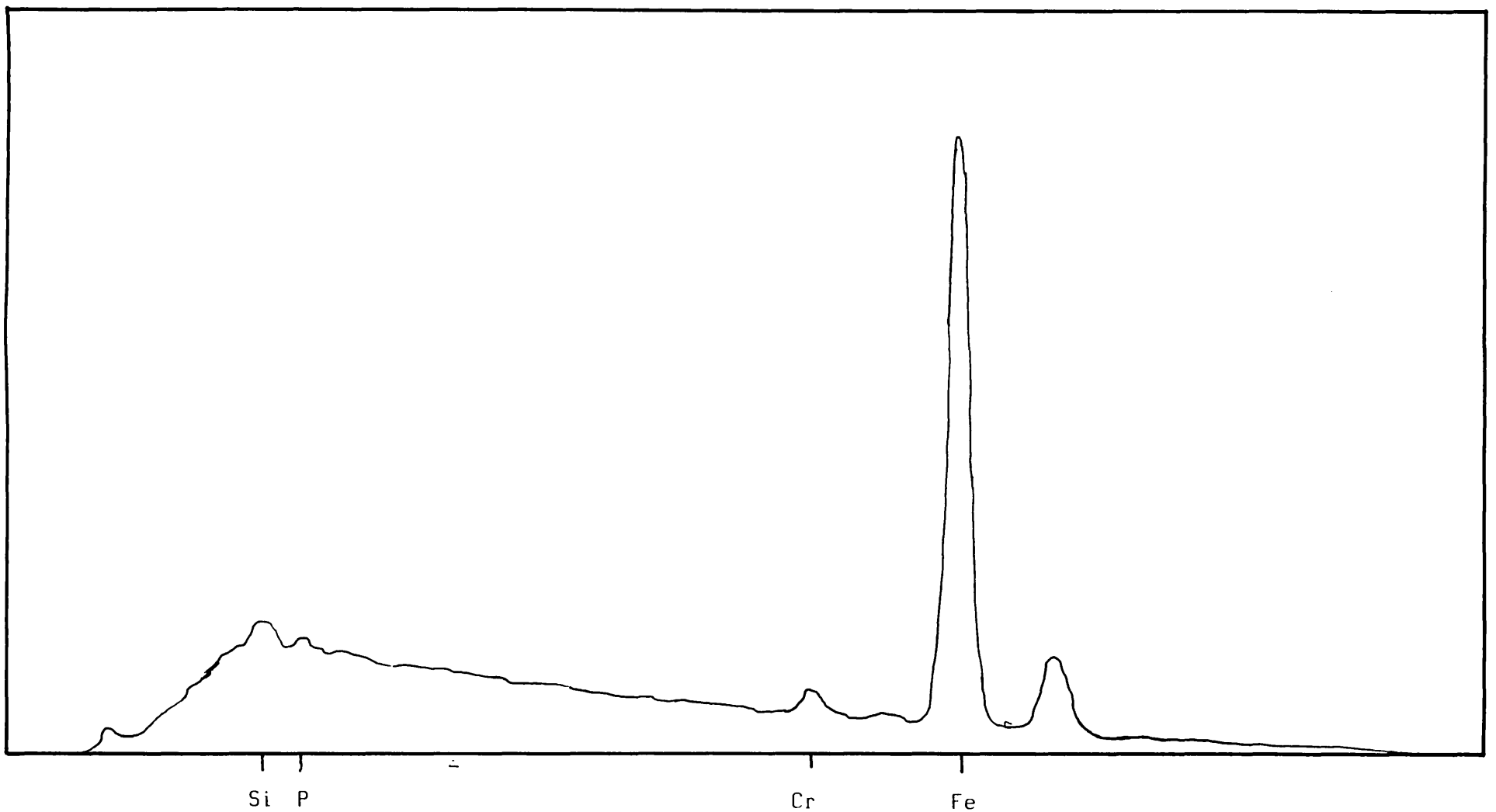


Figure 7.19 EDAX/ X ray emission spectrum of the surface of a ball from a bis octyl-phenyl phosphonate /SHC 234 lubrication test at 100°C.

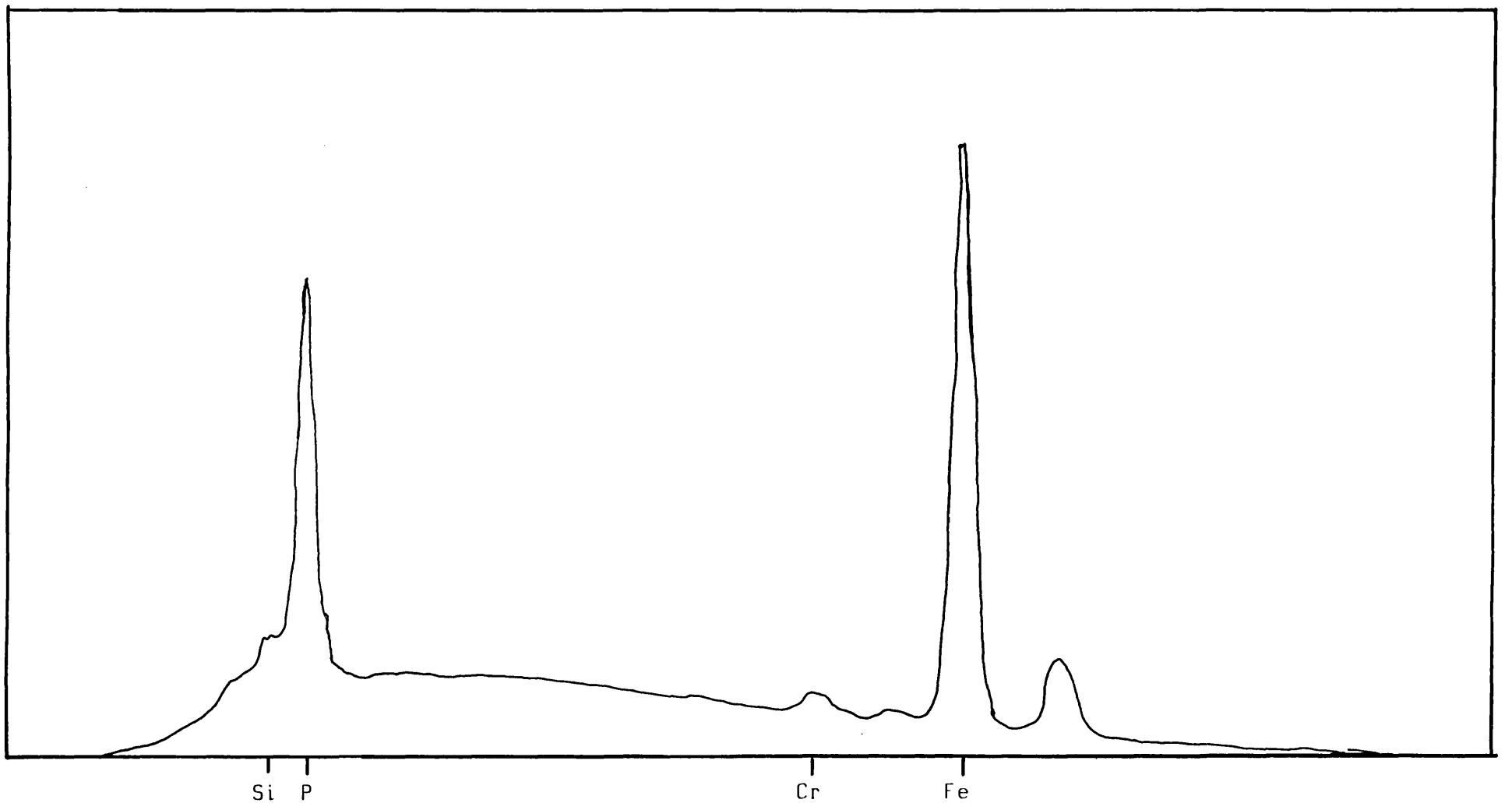


Figure 7.20 EDAX/ X ray emission spectrum of the surface (outside the rolling track) of a ball from a dihexyl phosphonate /SHC 234 lubrication test at 100°C.

In each case the spectrum reproduced is the median spectrum of the three recorded. The spectra show the K lines for phosphorus, iron and chromium, together with the lower intensity K lines for iron and chromium. In some of the spectra a low intensity peak corresponding to the K line of silicon (the fourth most common component of EN31 steel after iron, chromium and carbon) can be identified.

All the spectra of the used balls show the presence of phosphorus on the surface. The deposition was heaviest in the rolling track, but significant levels of phosphorus were found on the side of the dihexyl phosphonate ball. No phosphorus was found on the surface of the unused ball.

7.6.3 Infrared Spectra

Infrared spectra of the surface films observed on the cleaned, used balls was carried using a reflectance technique. These spectra were recorded on a Perkin Elmer 580 B infrared spectrometer using a 'Specac' 9000 Beam Condenser Unit. The infrared light of the sample beam was reflected and focussed onto the surface of the ball and thence to the detector using the beam condenser unit. Infrared spectra of the surface films were recorded using this technique.

The infrared spectra were recorded from the balls removed after lubrication tests with dihexyl, dioctyl, didodecyl and bis octyl-phenyl phosphonates, as described in section 7.4. The balls were cleaned before analysis in an ultrasonic bath with toluene followed by acetone.

The infrared spectra were recorded of the surface film present within the rolling track and outside the track, that is on the side of the ball, in the range 4000 to 600 cm^{-1}.

All the spectra recorded were similar, showing a number of common absorbances in the region 1800-800 cm^{-1}. None of the spectra showed any significant absorbances outside this region. The infrared spectra recorded in the wavelength region 1800 to 800 cm^{-1} are shown in figures 7.21 to 7.24 for balls used in dihexyl, dioctyl, didodecyl and bis octyl-phenyl phosphonate lubrication tests respectively.

As can be seen from figures 7.21 to 7.24 the four spectra display a number of common absorbances which are at approximately 1660, 1440, 1280, 1150, 1030 and 900 cm^{-1}. These peaks are tabulated in table 7.1.

Table 7.1

Absorbance Peaks in the Infrared Spectra of the Surface Films

Phosphonate used			
Dihexyl	Dioctyl	Didodecyl	bis Octylphenyl
1652	1650	*	1655
1438	1438	1455	1450
1252	*	*	1285
1168	1170	1150	1145
990 - 1020	1010 - 1030	*	1020
920 - 930	900 - 910	890	890

* absorbance not discernable

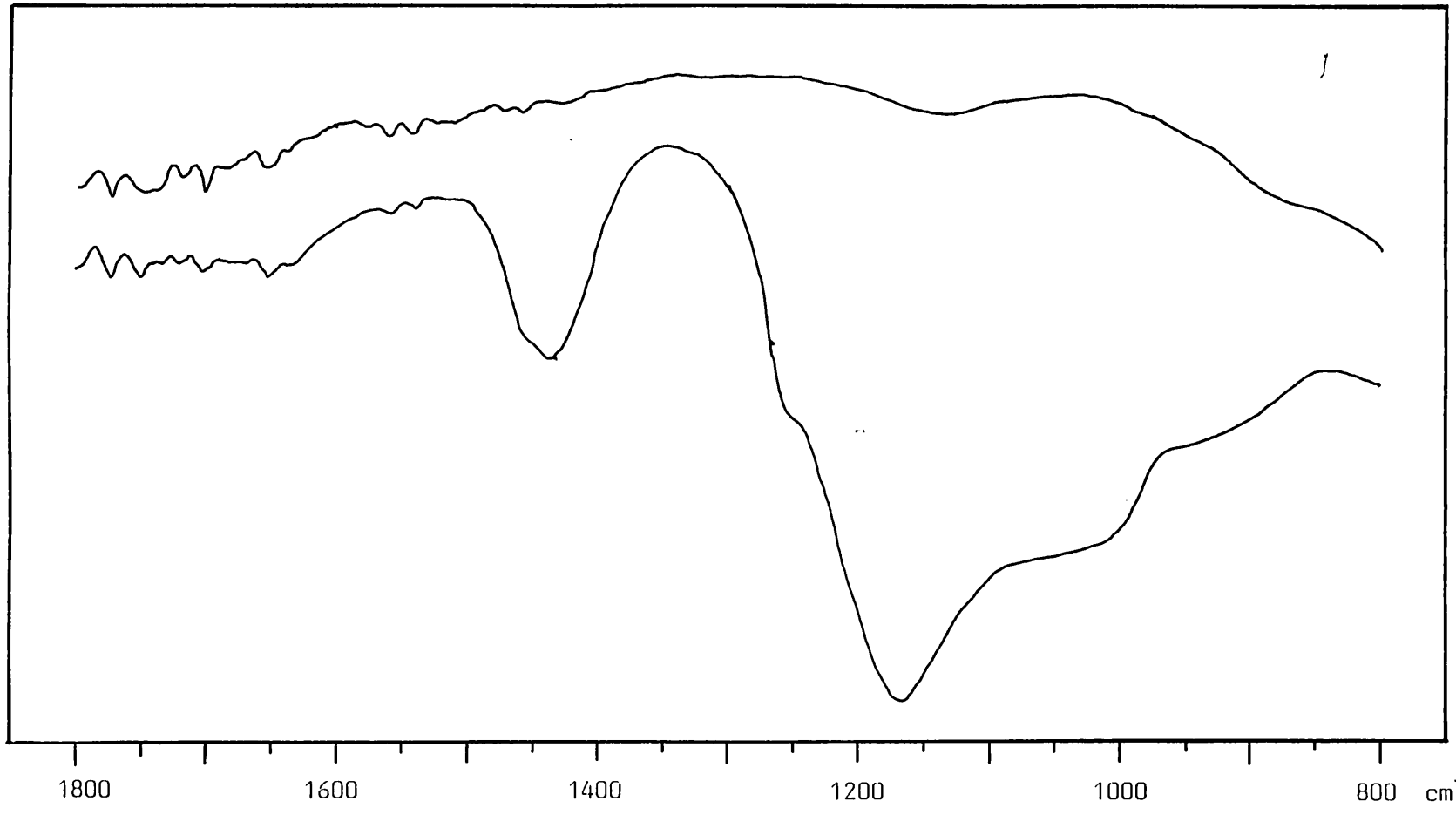


Figure 7.21 Infrared Spectra of the surface (inside & outside the rolling track) of a ball from a dihexyl phosphonate /SHC 234 lubrication test at 100°C.

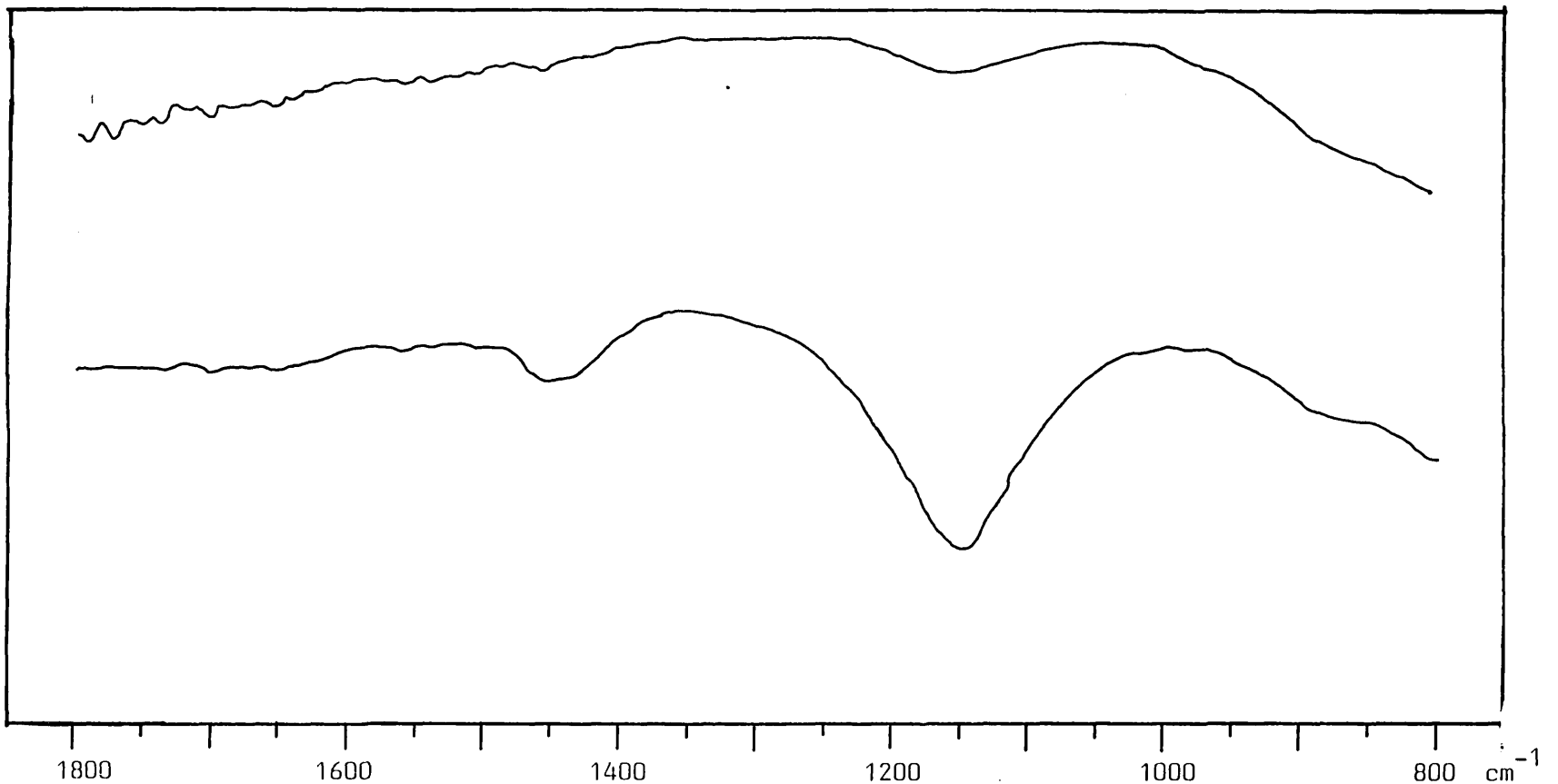


Figure 7.22 Infrared spectrum of the surface (inside and outside rolling track) of a ball from a didodecyl phosphonate /SHC 234 lubrication test at 100°C.

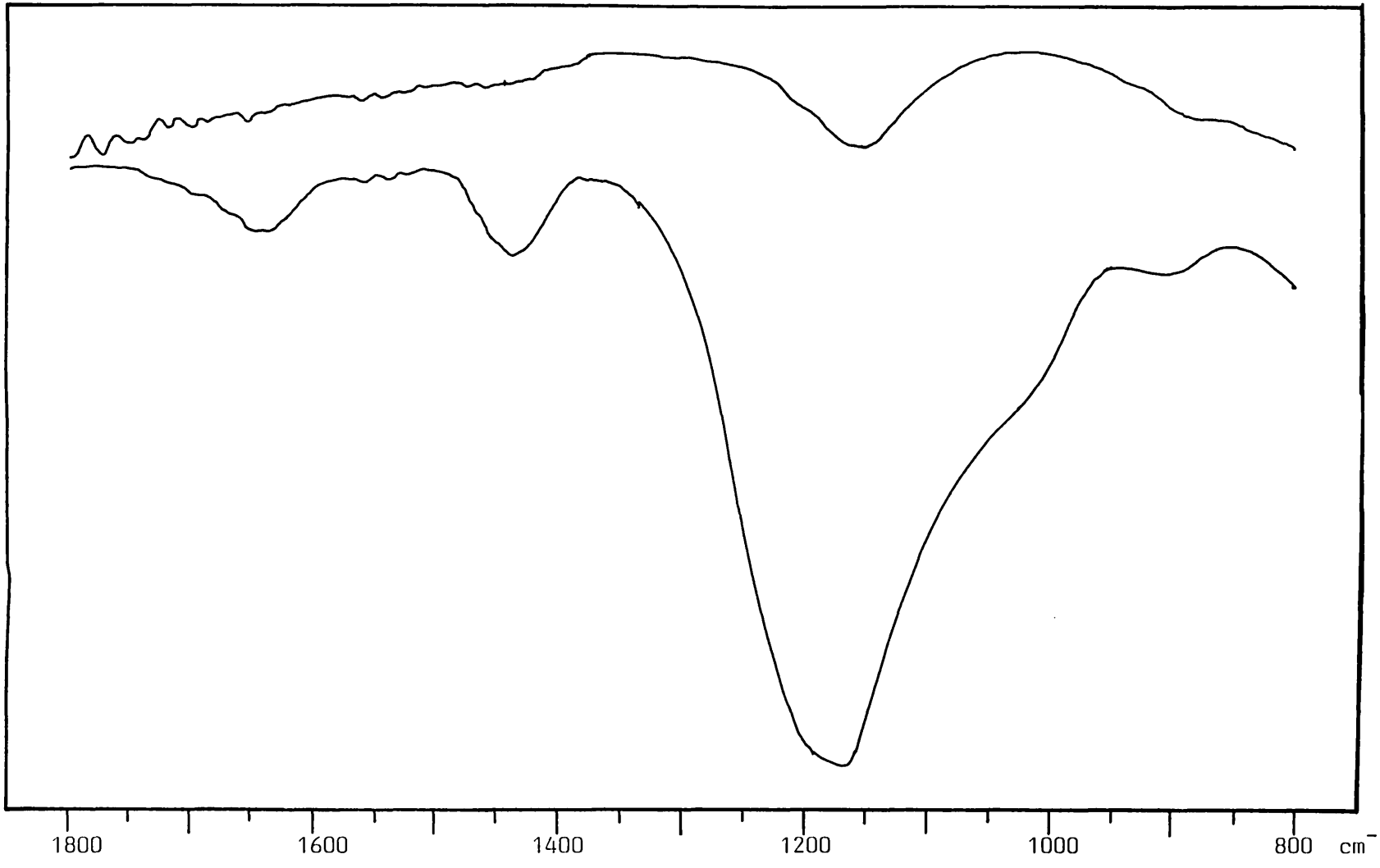


Figure 7.23 Infrared spectrum of the surface (inside and outside rolling track) of a ball from a dioctyl phosphonate /SHC 234 lubrication test at 100°C.

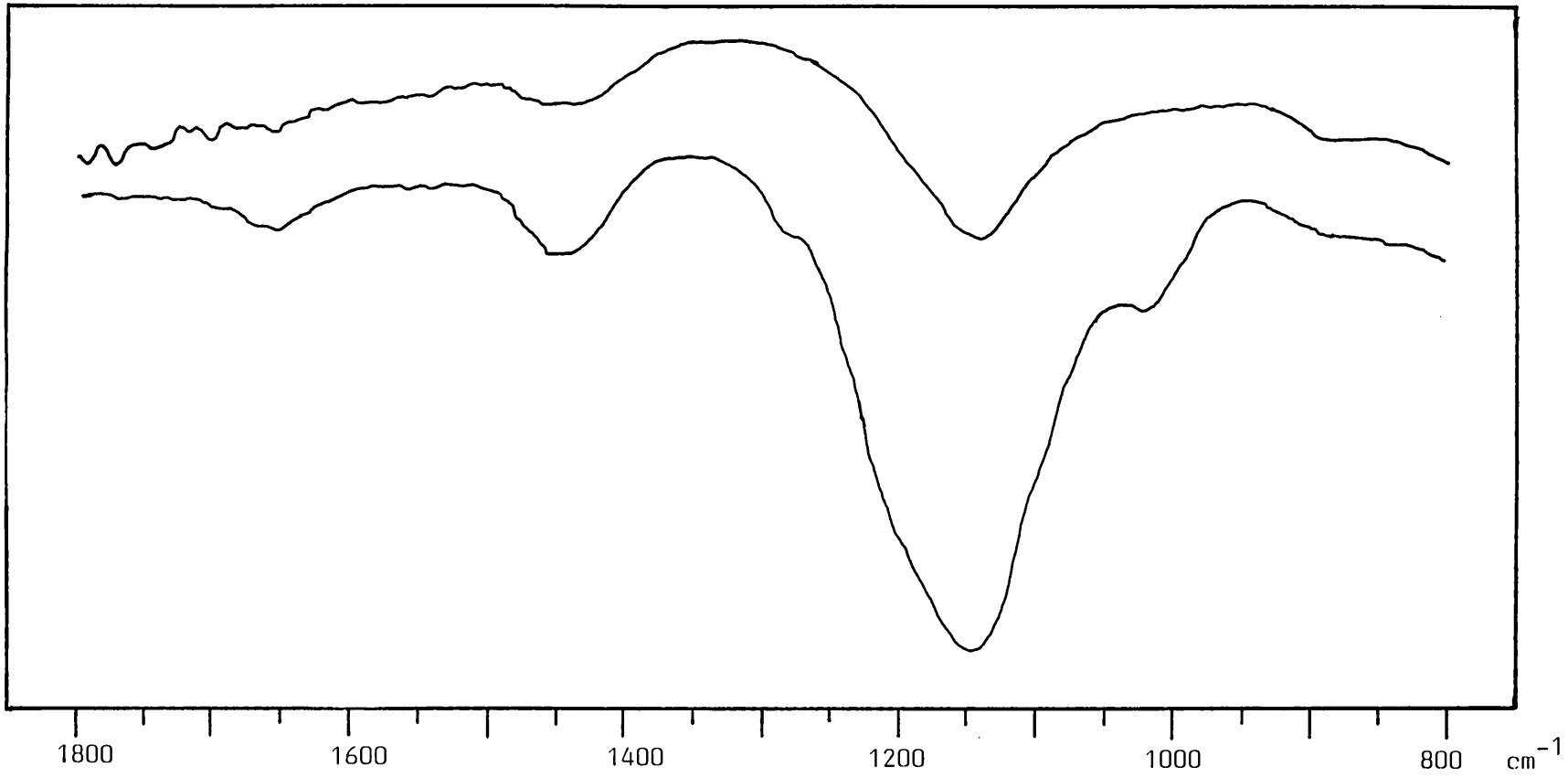


Figure 7.24 Infrared spectrum of the surface (inside and outside rolling track) of a ball from a bis octyl-phenyl phosphonate /SHC 234 lubrication test at 100°C.

The infrared spectra were recorded of the surface film present within the rolling track and outside the track, that is on the side of the ball, in the range 4000 to 600 cm^{-1}.

All the spectra recorded were similar, showing a number of common absorbances in the region 1800-800 cm^{-1}. None of the spectra showed any significant absorbances outside this region. The infrared spectra recorded in the wavelength region 1800 to 800 cm^{-1} are shown in figures 7.21 to 7.24 for balls used in dihexyl, dioctyl, didodecyl and bis octyl-phenyl phosphonate lubrication tests respectively.

As can be seen from figures 7.21 to 7.24 the four spectra display a number of common absorbances which are at approximately 1660, 1440, 1280, 1150, 1030 and 900 cm^{-1}. These peaks are tabulated in table 7.1.

Table 7.1

Absorbance Peaks in the Infrared Spectra of the Surface Films

Phosphonate used			
Dihexyl	Dioctyl	Didodecyl	bis Octylphenyl
1652	1650	*	1655
1438	1438	1455	1450
1252	*	*	1285
1168	1170	1150	1145
990 - 1020	1010 - 1030	*	1020
920 - 930	900 - 910	890	890

* absorbance not discernable

Of the six absorbances that are seen in the 1800 to 800 cm^{-1} region, the strongest is at approximately 1160 cm^{-1}. This absorbance is at a similar frequency to that observed for the donor phosphoryl bonds in the infrared spectra of the products of the reactions of heating the phosphonates with iron (section 6.1).

The absorbances at 1650 cm^{-1} and 900 cm^{-1} may indicate the presence of the P-O-H group (103,137). The higher frequency vibration (1650 cm^{-1}) is within the quoted limits for the P-O-H vibration in this region (103, 137). The 900 cm^{-1} vibration is at the lower limits quoted for this vibration (137).

Although the spectra show no significant C-H stretch (at 2900 cm^{-1}), the presence of the organic group is shown by the vibrations at 1440-1450 cm^{-1} and at 1000cm^{-1}. The former may be assigned to the C-H deformation vibration of the alkyl chain (206), whilst the latter corresponds to the P-O-C stretching vibration (102, 103, 105).

The weak absorbance at 1250-1280 cm^{-1} discernable in some of the spectra would appear to be due to the vibration of non-donor bonded phosphoryl bonds (102, 103, 104).

In conclusion therefore, the infrared spectra of the surface film deposited on the balls show the presence of a chemisorbed (since it was not removed using solvents) organophosphorus film. From the presence of absorbances corresponding to both P-OH and P=O, it seems likely that the film is an organophosphate.

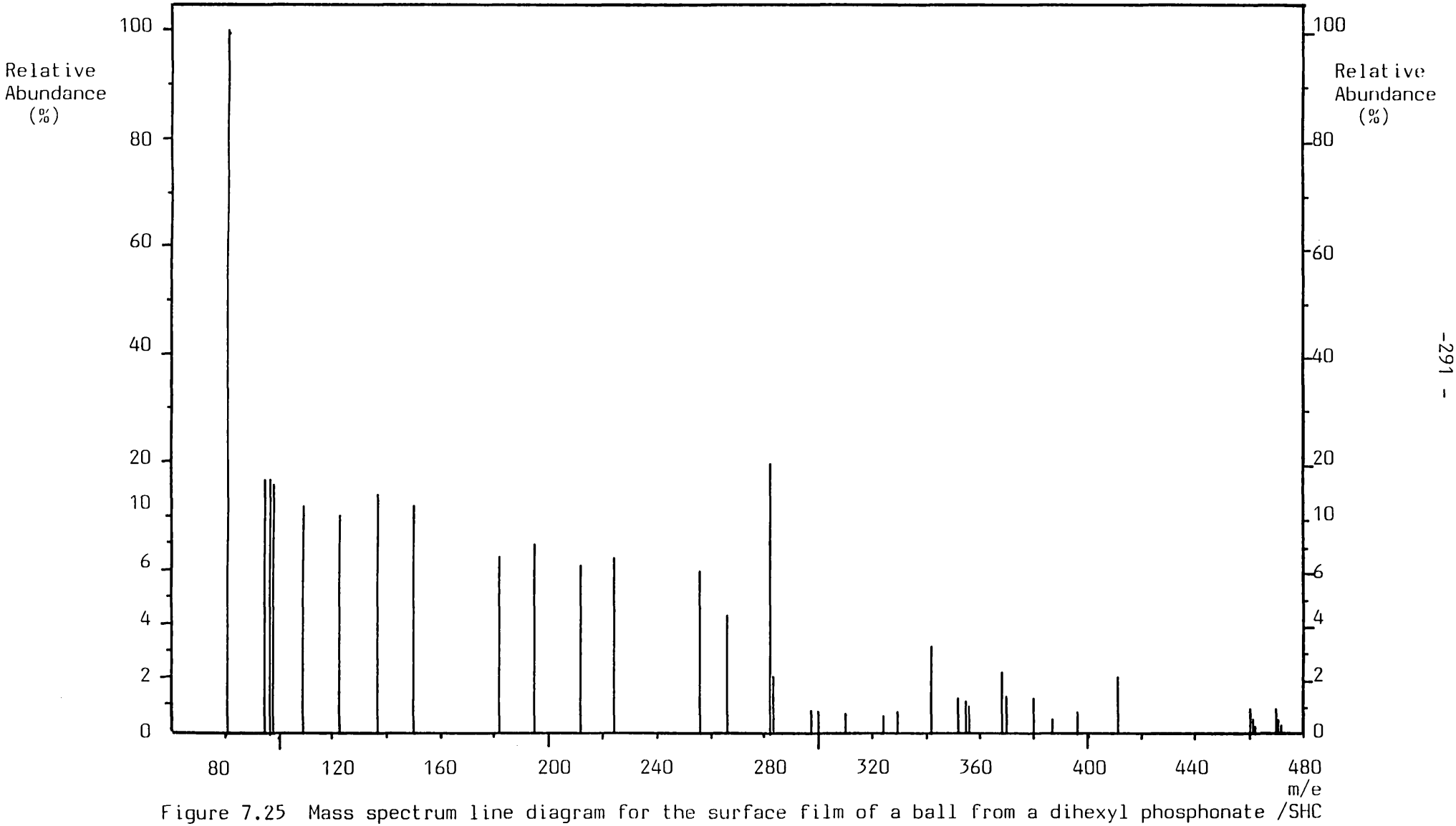


Figure 7.25 Mass spectrum line diagram for the surface film of a ball from a dihexyl phosphonate /SHC 234 lubrication test at 100°C.

7.6.4 Mass Spectral Analysis

As was mentioned in section 7.6.1 (Analysis of the Surface Film), the deposition of the surface film was sufficiently thick in parts to be physical removeable by scraping. This scraping off of the surface film can be seen in plates 7.8 and 7.90.

The mass spectra was recorded for a sample of the surface film removed from the ball used in a dihexyl phosphonate lubrication test. The surface film was removed by scraping it with the end of a glass "melting point tube" drawn to a fine point. Because the quantity of sample obtained was small (ca. 0.01g), the sample was transferred directly into the sample tube that was to be placed in the mass spectrometer. A stereo-microscope was used to monitor the film removal and transfer of the scraped film into the sample tube.

From the mass spectrum obtained, a line diagram was prepared, the preparation of which has already been described (section 4.4). This line diagram is shown in figure 7.25. For convenience this line diagram is prepared with the peak at m/e = 81 as the most abundant, and as in the line diagram in Chapter 6, with an expansion applied to the lower portion of the relative abundance axis. Peaks of m/e ratio less than 81 are present in the mass spectrum, many at a higher relative abundance than that of the m/e 81 peak. The inclusion of these peaks would only lead to a lowering of the relative abundance of the more important peaks of higher m/e values. The peaks of m/e values less than 81 represent a fragmentation of the alkyl group with charge retention on the alkyl fragment (111).

A comparison of this mass spectrum with that obtained in Chapter 6 (figure 6.8) for the dihexyl phosphonate-iron polymer shows that the two samples are not identical. This is understandable since the sample analysed in Chapter 6 was not purified in any way whilst the lubrication test sample was 'washed' before collection with heptane. The two mass spectra do however show considerable similarities when the line diagram of the lubrication test sample is analysed.

The presence of weak signals at m/e ratios of greater than 350 indicate the presence of a polymerisaction (cf. $(C_6H_{13}O)_3PO$ = 350). These high molecular weight peaks, like those present in the mass spectra of the phosphonate-iron reaction polymers, are not easily resolved. It is possible to assign the peak at m/e 470 to the formula $(RO)_3P_2O_3H$ Fe which may exist as $((RO)_2$ P(HO)Fe $(PO_2$ (OR)) (A) which allows the assignment of the m/e 471 and m/e 472 to the formulae $((RO)_2PH.O)$Fe (PO.OH(OR)) (A+1) and $((RO)_2PH.O)$Fe (OPH(OH)(OR)) (A+2) respectively, where R is the group C_6H_{13}. Fragmentation of these species can account for some of the peaks at lower m/e values, noticeably the 411 and 387 peaks. the assignment of lower peaks as resulting from a fragmentation of A, A+1 or A+2 is not possible, and a possible formation route is by fragmentation of the species $((RO)(OH)_2PO)_2$Fe (B) by the loss of alkenes. Thus the peaks at m/e 380, 368 and 352 may arise from the loss of C_3H_4, C_4H_4 and C_5H_8 from B. The presence of B is not indicated by the mass spectrum, but peaks corresponding to $(RO)_2$ P(OH)O and $(RO)(OH)_2PO$ are present at m/e 266 and at 182 respectively. Of the remaining high abundance peaks, that at m/e 282 may result from the loss of C_5H_8 from the trialkyl phosphate $(RO)_3PO$. The lower m/e peaks can be assigned to fragmentation peaks resulting from the loss of alkanes and alkenes from the alkyl group on the mono and dialkyl phosphates.

Of particular significance is the peak present at m/e = 98. As was reported in Chapter 6, this peak is resolvable only as $[P(HO)_3O]^+$, that is the resultant product of the "McLafferty rearrangement" of $(RO)P(OH)_2O$ (145, 146), which may be used as evidence of the presence of the monoalkyl phosphate, or of the presence of orthophosphoric acid $[H_3PO_4]$.

To conclude therefore, the mass spectra of the surface film formed in the dihexyl phosphonate lubrication test shows the presence of the monohexylphosphate, with an amount of the dihexyl phosphate present. The mass spectra show that polymerised species are present in the sample. The mass spectrum obtained shows considerable similarity to that recorded for the dihexyl phosphonate-iron reaction polymers. It is reasonable to conclude therefore that product produced under rolling EHD conditions is similar to that obtained in the reactions observed on heating the phosphonate with iron powder.

7.6.5 Summary of the Analysis of the Surface Film

The three methods of analysis used to investigate the surface film formed have produced results which are complementary. All the methods have shown the presence of phosphorus in the surface film, each method with a different amount of detail.

Clear evidence of the presence of phosphorus is provided by the results of the electron microscopy analysis. These analyses showed that a phosphorus containing film was deposited over the whole surface of the used, cleaned balls. The film was thickest in the rolling track, but with significant amounts of phosphorus present outside this track.

The infrared spectra of the surface film similarly showed a greater film deposition within the rolling track. The infrared spectra indicated that the surface film was composed of an organophosphate, with the phosphoryl oxygen donor bonded to the iron atom, as was observed with the phosphonate-iron reaction polymers (see Chapter 6).

Further evidence for the presence of an organophosphate in the surface film came from the mass spectra of the dihexyl phosphonate surface film. As with the polymers obtained by heating the phosphonates with iron powder, the mass spectra of the surface film shows both polymeric species and the presence of the mono and di hexyl phosphates. Although the mass spectra show some considerable differences, it was considered that these arose from the partial purification carried out on this surface film. The major differences in these mass spectra was largely due to the different amounts of phosphonates in the samples, which, before the surface film was analysed, were reduced by the rinsing with heptane.

The results of these analyses show that the films formed on the rolling surfaces in the lubrication tests are very similar to those formed in the heated phosphonate-iron reactions, that is a polymeric iron organophosphate. This film is deposited over the entire surface, but is concentrated into the rolling track.

7.7 Discussion

The four additives tested all showed a similar ability to produce an increase in the thickness of the EHD film formed under rolling conditions by the formation of a chemical film in the rolling surface. All four phosphonates show, therefore, the behaviour previously reported for a bis nonyl phenyl phosphonate (1,2). The rate of formation of this film is dependent on temperature but unlike previous work (2), the build-up of a chemical film was observed at quite low temperatures. In earlier work no details of studies carried out at temperatures below 99°C were given, and the failure to observe a film build-up may have resulted from not allowing the test to run for a sufficiently long time.

The film formed in rolling and sliding appears, as suggested by Fowles et al (2), to be incremental to the EHD film thickness. At the beginning of a test the EHD film predicted by theory is obtained. The film thickness then builds up steadily at constant speed over a period of some hours. Comparision of the tests at constant speed with those at constant film thickness are consistent with there being the original EHD film plus a gradually increasing chemical film.

This is shown in Figure 7.26. The lower curve is an experimental constant speed test, starting at the first red interference fringe, at 165nm. The upper curve has been calculated from the constant film thickness test results of Figure 7.11. These latter were carried out at the first blue interference fringe, i.e. at approximately 240nm. On the assumption that the chemical film is independent of the EHD film, the reduction in EHD film thickness throughout the test in Figure 7.11 can be chartered from the reduced speed.

EHD film thickness at time t, h_{Et}, is the given by:

$$h_{Et} = h_o (U_t/U_o)^{0.7}$$

where suffix o refers to the initial, pure EHD condition, at t = 0. This allows calculation of the residual chemical film in the contact speed test, h_{ct}

$$h_{ct} = h_t - h_{Et}$$

where h_t is 240nm, and thus permits conversion of constant film thickness to notional constant speed results. The result, shown in Figure 7.26 is strikingly similar to the experimental contact speed test, supporting the original contention, that the chemical film is independent of, and additional to, the EHD film.

The presence of a corrosion inhibitor does not affect this chemical film formation, although the barium napthalene sulphonate could not be directly tested due to the coagulation observed between the two additives. Thus it may be speculated that these phosphonate additives will perform in much the same manner in a formulated oil in a practical situation, as under experimental situations.

The film formed in the surface under rolling conditions has a considerable strength, and is not removed by sliding forces present in the contact. It is clear, therefore, that the film produced is chemically bound to the metal surface, and not an adsorbed film. The surface film was shown to be a chemical film by the variation in the rate of build-up of the film that was observed if the test rig was not adequately cleaned after a previous test. Surface film remaining from a previous test evidently catalysed further film formation, as might be expected for a polymerisation process.

This variation in rate of film build-up meant that a clear comparison of the different phosphonates could not be made. However the effect of previously formed surface film is very important in practical applications, since it would indicate that little detrimental loss of film would occur after an oil change.

The various analyses of the surface film have shown that similar films are formed on the surface to those obtained in the heated-phosphonate-iron reactions. This indicates that no other reaction is initiated by the high pressure conditions encountered within the rolling contact. Since the surface film is apparently similar to that obtained in the heated phosphonate-iron reaction tests, it may be assumed that their properties are similar, in particular the rheopecticity observed. This rheopecticity may account for the "exceptional antiwear properties" observed for a nonyl-phenyl phosphonate (1,2) and the film formation of the four phosphonates tested in this work.

The analysis of the surface film indicated the presence of a organophosphate film. The formation of organophosphate films from phosphonate additives has been previously reported (17,21,24,25). Polymeric phosphates formed with transition metals are known (178) but are not as well documented as those formed by phosphinates. They do, however, share many similar properties notably thermal stability. It is interesting to note that the phosphinate polymers are used as antiwear agents in lubricating greases (207) and as viscosity stabilisers in hydraulic fluids and phosphate ester lubricants (208).

EHD Film Thickness

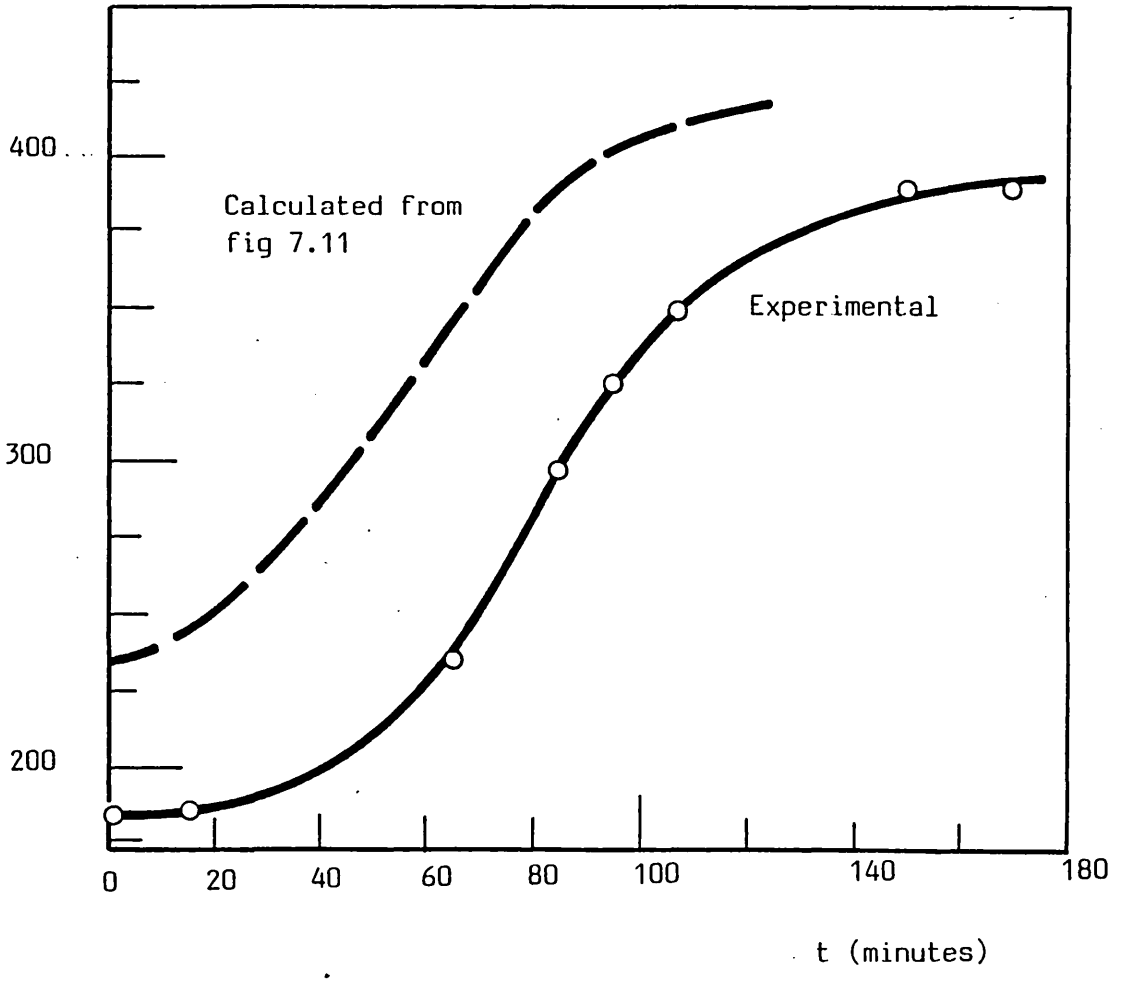


Figure 7.26

Chapter 8.

Summary and General Conclusions

8.1 The Reaction of Phosphonates with Iron

All the dialkyl and diaryl phosphonates tested were found to undergo a chemical reaction on being heated with iron. The reactions produce polymeric ferro-organophosphorus compounds which differ by the organic group present in the parent phosphonate. The rate of the reaction with iron depends on the nature of the organic group present, the temperature of reaction and whether oxygen or water are present. The observed reaction appears to be a general reaction of di-substituted phosphonates.

Analysis of these reaction products indicated that they are largely composed of the Iron (III) mono alkyl (or aryl) phosphate linked into polymer chains. The formation of phosphate surface films from phosphonate esters under rolling conditions has been previously reported (17,21,24,25) both as iron inorganic phosphates and as iron organophosphates. The polymeric nature of the phosphonate-iron reaction products was described in Chapter 6. The properties of these reaction products are similar to those reported for polymeric phosphates and phosphinates (176-8). Although previous EHD work has not suggested the presence of polymeric phosphate films, the reaction products of dialkyl phosphonates and iron have been reported as having wax-like consistencies (10,26). These reaction products, however, were considered to be iron (III) mono alkyl phosphonates, and not phosphates as found in this work.

The results of phosphonate-iron reactions showed that both the presence of oxygen, and of surface oxide on the iron increase the rate of reaction. The typical reactions of dialkyl phosphonates are those of nucleophilic addition (125), and phosphonates show considerable resistance to oxidation (54,55). Thus it seems that the role of oxygen is to oxidise the iron surface. The oxidation of the phosphonate probably follows its adsorption on the surface. The formation of the donor phosphoryl bond will help any nucleophilic attack as a consequence of the electron displacement along this phosphoryl bond away from the phosphorus atom. Further discussions on the possible mechanism will be presented in section 8.3. The beneficial effects of both oxygen and surface oxide on the surface levels of phosphorus caused by dialkyl phosphonates has been previously reported (21,24,25). It has been previously proposed (21,25) that oxidation of the phosphonate occurs on the metal surface and not in solution.

The reaction process has been produced in static tests using pure iron powder and thus shown not to require the high shear of an EHD contact. Static tests have also enabled a proper chemical analysis to be achieved. The results of this indicate that the iron is entering into a reasonably symmetrical complex with acid phosphate and/possibly also phosphonate ester. Because these acid esters have at least two P-O groups they can act as chelating agents, occupying two iron co-ordination sites at once. In such cases, most chelating agents tend to bond to the same iron atom, but acid phosphorus esters prefer to bridge two iron atoms, these giving rise to a linked iron-phosphorus ester polymer.

This characteristic has been noted for phosphinates by Block (177), who states "It is interesting to note that phosphinate anions were being studied as potential chelating groups at about the same time but that the experimental results were considered more in occurrence with bridging than chelating phosphonate groups".

The same bridging effect has also been found for dialkyl acid phosphate esters, where it has been noted that at low metal concentrations, singly complexed ions were formed, but that bridging occurred as the metal concentration was raised (179). This is likely to be the pattern of behaviour in rolling contacts. Then longer chain iron (III) acid phosphate esters, which are slightly soluble in oils, most probably dissolve into the boundary layer of fluid coating the rubbing track. As this continues, the iron content increases until viscous, bridged polymers form, which have only very limited tendency to disperse further into solution. Instead they form a thick, viscous, adherent coating.

The lack of reactivity with chromium may be a consequence of the differences in the surface oxides, with no reaction occurring with the Cr_2O_3 surface oxide. Dialkyl phosphonates have been shown to give rise to lower surface phosphorus levels on steels with a high chromium content compared to low chromium steels (25).

Like oxygen, water was shown to have a beneficial effect on the rate of the phosphonate-iron reaction. From the analysis of the reaction products both hydrolysis and oxidation occur. Although the role of water has not been determined, it probably encourages both the oxidation and hydrolysis reactions. A similar effect has previously been reported for dialkyl phosphonates (10).

8.2 The EHD Film Forming Properties

Four of the five phosphonates studied in this work were shown to produce a chemical film in the rolling track which 'grew' as the lubrication test proceeded. (The exception was diphenyl phosphonate which proved too corrosive to be tested in the optical EHD test rig). The film forming properties previously reported for bis nonyl-phenyl phosphonate (1,2) appear therefore to be a general property of di-substituted phosphonates.

The analyses carried out on the surface films showed that they were similar to the products of the reactions of the phosphonates and iron on heating. This reaction with iron would appear to be a general reaction of disubsituted phosphonates. The antiwear properties of phosphonates thus arise from their reaction with the steel (or iron) surface to form a polymeric ferro-organophosphate surface film. The "phosphonate additive" (bis nonylphenyl phosphonate) tested by Fowles et al. (2) and by other workers had been reported as forming strongly bonded films on steel surfaces (42).

The superior antiwear properties reported by several workers (5,7,8,10) for di-phosphonates compared to the corresponding phosphates would, therefore, appear to result from the ability of the phosphonates to react with the iron to form a surface film in a way that phosphate compounds cannot react. The formation of the surface film was shown to involve oxidation of the phosphonate. Clearly further oxidation of phosphate esters is not possible, and thus phosphate additives cannot interact with the iron in a similar way to phosphonates.

If the surface films are, as concluded, identical to the products obtained in the heated phosphonate-iron reactions, then they would be expected to exhibit the same physical properties, in particular, the rheopecticity exhibited by the phosphonate-iron reaction products. It is not clear how important this may prove under rolling conditions. In any rolling contact a certain amount of shear force exists in the contact, and a rheopectic coating may produce an increase in viscosity within the rolling contact compared to that outside the contact. Thus a higher film separation would be obtained due to the contribution from the thickness of the surface film and possibly also a greater EHD film thickness than would otherwise be expected due to a viscosity increase within the contact.

The formation of polymeric films has been reported for zinc dialkyl dithiophosphates (209,210,211). Thus the good antiwear and antifatigue properties found for these additives may also result from the formation of thick chemical films on the rolling surfaces.

8.3 A Possible Mechanism of Interaction

The reaction which takes place between the di-substituted phosphonates and iron under both "bulk-heating" and EHD conditions has two oxidation steps. Metallic iron is oxidised to iron (III) and the phosphonate is oxidised to the phosphate. It was reported earlier that phosphonates are fairly resistant to oxidation and that their reactions are usually those of nucleophilic addition at the phosphorus atom. Iron metal is oxidised readily in the presence of oxygen or water (127, 128). It may be assumed that even under "nitrogenated" conditions an amount of oxygen is present.

Simple analysis of the rate of iron uptake in Figure 5 suggests that 3 x 10^{-3} moles 0 were needed in the dihexyl phosphonate test. Estimates for available "0" are (i) from nitrogen gas bubbled in, 0.5 x 10^{-5} moles 0/hour, (ii), from dissolved oxygen, 6 x 10^{-3} moles 0/hour, (iii) from a 10_um metal oxide layer, 9 x 10^{-3} moles 0.

Thus even in this "oxygen free" environment, enough oxygen would be present to cause the effect observed for dihexyl phosphonate. The iron, oxidised probably due to the presence of oxygen, is converted to a nucleophile (FeO or other species) which attacks the phosphonate group. If this phosphonate group is donor bonded to an iron atom, nucleophilic attack at the phosphorus is enhanced due to the decrease in electron density at the phosphorus atom. Nucleophilic attack, by an iron oxide species, produces firstly the iron diphosphate and secondly the iron monophosphate after elimination of ROH.

The sequence of events described above is open to considerable speculation. Clearly a considerable amount of work is entailed in determining the exact mechanism.

8.4 Implications

The formation of a "thick" mechanically strong surface film on the rolling contact has considerable beneficial implications in terms of reducing wear and fatigue under elastohydrodynamic lubrication conditions and consequently reducing fatigue. The chemical film results in a greater separation of the rolling surfaces than the bulk oil properties, contact geometry and loading would predict. A greater separation of the rolling surfaces will result in a lower number of asperity contacts and thus lower amounts of wear and fatigue.

Fatigue life is proportional to the specific film thickness, , where is defined as:-

$$= \frac{\text{minimum film thickness ho}}{\text{composite surface roughness}}$$

and composite surface roughness = $\sqrt{RMS_1^2 + RMS_2^2}$

where RMS_1 and RMS_2 are the surface roughness of surfaces 1 and 2 Fatigue life is proportinal to ( )^x where x is in the range 0.8 to 2.1 (213).

This formation of thick film has considerable practical implications. It is now recognised that the severity of a mixed EHD, boundary lubricating system is well expressed by the prevailing lamda value or specific film thickness

$$= \frac{h_o}{(Rq_1^2 + Rq_2^2)}$$

where h_o is the minimum EHD film thickness and Rq_1 Rq_2 are the RMS roughness of the two surfaces. Fatigue (214), wear (215) and scuffing have all been show to depend quite critically on this value , especially for <2. The converntional methods of increasing are to increase oil viscosity (or pressure viscosity coefficient), increase rolling speed and increase contact conformity. In many situations these expedients are either not practical, or, often, product a rise in temperature which in turn reduces EHD film thickness.

The formation of thick chemical films suggests an alternative approach to the problem. In this study film thickness was increased typically from 150 to 400nm with greater increases dependent on the quantity of additive available. The maximum film thickness measured was circumscribed by the optics rather than film growth, but was over 600nm. Such a thickness with realistic surface roughnesses of 0.5mm. RMS would increase values from 0.2 to 0.8. Sastry et al (215) have found such a change to produce a greater than ten-fold reduction in wear.

An important point to be borne in mind about these findings is that the class of additives studied here have already been shown to be effective antifatigue additives. Thus these additives have been shown to be useable in practical lubrication situations and are compatible with formulated oils. The work reported in Chapter 7 showed that "thick" chemical films were formed when commercial corrosion inhibitors were present. It may therefore be concluded that the known high performance of these additives is due to thick film formation.

8.5 General Conclusions

From the results obtained from the work described in this thesis, the following general conclusions about the antiwear performance of dialkyl phosphonates can be drawn:

i) Di-alkyl and di-aryl phosphonates react with iron to form similar polymeric ferro-organophosphorus compounds which are mainly composed of iron (III) monoalkyl (or aryl) phosphate groups linked into polymeric chains.

ii) These phosphonates show good antiwear film forming properties under rolling EHD conditions. These films are of sufficiently high a mechanical strength to be able to withstand moderate (10%) sliding forces.

iii) Analysis of the EHD chemical films shows that they are similar to the products obtained on heating the phosphonates with iron.

iv) The antiwear properties of the phosphonates do not result from the formation of 'thin' chemical films which easily shear under rolling conditions so reducing wear. Rather these phosphonates perform in an antiwear capacity by forming "thick", mechanically strong, chemically bonded surface films within the rolling track which reduce wear by greatly increasing the metal-to-metal separation without affecting the bulk oil properties.

Chapter 9

Suggestions for Future Work

Future work arising from the results presented in this thesis can be divided into two broad, but overlapping areas. These are, further investigations into the antiwear behaviour of the disubstituted phosphonates, and investigations into the differences in antiwear activities of the disubstituted phosphonates and other types of antiwear additives.

In investigating further the antiwear properties of the disubstituted phosphonates, it will be important to determine the effect of the several parameters studied in the "bulk heated" tests reported in this thesis. Notably the effect of water and oxygen were not investigated, all tests being carried out in air. Careful thought into the design of a rig capable of running in an oxygen-free atmosphere would be necessary, the main problem being the form of heating used.

The analytical techniques used to study the thick films present opportunities for further development in particular mass spectroscopy. Developments in mass spectrometers, notably combined SIMS/FABS instruments (Secondary Ion Mass Spectroscopy/Fast Atom Bombardment Spectroscopy) should allow direct analysis of the specimen surface without the need to remove the film for analysis.

Clearly there is a very large amount of information to be gained from an extensive mass spectroscopic investigation of the surface films. The sampling technique may be capable of extension so as to allow analysis of the film by ^{31}P n.m.r.

The rheology of the phosphonate-iron reaction polymers was discussed in Chapters 5 and 7 and needs further investigation. It has not been possible to study the rheology of the chemical film formed under rolling EHD conditions in the present work. If the chemical films generated under EHD conditions exhibit the same rheopecticity that "bulk reaction" products show this will be an important area of study, especially for circumstances involving mixed rolling and sliding. It is this factor that may dictate whether thick films form in contacts of other geometries (e.g. line contact).

No indication of the role of impurities in the formation of the thick films was obtained. In the light of the results the presence of the mono- and tri- substituted esters and the parent alcohol may considerably influence the antiwear performance. The presence of phosphate impurities should also have an influence on the antiwear performance of the di-substituted phosphonates.

An important aspect of these results is whether other currently used antiwear additives will also, under similar conditions, form 'thick' films. This study should therefore include other phosphonates (i.e. the mono- and tri- esters), phosphates and ZDDP's. Two points of interest exist here, whether these additives form 'thick' films or not and, if not, why they do not form such films.

The suggestions for future work may thus be summarised into the following points:-

a) a further study of the nature and mechanism of formation of the 'thick' films formed by the di-substituted phosphonates

b) An investigation of the effect of water, absence of oxygen and impurities on the rate of formation of the thick films generated by the di-substituted phosphonates

c) A study of the physical and mechanical properties, especially the rheology, of the thick films including a further study of the effect of sliding and of load on their formation and stability.

d) An investigation into whether other currently used additives produce thick films or not. Notable compound types should include mono phosphonates, tri phosphites, phosphates and ZDDP's.

References

1. Parker R.J. and Kannell J.W. "Elastohydrodynamic Film Thickness between Rolling Discs with a Synthetic Paraffinic Oil to 589K (600°F)", NASA Technical Note TN-D6411 (1971)

2. Fowles P.E., Jackson A. and Murphy W.R. "Lubricant Chemistry in Rolling Contact Fatigue - The Performance and Mechanism of one Antifatigue Additive", ASLE Trans., 24, (1981), 107-118

3. Jackson A., Private Communication

4. Barcroft F.T. and Daniel S.G. "The Action of Neutral Organic Phosphates as E.P. Additives", J. Bas. Engng. Trans 87, (1965), 761-770

5. Davey, W. "Extreme Pressure Lubricants - Phosphorus Compounds as Additives", Ind. & Eng. Chem., (1950) 1841-7

6. Beeck O., Givens J.W. and Williams F.C., "On the Mechanism of Boundary Lubrication; II, Wear Prevention by Additive Agents", Proc. Roy. Soc. L., A 177, (1940), 103-118

7. Hall J.M. "Antiwear Additives in Neopentyl Ester Oils", ASLE. Trans., 14, (1971), 292-300

8. Yamamoto Y. and Hirano F., "Effect of different Phosphate Esters on Frictional Characteristics", Trib. Int., 13, (1980), 165-9

9. Yamamoto Y. and Hirano F., "The Effect of the Addition of Phosphate Esters to Paraffinc Base Oils on their Lubricating Performance under Sliding Conditions", Wear, 78, (1982) 285-296

10. Forbes E.S. and Battersby J., "The Effect of Chemical Structure on the Load Carrying and Adsorption Properties of Dialkyl Phosphites", ASLE Trans, 17, (1974), 263-270

11. Forbes E.S., Neustader B.L., Silver H.B. and Upsdell N.T., "The Effect of Chemical Structure on the Load Carrying Properties of Amine Phosphates" Wear, 18, (1971), 269-278

12. Forbes E.S. and Silver H.B., "The Effect of Chemical Structure on the Load Carrying Properties of Organo Phosphorus Compounds", J. Inst. Pet., 56, (1970), 90-98

13. Godfrey D., "The Lubrication Mechanism of Tri Cresyl Phosphate on Steel", ASLE Trans., 8, (1965), 1-11

14. Sakurai T. and Sato K., "Chemical Reactivity and Load Bearing Capacity of Lubricating Oils containing Organic Phosphorus Compounds", ASLE Trans., 13, (1970), 252-261

15. Forbes E.S., "Antiwear and Extreme Pressure Additives for Lubricants", Trib. Int., 3, (1970), 145-152

16. Forbes E.S., Upsdell N.T. and Battersby J., "Current Thoughts on the Mechanism of Action of TCP as a Load Carrying Additive", I. Mech. E., 3rd Intl. Lub. Symp., Paisley (1971), Paper 9/71

17. Goldblatt I.L. and Appeldoorn J.K., "The Antiwear Behavious of TCP in Different Atmospheres and Different Base Stocks", ASLE Trans., 13, (1970), 203-214

18. Gauthier A., Montes H. and Georges J.M., "Boundary Lubrication with Tri Cresyl Phosphate (TCP) - Importance of Corrosive Wear", ASLE Trans., 25, (1982), 445-455

19. Rounds F.G., "Effect of Additives on the Friction of Steel on Steel, (i) Surface Topography and Film Composition Studies", ASLE Trans., 7, (1964), 11-23

20. Wiegand H. and Broszeit E., "Zum Mechanismus der AdditivWirkung Modelluntersuchungen mit Trikresyl Phosphate", Wear, 21 (1972), 289-302

21. Rounds F.G., "Some Environmental Factors affecting Surface Coating Formation with Lubricating Oil Additives, ASLE Trans., 9, (1966), 88-100

22. Rounds F.G., "Effects of Additives on the Friction of Steel on Steel (ii) Additive-Base Oil Interactions", ASLE Trans., 8, (1965) 21-28

23. Rounds F.G., "Some Effects of Nonhydrocarbon Base of Constituents on the Friction and Surface Coating Formation obtained with three additives", ASLE Trans., 11, (1968), 19-30

24. Rounds F.G., "Effect of Aromatic Hydrocarbons on Friction and Surface Coating Formation with three Additives", ASLE Trans., 16, (1973), 141-149

25. Rounds F.G. "Influence of Steel Composition on Additive Performance", ASLE Trans., 11, (1968), 54-66

26. Barber R.I., "The Preparation of some Phosphorus Compounds and their Comparison as Load Carrying Additives by the Four Ball Machine, "ASLE Trans., 19, (1975), 319-328

27. Klaus E.E. and Bieber H.E., "Effects of ^{32}P impurties on the Behaviour of Tricresylphosphate - 32 as an antiwear additive", ASLE Trans., 8 (1965), 12-20

28. Bieber H.E., Klaus E.E. and Tewkesbury E.J., "A Study of TriCresyl Phosphate as an Additive for Boundary Lubrication", ASLE Trans., 11, (1968), 155-161

29. Cottington R.L. and Ravner H., "Interactions in Neopentyl Palyol Ester - Tri Cresyl Phosphate - Iron systems at 500°F" ASLE Trans., 12, (f1969), 280-6

30. Lindinger H., "Studies on the Formation of Reaction Layers on Metal Surfaces by Lubricant Blending", Dtsch. Luft-Raumfahrt Forshungsber, 1977, DLR-FB 77-31. ex. CA, 89, (1978), 112625

31. Bamberger E.N. "Bearing Fatigue Investigation - Final Report", NASA CR-72290 (1967)

32. Bamberger E.N., Zaretsky E.V. and Anderson W.J., "Fatigue Life of 120mm bore ball bearings at 600°F with Fluorocarbon, Polyphenyl Ether and Synthetic Paraffinic Base Lubricants "NASA TN-D4850 (1968)

33. Bamberger E.N., Zaretsky E.V. and Anderson W.J., "Effect of three Advanced Lubricants on High Temperature Bearing Life", J. Lub. Tech., 92, (1970), 23-33

34. Parker R.J. and Zaretsky E.V. "Effect of Oxygen Concentration of the Performance of Synthetic Paraffinic Oils in Short Term Bearing Tests from 400° to 500°F", NASA TN-D5152 (1969)

35. Parker R.J., Bamberger E.N. and Zaretsky E.V., "Evaluation of Lubricants for High Temperature Ball Bearing Applications", J. Lub. Tech., 90, (1968), 106-112

36. Sibley L.B. and Peacock L.A., "Extreme Temperature Aerospace Bearing Lubrication Systems" NASA CR-72292 (1967)

37. Wachendorfer C.J. and Sibley L.B., "Bearing-Lubricant Endurance Characteristics at High Speeds and High Temperatures" NASA CR-74097 (1965)

38. Zaretsky E.V. and Anderson W.J., "Preliminary Determinations of Temperature Limitations of Ester, Ether and Hydrocarbon Base Lubricants in 25mm bore Ball Bearings", NASA TN-D4146 (1967)

39. Zaretsky E.V. and Bamberger E.N. "Advanced Air Breathing Engine Lubricants Study with a Tetraester Fluid and a Synthetic Paraffinic Oil at 492K (425° F)", NASA TN-D6771 (1972)

40. Gentle C.R. and Day R.S. "Effect of Some Antiwear Additives on the Elastohydrodynamic Lubrication of a Point Contact", Proc. Trib. Conv. 1972, paper C81/72

41. Myers H. "Lubricating Oils containing Phosphorus Products" U.S. Patent 3,329,742 (1966)

42. Raich H. "Method for applying Fatigue Resistant Surface Coating", U.S. Patent 4,054,694 (1977)

43. Schmitt K.D. "Process for Preparing Tertiary Alkylphosphordichloridites", U.S. Patent 4,120,917 (1978)

44. Parker R.J. Bamberger E.N. and Zaretsky E.V. "Bearing Torque and Fatigue Life Studies with Several Lubricants for Use in the Range 500° to 700°F", NASA TN-D3948 (1967)

45. Wachendorfer C.J. and Sibley L.B. "Bearing-Lubricant Endurance Characteristics at High Speeds and High Temperatures, Final Report 1 Sept. 1962-31 Aug 1965", SKF Report AL65TO68

46. Parker R.J., Bamberger E.N. and Zaretsky E.V. "Evaluation of lubricants for High Temperature Ball Bearing Applications", NASA TM-X-52321 (1967)

47. Trachman E.G. and Cheng H.S. "Traction in EHD line Contacts for two Synthesised Hydrocarbons"., ASLE Trans., 17, (1974), 271-9

48. (not used)

49. Zaretsky E.V., Anderson W.J. and Bamberger L.N. "Rolling Element Bearing Life from 400° to 600°F", NASA TN-D5002 (1968)

50. Chiu Y.P. Hahn D. and Rosenberg N. "Exploratory Analysis of EHD Properties of Lubricants", SKF Report SKF-AL 72 POO1. (1972)

52. Jones W.R., Johnson R.L., Winer W.O. and Sanborn D.M. "Pressure-Viscosity Measurements for several lubricants to 5.5 x 10^8 Nm^{-2} (8 x 10^4 p.s.i.) and 149°C (330°F)", NASA TN D-7736 (1974)

52. Jones W.R., Johnson R.L., Winer W.O. and Sanborn D.M. "Pressure-Viscosity Measurements for several Lubricants", ASLE Trans., 18, (1975), 249-262

53. Cameron A. and Gohar R., "Theoretical and Experimental Studies of the Oil Film in Lubrication Point Contact", Proc. Roy. Soc. L., A291, (1966), 520-536

54. Cotton F.A. and Wilkinson G. "Advanced Inorganic Chemistry", 3rd Edition, Interscience, New York, 1972 pp. 394-5

55. Kirby A.J. and Warren S.G. "The Organic Chemistry of Phosphorus", Elsevier, Amsterdam, 1967, pp. 20-23

56. Arbuzor B.A. and Vinogradora V.S. "The Structure of Dialkylphosphorus Acids", Bull. Acad. Sci. URSS, Classe. Sci. Chim. (1947), 617-22, ex. CA, 42, (1948), 5844

57. Corbridge D.E.C., "Phosphorus", Elsevier, Amsterdam, 1978, pp. 206-7

58. Anon. "Editorial Report on Nomenclature, 1952, Appendix 3", J. Chem. Soc., 1952, 5122-31

59. Kosolapoff, G.J. and Maier L. (Eds.) "Organic Phosphorus Compounds", vol 5. Wiley-Interscience, New York, 1973, p 24-6

60. Corbridge D.E.C. (57) p. 206

61. Gerrard W. "The Interaction of n-Butyl Alcohol and the Chlorides and Oxychlorides of Phosphorus in the Absence and Presence of Pyridine", J. Chem. Soc., 1940 (ii), 1464-9

62. Corbridge D.E.C. (57) p. 68

63. Bloch H.S. "Preparation of Dialkyl Phosphites", U.S. Patent 2,570, 512 (1951)

64. Mark V. and Van Wazer J.R., "Tri-t-butyl phosphite and some of its Reactions", J. Org. Chem. 29, (1964), 1006-8

65. Gerard W. and Shepherd B.D., "Formation of Sulphites, Phosphites and Phosphates of Alcohols containing an Aryl Group", J. Chem. Soc., (1953), 2069-74

66. Anschutz R. and Emery W.O., "Uber die Einwirkung von Phosphortirichlorid auf Salicylsaure und auf Phenol", Ann. Chem., 239, (1887), 301-313

67. Kim S.G., Han B.D., Lee D.M. and Kim B.K., "Preparation of Trialkyl Phosphites", Hwahak Kwa Hwahak Kongop, (1971), 312-4; ex CA, 77, (1972), 139504

68. Chadwick D.H. and Reetz T., "Phosphorous Acid Esters and Method of Making Same", U.S. Patent 2,865,942 (F1958)

69. Ford-Moore A.H. and Williams J.H., "The Reaction between Trialkyl Phosphites and Alkyl Halides", J. Chem. Soc. (1947) 1465-1467

70. Virginia-Carolina Chemical Corp., "Alkyl and Aryl Esters of Phosphorous Acid", U.K. patent 853,982 (1960)

71. Schliebs R., "Neutral Esters of Phosphorus Acid", U.K. Patent 749,550 (1956)

72. Hurwitz M.J. and Carson A., "Trialkyl Phosphites", US patent 3.087,958 (1963)

73. Reetz T., "Tralkyl Phosphites", U.S. Patent 2,859,238 (1958)

74. Schliebs R., "Trialkyl Phosphites", German Patent 1,079,022 (1961)

75. Schliebs R., "Ester of Phosphorus (III) Acids", German Patent 1,088,955 (1960)

76. Hoffman F.W., Ess R.J. and Usinger R.P., "Transesterification of Trialkyl Phosphites with Alphatic Alcohols", J.A.C.S., 78, (1956), 5817-22

77. Rosin J. and Birsten O.G. "Trimethyl and Triethyl Phosphite", U.S. Patent 2,970,166 (1961)

78. Yamazaki N. and Higashi F. "Triphenyl Phosphite", Japan Kokai, 77 42,858 (1977) ex CA., 87, (F1977), 134558

79. Cambell C.H., Chadwick D.H. and Kaufman S., "Dialkyl Phosphites", Ind. Eng. Chem., 49, (1957), 1871-4

80. Cook H.G., McCombie H. and Saunders B.C., "Esters containing Phosphorus. Part II", J. Chem. Soc., (1945), 873-4

81. McIvor R.A., McCarthy G.D. and Grant G.A., "Preparation and Toxicity of some Alkyl Thiopyrophosphates", Can. J. Chem., 34, (1954), 1819-

82. McCombie H., Saunders B.C. and Stacey G.J., "Esters containing Phosphorus. Part I", J. Chem. Soc., (1945), 380-2

83. Arbuzov B.A. and Vinogradova V.S., "Preparation of Higher Dialkyl Phosphites by Transesterification", Doklady Akod. Nauk. SSSR, 83, (1952), 79; ex CA, 47, (1953), 2685

84. Bliznyuk N.K. Protasova L.D., Sakharchuck T.A., Klopkova R.S. and Klimova T.A., "Dialkyl Phosphites", U.S.S.R. Patent 488,280 (1975); ex CA, 84, (1976), 4473

85. Chadwick D.H., "Method of Producing Mono and Dialkyl Hydrogen Phosphites", U.S. Patent 2,834,797 (1958)

86. Gunderlay F.C. "Synthesis of Partial Esters and Phosphorus Acids and Salts thereof", U.S. Patent 3,019,249 (1958)

87. Walsh E.N., "Conversion of Tertiary Phosphites to Secondary Phosphonates. Diphenyl Phosphonate", J.A.C.S., 81, (1959), 3023

88. Walsh E.N., "Possibly Substituted Diphenyl Phosphites", German Patent. 1,078,136 (1961)

89. Yamazaki N, "Diphenyl Phosphite", Japan Kokai 77 42,857 (1977) ex CA, 87, (1977), 134557

90. Schimmelschmidt K. and Kleiner H.-J., "Dialkyl Phosphites", U.K. Patent 1,298,156 (1972)

91. Schimmelschmidt K. and Kleiner H.J., "Dialkyl Phosphites from ROH and H_3PO_3", German Patent 1,668,031 (1973)

92. Schimmelschmidt K. and Kleiner H.-J., "Dialkyl Phosphites", Japan Patent 77 27,141 (1977) ex CA, 88, (1978), 22137

93. Jenker H., "Alkyl Phosphites" U.K. Patent 1,22,550 (1968)

94. Gilbert E.E. and Otto J.A., "Dailkyl Hydrogen Phosphites", U.S. Patent 2,745,862 (1956)

95. Corbridge D.E.C. (57) p.51

96. Bliznyuk N.K. and Protosova L.D., "Higher Dialkyl Phosphites", U.S.S.R. Patent 473,717 (1975)

97. Nifant'er E.E. and Levitan L.P., "Monoalkyl Phosphites, Probl. Organ. Sinteza., Akad, Nauk SSSR, Otd., Obshch i Teckhn. Khim., (1965), 293-6 ex. CA, 64, (1966), 11074

98. Blyznyuk N.K., Protasova L.D. and Klopkova R.S., "Mono Alkyl Phosphonates", U.S.S.R. Patent 487,081 (1976) ex. CA, 84, (1976), 4471

99. Nifant'er E.E., Blagoveshchenskii V.S., Sokurenko A.M. and Skylarksii L.S., "Monoalkyl Phosphonats". U.S.S.R. Patent, 363,708 (1972), ex. CA, 78, (1973), 159865

100. Corbridge D.E.C. (57) p. 211

101. Michalski J. Modro T. and Zwierzak A., "Anhydrides of Organophosphorus Acids. Part II; The Synthesis of Tri and Tetra Alkyl Esters of Phosphorous Phosphoric Anhydrides", J. Chem. Soc., (1961) 4904-6

102. Bellamy L.J. "The Infrared Spectra of Complex Molecules", Vol. 1, 3rd Edn., Chapman & Hall, London, 1975, pp. 348-353

103. Pouchert C.J., "The Aldrich Library of Infrared Spectra", Aldrich Chemical Company Inc., 1975, pp 407-415 and 865-872

104. Thomas L.C. and Chittenden R.A., "Characteristic Infrared Absorption Frequencies of Organophosphorus Compounds - I - The Phosphoryl (P=O) group.", Spec. Acta, 20, (1964), 467-487

105. Thomas L.C. and Chittenden R.A., "Characteristic Infrared Absorption Frequencies of Organophosphorus Compounds - II - P - O - (X) bonds", Spec. Acta, 20, (1964), 489-502

106. Corbridge D.E.C., "Infrared Analysis of Phosphorus Compounds", J. Appl. Chem., 6, (1956), 456-465

107. Thomas L.C., Chittenden R.A. and Hartley H.E.R., "Hydrogen Bonding in Alkyl Phosphonic and Alkyl Phosphonothionic Acids", Nature, 192, (1961), 1283-4

108. Arbuzor B.A. and vinogradova V.S. "The Structure of Dialkyl Phosphorous Acids", Bull, Acad. Sci. URSS, Classe Sci. Chem. (f1947) 617-22 ex CA, 42, (1948), 5844

109. Smith A.L. "Applied Infrared Spectroscopy" Wiley, New York, 1979, pp 117-8

110. Emsley J.W., Feeney J. and Sutcliffe L.H., "High Resolution Nuclear Magnetic Spectroscopy", Vol 1, Pergamon Press, Oxford, 1965.

111. Kemp W., "Qualitative Organic Analysis" Revised Edition, McGraw-Hill, London 1979, pp 151-165

112. McLafferty F.W., "Interpretation of Mass Spectra", W.A. Benjamin Inc., New York, 1966

113. Hill H.C., "Introduction to Mass Spectrometry", Heyden, London, 1966

114. Biemann K. "Mass Spectrometry. Organic Chemical Applications" McGraw-Hill, New York, 1962

115. Dixon J.P., "Modern Methods in Organic Microanalysis" Van Nostrand, London, 1968

116. Bance S. "Handbook of Practical Organic Microanalysis" Ellis-Horwood, Chichester, 1980

117. Elemental Micro Analysis Ltd., Catalogue of available analytical services

118. Tennent R.M. (Ed.) "Science Data Book", Oliver & Boyd, Edinburgh, 1971, p. 60

119. Siddiqui I.H. and Davies D.A., Private Communication, Albright and Wilson Ltd., Phosphates Division, London E15

120. Smith A.L., (109), pp 220-222

121. Smith A.L., (109), pp 223-228

122. Blair G.W.S. "Elementary Rheology" Academic Press, London, 1969, 33-37

123. Cotton F.A. and Wilkinson G., (54) p 858

124. Alder R.W., Baker R., and Brown J.M., "Mechanism in Organic Chemistry", pp. 310-348

125. Corbridge D.E.C. (57) 202-211

126. Morrison R.T. and Boyd R.N. "Organic Chemistry" Third Edition, Allyn and Bacon, Boston, 1973, p. 628

127. Cotton F.A. and Wilkinson G. (54) p. 857

128. Cotton F.A. and Wilkinson G. (54) p. 860

129. Goto K., Tamura H. and Nagayama M., "The Mechanism of Oxygenation of Ferrous Ion in Neutral Solution," Inorg. Chem., 9, (1970), 963-4

130. Morrison R.T. and Boyd R.N. (126) pp 32-3

131. Cotton F.A. and Wilkinson G. (f54) p. 863

132. Jackson J.S. and Wadsworth M.E., "A Kinetic Study of the Dissolution of Allard Lake Ilmenite in Hydrochloric Acid", Light Met. Proc. Sess., A.I.M.E. Ann. Meet. 1976, 1, 481-540

133. Cotton F.A. and Wilkinson G. (54) p. 831

134. Morrison R.T. and Boyd R.N. (126) p. 660-2

135. Corbridge D.E.C.

136. Morrison R.T. and Boyd R.N. (126) pp. 797-8

137. Morrison R.T. and Boyd R.N. (126) pp. 677-681

138. Thomas L.C., "Identification of Functional Groups in Organophosporous Compounds", Academic Press, London, 1974, 23-48

139. Bellamy L.J., "The Infrared Spectra of Complex Molecules" Vo. 1. 3rd Edn., Chapman & Hall, London, 1975 pp 348 and 351

140. Thomas L.C. "Interpretation of Infrared Spectra of Organophosphorus Compounds", Heyden, London

141. Guilbault G. and Das J. "Chemisorption Reactions and Disopropyl methyl phosphonate with Transition Metal Salts". J Phys. Che., 73 (1969), 2243-7

142. Cambell I.G.M. Fowles G.W.A. and Nixon L.A. "Organometallic Compounds Containing a Tin-Phosphorus Bond.", J. Chem. Soc., (1964), 1389-96

143. Coates G.E. and Golightly D.S., "Cobalt (II) Methyl-and Phenyl-phosphinates" J. Chem. Soc., (1962), 2523-5

144. Finegold H., "Complementary Use of n.m.r. and Infrared Absorption Studies in Organic Phosphorus Chemistry", Ann. N.Y. Acad. Sci, 70 (1958), 875-889.

145. Morrison & Boyd (126) pp. 163 & 360

146. McLafferty F.W. (112) p 123

147. McLafferty F.W., "Interpretation of Mass Spectra" 2nd Edition, W.A. Benjamin Inc., New York, 19, p. 68-9

148. Pake G.E. "Paramagnetic Resonance" W.A. Benjamin Inc., New York, 1962, pp. 16-47

149. Pake G.E. and Estle T.L., "The Physical Principles of Electron Paramagnetic Resonance" 2nd Edn., W.A. Benjamin Inc., Reading Mass., 1973, pp. 14-57

150. Cotton F.A. and Wilkinson G. (54), 536-7

151. Pake G.E., "Paramagnetic Resonace", W.A. Benjamin Inc., New York 1962, 3-47

152. Pake G.E. and Estle T.L., "The Physical Principles of Electron Paramagnetic Resonance", W.A. Benjamin Inc., Reading Mass., 1973, 1-57

153. Feher G., "Electron Paramagnetic Resonance with Applications to Selected Problems in Biology", Gordon and Breach, New York 1970, 2-28

154. Cotton F.A. and Wilkinson G. (54), 562

155. Feher G. (153), 49-52

156. Cotton F.A. and Wilkinson G. (54), 546

157. Pake G.E. (151), 68

158. Pake G.E. and Estle T.L. (152), 108-11 and 131-149

159. Pake G.E. and Estle T.L. (152), 300-1

160. (not used)

161. Gibb T.C., "Principles of Mossbauer Spectroscopy", Chapman & Hall, London, 1975, 1-21

162. Greenwood N.N. and Gibb T.C., "Mossbauer Spectroscopy", Chapman & Hall, London, 1971, 1-45

163. May L. (Ed.), "An Introduction to Mossbauer Spectroscopy", Chapman & Hall, Adam Hilger, London, 1971, 1-44

164. Greenwood N.N. and Gibb T.C., (162), 54-56

165. (not used)

166. Gibb T.C. (161), 76

167. (not used)

168. Gonser U. (Ed.), "Mossbauer Spectroscopy" Springer-Verlag, Berlin, 1975, 16 and 26.

169. Danon J. "Lectures on the Mossbauer Effect", Gordon and Breach, New York, 1968, p. 96

170. Goldanskii V.I. and Herber R.H. "Chemical Applications of Mossbauer Spectroscopy", Academic Press, New York, 1968, pp 63-4

171. Gibb T.C. (F160) p 33

172. May L. (163) p. 102

173. Gibb T.C. (f161) pp 102-3

174. Danon J. (169) p. 269

175. Cotton F.W. and Wilkinson G. (54) pp 857 and 864

176. Corbridge D.E.C. (57) 1-11

177. Block B.P. "Polymeric Metal Phosphinates", Inorg. Macromol. Rev., 1, (1970) 115-125

178. Smith L.S., Newman P.R., Heeger A.J., Garito A.F., Gillman H.D. and Nannelli P., "Phosphorus - 31 n.m.r. Studies of the Linear Chain Magnets: Poly (metal phosphinates)., J. Chem. Phys. (1977), 66, 5428-32

179. Hardy C.J. and Fletcher P.R. "Polymers of Heavy Metals with Dialkyl Phosphonic Acids", AERE Report R-4281, (1963)

180. Corbridge D.E.C. (57) 1-11

181. Wedeven L.D., "What is EHD?", Lubr. Eng., 31, (1975), 291-6

182. Martin H.M., "The Lubrication of Gear Teeth", Engineering, London, 102, (1916), 119-121

183. Cameron A., "Principles of Lubrication", Longmans, London, 1966

184. Dowson D. and Higginson G.R., "New Roller Bearing Lubrication Formula", Engineering, 192, (1961), 158-9

185. Dowson D. Higginson G.R. and Whitaker A.V., "Elastohydrodynamic Lubrication" A Survey of Isothermal Solutions", J. Mech. Eng. Sci. 42, (1962), 121-6

186. Archard G.D., Gair F.C. and Hirst W., "The Elastohydrodynamic Lubrication of Rollers" Proc. Roy. Soc., A262, (1961) 51-72

187. Archard J.F. and Cowking E.W., "Elastohydrodynamic Lubrication at Point Contacts", Proc. Inst. Mech. Engrs., 180 pt. 3B, (1965-6), 47-56

188. Cheng H.S. "A Numerical Solution of the Elastohydrodynamic Film Thickness in an Elliptical Contact", J. Lub. Tech 92, (1970)

189. Ranger A.P., Ettles C.M.M. and Cameron A., "The Solution of the Point Contact Elastohydrodynamic Problem" Proc. Roy. Soc. London, A346, (1975), 227-244

190. Oh K.P. and Rohde S.M., "Numerical Solution of the Point Contact Problem using the Finite Element Method", Int. J. Num. Methods in Eng., 11 (1977), 1507-18

191. Hamrock B.J. and Dowson D., "Isothermal Elastohydrodynamic Lubrication of Point Contacts Part 1 - Theoretical Formulation", J. Lub Tech., 98, (1976) 223-9

192. Hamrock B.J. and Dowson D., "Isothermal Elastohydrodynamic Lubrication of Point Contacts Part 2 - Fully Flooded Results, J. Lub. Tech. 99, (1977), 264-274

193. Cameron A. and Gohar R., "Optical Measurement of Oil Film Thickness under Elastohydrodynamic Lubrication", Nature, 200, (1963), 458-9

194. Gohar, R. and Cameron A., "The Mapping of Elastohydrodynamic Contacts" ASLE Trans., 10, (1966), 215-225

195. Foord, C.A. Hamman W.C. and Cameron A., "Evaluation of Lubricants using Optical Elastohydrodynamics", ASLE Trans. II, (1968), 31-43

196. Foord C.A., Wedeven L.D. Westlake F.J. and Cameron A., "Optical Elastohydrodynamics", Proc. Inst. Mech. Eng. Pt. 1, 184, (1969-70), 487-503

197. Wedeven L.D., "Optical Measurements in Elastohydrodynamic Rolling-Contact Bearings", Ph.D. Thesis, University of London (1970)

198. Gentle C.R., "Traction in Elastohydrodynamic Point Contact", Ph.D. Thesis, University of London (1972)

199. Paul G.R. and Cameron A., "An absolute High-Pressure Microviscometer based on Refractive Index", Proc. Roy. Soc. London, A331, (1972), 171-184

200. Kaye K.A. and Winer W.O. "An Experimental Evaluation of the Hamrock and Dowson minimum Film Thickness Equation for Fully Flooded EHD Point Contacts "J. Lub. Tech., 103, (1981), 284-294

201. Hares J.A., "The Commissioning of an Elastohydrodynamic Lubrication Rig", Int. Rep., Imperial College, (1978-9).

202. R.T. Vanderbilt Co. Inc., "NA-SUL Rust Inhibitors - A Summary of Their Properties and Uses" Technical Bulletin 711, R.T. Vanderbilt Company Inc., Norwalk Conneticut, U.S.A.

203. Scott V.D. and Love G., "Quantitative Electron Probe Microanalysis", Ellis Horwood, Chichester, 1983, Chapters 2,4 and 5

204. Goldstein, J.I. and Yakowitz H. (Eds.), "Practical Scanning Electron Microscopy", Plenum Press, New York, 1975, Chapters 9 and 11

205. Goldstein J.I. and Yakowitz H. (204), p. 356

206. Kemp. W (111) p. 47

207. Saraceno A.J., "Lubricating Greases", U.S. Patent 3,331,775 (1967)

208. Saraceno A.J., "Phosphate Esters containing Co-ordination Polymers" U.S. Patents 3,328,296 (1967) and 3,384,605 (1968)

209. Feng. I. Ming., Perilstein W.L. and Adams M.R., "Solid Film Deposition and Non-Sacrificial Lubrication", ASLE Trans., 6, (1963), 60.

210. Watkins R.C., "The Antiwear Mechanism of ZddP's part 2", Trib. Int., 15, (1982), 3

211. Jones R.B. and Coy R.C., "The Chemistry of the Thermal Degradation of Zinc dialkyl dithiophosphonate Additives", ASLE Trans., 24, (1980), 91

212. Bamberger E.N. et al., "Life Adjustment Factors for Ball and Roller Bearings - An Engineering Design Guide", ASME, New York, 1971

213. Rowe C.N., "Specific Film Thickness - The Effects of EHL Film Thickness and Surface Roughness on Bearing Fatigue", ASLE Preprint 80-LC-4A-1

214. "Life Adjustment Factor for Ball & Roller Bearings", ASME Eng. Design Guide (1971).

215. Sastry, V.R.F., Sethuramiah, A. and Singh, D.V., "A Study of Wear under partial EHL Conditions", Proe, Leeds/Lyon Symposium 1984 (to be published).

216. Michaelis, A. and Ananoff, J., "Verber Aromatische Phosphor verbunding", Ber. Deutsch. Chem. Ges., 7, (1874), 1688-1693.